The Interaction between Aluminium Toxicity and Drought Stress in Common Bean (*Phaseolus vulgaris* **L.**)

Physiological and Molecular Aspects

Von der Naturwissenschaftlichen Fakultät der

Gottfried Wilhelm Leibniz Universität Hannover

zur Erlangung des Grades

Doktor der Naturwissenschaften

Dr. rer. nat.

genehmigte Dissertation

von

Master of Agriculture Zhongbao Yang

geboren am 28.11.1979 in Tancheng, VR China

2011

Referent: Prof. Dr. rer. agr. Walter J. Horst

Gottfried Wilhelm Leibniz Universität Hannover

Korreferent: Prof. Dr. rer. nat. Hans-Peter Braun

Gottfried Wilhelm Leibniz Universität Hannover

Tag der Promotion: 07.Juli 2011

ABSTRACT

Aluminium (Al) toxicity and drought are two major abiotic stress factors limiting common bean (*Phaseolus vulgaris* L.) production in the tropics. The Al-impeded root growth may strongly limit the water exploitation of roots from subsoil and thus less ability to withstand drought stress in the acid soils. In light of the importance of root development under Al toxicity and drought stress, in this study the short-term effects of combined Al toxicity and drought stress on root growth with special emphasis on physiological and molecular mechanisms in the root apex was investigated.

Using hydroponics, PEG 6000 (polyethylene glycol)-induced osmotic (drought) stress reversed the Al-induced inhibition of root elongation by reducing Al accumulation in the root tips in the Al-sensitive genotype VAX 1, which was related to the reduction of cell-wall (CW) porosity resulting from PEG 6000-induced dehydration of the root apoplast. Less Al stress in PEG-treated roots was confirmed by the expression of the Al-sensitivity indicator genes: multidrug and toxin extrusion family protein (*MATE*) and 1-aminocyclopropane-1-carboxylic acid oxidase (*ACCO*). Transcriptional analysis using SuperSAGE (serial analysis of gene expression) and quantitative RT-PCR (qRT-PCR) suggested that genes related to CW assembling and modification such as xyloglucan endotransglucosylase/hydrolase (*XTH*), glucan endo-1,3-beta-glucosidase (*BEG*) and hydroxyproline-rich glycoprotein (*HRGP*) play important roles in PEG-induced decrease of CW porosity leading to reduced Al accumulation in root tips. A large-scale proteomic analysis revealed that dehydrin (DHN) may play a key role in the protection of osmotic stress-induced physical breakage of CW and thus the maintenance of reversible CW extensibility.

Under soil conditions, drought reduced Al toxicity in the common bean genotype VAX 1, indicated as the reversion of Al-induced enhancement of callose content and of *MATE* gene expression in the root tips. However, in contrast to PEG-induced reduction of Al injury in hydroponics, combined Al and drought stress in soil resulted in a more severe inhibition of root elongation than either stress alone. This is consistent with enhanced further up-regulation by Al of the drought-induced *ACCO* gene involved in the biosynthesis of ethylene by Al and the down-regulation by Al of drought-induced genes/transcription factors in the root tips: the 9-cis-epoxycarotenoid dioxygenase (*NCED*) gene involved in ABA biosynthesis, the transcription factors *bZIP* and *MYB* involved in the regulation of ABA-dependent genes, the ABA-dependent sucrose synthase (*SUS*) gene, the late embryogenesis abundant (*PvLEA18*) gene, the KS-type dehydrin (*KS-DHN*) gene, and the lipid transfer family protein (*LTP*) gene.

Together, the results provide circumstantial evidence that PEG-induced osmotic stress and low soil moisture alleviates Al toxicity, but Al renders the root apex more sensitive to low soil moisture particularly by impacting the gene regulatory network involved in ABA signal transduction and ABA signal cross-talk with other phytohormones necessary for maintaining root growth under drought.

Key words: aluminium toxicity and drought stress, common bean, cell wall porosity

KURZZUSAMMENFASSUNG

Aluminium (Al)-Toxizität und Trockenstress sind zwei wichtige abiotische Stressfaktoren, die die Produktivität von Buschbohne (*Phaseolus vulgaris* L.) in den Tropen begrenzen. Durch Al-Angebot gehemmtes Wurzelwachstum kann die Wasseraufnahme aus dem Unterboden stark beeinträchtigen und damit die Trockenresistenz von Buschbohne auf sauren Böden vermindern. Angesichts der Rolle des Wurzelwachstums für Al-Toxizität und Trockenstress wurde in dieser Arbeit die kurzfristige Wirkung von kombiniertem Al und Trockenstress auf das Wurzelwachsum mit besonderer Berücksichtigung physiologischer und molekularer Mechanismen in der Wurzelspitze untersucht.

In Hydroponik verminderte PEG 6000 (Polyethylenglycol) induzierter osmotischer (Trocken) Stress die Hemmung des Wurzellängenwachstums durch Al durch eine verminderte Al Akkumulation in der Wurzelspitzen im Al-sensitiven Buschbohnengenotyp VAX 1. Dies wurde zurückgeführt auf eine Verminderung der Zellwandporosität hervorgerufen durch die Dehydrierung des Wurzelapoplasten durch PEG. Geringerer Al Stress in PEG behandelten Wurzeln wurde bestätigt durch eine verminderte Expression Al-sensitiver Indikatorgene: multidrug and toxin extrusion family protein (*MATE*) and 1-aminocyclopropane-1-carboxylic acid oxidase (*ACCO*). Eine Transcriptionsanalyse mit SuperSAGE (serial analysis of gene expression) und quantitative RT-PCR (qRT-PCR) ergab, dass an der Zellwandsynthese und -struktur beteiligte Gene wie z.B. Xyloglucan endotransglucosylase/hydrolase (*XTH*), Glucan endo-1,3-beta-glucosidase (*BEG*) und Hydroxyproline-rich glycoprotein (*HRGP*) eine wichtige Rolle bei der durch PEG verursachten verminderten Zellwandporisität, die zu einer verminderten Al Akkumulation in Wurzelspitzen führt, spielen. Eine umfassende proteomische Analyse ergab, dass Dehyrin eine Schlüsselrolle für den Schutz der Zellwand vor irreversibler Schädigung durch Entwässerung bei osmotischem Stress durch PEG zukommen könnte.

Im Boden führte Trockenstress zu verminderter Al Toxizität. Hierauf ließ eine geringere Al-induzierte Kallose-Bildung und Expression des *MATE* Genes schließen. Im Unterschied zu einer geringeren Hemmung des Wurzelwachstums durch Al in Gegenwart von PEG in Hydroponik, erhöhte Al-Angebot im Boden die Hemmung des Wurzelwachstums durch Trockenstress. Dies ist konsistent mit einer verstärkten Heraufregulierung durch Al des an der Ethylen-Synthese beteiligten *ACCO* Gens und der Herunterregulierung durch Al von durch Trockenstress verstärkt exprimierten Genen/Transkriptionsfaktoren in den Wurzelspitzen: des an der ABA-Synthese beteiligten 9-cis-Epoxycarotenoid dioxygenase (*NCED*) Gens, den Transkptionsfaktoren *bZIP* and *MYB*, die an der Regulation ABA abhängiger Gene beteiligt sind, des ABA abhängigen Sucrose synthase (*SUS*) Gens, des Late embryogenesis abundant (*PvLEA18*) Gens, des KS-type dehydrin (*KS-DHN*) Gens und des Lipid transfer family protein (*LTP*) Gens. Insgesamt lassen die Ergebnisse darauf schließen, dass PEG indizierter osmotischer Stress und Trockenstress Al Toxizität vermindern. Aluminium-Angebot im Boden macht die Wurzelspitze allerdings empfindlicher gegenüber Trockenstress, da Al insbesondere das die ABA Signaltransduktion regulierende Gen-Netzwerk und die Kommunikation von ABA mit anderen Phytohormonen, was Voraussetzungen für die Aufrechterhaltung des Wurzelwachstums unter Trockenstress sind, beeinträchtigt.

Schlagworte: Aluminium-Toxizität und Trockenstress, Buschbohne, Zellwandporosität

CONTENTS

ABBREVIATIONS

2D	Two dimensional
AAO	abscisic aldehyde oxidase
ABA	Abscisic acid
ABRE	ABA-responsive element
ACCO	1-aminocyclopropane-1-carboxylic acid oxidase
ACO	aconitase
ALMT	Al-activated malate transporter
ANOVA	analysis of variance
AQP	aquaporin
BEG	Glucan endo-1,3-beta-glucosidase
bp	base pair
bZIP	basic domain/leucine zipper
CBB	Coomassie Brilliant Blue
CK	cytokinin
CKX	cytokinin oxidase/dehydrogenase
CPC	cytosolic protein contamination
CS	citrate synthase
CW	cell-wall
CWP	cell wall protein
CYP701A	cytochrome P450 monooxygenase CYP701A
CYP735A	cytochrome P450 monooxygenase 735A
cZ	*cis*-zeatin
cZR	*cis*-zeatin riboside
cZRMP	cZR 5'-monophosphate
DHN	dehydrin
DM	degree of methylation
DMAPP	dimethylallyl diphosphate
DMT	dialysis membrane-tube
DPS	Diamond Phosphoprotein Stain
DTZ	distal transition zone
DZ	dihydrozeatin
DZR	dihydrozeatin riboside
DZRMP	DZR 5'-monophosphate
ECEC	effective cation exchange capacity
EST	expressed sequence tag
EZ	elongation zone

GaE	galacturonic acid equivalent
GFAAS	graphite furnace atomic absorption spectrophotometer
GO	gene ontology
HESI	heated electrospray ionization
HPLC	high pressure liquid chromatography
HRGP	hydroxyproline-rich glycoprotein
IAA	indole-3-acetic acid
ICDH	isocitrate dehydrogenase
ICP-MS	inductively coupled plasma mass spectroscopy
IEF	isoelectric focusing
iP	N^6-(Δ^2-isopentenyl)-adenine
IPG	immobilized pH gradient
iPR	N^6-(Δ^2-isopentenyl)-adenine riboside
iPRDP	iP riboside 5'-diphosphate
iPRMP	iP riboside 5'-moophosphate
iPRTP	iP riboside 5'-triphosphate
IPT	adenosine-phosphate isopentenyl-transferase
JA	jasmonic acid
KDa	kilodalton
kPa	kilopascal
KS-DHN	KS-type dehydrin
LA-ICP-MS	laser ablation inductively coupled plasma mass spectrometry
LEA	late embryogenesis abundant
LMW	low molecular weight
LTP	lipid transfer protein
MATE	multidrug and toxic compound extrusion
MDH	malate dehydrogenase
MetS	methionine synthase
MIPS	*myo*-inositol 1-phosphate synthase
MS	mass spectrometry
MWCO	molecular weight cut off
NCED	9-*cis*-epoxycarotenoid dioxygenase
OA	organic acid
OP	osmotic potential
OS	osmotic stress
P5CS	Δ1-pyrroline-5-carboxylate synthase
PAGE	polyacrylamide gel electrophoresis
PCV	pyrocatechol violet
PEG	polyethylene glycol

PEPC	phosphoenolpyruvate carboxylase
PGM	phosphoglycerate mutase
PHGDH	D-3-phosphoglycerate dehydrogenase
PIP	plasma membrane intrinsic protein
PME	pectin methylesterase
PR	Pathogenesis-related protein
PRP	proline-rich protein
qRT-PCR	quantitative real-time polymerase chain reaction
RC	recovery
RNA	ribonucleic acid
ROS	reactive oxygen species
SA	salicylic acid
SAGE	serial analysis of gene expression
SAM	S-adenosylmethionine
SAMS	S-adenosylmethionine synthethase
SDS	sodium dodecyl sulphate
SEM	scanning electron microscope
SSH	suppression subtractive hybridization
SUS	sucrose synthase
SWP	soil water potential
Tris	tris(hydroxymethyl)aminomethane
TZ	transition zone
tZ	*trans*-zeatin
tZR	*trans*-zeatin riboside
tZRDP	tZR 5'-diphosphate
tZRMP	tZR 5'-monophosphate
tZRTP	tZR 5'-triphosphate
UDP	Uridine diphosphate
UniTags	unique transcripts
XET	xyloglucan endotransglucosylase
XTH	xyloglucan endotransglucosylase/hydrolase
ZEP	zeaxanthin epoxidase
ZOG	zeatin-O-glucoside
ZOGT	zeatin-O-glucosyltransferase
ZR	zeatin-riboside
βGlc	β-glucosidase

GENERAL INTRODUCTION

Acid soils and major constraints

Soil acidity with pH $\leq$ 5.5 is one of the most important factors limiting crop production worldwide on approximately 30% of the world's total land area and as much as 50% of the world's potentially arable lands. The tropics and subtropics account for 60% of the acid soils in the world. In tropical areas about 43% of soils are acidic comprising about 68% of tropical America, 38% of tropical Asia, and 27% of tropical Africa (von Uexküll and Mutert, 1995). The factors that contribute to acid soil infertility and subsequent stunted plant growth in acid soils are complex. In acid mineral soils, a variety of individual chemical constraints and interactions among them limit plant growth. For example, in low pH soils, it is not usually the hydrogen ion toxicity which affects plant growth but rather other toxicities, such as aluminium (Al) and manganese, and deficiencies of phosphorus, nitrogen, potassium, calcium, magnesium, sulfur, zinc, and molybdenum (Rao et al., 1993). Aluminium toxicity is particularly severe at soil pH values of 5.0 or below (Foy, 1974). And on many acid soils, dry spells during the main growing period of crops are becoming an increasingly important yield-limiting factor (Welcker et al., 2005) with the changing global climate. The use of lime, phosphate fertilizers, organic matter and irrigation is more productive on acid soils, as practiced in the temperate climates of North America and Europe. However, it is not an economically realistic alterative in many developing tropical countries because the high cost is beyond the ability of low input resource-poor farmers. Also, the utilization of fertilizers or chemicals may seriously threaten the environment (Rao et al., 1993; Miklas et al., 2006). On the other hand, even if liming can raise soil pH and overcome toxicity problems, the subsoil usually remains unaffected, since deep lime incorporation is technically difficult and even more expensive.

The traits of aluminium toxicity in plants

When the soil pH drops below 5, Al^{3+} is solubilized into the soil solution and become a major constraint for plant growth and development in acidic soils (Kinraide et al., 1992). The easily observable symptom of Al toxicity is a rapid (minutes to few hours) inhibition of root growth (Horst et al., 1992; Delhaize and Ryan, 1995), resulting in a reduced and damaged root system that limits mineral nutrient and water uptake (Kochian et al., 2004). The rapidity of this response indicates that Al first inhibits root cell-expansion and

elongation and consequently cell division over the longer term (Kochian, 1995; Delhaize and Ryan, 1995). The role of the root apex in the perception of Al toxicity was firstly proposed by Ryan et al. (1993) in maize (*Zea mays*). Subsequently, Sivaguru and Horst (1998) specified that the distal part of the transition zone (DTZ, 1-2 mm) is the most Al-sensitive apical root zone in Al-sensitive maize cultivar 'Lixis'. In common bean, Rangel et al. (2007) showed that both the transition zone (TZ, 1-2 mm) and elongation zone (EZ) are targets of Al injury. It has been suggested that the Al toxicity results from the interactions of Al with either apoplastic (Horst, 1995; Blamey, 2001; Horst et al., 2010), plasma membrane (Zhao et al., 1987; Wagatsuma et al., 1985; Ishikawa and Wagatsuma) or symplastic targets (Kochian, 1995; Barceló and Poschenrieder, 2002; Kochian et al., 2005). However, the mechanisms of Al-induced inhibition of root elongation are still not well defined. Recently, it has been speculated that the Al-induced inhibition of root growth is due to enhanced gene expression and enzyme activity of 1-aminocyclopropane-1-carboxylic acid oxidase (ACCO) resulting in increased ethylene production in *Lotus japonicus* and *Medicago truncatula* (Sun et al., 2007) and the ethylene-mediated inhibition of polar auxin transport controls Al-induced inhibition of root elongation in Arabidopsis (Kollmeier et al., 2000; Sun et al., 2010). Also in common bean, Eticha et al. (2010) observed that initial Al-induced inhibition of root elongation was correlated with the expression of the *ACCO* gene, which is involved in the ethylene biosynthesis, in both common bean genotypes, Quimbaya (Al-resistant) and VAX 1 (Al-sensitive).

The induction of callose synthesis has been proposed as another sensitive indicator of Al injury in roots (Wissemeier et al., 1987; Staβ and Horst, 2009), particularly in the root apex (Wissemeier and Horst, 1995; Sivaguru et al., 2006). The high sensitivity of Al-induced callose formation to Al is also a reliable parameter for the classification of genotypes of different plant species in terms of Al resistance (Wissemeier et al., 1992; Horst et al., 1997; Collet and Horst, 2001; Eticha et al., 2005).

The role of the root apoplast in aluminium toxicity and resistance

The accumulation of Al in the root tips is characterized by a rapid initial phase and a low rate at later stages (Zhang and Taylor, 1989; 1990). The rapid initial phase reflects the binding of Al in the apoplast (Taylor et al., 2000; Wang et al., 2004; Horst et al., 2007; Rangel et al., 2009) in which the negatively charged carboxylic groups of pectin provide the Al^{3+} binding sites (Blamey et al., 1990; Chang et al., 1999). The negative charge of pectin depends on its degree of methylation (Eticha et al., 2005), which is controlled by

pectin methylesterase (PME) (Bordenave, 1996; Gerendás, 2007). Schmohl et al. (2000) provided evidence that the degree of methylation (DM) of CWs modulates the Al accumulation and Al sensitivity of maize suspension cells. Also, short-term PME treatment of intact maize roots elevated Al accumulation and Al-induced inhibition of root elongation (Horst et al., 2007). It has been reported that short-term Al accumulation of roots was closely related to the pectin content in apical root sections of maize and faba bean (*Vicia faba*) and the binding of Al to the pectic matrix was closely positively correlated with Al-induced callose formation and thus Al sensitivity (Horst et al., 1999).

The high affinity of Al to the pectic matrix may prevent the binding of Ca^{2+} to the CW, which plays a key role in controlling CW extensibility by the formation and cleavage of Ca bonds during cell elongation (Boyer, 2009). It has been revealed that Al treatment reduces root CW extensibility (Tabuchi and Matsumoto, 2001; Ma et al., 2004). Strong binding of Al to the pectic matrix may present CW extension physically and/or physiologically by decreasing the effectiveness of CW-loosening enzymes (Wehr et al., 2004). Recently, Yang et al. (2011) observed that the Al-induced reduction of the activity of CW loosening enzyme xyloglucan endotransglucosylase (XET) was related to Al-inhibited root elongation in Arabidopsis, and the reduction of the activity of this enzyme was accompanied with callose deposition in roots. Therefore, it appears the binding of Al to pectins is closely related to Al sensitivity, since it was also reported that the Al-induced increase in pectin content of Al-sensitive cultivars was greater than that of Al-resistant cultivars (Eticha et al., 2005; Yang et al., 2008). Also in common bean, Rangel et al. (2009) found that the Al-induced root growth was closely negatively related to free apoplastic and particularly strongly bound CW Al. This suggests that the strong binding of Al to the pectic matrix of the CW is a main factor in Al toxicity rather than a resistance mechanism in common bean. However, some studies indicated that the increased pectin content was related to Al resistance (Van et al., 1994) since the free carboxyl groups of pectin can bind or chelate Al^{3+} ions and cause cross-link of pectin molecules (Klimashevskii and Dedov, 1975).

In fact, the involvement of pectin in Al resistance mainly depends on its degree of methylation (DM), since the DM is responsible for the negativity of the CW as mentioned above. In *Petunia inflate*, higher Al accumulation and callose production in the roots and more inhibition of root growth were found in transgenic potato plants with higher PME expression than wild type when exposed to Al (Schmohl et al., 2000). In two differential Al-resistant cultivars of maize, Eticha et al. (2005) observed that the Al-sensitive cultivar

had lower DM and more Al accumulation, and thus were more severely injured by Al compared with the Al-resistant cultivar, while no difference was found in pectin content. Similarly, in rice (*Oryza sativa*), Yang et al. (2008) found that CW PME activity in the root tips was higher leading to a higher demethylated pectin content in the Al-sensitive cultivar than the Al-resistant cultivar. This indicates that the higher proportion of free pectic acid residues in the CW causes a corresponding higher Al accumulation in the root tips and the CW. Also, transcriptional analysis of Al resistance in maize by Maron et al. (2008) revealed that Al up-regulated the expression of *PME* gene in both Al-resistant and Al-sensitive genotypes, while the level of up-regulation of PME was higher in Al-sensitive genotypes.

On the other hand, there is no doubt that more Al accumulation in the CW will also affect the plasma membrane. The interaction between CW and plasma membrane appears to be potentially harmful (Delhaize and Ryan, 1995), although the low rates of transport observed through the plasma membrane will favor the accumulation of Al in the apoplast (Rengel and Reid, 1997). It has been proposed that the interaction of apoplastic Al with the cell wall - plasma membrane - cytoskeleton continuum play major role in the Al-induced inhibition of root growth (Horst et al., 1999; Sivaguru et al., 2000).

Aluminium exclusion from the apoplast by the release of organic acid anions

It is widely accepted that the release of Al-complexing solutes, particularly organic acid anions, from the root apex, play a key role in Al resistance by complexation of Al and thereby detoxifying rhizotoxic Al (Ma et al., 2007; Ryan et al., 2001; Kochian et al., 2004; Delhaize et al., 2007; Ryan and Delhaize, 2010; Horst et al., 2010). It has been well established that the Al-induced release of malate in wheat (*Triticum aestivum*) (Delhaize et al., 1993), citrate in maize, soybean (*Glycine max*) and common bean (Miyasaka etal., 1991; Kollmeier et al., 2001; Yang et al., 2000; Rangel et al., 2010), and oxalate in buckwheat (*Fagopyrum esculentum*) (Zheng et al., 1998). In common bean, Rangel et al. (2010) showed that the initial (0-4 h) genotype-independent Al injury was related to the absence of citrate exudation from the root tips in both genotypes (Quimbaya, Al-resistant; VAX-1, Al-sensitive) in spite of high amounts of citrate in the root apical tissues particularly in Quimbaya. Thereafter (5-9 h), in both genotypes recovery of root elongation was related to an Al-enhanced exudation of citrate typical for pattern-II type Al-induced release of organic acid anions (Ma et al., 2001).

The role of the metabolism of organic acids in Al resistance is still under debate. Most studies have shown no clear relationship between the root content and exudation of organic acid anions (Ryan et al., 2001). Ryan and Delhaize (2010) suggested that the convergent evolution of Al resistance in Al-excluder species mainly resulted from the mutation of transport proteins. However, some evidences indicate that the release of organic acid requires enhanced synthesis of organic acids to maintain the cytosolic pool. For example, in maize, Kollmeier and Horst (2001) showed that an Al-sensitive cultivar was not capable of maintaining the level of citrate in the root apical tissues in spite of a lower exudation rate. This was in agreement with Al-enhanced activities of enzymes involved in citrate synthesis such as malate dehydrogenase (MDH) and phosphoenolpyruvate carboxylase (PEPC) (but not citrate synthase (CS)) in the Al-resistant cultivar and of citrate degradation aconitase (ACO) in the Al-sensitive cultivar. Similarly, in common bean, Rangel et al. (2010) revealed that citrate release requires the activation or expression of an organic anion permease in the plasma membrane and is initially mainly derived from the internal organic acid pool. The sustained recovery from Al stress through citrated exudation in the Al-resistant genotype Quimbaya after 24 h Al treatment relied on restoring the internal citrate pool and a constitutively high activity of CS fuelled by high PEPC activity, while, in the Al-sensitive genotype VAX 1 the citrate exudation, and thus Al exclusion and root elongation, could not be maintained due to the exhaustion of the internal citrate pool and low CS and PEPC activities.

Genes encoding organic acid anion transporters in the plasma membrane belonging to two families, ALMT (Al-activated malate transporter) and MATE (multidrug and toxic compound extrusion) have been identified to mediate the exudation of organic acid anions from the root and thus Al resistance. The ALMT facilitate malate efflux in plant species that depend on malate exudation as the main Al resistance mechanism (Sasaki et al., 2004; Delhaize et al., 2004; Hoekenga et al., 2006; Ligaba et al., 2006), and the MATE proteins play a decisive role in Al-induced citrate exudation (Furukawa et al., 2007; Magalhaes et al., 2007; Ryan et al., 2009). However, these genes related to Al resistance, they may not fully explain the genotypic variation (Ryan et al., 2011), which may depend on the plant species. For example, in sorghum (*Sorghum bicolor*), *SbMATE* was expressed only in the root tips of the Al-resistant genotype in an Al-inducible way (Magalhaes et al., 2007). Similarly, in barley (*Hordeum vulgare*) *HvMATE* expression in the root apices correlated with Al-activated citrate exudation and Al resistance in a set of barley cultivars (Furukawa et al., 2007). However, in contrast to these plant species, studies in common bean showed,

that the *MATE* gene was highly expressed by Al within 4 hours of treatment in both an Al-resistant (Quimbaya) and an Al-sensitive (VAX 1) genotype. The expression of *MATE* was a prerequisite for citrate exudation, but the build-up of Al resistance within 24 h in Quimbaya exclusively depended on the capacity to sustain the synthesis of citrate for maintaining the cytosolic citrate pool that enabled continuous exudation (Eticha et al., 2010; Rangel et al., 2010).

The response of roots to drought

When plants are grown in drying soil, the growth of shoots is rapidly inhibited (Van Volkenburgh and Boyer, 1985; Chazen and Neumann, 1994) while in contrast, roots can still maintain elongation (Westgate and Boyer, 1985; Sharp et al., 1988). The differential response of roots and shoots to drought is considered an important feature of the adaptation of plants to water-deficit conditions since the maintenance of the root elongation facilitates water exploitation from deep soil (Sharp and Davis, 1989; Wu and Cosgrove, 2000; Sharp et al., 2004). It has been found that the elongation is maintained preferentially towards the root apex during water deficit (Sharp et al., 1988). Detailed studies indicate that root elongation was maintained in the apical 0-3 mm in maize (Liang et al., 1997; Spollen and Sharp, 1991) and 0-4 mm in soybean (Yamaguchi et al., 2010) under reduced water supply. It has been proposed that three potential mechanisms are involved in the maintenance of root elongation under low soil moisture conditions: (i) osmotic adjustment; (ii) modification of cell-wall extension; (iii) the accumulation of abscisic acid (ABA) (Sharp et al., 2004; Yamaguchi and Sharp, 2010).

The deposition of osmotica in the root tips appears most important to maintain the turgor of cells during limited water supply. It was reported that the rate of proline deposition increased dramatically along the root apex under drought conditions, and the resulting enhancement in proline accumulation was responsible for about 45% of the total osmotic adjustment (Voetberg and Sharp, 1991; Yamaguchi and Sharp, 2010). However, the role of other osmolytes such as the widely recognized cellular solutes sugars, amino acids, organic acids and inorganic ions (Morgan, 1984) for osmotic adjustment cannot be disregarded since dehydration resulting from osmotic stress increased sugar (fructose, glucose and sucrose) accumulation in the roots of mung bean (*Vigna mungo*) seedlings (Itoh et al., 1987).

Although the osmotic adjustment is a prerequisite for root elongation, it is insufficient to

maintain root growth under drought, since it additionally requires maintenance of CW extensibility (Sharp et al., 2004; Yamaguchi and Sharp, 2010). It appears that the modification of CW composition is important for the maintenance of CW structure and the avoidance of CW collapse during water loss from the apoplast. Since the water is the most abundant component of the CW making up about two thirds of the CW mass in growing tissues (Cosgrove, 1997), the loss of water from the CW matrix probably will result in serious disruption to polymer organization and consequently polymers will be brought in close proximity to each other, thus causing polymer adhesion or cross-linking (Moore et al., 2008). Cellulose microfibrils are the major tensile components of the wall and interact with the matrix components such as hemicellulose, pectin and structural proteins (Cosgrove, 2005). The interaction between the polymers endow the wall with strength or stiffness, whereas during the elongation the primary CW still allows the CW expansion, which can be modified by several CW-loosening enzymes such as expansin, XET and glucannase, or the synthesis and integration of new elements into the CW from the symplast (Wu and Cosgrove, 2000). Maize roots subjected to drought treatment have demonstrated that the CW of the apical 0-3 mm segments of root tips maintains a flexible state and thus allows elongation to continue (Wu and Cosgrove, 2000; Fan and Neumann, 2004), while the segments of 3-9 mm region of root apex remain inextensible leading to a cessation of further growth in this apical root section (Fan et al., 2006). The cessation of root growth in the basal region of the root apex is supposed to result from the accumulation of phenolics and lignin (Fan and Neumann, 2004). Usually the phenolics and lignin monomers can covalently cross-link the wall matrix via peroxidase and oxidase enzymes. The phenolic cross-links will tighten the wall structure, while lignin formation is accompanied by removal of water from the wall (Brett and Waldron, 1996; Moore et al., 2008). The apical walls increase in extensibility, and thus elongation has been shown to be related to the enhancement of expansin and XET activity (Wu et al., 1994; 1996). However, there is also evidence showing that drought did not affect the XET activity in the root tips region, when maize roots were exposed to polyethylene glycol (PEG)-simulated water deficit (Pritchard et al., 1993). Also a proteomic analysis of root apical CW proteins showed that water deficit even decreased the XET formation particularly in the apical 0-3 mm region of maize root apex (Zhu et al., 2007).

In addition, the accumulation of ABA in the root tips has been shown to be required for the maintenance of maize primary root elongation at low water potentials (Sharp et al., 2004). Using the ABA-deficient mutant *vp5* and a chemical inhibitor of ABA biosynthesis

to decrease endogenous ABA levels in seedlings growing at low water potentials, Sharp et al. (2004) reported that reduced ABA accumulation in maize primary roots was associated with more severe inhibition of root elongation. Under drought, ABA accumulated mainly towards the root apex (Saab et al., 1992) indicating that it was required for the maintenance of elongation in the distal elongation zone at low water potentials (Yamaguchi and Sharp, 2010). Several studies have clearly shown that ABA can suppress ethylene production, and the maintenance of root elongation under water deficit conditions requires increased ABA levels to prevent excess ethylene production (Sharp et al., 2000; Spollen et al., 2000; Sharp, 2002; LeNoble et al., 2004). Also it is suggested that ABA accumulation may play an important role in cellular protection from reactive oxygen species (ROS)-induced oxidative damage in drought-subjected roots of both maize and soybean (Yamaguchi and Sharp, 2010). Using the ABA-deficit mutant *vp14*, they found that the primary root elongation zone exhibits an enhanced cytosolic ROS level under drought conditions.

Common bean: An aluminium and drought-sensitive crop

Common bean (*Phaseolus vulgaris* L.) is the most important grain legume for direct human consumption worldwide, and it is a staple crop for small farmers and the urban poor in many Latin American and African countries. Total production exceeds 23 million metric tones, of which 7 million metric tones are produced in Latin America and Africa. It is also the second important source of protein (65% of all protein consumed) and the third most important caloric source (32% of all calories consumed) after cassava (*Manihot esculenta* Crantz) and maize (*Zea mays* L.) (Rao, 2001; Broughton et al., 2003). The higher production of beans can bring more profit for small farmers in less developed countries of Latin American and Africa. However, under field conditions, the production of common bean in the tropics is often limited by two major abiotic stresses, Al toxicity and drought (Thung and Rao, 1999; Singh, 2001; Ishitani et al., 2004). About 40% of the common bean-production areas in Latin America and 30 to 50% of central, eastern, and southern Africa are affected by Al phytotoxicity resulting in yield reduction from 30 to 60% (CIAT, 1992). And as much as 60% of the common bean production in the developing world occurs under conditions of drought stress (Graham and Ranalli, 1997; Beebe et al., 2008) and consequently leads to a low average global yield (< 900 kg ha^{-1}) of beans (Singh, 2001; Thung and Rao, 1999). Since the major phytotoxic site of Al is the root apex and the inhibition of root elongation is the primary symptom of Al toxicity (see above), the exploitation of the subsoil for water and thus the ability of the plants to withstand drought

stress may be strongly impeded by Al toxicity in acid subsoils (Goldman et al., 1989). Thus on acid soils that physically permit deep rooting both Al and drought resistance are required for yield improvement particularly in common bean, a generally Al and drought-sensitive crop (Rao, 2001; Beebe et al., 2008). Studies on these two combined growth and yield limiting factors are important and necessary to clarify the opportunities and constraints in breeding for adaptation to these abiotic stresses.

Based on the above information, the short-term effects of combined Al toxicity and drought on root growth with special emphasis on Al/drought interaction in the root apex was investigated at physiological and molecular level in the present study:

(i)   Physiological analysis of the interaction between Al toxicity and PEG-simulated drought stress in common bean grown in hydroponics (Chapter 1).

(ii)   Transcriptional analysis of the interaction between Al toxicity and PEG-simulated drought stress in common bean grown in hydroponics (Chapter 2).

(iii)   Proteomic analysis of the PEG-simulated drought stress in root tips of common bean grown in hydroponics (Chapter 3).

(iv)   Physiological and molecular analysis of the interaction between Al toxicity and drought stress in common bean under soil conditions (Chapter 4).

CHAPTER 1

Alteration of cell-wall porosity is involved in osmotic stress-induced enhancement of aluminium resistance in common bean (*Phaseolus vulgaris* L.)

Zhong-Bao Yang[1], Dejene Eticha[1], Idupulapati Madhusudana Rao[2], Walter Johannes Horst[1]

[1] Institute of Plant Nutrition, Leibniz Universität Hannover, Herrenhaeuser Str. 2, D-30419 Hannover, Germany

[2] International Center for Tropical Agriculture (CIAT), AA 6713, Cali, Colombia

Abstract

Aluminium (Al) toxicity and drought are the two major abiotic stress factors limiting common bean production in the tropics. Using hydroponics, we investigated short-term effects of combined Al toxicity and drought stress on root growth and Al uptake into the root apex. In the presence of Al stress, PEG 6000 (polyethylene glycol)-induced osmotic (drought) stress lead to amelioration of Al-induced inhibition of root elongation in the Al-sensitive genotype VAX 1. PEG 6000 ($\gg$ PEG 1000) treatment greatly decreased Al accumulation in the 1-cm root apices even when the roots were physically separated from the PEG solution using dialysis membrane-tubes. Upon removal of PEG from the treatment solution, the root tips recovered from osmotic stress and the Al accumulation capacity was quickly restored. The PEG-induced reduction of Al accumulation was not due to lower phyto-toxic Al concentration in the treatment solution, reduced negativity of the root apoplast, or enhanced citrate exudation. Also cell-wall (CW) material isolated from PEG-treated roots showed a low Al-binding capacity which, however, was restored after destroying the physical structure of the CW. The comparison of the Al^{3+}, La^{3+}, Sr^{2+}, and Rb^+ binding capacity of the intact root tips and the isolated CW revealed the specificity of the PEG 6000 effect for Al. This could be due to the higher hydrated ionic radius of Al^{3+} compared to other cations ($Al^{3+} \gg La^{3+} > Sr^{2+} > Rb^+$).

In conclusion, the results provide circumstantial evidence that the osmotic stress-inhibited Al accumulation in root apices and thus reduced Al-induced inhibition of root elongation in the Al-sensitive genotype VAX 1 is related to the alteration of CW porosity resulting from PEG 6000-induced dehydration of the root apoplast.

Keywords: aluminium, apoplast, drought stress, intercellular space, organic acids, polyethylene glycol, root elongation

Introduction

Soil acidity (pH < 5.5) is one of the important limitations to crop production worldwide. Acid soils make up approximately 30% of the world's total land area and more than 50% of the world's potentially arable lands, particularly in the tropics and subtropics (von Uexküll and Mutert, 1995; Kochian et al., 2004). When the pH drops below 5, aluminium (Al) is released into the soil solution and becomes the single most important factor limiting crop production on 67% of the total acid soil area (Eswaran et al., 1997).

Common bean (*Phaseolus vulgaris* L.) is the most important food legume for direct human consumption in the world, and it is a staple food crop for small farmers and the urban poor in many Latin American and African countries. It is also the second most important source of protein (65% of all protein consumed) and the third most important caloric source (32% of all calories consumed) after cassava (*Manihot esculenta* Crantz) and maize (*Zea mays* L.) (Rao, 2001; Broughton et al., 2003). Under field conditions, common bean often experiences different abiotic stresses including drought, toxicities of Al and manganese, low soil fertility, and high temperatures (Thung and Rao, 1999; Singh, 2001; Ishitani et al., 2004). Among these, Al toxicity and drought are the two major abiotic stresses for bean production in the tropics (Ishitani et al., 2004). About 40% of the common bean-production areas in Latin America and 30 to 50% of central, eastern, and southern Africa are affected by Al phytotoxicity resulting in yield reduction from 30 to 60% (CIAT, 1992).

The easily observable symptom of Al toxicity is a rapid (minutes to few hours) inhibition of root growth (Horst et al., 1992; Delhaize and Ryan, 1995), resulting in a reduced and damaged root system that limits mineral nutrient and water uptake (Kochian et al., 2004). Ryan *et al.* (1993) found that the root apex is the most Al-sensitive root zone, and Sivaguru and Horst (1998) identified the distal transition zone (DTZ) as the specific site of Al injury in maize. However, in common bean, Rangel et al. (2007) showed that both the transition zone (TZ, 1-2 mm) and elongation zone (EZ) are targets of Al injury. Aluminium resistance was related to a lower Al accumulation in the root tip (Shen et al., 2002; Rangel et al., 2007). Under short-term Al supply Al accumulates primarily in the root apoplast (Taylor et al., 2000; Wang et al., 2004; Rangel et al., 2009), where Al^{3+} strongly binds to the negatively charged binding sites (Zhang and Taylor, 1989; Blamey et al., 1990; Horst et al., 2010) provided by unmethylated pectin in the cell wall (CW) (Schmohl et al., 2000; Eticha et al., 2005). Thus, a lower CW negativity reducing Al

accumulation (Horst, 1995) and the detoxification of Al in the apoplast through root exudates play an important role in Al resistance. Lower Al accumulation in the root tips and thus Al resistance is mediated by citrate exudation in common bean (Mugai et al., 2000; Shen et al., 2002; Rangel et al., 2010).

Drought stress is another important limiting factor for common bean production in the developing world, since as much as 60% of the common bean production occurs under conditions of drought stress (Graham and Ranalli, 1997; Beebe et al., 2008). Particularly on many acid soils, dry spells during the main growing period of crops are a major yield-limiting factor (Welcker et al., 2005). Adaptation to drought involves complex multigenic components that interact holistically in plant systems (Cushman and Bohnert, 2000). In plants growing in dry soil, both shoot and root growth is hampered (Westgate and Boyer, 1985; Sharp et al., 1988). The maintenance of root growth during water deficit facilitates water uptake from the subsoil (Sponchiado et al., 1989; Serraj and Sinclair, 2002). However, the exploitation of the subsoil for water and thus the ability of the plants to withstand drought stress may be strongly impeded by Al toxicity in acid subsoils (Goldman et al., 1989). Thus on acid soils that permit deep rooting both Al and drought resistance are required for yield improvement particularly in common bean, a generally Al and drought-sensitive crop (Rao, 2001; Beebe et al., 2008). Therefore, studies on individual and combined stress factors of these two limitations are important to clarify the opportunities and constraints in breeding for adaptation to these abiotic stresses.

In light of the importance of root development under conditions of Al toxicity and drought, short-term effects of combined Al toxicity and drought stress on root growth with special emphasis on Al/drought interaction in the root apex was investigated in the present study in hydroponics which allow a detailed study of Al toxicity. Drought stress was imposed through the application of polyethylene glycol (PEG). PEG 6000 is a high molecular weight solute, which cannot enter the apoplastic space (Carpita et al., 1979, Hohl and Schopfer, 1991). It thus is being amply used as a non-absorbed osmoticum to induce osmotic stress and allows to mimic the response of plants to drought stress in hydroponic studies (Jia et al., 2001; Fan and Neumann, 2004).

Materials and Methods

Plant materials and growing conditions

Seeds of the four common bean genotypes, Quimbaya, G 21212, BAT 477 and VAX 1 were germinated in filter paper sandwiched between sponges. After three to four days, uniform seedlings were transferred to a continuously aerated simplified nutrient solution containing 5 mM $CaCl_2$, 1 mM KCl and 8 μM H_3BO_3 (Rangel et al., 2007). Plants were cultured in a growth chamber under controlled environmental conditions of a 16/8 h light/dark cycle, 27/25 °C day/night temperature, 70% relative air humidity, and a photon flux density of 230 μmol m^{-2} s^{-1} of photosynthetically active radiation at plant height. The pH of the nutrient solution was gradually lowered to 4.5 within two days. Then the plants were transferred to treatment solutions containing a factorial combination of Al (0, 25 μM) and PEG 6000 (Sigma-Aldrich Chemie GmbH, Steinheim, Germany) (0, 200 g L^{-1}) for 24 h in the simplified nutrient solution, pH 4.5. At harvest, the culture solutions were collected and filtered immediately through 0.025 μm nitrocellulose membranes. Mononuclear Al (Al_{mono}) concentrations were measured colorimetrically using the pyrocatechol violet method (PCV) according to Kerven et al. (1989). The Al_{mono} concentration of the Al treatment solution was kept at 25 μM by adding Al stock solution when necessary to prevent a decrease of the Al_{mono} concentration in the solution owing to the Al absorption by the roots. There was no difference between the PEG treatments (data not shown), suggesting that PEG supply did not lead to precipitation or complexation of Al in the treatment solution.

If not otherwise mentioned PEG 6000 (PEG) was used. In some experiments different PEG 6000 concentrations were used. The corresponding osmotic potentials (OPs) of the 0, 50, 100, 150, 200 and 250 g L^{-1} PEG 6000 solutions were 0.00, -0.06, -0.24, -0.60, -1.20 and -2.10 MPa, respectively, measured with a cryoscopic osmometer (Osmomat 030, Gonotec GmbH, Berlin, Germany).

Dialysis membrane-tubes (DMTs) (3,500 Dalton MWCO, Spectra/Por, California, USA) were used to separate the roots from the PEG 6000 solution. After 2 days of acclimation, plants were transferred into DMTs, and then the DMTs were transferred into 200 g L^{-1} PEG treatment solution and kept in an upright position in solution for 8 h, then the DMTs were transferred to 100 μM Al treatment solution without or with 200 g L^{-1} PEG for 1 h. In parallel, experiments without DMT were conducted for comparison. The PEG and Al

concentrations in the parallel experiments were 150 g L^{-1} and 25 µM, respectively. When treating the plants in the DMTs with 200 g L^{-1} PEG and 100 µM Al, inhibition of root elongation and Al contents were comparable to the treatment of the plants without DMTs at 150 g L^{-1} PEG and 25 µM Al, respectively (data not shown). Thus different concentrations of Al and PEG were used in the different growing systems.

Diffusion of low molecular weight (LMW) PEG through DMTs and the effect of LMW PEG on root growth and Al accumulation in the root apex

Two hundred fifty ml PEG 6000 (200 g L^{-1}) solution in DMTs was incubated in 1.0, 1.5, and 2.0 L distilled water for 4 h. During this period, the external solution was stirred gently and subsamples were collected in 15 min interval. In these samples the OP was determined with a cryoscopic osmometer either directly or after concentrating ten times with a rotational-vacuum-concentrator RVC 2-25 (Martin Christ Gefriertrocknungsanlagen GmbH, Osterode/Harz, Germany).

To compare the effect of different molecular weight PEG on root growth and Al accumulation in root apices, plants were pre-treated with PEG 1000, 3000 and 6000 (Sigma-Aldrich Chemie GmbH, Steinheim, Germany) at different OPs (0, -0.06, -0.24, -0.60 MPa) for 8 h in simplified nutrient solution, pH 4.5. Then half of the plants were harvested for the determination of root elongation. The remaining plants were continued to grow for 1 h in the same solutions in the presence of 25 µM Al, pH 4.5. After the Al treatment 1-cm root tips were excised for Al analysis.

Measurement of root-elongation rate

Two hours before the treatment was initiated tap roots were marked three centimetres behind the root tip using a fine point permanent marker (Sharpie blue, Stanford) which did not affect root growth during the experimental period. Afterwards, the plants were transferred into a simplified nutrient solution (see above) without or with PEG in the absence or presence of 25 µM Al. Root elongation was measured after the treatment period using a mm scale.

Collection of root exudates and determination of organic acids in exudates and root apices

To collect root exudates from root apices, plants were pre-treated with 0 or 25 µM Al in the

absence or presence of 150 g L^{-1} PEG for 3, 7 and 23 h, then ten plants were bundled in filter paper soaked with nutrient solution. Approximately 1 cm of the main root apex of each plant was immersed into 15 mL of a constantly aerated incubation solution containing 5 mM CaCl$_2$, 1 mM KCl, 8 μM H$_3$BO$_3$, and 0 or 40 μM AlCl$_3$, pH 4.5. During this treatment process, the basal part of the root system was constantly moistened with incubation solution (see above) to prevent dryness but avoiding dripping into the columns. After 2 h, the incubation solution containing the root exudates were immediately frozen at -20 ℃. After thawing, the incubation solution was passed through 5 g of a cation-exchange resin (AG50W-X8 with a 75 – 150 μm mesh) in 20 mL poly-prep columns with a 200 – 400 μm mesh filter at the bottom of the column, at a flow rate of 1 mL min^{-1}. The resulting solution containing the organic acids (OA) was concentrated to dryness in a rotary vacuum evaporator (RCT 10-22T, Jouan, Saint-Herblain, France). The residue from each sample was re-dissolved in 500 μL (10 mM) perchloric acid, sonicated for 15 min, filled into micro filtration tubes with a membrane pore size of 0.45 μm (GHP Nanosep MF Centrifugal Device, Pall Life Sciences, Ann Arbor, USA), and filtered by centrifugation at 20,000 g for 25 sec. The filtered samples were immediately used for measurement or frozen.

The OA content of root tips was determined by the modified method of de la Fuente *et al.* (1997). Plants were treated with 0 or 25 μM Al in the absence or presence of 150 g L^{-1} PEG for 4, 8 and 24 h, then the root tips (1-cm) were excised and frozen immediately in liquid nitrogen. Before thawing, 400 μL of cold 70 % (v/v) ethanol was added to the samples which were then homogenized in a micro-homogenizer (MM200 Retsch, Haan, Germany) for 3 min at 20 cycles sec^{-1}. OAs were extracted at 75 ℃ for 1 h with intermittent shaking on a vortex every 15 min. Thereafter, the samples were centrifuged at 23,000 *g* for 10 min and the supernatant was transferred into a new Eppendorf tube. The supernatant was concentrated to dryness in a rotary vacuum evaporator. The concentrated residue from each sample was re-dissolved in 200 μL 10 mM perchloric acid, sonicated for 15 min, transferred to centrifugal micro filtration tubes with a membrane pore size of 0.45 μm, and centrifuged at a speed of 20,000 *g* for 25 sec. The samples were immediately used for measurement or frozen.

The concentrations of OAs in the root exudates as well as in the extracts of root tissue were measured by isocratic High Pressure Liquid Chromatography (HPLC, Kroma System 3000, Kontron Instruments, Munich, Germany). The OAs were detected through a 20 μL loop-injector (Auto-sampler 360) of the HPLC, separating different OAs on an Animex

HPX-87H (300 x 7.8 mm) column (BioRad, Laboratories, Richmond, California, USA), supplemented with a cation H^+ micro-guard cartridge, using 10 mM perchloric acid as eluent at a flow rate of 0.5 mL per minute, at a constant temperature of 35 ℃ (Oven 480), and with a pressure of 7.4 kPa. Measurements were performed at $\lambda = 214$ nm (UV Detector 320).

Freeze-fracture scanning electron microscopy

The effect of PEG on the structure of the root tips was studied at the Research Centre of Bayer CropSciences at Monheim, Rhein, Germany, in cooperation with P. Baur and S. Teitscheid. After treating the plant with PEG 6000 and PEG1000 (-0.60 MPa OP) for 4 h, root tips (1 - 5 mm from the root apex) were excised and placed onto a specimen holder, then shock frozen with liquid nitrogen. Frozen specimens were transferred to a pre-cooled (–150 ℃) specimen stage in a vacuum-cryo-shuttle into the preparation-chamber, fractured with knife and etched (sublimated) in the specimen-chamber for 10 min at –100 ℃ under 10^{-4} mbar to remove surface ice. The structure of root-tip cross-sections was examined using a scanning electron microscope (SEM, JSM-5600 LV, Jeol, Tokyo, Japan) after gold sputtering.

Isolation of cell-wall material

After pre-treating with PEG (0 – 200 g L^{-1}) for 24 h, thirty root tips of 1-cm length were excised and transferred to 1 mL of 96% ethanol (method A) or immediately frozen in liquid nitrogen and then ground to fine powder with mortar and pestle in liquid nitrogen before 1 ml of 96% ethanol was added (method B). Cell-wall material was prepared as alcohol-insoluble residue after repeated washing with ethanol, modified after Schmohl and Horst (2000). Root samples were thoroughly homogenized in ethanol using a mixer mill at a 30 cycles s^{-1} for 2 min. The homogenization was repeated two times. Then the samples were centrifuged at 23,000 *g* for 15 min and the supernatant was discarded. One millilitre of 96% ethanol was added and the pellet was re-suspended. The washing procedure was repeated twice. The remaining CW material was dried using a centrifugal evaporator (RC10-22T, Jouan SA, France), weighed, and stored at 4 ℃ for further use.

Determination of pectin and its degree of methylation

The dried cell-wall material isolated from 1-cm root tips was weighed, hydrolysed according to Ahmed and Labavitch (1977) extending the incubation time to 10 min in

concentrated H_2SO_4 and 2 h after each step of water addition. The uronic acid content was determined colorimetrically according to Blumenkrantz and Asboe-Hansen (1973) using a microplate spectrophotometer (μQuant[TM]; Bio-Tek Instruments, Winooski, VT, USA). Galacturonic acid was used as a calibration standard; thus the root pectin content was expressed as galacturonic acid equivalent (GaE).

For the determination of the degree of methylation (DM), the cell-wall material from root apices was prepared in the same way as for pectin determination. Methanol was released from the cell-wall material by saponification according to Fry (1988), modified after Wojciechowski and Fall (1996). After addition of 2 units of alcohol oxidase (EC 1.1.3.13 from *Piccia pastoris*; Sigma, Deisenhofen, Germany) the complex of formaldehyde with Fluoral-P (15 mg mL^{-1}) (Molecular Probes, Leiden, The Netherlands) was measured fluorometrically (excitation $\lambda = 405$ nm, emission $\lambda = 503$ nm). The degree of methylation (%) was calculated as the molar ratio of methanol/uronic acid $\times 100$.

Cell-wall binding-capacity and uptake of Al^{3+}, La^{3+}, Sr^{2+}, Rb^{2+} in 1-cm root apices

The isolated cell-wall material from 30 root tips (approximately 3 mg) was incubated for 30 min in 1 mL of a solution (pH 4.3) containing 300 μM $AlCl_3$ or 300 μM $LaCl_3$, 450 μM $SrCl_2$ or 900 μM RbCl without or with 150 g L^{-1} PEG. Then the suspension was centrifuged at 23,000 *g* for 10 min. The supernatant was discarded. The pellet was re-suspended in one ml of ultra-pure deionized water and centrifuged again. The procedure was repeated twice. Then the residues were prepared for Al, La, Sr and Rb determination.

To study the effect of PEG on the accumulation of La^{3+}, Sr^{2+} and Rb^+ in the root apices, intact plants were pre-treated with the simplified nutrient solution and 0 or 50, 100, 150, 200 g L^{-1} PEG (pH 4.5) for 8 h. Then the plants were treated with 25 μM $AlCl_3$, 5 μM $LaCl_3$, 2.5 mM $SrCl_2$, or 0.5 mM RbCl minus or plus 150 g L^{-1} PEG in the same nutrient solution for 1 h, pH 4.5.

Determination of Al, La, Sr, and Rb

For the determination of Al, La, Sr, and Rb, 1-cm root tips or cell-wall material were digested in 500 μL ultra-pure HNO_3 (65%, v/v) by overnight shaking on a rotary shaker. The digestion was completed by heating the samples in a water bath at 80 °C for 20 min. Then 1.5 mL ultra-pure deionised water was added after cooling the samples in an ice-water bath. Aluminium was measured with a Unicam 939 QZ graphite furnace atomic

absorption spectrophotometer (GFAAS; Analytical Technologies Inc., Cambridge, UK) at a wavelength of 308.2 nm after appropriate dilution, and an injection volume of 20 μL. La, Sr, and Rb were measured by inductively coupled plasma mass spectroscopy (ICP-MS) (7500cx, Agilent Technology, Santa Clara, California, USA) after appropriate dilution.

Statistics analysis

A completely randomized design was used, with four to twelve replicates in each experiment. Statistical analysis was carried out using SAS 9.2. Means were compared using t or Tukey test depending on the number of treatments being compared. *, **, *** and ns denote significant differences at $P < 0.05$, 0.01, 0.001, and not significant, respectively.

Results

Four common bean genotypes differing in Al resistance were selected to investigate the relationship between Al toxicity and drought stress. The genotypes responded to Al treatment as previously reported, with Quimbaya as most Al-resistant and VAX 1 as most Al-sensitive (Fig. 1A; Rangel et al., 2005). PEG treatment led to severe osmotic stress and thus inhibition of root growth. Although the comparison of means did not show significant differences between genotypes in response to PEG, the ANOVA showed a highly significant genotype*Al interaction with genotype Quimbaya showing the highest and BAT 477 the lowest root growth in presence of PEG. Combined Al and PEG stress did not lead to further root-growth inhibition. On the contrary, PEG in addition to Al stress enhanced root growth compared to Al stress alone (highly significant PEG*Al interaction) particularly in genotype VAX 1 (highly significant genotype*PEG*Al interaction). The lack of Al-induced inhibition of root elongation and even the positive effect of PEG on root growth in presence of Al can be explained by a strongly reduced Al accumulation in the root tips (Fig. 1B).

Since among the tested genotypes the PEG-improved root growth in presence of Al was most marked in VAX 1, the study was continued with this genotype only. The lower Al accumulation in the root apices of PEG-stressed plants could be due to an enhanced synthesis and exudation of organic acids because citrate exudation has been reported as one of the most important mechanisms of Al resistance in common bean. Therefore, the contents and the exudation rates of organic acids were determined after 4, 8, and 24 h of PEG and Al treatment in order to take into account the adaptations to Al (Rangel et al., 2007) and PEG (data not shown) over the treatment period.

Whereas Al treatment decreased the contents of most organic acids with increasing treatment duration, PEG treatment/drought stress strongly enhanced OA contents in the root tissue, particularly of citrate and malate independent of the Al treatment (Fig. 2). Since organic acids could not be analyzed in the presence of PEG and PEG could not be satisfactorily separated from the solution, organic acid anion exudation had to be determined during a two hour period without PEG (but with Al) supply after the corresponding PEG pre-treatment. After removing of PEG from the treatment solution, the amount of organic acid in 1-cm root apical tissues did not change during the subsequent 2 h exudate collection-period and confirmed the organic acid contents (data not shown). Only malate, but not citrate exudation was affected by PEG treatment (Fig. 3). On the other

hand, Al significantly enhanced citrate exudation independent of the PEG pre-treatment up to 9 h treatment (Fig. 3).
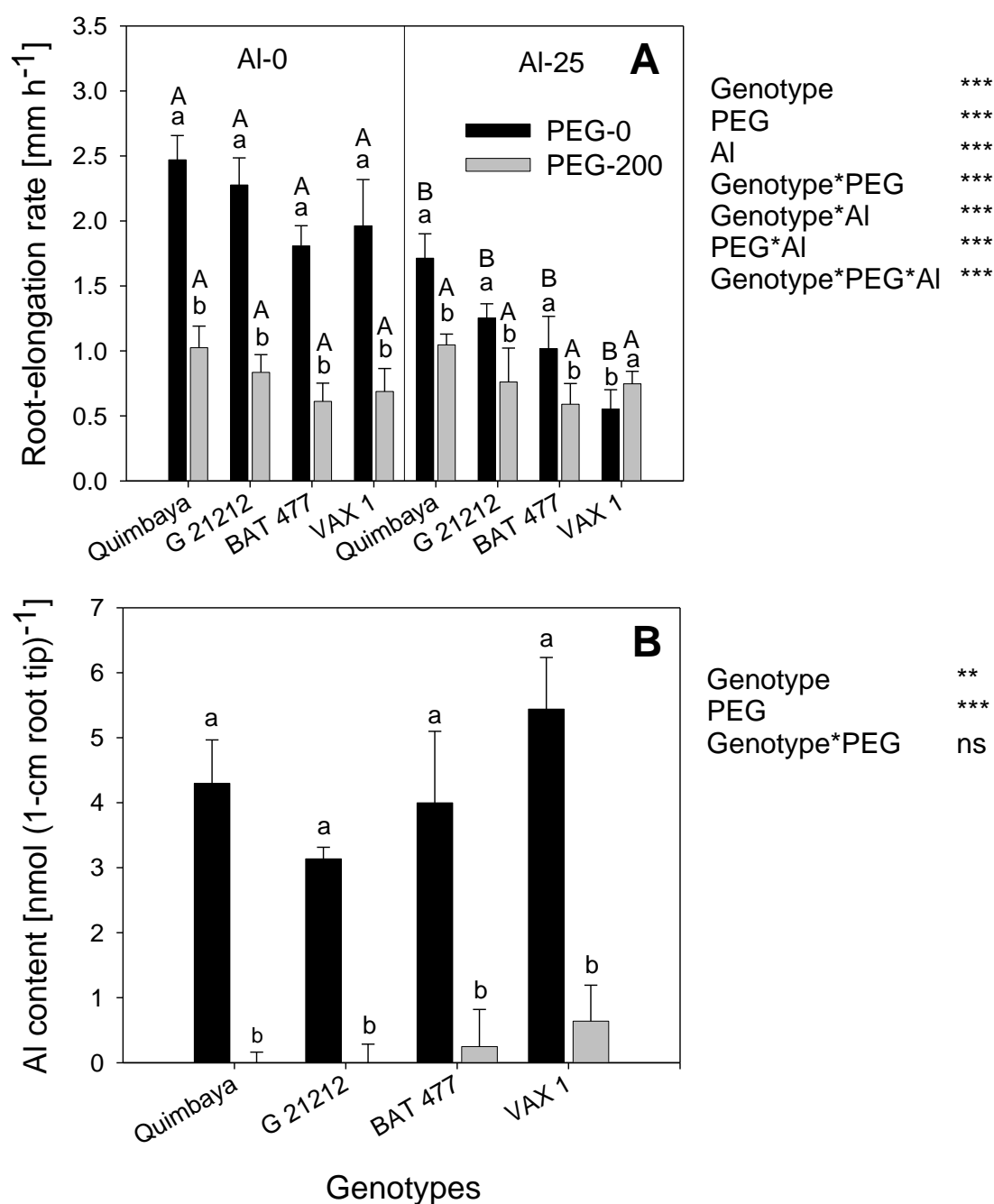
Figure 1 Root-elongation rate (A) and Al content of 1-cm root tips (B) of four common bean genotypes under osmotic (200 g L^{-1} PEG) and Al stress (25 μM Al). Plants were pre-cultured in a simplified nutrient solution containing 5 mM CaCl$_2$, 1 mM KCl, and 8 μM H$_3$BO$_3$ for 48 h for acclimation and pH adaptation, then treated without or with 25 μM Al in the absence or presence of 200 g L^{-1} PEG in the simplified nutrient solution for 24 h, pH 4.5. Bars represent means $\pm$ SD, n = 12 for (A) and n = 4 for (B). Means with the same small letter and capital letter are not significantly different at $P < 0.05$ (t test) for the comparison of PEG treatments within Al supplies and comparison of Al treatments within PEG supplies, respectively. For the ANOVA, **, *** denote significant differences at $P < 0.01$, $P < 0.001$, respectively; ns = not significant.
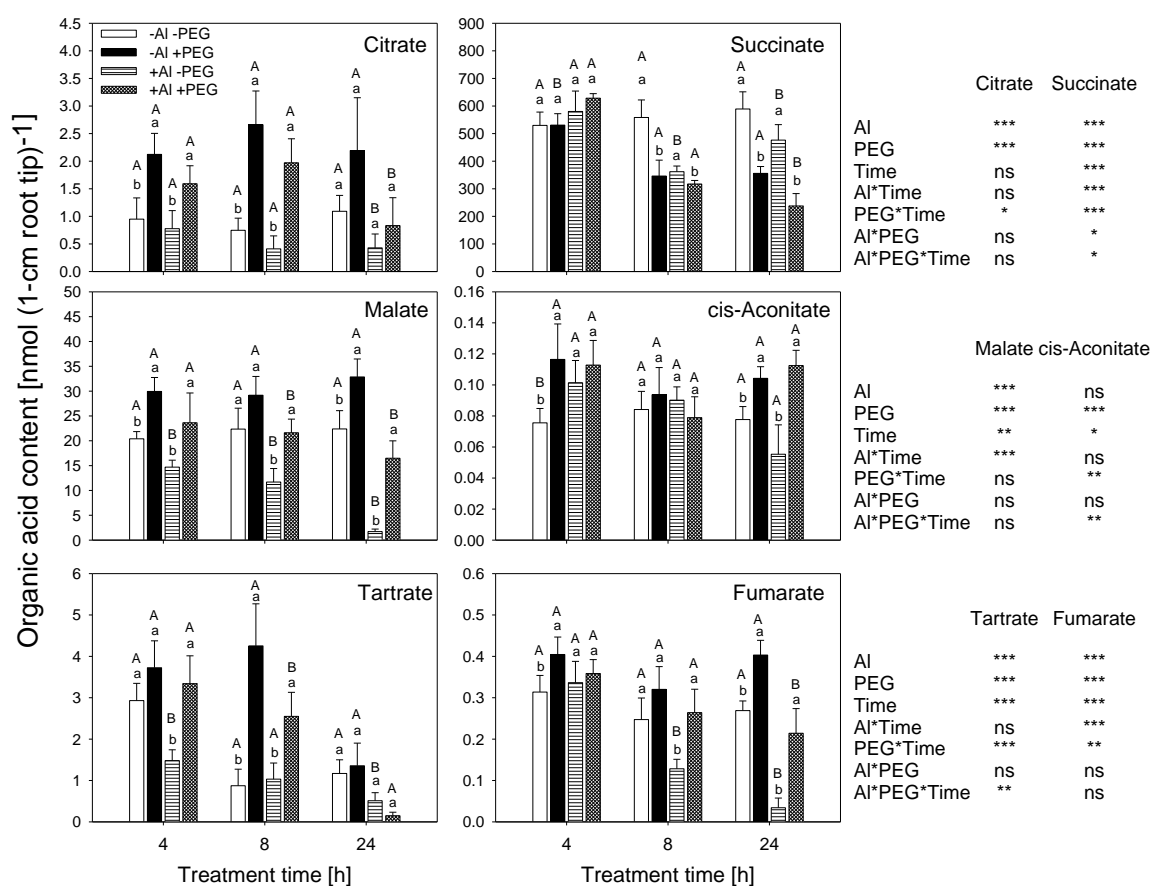
Figure 2 Organic acid contents in 1-cm apical roots of common bean genotype VAX 1 (Al-sensitive) affected by osmotic stress and Al supply. Plants were pre-cultured in a simplified nutrient solution containing 5 mM $CaCl_2$, 1 mM KCl, and 8 μM H_3BO_3 for 48 h for acclimation and pH adaptation, then treated without or with Al (25 μM) in the absence or presence of PEG (150 g L^{-1}) in the simplified nutrient solution for 4, 8 and 24 h, pH 4.5. Bars represent means $\pm$ SD, n = 4. Means with the same small letter and capital letter are not significantly different at $P < 0.05$ (t test) for the comparison of PEG treatments within Al supplies and comparison of Al treatments within PEG supplies, respectively. For the ANOVA, *, **, *** denote significant differences at $P < 0.05$, $P < 0.01$, $P < 0.001$, respectively; ns = not significant (F test).

Another reason for the impeded Al accumulation in the root apices could be a lower negativity of the CWs formed in the presence of PEG. The cell-wall pectin-content and its degree of methylation determine the Al binding capacity of the root cell-wall (Schmohl and Horst, 2000). PEG treatment reduced total CW pectin content but also decreased the degree of methylation of pectin in 1-cm root tips. Thus the content of unmethylated pectin representing the negativity of the CWs remained unaffected by the PEG treatment (Fig. 4).
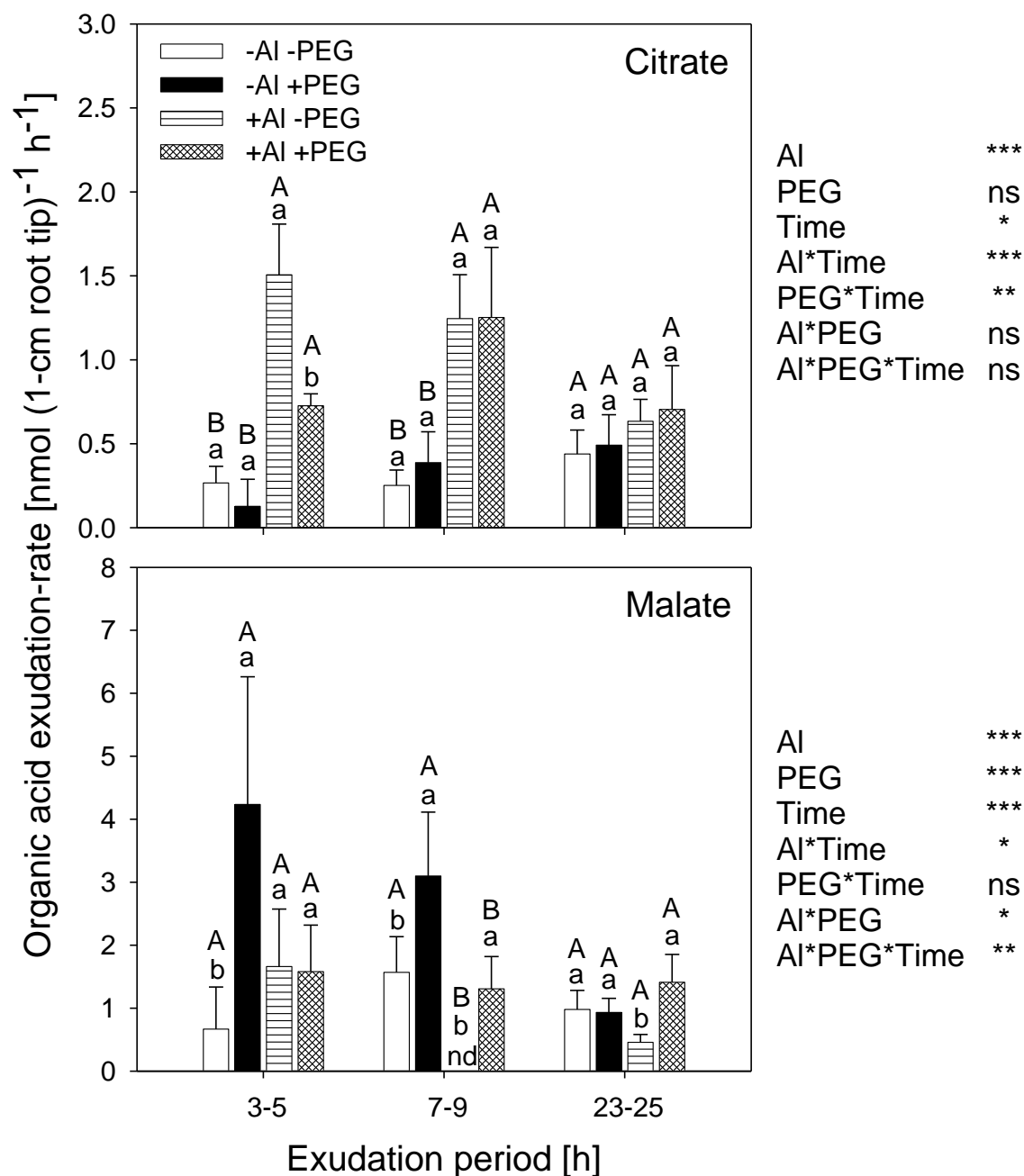
Figure 3 Effect of PEG and Al treatment on organic acid exudation from 1-cm root apices of Al-sensitive common bean genotype (VAX 1). Plants were pre-cultured in a simplified nutrient solution containing 5 mM $CaCl_2$, 1 mM KCl, and 8 μM H_3BO_3 for 48 h for acclimation and pH adaptation and then treated without or with Al (25 μM) in the absence or presence of PEG (150 g L^{-1}) for 3, 7 and 23 h. Thereafter, the roots of 10 plants were bundled and the root tips (1 cm) were incubated in 15 mL of Al (0, 40 μM) treatment solution containing the above simplified nutrient solution without PEG for 2 h. Bars represent means ± SD, n = 4. Means with the same small letter and capital letter are not significantly different at $P < 0.05$ (t test) for the comparison of PEG treatments within Al supplies and comparison of Al treatments within PEG supplies, respectively. For the ANOVA, *, **, *** denote significant differences at $P < 0.05$, $P < 0.01$, $P < 0.001$, respectively; ns = not significant (F test). nd = not detected.
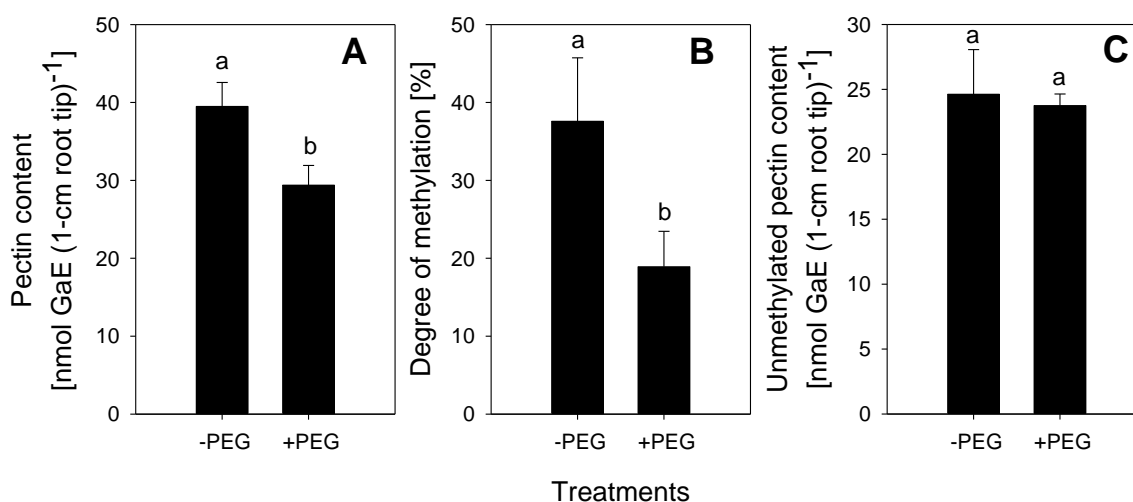
Figure 4 Total cell-wall pectin-content (A), its degree of methylation (B) and unmethylated pectin content (C) in 1-cm root tips of Al-sensitive common bean genotype (VAX 1). Plants were pre-treated without or with 150 g L^{-1} PEG in a simplified solution (pH 4.5) containing 5 mM $CaCl_2$, 1 mM KCl and 8 µM H_3BO_3 for 24 h, then 30 root tips (1-cm) were harvested and cell-wall material was isolated according to Method A described in materials and methods for determination of pectin content and degree of methylation. Bars represent means ± SD, n = 4. Means with the same letters are not significantly different at $P < 0.05$ (t test).

In order to differentiate between a direct effect of PEG accumulation on/in the root and of PEG-induced osmotic stress on Al accumulation in the roots, the roots were enclosed in a DMT, which has a molecular weight cut off (MWCO) of 3,500 Dalton and does not allow PEG 6000 to cross the membrane. Thus, the direct contact of PEG with the root was prevented while maintaining the osmotic stress. Higher PEG and Al concentrations were used with rather than without DMT according to preliminary experiments to compensate for impeded PEG and Al diffusion through the DMT (data not shown). As shown above, presence of PEG during the Al treatment period of 1 h reduced the Al accumulation in the root tips to low levels even in plants not exposed to PEG during the 8 h pre-treatment period (-/+ PEG) (Fig. 5A). Discontinuing the PEG treatment during the 1 h Al treatment period after 8 h PEG pre-treatment (+/- PEG) completely restored the Al accumulation capacity of the root apices. This recovery is a very rapid process since as early as 15 min after interrupting the PEG treatment the difference in Al accumulation between PEG-treated and untreated plants disappeared (Fig. 5C). When the roots were protected against direct contact with PEG using DMT (Fig. 5B) Al accumulation by the roots was similarly reduced when osmotic stress was applied during the 1 h Al uptake period. However, when the osmotic stress was discontinued during the Al uptake period (+/- PEG) the Al uptake capacity was not fully restored as to the level observed without DMT. This

suggests a slower recovery from osmotic stress in the dialysis tubes.
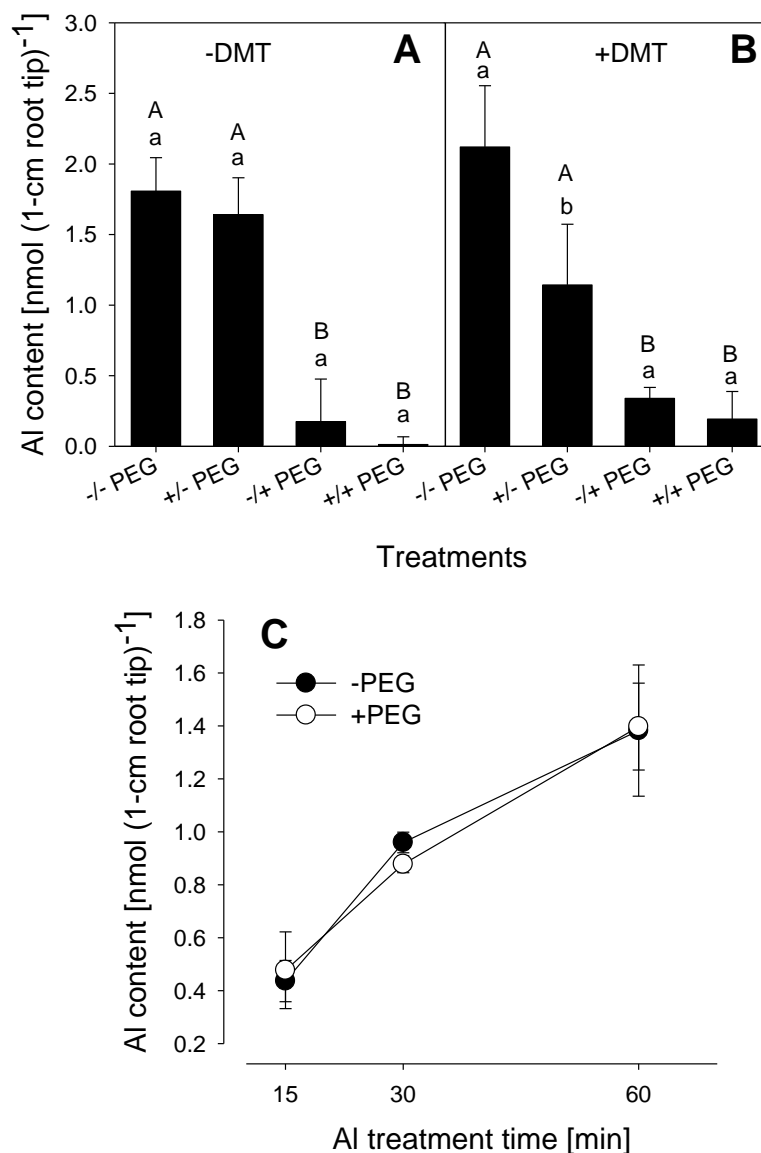
Figure 5 Al content in 1-cm root tips of Al-sensitive common bean genotype (VAX 1). (A) Without dialysis membrane tubes (DMT); plants were pre-treated without or with 150 g L^{-1} PEG solution for 8 h, and then treated with 25 μM Al in the absence or presence of 150 g L^{-1} PEG solution for 1 h. (B) With DMT; plants were pre-treated without or with 200 g L^{-1} PEG for 8 h, then treated with 100 μM Al in the absence or presence of 200 g L^{-1} PEG solution for 1 h. (C) Without DMT; plants were pre-treated without or with 150 g L^{-1} PEG solution for 8 h, and then treated with 25 μM Al solution for 15, 30 and 60 min. The background solution of the above treatment solution was the simplified solution containing 5 mM $CaCl_2$, 1 mM KCl, and 8 μM H_3BO_3, pH 4.5. -/- PEG: without PEG during pre-treatment and Al treatment; +/- PEG: with PEG during pre-treatment, without PEG during Al treatment; -/+ PEG: without PEG during pre-treatment, with PEG during Al treatment; +/+ PEG: with PEG during pre-treatment and Al treatment. Bars represent means ± SD, n = 4. Means with the same small letter and capital letter are not significantly different at $P < 0.05$ (t test) for the comparison of PEG pre-treatments within PEG re-treatments and comparison of PEG re-treatments within PEG pre-treatments, respectively.

Since the presence and thus penetration of the DMT by LMW PEG in PEG 6000 cannot be excluded we studied the OP as an indirect measure of the presence of LMW PEG in the solution passing through the DMT in a model experiment in which the PEG 6000-filled DMT was incubated for 4 hours. There was only a slight decrease of the OP which was only significant in the ten times concentrated incubation solution (Fig. S1). Even then the OP did not decrease beyond -0.06 MPa which did not affect root growth (Fig. 6A). This suggests that there is only a low amount of LMW PEG in the PEG 6000 product used for our experiments.

To clarify how LMW PEG affect Al accumulation in the root apex, the effect of PEG 6000, PEG 3000, and PEG 1000 on Al contents in the root tips was compared at the same OPs corresponding to PEG 6000 concentrations of 0, 50, 100, 150 g L^{-1}. The root elongation rate was decreased with decreasing OP independent of the molecular weight of the PEG (Fig. 6A). However, PEG 6000 reduced the Al contents of the root tips much more efficiently than PEG 3000 and particularly PEG 1000 (Fig. 6B).

The effect of different molecular weight PEG on the root-tip structure has been studied using freeze-fracture electron microscopy. The resolution of the technique did not allow to draw any conclusion about the cell wall structure. However, the root cross-sections shown in Fig. S2 clearly showed that in spite of comparable osmotic stress induced by the different molecular weight PEG (compare Fig. 6A) the effects on the root structure were different. In roots exposed to PEG 6000 (Fig. S2C, F) the epidermis and the outer cortical cell layers were very closely packed and nearly all intercellular spaces disappeared. In contrast, PEG 1000 (Fig. S2B, E) did hardly affect the intercellular space compared to the control (Fig. S2A, D) indicating that in addition to osmotic stress PEG 6000 dehydrates the root apoplast more than PEG 1000.

The specificity of the PEG 6000 effect on Al uptake into the root apex was evaluated using La, Sr and Rb uptake for comparison (Fig. 7). PEG pre-treatment did not affect La uptake, while PEG applied together with La slightly but significantly decreased La accumulation (Fig. 7A). In contrast, neither PEG pre-treatment (+/- PEG) nor re-supply of PEG (-/+ PEG) during the Sr uptake period affected Sr (as a tracer of Ca) accumulation in the root apices (Fig. 7B). However Rb (as a tracer of K) accumulation was reduced by PEG pre-treatment (+/- PEG) and PEG application (-/+ PEG) during the Rb exposure period (Fig. 7C), which might be explained by a significant increase of the K content in the root tips (from 212 to 342 nmol root-tip^{-1}, data not shown) caused by osmotic stress.
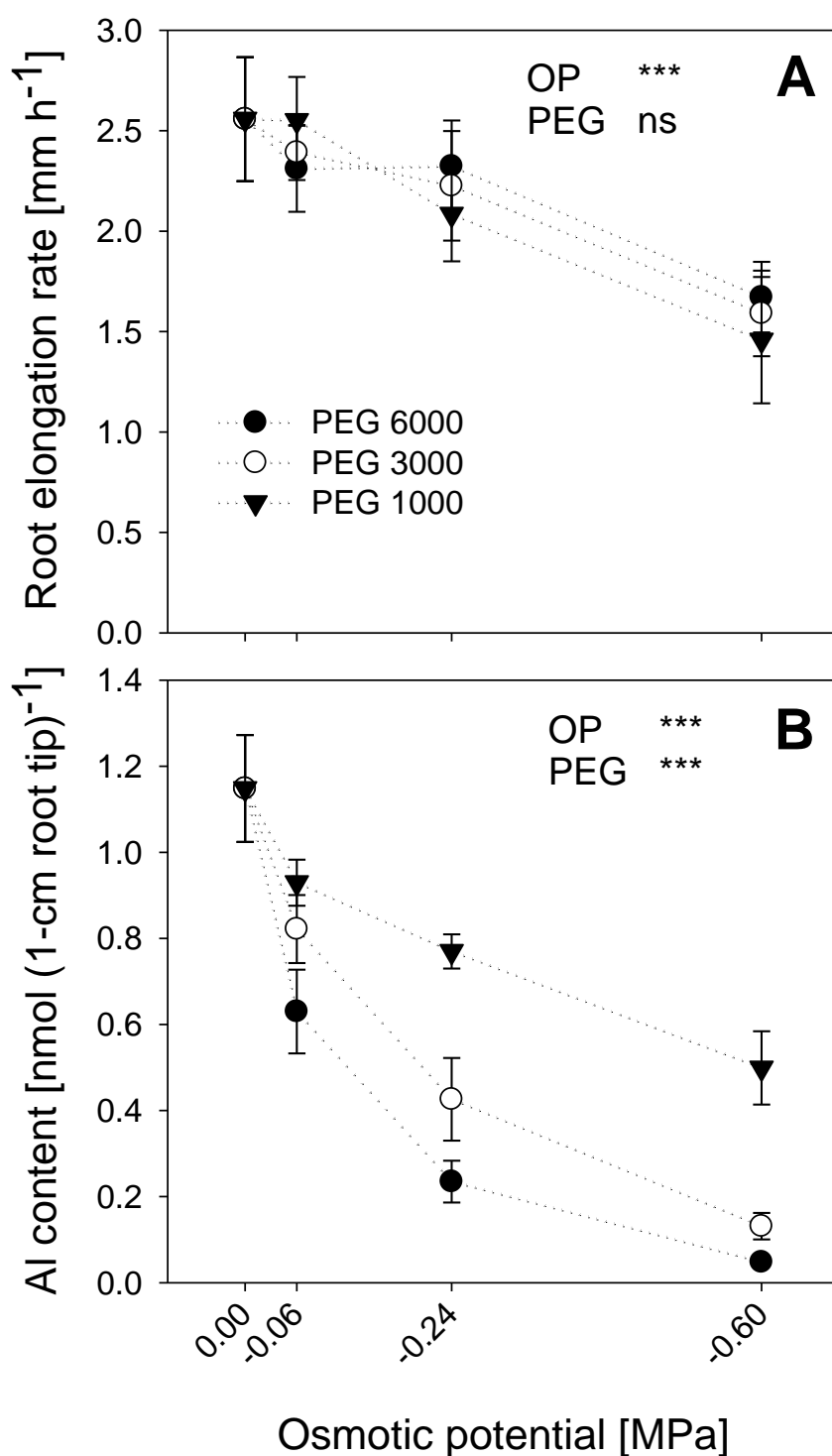
Figure 6 Effect of different molecular weight PEGs on root growth and Al accumulation in root tips of Al-sensitive common bean genotype (VAX 1). (A) Plants were pre-treated with different molecular weight PEGs at different osmotic potentials for 8 h. (B) Plants were pre-treated with different molecular weight PEGs at different osmotic potentials for 8 h, and then treated with 25 μM Al for 1 h in the presence of different molecular weight PEGs for 1 h. The background solution of the above treatment solution was the simplified solution containing 5 mM $CaCl_2$, 1 mM KCl, and 8 μM H_3BO_3, pH 4.5. Bars represent means ± SD, n = 4. For the ANOVA, *** denote significant differences at $P < 0.001$; ns = not significant (F test).
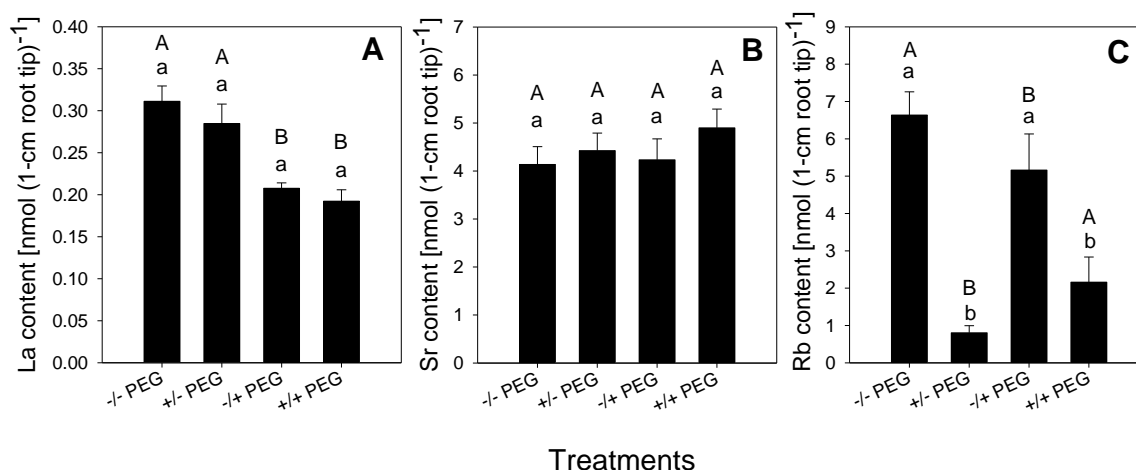
Figure 7 Effect of PEG pre-treatment/treatment on La (A), Sr (B) and Rb (C) accumulation of 1-cm root tips in Al-sensitive common bean genotype (VAX 1). Plants were pre-treated without (- PEG) or with 150 g L^{-1} PEG (+ PEG) in a simplified solution (pH 4.5) containing 5 mM CaCl$_2$, 1 mM KCl and 8 μM H$_3$BO$_3$ for 8 h. Then the plants were supplied with 5 μM LaCl$_3$, 2.5 mM SrCl$_2$ or 0.5 mM RbCl in absence (-/-, +/- PEG) or presence of 150 g L^{-1} PEG (-/+, +/+ PEG) in the same nutrient solution as described above for 1 h. Bars represent means ± SD, n = 4. Means with the same small letter and capital letter are not significantly different at $P < 0.05$ (t test) for the comparison of PEG pre-treatments within PEG re-treatments and comparison of PEG re-treatments within PEG pre-treatments, respectively.

Cell-wall material isolated from 1-cm root apices of plants treated without or with PEG (150 g L^{-1}) was exposed to Al, La, Sr, or Rb for 30 min in the absence or presence of PEG. PEG pre-treatment strongly reduced Al binding to the CWs (Fig. 8A). In contrast to Al, La accumulation was only slightly reduced (Fig. 8B), and Sr and Rb accumulation was not affected by PEG (Fig. 8C, D). Application of PEG only during the Al loading period did not affect the Al-binding properties of the isolated cell-wall material (Fig. 8A). Moreover, the different effects of osmotic stress on Rb accumulation *in vivo* (Fig. 7C) and *in vitro* (Fig. 8D) conditions suggest that the apoplast is not the main binding site of Rb, which may play an important role in the osmotic adjustment of the cytoplasm similar to K (Ogawa and Yamauchi, 2006).

Al accumulation in 1-cm root apices of intact plants (Fig. 9A) and Al binding to the CWs of these root tips (Fig. 9A′) decreased with increasing PEG concentration (0 - 150 g L^{-1}) in the treatment solution. A similar decreasing tendency was also observed for La, although the relative change was much lower compared to Al (Fig. 9B, B′). Unlike that of Al and La, Sr uptake/binding was not reduced by PEG treatment (Fig. 9C, C′). A higher concentration of PEG (200 g L^{-1}) did not further reduce Al and La uptake and its binding to the CW of root tips (Fig. 9). A PEG supply of 250 g L^{-1} was found to be lethal to the plants

since it seriously damaged the root system (data not shown).
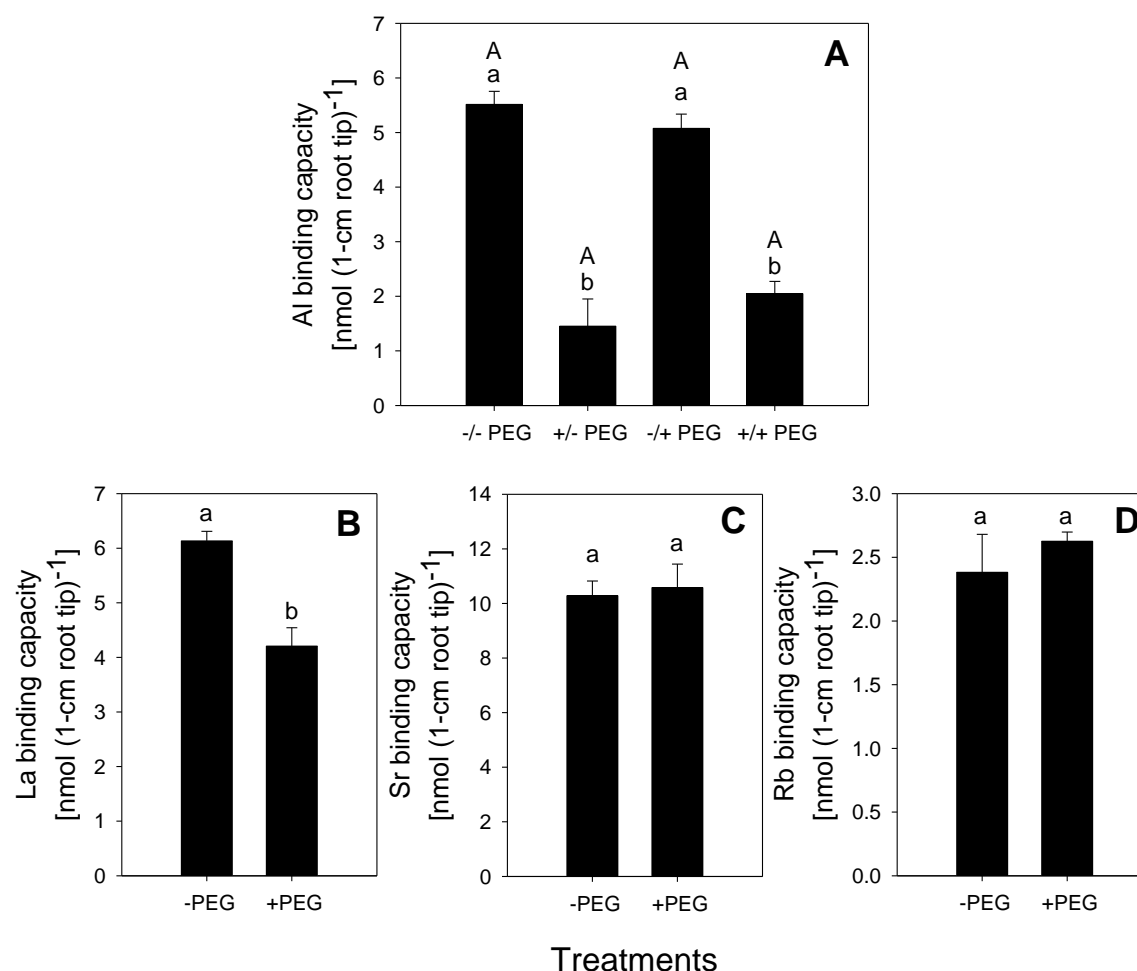
Figure 8 Al^{3+} (A), La^{3+} (B), Sr^{2+} (C) and Rb^+ (D) binding of cell-wall material isolated from of 1-cm root tips of Al-sensitive common bean genotype (VAX 1). Plants were pre-treated without or with 150 g L^{-1} PEG for 24 h in a simplified solution (pH 4.5) containing 5 mM $CaCl_2$, 1mM KCl and 8 μM H_3BO_3. Then 30 root tips (1-cm) were harvested for each sample and cell-wall material isolated according to Method A described in materials and methods. Then the isolated cell-wall material was treated with 1 mL 300 μM Al minus or plus 150 g L^{-1} PEG, 300 μM $LaCl_3$, 450 μM $SrCl_2$, or 900 μM RbCl for 30 min, pH 4.3. -/- PEG: without PEG during pre-treatment and Al treatment; +/- PEG: with PEG during pre-treatment and without PEG during Al treatment; -/+ PEG: without PEG during pre-treatment and with PEG during Al treatment; +/+ PEG: with PEG during pre-treatment and Al treatment. Bars represent means $\pm$ SD, n = 4. Means with the same small letter and capital letter are not significantly different at $P < 0.05$ (t test) for the comparison of PEG pre-treatments within PEG re-treatments and comparison of PEG re-treatments within PEG pre-treatments, respectively.
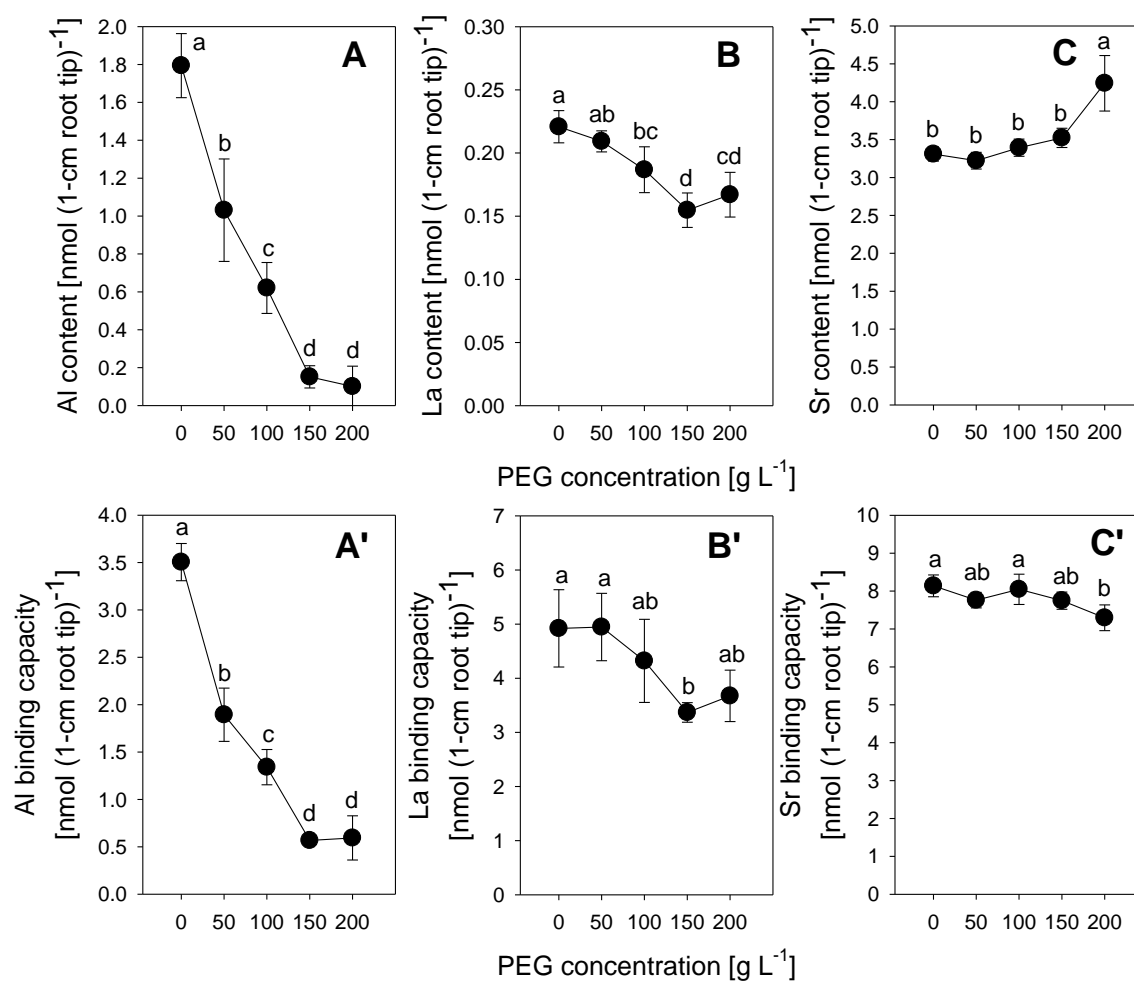
Figure 9 Effect of PEG treatment on Al, La and Sr accumulation of 1-cm root tips (A, B, C) and binding of cell-wall material isolated from 1-cm root tips (A′, B′, C′) of Al-sensitive common bean genotype (VAX 1). (A, B, C) Plants were pre-treated with PEG (0 - 200 g L^{-1}) for 8 h in a simplified solution (pH 4.5) containing 5 mM CaCl$_2$, 1 mM KCl and 8 μM H$_3$BO$_3$. Then the plants were supplied with 25 μM AlCl$_3$, 5 μM LaCl$_3$, or 2.5 mM SrCl$_2$ in the presence of PEG (0 - 200 g L^{-1}) in the same nutrient solution for 1 h as described above. (A′, B′, C′) Plants were pre-treated with PEG (0 - 200 g L^{-1}) for 24 h in the simplified solution. Then 30 root tips (1-cm) were harvested for each sample and cell-wall material isolated according to Method A described in materials and methods. Then the isolated cell-wall material was treated with 1 mL 300 μM Al, 300 μM LaCl$_3$, or 450 μM SrCl$_2$ for 30 min, pH 4.3. Bars represent means ± SD (n = 4). Means with the same letters are not significantly different at $P < 0.05$ (Tukey test).

To elaborate the role of PEG-induced alteration of cell-wall structure on Al binding, a simple physical method (method B) was used to destroy the CW structure by vigorously grinding the root apices with mortar and pestle in liquid nitrogen. PEG pre-treatment resulted in about 70% reduction of Al binding when the CW structure was widely unaltered (method A; Fig. 10). But by destroying the CW structure (method B) Al binding was restored in the PEG pre-treated samples. This indicates that PEG reduces CW porosity and

restricts the access of Al ions to binding sites.
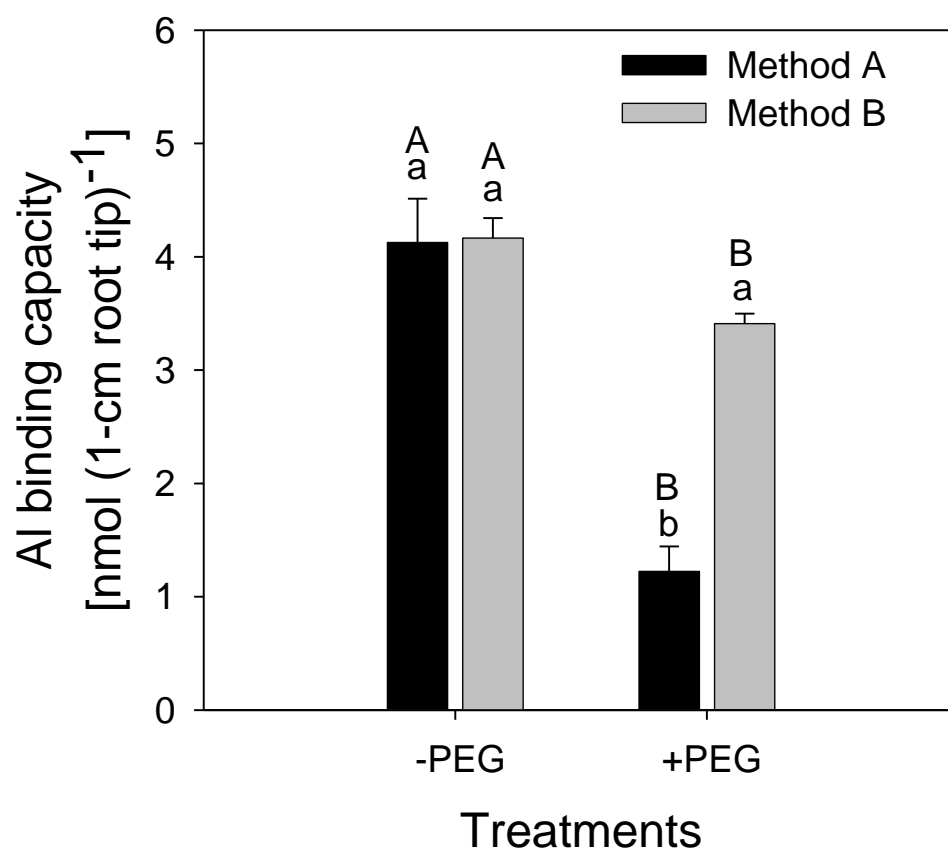
Figure 10 Al^{3+} binding of cell-wall material isolated from 1-cm root tips of Al-sensitive common bean genotype (VAX 1). Plants were pre-treated without or with 150 g L^{-1} PEG for 24 h in a simplified solution (pH 4.5) containing 5 mM $CaCl_2$, 1 mM KCl and 8 μM H_3BO_3. Then, thirty root tips (1-cm) were harvested and cell-wall material was isolated according to method A or method B, described in materials and methods. Then the isolated fine cell-wall powder was treated with 1 ml 300 μM Al for 30 min, pH 4.3. Bars represent means $\pm$ SD, n = 4. Means with the same small letter and capital letter are not significantly different at $P <$ 0.05 (t test) for the comparison of the method of CW isolation within PEG pre-treatments and comparison of PEG pre-treatments within the method of CW isolation, respectively.

Discussion

Generally, there is a positive relationship between Al-induced short-term inhibition of root elongation and Al accumulation in the root-tip apoplast of common bean (Rangel et al., 2009) indicating that Al resistance involves exclusion of Al from the root-tip apoplast (Horst et al., 2010). In the present study, PEG 6000-induced osmotic stress significantly inhibited Al accumulation in the root tips reaching almost the level of the control (Fig. 1B). Consequently, there was no Al toxicity which is reflected by the lack of any additional Al effect on the root elongation of PEG 6000-stressed plants (Fig. 1A). The possibility that PEG or contaminants associated with the PEG may decrease Al uptake into the root apex by complexing or precipitating Al in the treatment solution can be excluded because PEG application did not affect the mononuclear phytotoxic Al concentration of the treatment solution (data not shown).

Citrate exudation contributes to Al resistance of common bean by excluding Al from the root apex. In the present study, Al stress significantly increased citrate exudation from root apices during the early Al injury period (3 – 9 h), but the exudation was reduced with time (Fig. 3), which is typical for this Al-sensitive genotype VAX 1 (Rangel et al., 2010). The reduction of citrate exudation was related to the decreasing citrate content in the root apex (Fig. 2). These results confirm our previous studies that Al resistance of common bean through citrate exudation requires the maintenance of the cytosolic citrate concentration through up-regulated synthesis and down-regulated degradation (Rangel et al., 2010, Eticha et al., 2010). Abscisic acid (ABA), known as a stress-inducible phytohormone, plays important regulatory roles in the adaptation of root growth to drought and salt stress (Sharp, 2002; Ren et al., 2010). As an early Al-stress signal it may also regulate citrate exudation since exogenous application of ABA increased the activity of citrate synthase (CS) and citrate exudation, thus decreasing Al accumulation in the root apex of soybean (Shen et al., 2004). Therefore, we speculate that drought stress-induced ABA synthesis may directly or indirectly enhance citrate exudation through stimulating citrate production in the root apex which detoxifies Al and contributes to improved root growth under Al stress condition. Under medium-term (4 – 24 h) Al stress, the citrate content in the root apex was enhanced by PEG (osmotic stress) treatment (Fig. 2). However, PEG pre-treatment did not affect citrate exudation from the root apex (Fig. 3), suggesting that osmotic stress did not induce the exclusion of Al from root apices by increasing citrate exudation. Since relieving of the osmotic stress by withdrawing PEG from the solution

rapidly restored the Al accumulation capacity of the root apices (Fig. 5), the contribution of citrate exudation in reducing the Al binding capacity in presence of PEG cannot be unequivocally ruled out.

The apoplast of the root apex has been proposed to be the primary site of Al toxicity (Horst, 1995; Horst et al., 2010). Many reports indicate that Al in the root primarily accumulates in the CW. Rangel et al. (2009) found that about 80% of the total Al in the root of common bean was bound in the CW. Similar findings were reported for soybean (Yang et al., 2009). The density of the negative charge carried by the CW is determined by the degree of methylation (DM) of pectin which thus determines the Al binding capacity of roots (Schmohl et al., 2000; Eticha et al., 2005; Yang et al, 2008). Therefore, reduced Al accumulation in PEG-stressed plants could be due to CW modification. However, in disagreement with salt (NaCl)-induced osmotic stress of our previous studies in maize, which led to increased pectin content in root apices, enhanced Al accumulation, and thus higher Al sensitivity (Horst et al., 1999), our present results showed that PEG-induced osmotic stress did not affect the content of unmethylated pectin in root apices of common bean (Fig. 4). Therefore, the results do not support the assumption that osmotic stress leads to low Al accumulation by decreasing the CW negativity.

The use of PEG in studies on osmotic stress relies on the assumption that this high molecular weight solute cannot enter the symplastic space of the root (see introduction). However, there are several reports clearly showing that PEG may be accumulated in roots and even transported to the shoot (Lawlor, 1970; Janes, 1974; Yaniv and Werker, 1983; Jacomini et al., 1988). This may depend on the plant species, PEG source (contamination by LMW PEG) and concentration, time of exposure and root damage. If PEG accumulates at the root surface or enters the root apoplast it may physically interfere with Al uptake and its binding to the CW. Therefore, in order to clarify the importance of apoplastic PEG or PEG-induced osmotic stress decreased Al accumulation in root tips, the roots were separated from the PEG in solution using DMT which has a molecular weight cut off of 3,500 Dalton. Aluminium accumulation in the root tips grown in DMTs was also strongly reduced by PEG treatment (Fig. 5) suggesting that not the physical presence of PEG 6000 but the PEG 6000-induced osmotic stress was the cause for lower Al accumulation. A possible contribution of LMW PEG present in the PEG 6000 used for the experiments is unlikely because of two lines of evidence: (i) LMW PEG diffusing through the DMT reduced the OP of the equilibrium solution only to an OP value which hardly affected the Al binding of the roots (Fig. S1, Fig. 6B); (ii) PEG 6000 reduced the Al binding of the

roots more than PEG 3000 and particularly PEG 1000 in spite of similar osmotic stress and inhibitory effects on root elongation rate (Fig. 6).

In comparison with La, Sr, and Rb, the strong reduction of cation accumulation in the root apex by osmotic stress appears to be specific to Al. Osmotic stress had only a much smaller, yet, significant effect on La accumulation (Fig. 7, Fig. 9). In contrast, neither PEG pre-treatment nor re-supply of PEG during the Sr uptake period affected Sr accumulation in the root apices (Fig. 7B). Rubidium accumulation was reduced by PEG pre-treatment and PEG application during the Rb exposure period (Fig. 7C). The reduction of Rb accumulation was only found under *in vivo* conditions. Binding of Rb to the isolated CW of root apices *in vitro* was not affected by PEG pre-treatment (Fig. 8D). This suggests that the apoplast is not the main binding sites of Rb, which may play an important role in the osmotic adjustment of the cytoplasm similar to K (Premachandra et al., 1995; Ogawa and Yamauchi, 2006).

The specificity of cation accumulation might be related to the hydrated ionic radius of the cations: Al^{3+} (0.475 nm) > La^{3+} (0.452 nm) > Sr^{2+} (0.412 nm) = Ca^{2+} (0.412 nm) > K^+ (0.331 nm) > Rb^+ (0.329 nm) (Nightingale, 1959). Since the pore size of the CW plays an important role in apoplastic transport of water, ions, metabolites and proteins (Carpita et al., 1979; Brett and Waldron, 1996; Cosgrove, 2005), the differences between the ions in Al accumulation of the PEG-exposed root apices may suggest that PEG (osmotic stress) affects CW porosity. This assumption is supported by the fact that a similar reduction in accumulation specific for Al could also be observed in cell walls isolated from PEG-treated root tips (Fig. 8). Microscopic evaluation showed that the CW material was fairly intact (not shown) indicating that the CW porosity was not disrupted. After physically destroying the structure of the CW, Al binding to the CW was almost restored (Fig. 10).

The CW porosity is reported to be largely controlled by the pectin matrix (Baron-Epel et al., 1988). Schmohl and Horst (2000) suggested that the cross-linking of pectins by Al reduces the permeability of the CW for macromolecules such as proteins by reducing the CW porosity. McKenna et al. (2010) showed that Al and other metals reduced the hydraulic conductivity of bacterial cellulose–pectin composites, used as plant cell-wall analoges to about 30% of the initial flow rate. SEM revealed changes in the ultrastructure of the composites suggesting that metal binding decreased the hydraulic conductivity through changes in pectin porosity.

Pectin can form hydrated gels that push microfibrils apart, easing their sideway slippage

during cell growth, while also locking them in place when growth ceases (Baron-Epel et al., 1988; Fleischer et al., 1999; Cosgrove, 2005). For example, Jarvis (1992) indicated that pectin may act as a hydrophilic filler to prevent aggregation and collapse of the cellulose network. Therefore, the reduction of pectin in the CW of root apices under osmotic stress (Fig. 4) may change the structure of the CW, consequently resulting in a rearrangement of wall polymers and affecting the porosity.

Generally, the pore diameter of the plant CW is in the range of 3.5 - 5.5 nm, which mainly depends on CW structure, hydrophobicity, CW chemical composition and physical properties (Carpita et al., 1979; Chesson et al., 1997). Thus any change of these factors may result in subsequent alteration of porosity. For example, Bauchot et al. (1999) reported that low temperature decreased the pore size of the CW of kiwifruit by modifying CW composition. Addition of boric acid to growing borate-deficient suspension-cultured *Chenopodium album* L. cells rapidly decreased the pore size of the CW by the formation of a borate ester cross-linked pectic network in the primary walls (Fleischer et al., 1999). However, although it is reported that plant cells interact with their environment through the porous network of the CW (Carpita et al., 1979), and water stress can induce changes in CW composition and CW properties of roots (Iraki et al., 1989a, b; Wakabayashi et al., 1997; Leucci et al., 2008), to our knowledge, there is no report addressing the effect of drought stress on CW porosity.

Water is the most abundant component of the CW making up about two thirds of the wall mass in growing tissues. This water is located mainly in the matrix ($\approx 75 - 80\%$ water), which suggests that the matrix has properties of a relatively dense hydro-gel (Cosgrove, 1997). This visco-elastic nature of the plant CW allows it to respond to stresses and limitations imposed upon it (Moore et al., 2008). Loss of water from the wall matrix can result in serious disruption to polymer organization. One obvious effect is that polymers usually well separated in the hydrated wall are brought in close proximity to each other, thus causing polymer adhesion or cross-linking under water stress. A model illustrating the effect of water loss on CW polymer organization was presented by Moore et al. (2008).

The extent of loss of water from the apoplast and consequently shrinkage of the root structure appeared to be dependent of the molecular size of the applied PEG: PEG 6000 > PEG 3000 >> PEG 1000 (Fig. S2). The difference between the PEG sources at the same OP of -0.60 MPa might be related to the penetration of the PEG molecules into the root

apoplast: the higher the hydrodynamic radius the better the exclusion from the apoplast and consequently the dehydration of the apoplast. The estimated hydrodynamic radii of PEG 6000, 3000, and 1000 are 2.7, 1.6, and 0.89 nm, respectively (Kuga, 1981).

Also, the rapid recovery of Al accumulation in the living root apex after transfer of the roots into PEG-free solution (Fig. 5C) suggests that the water content of the apoplast is a decisive factor for PEG-induced alteration of CW porosity. However, the CW extension of living cells must involve biochemical (enzymatic) cleavage of load-bearing cross-linkages between wall polymers. Since the restoration of the Al accumulation capacity of the cell walls after the cessation of the PEG stress could only be observed in living root apices (Fig. 5) but not in ethanol-insoluble CW material isolated from root apices pre-treated with PEG (Fig. 8A), a role of enzymes mediating the inhibition of Al accumulation has to be postulated. Several CW proteins/enzymes are believed to play important roles in modifying the wall network and thus, possibly, the wall's ability to extend, such as expansin, xyloglucan endotransglycosylase (XET), glucanase (Wu and Cosgrove, 2000). Therefore, it is speculated that some proteins related to the modification of the CW structure are involved in the PEG 6000 (osmotic stress)-induced alteration of CW porosity. This needs to be substantiated through further physiological and molecular studies.

In conclusion, the observed results provide circumstantial evidence that the osmotic stress-inhibited Al accumulation in root apices and thus reduced Al-induced inhibition of root elongation in the Al-sensitive common bean genotype VAX 1 is related to the alteration of CW porosity resulting from PEG 6000-induced dehydration of the root apoplast.

CHAPTER 2

Physiological and molecular analysis of polyethylene glycol-induced reduction of aluminium accumulation in the root tips of common bean (*Phaseolus vulgaris* L.)

Zhong-Bao Yang[1], Dejene Eticha[1], Björn Rotter[2], Idupulapati Madhusudana Rao[3], Walter Johannes Horst[1]

[1] Institute of Plant Nutrition, Leibniz Universität Hannover, Herrenhaeuser Str. 2, D-30419 Hannover, Germany

[2] GenXPro GmbH, Altenhöferallee 3, 60438 Frankfurt am Main, Germany

[3] International Center for Tropical Agriculture (CIAT), AA 6713, Cali, Colombia

Abstract

Aluminium (Al) toxicity and drought are two major stress factors limiting common bean (*Phaseolus vulgaris* L.) production on tropical acid soils. Polyethylene glycol (PEG) treatment reduced Al uptake and Al toxicity. The effect of PEG 6000-induced osmotic stress (OS) on the expression of genes was studied using SuperSAGE combined with next generation sequencing and quantitative RT-PCR (qRT-PCR) for selected genes. Less Al stress in PEG-treated roots was confirmed by decreased Al-induced up-regulation of *MATE* and *ACCO* genes. Withdrawing PEG from the Al treatment solution restored the Al accumulation and reversed the *MATE* and *ACCO* genes expression to the level of the treatment with Al alone. Using SuperSAGE, we identified 611 up- and 728 down-regulated genes in PEG-treated root tips, and the results were confirmed by qRT-PCR using 46 differentially expressed genes. Among the 12 genes studied in more detail, *XTHa*, *BEG* (down-regulated by PEG) and *HRGP*, *bZIP*, *MYB* and *P5CS* (up-regulated by PEG) recovered completely within two hours after removal of PEG stress. The results suggest that genes related to CW assembling and modification such as *XTHs*, *BEG* and *HRGP* play important roles in PEG-induced decrease of CW porosity leading to reduced Al accumulation in root tips.

Key words: aluminum, cell wall, common bean, drought, osmotic stress, porosity, qRT-PCR, SuperSAG

Introduction

Common bean (*Phaseolus vulgaris* L.) is the major food legume for human nutrition in the world, and a major source of calories and protein particularly in many Latin American and African countries where middle and low income families are often unable to produce, or afford sufficient animal protein (Graham, 1978; Rao, 2001). However, in these tropical countries, the production of common bean is often limited by the adverse acidic soil conditions, particularly with aluminium (Al), proton, and manganese toxicity together with nutrient deficiencies and seasonal dry spells (Graham and Ranalli, 1997; Thung and Rao, 1999; Yang et al., 2010).

Common bean is generally less adapted to acid soil environments and is also a drought-sensitive crop (Rao, 2001; Beebe et al., 2008). The crop yield on acid soils is mainly limited by Al toxicity. Al resistance in common bean is attributed to the release of citrate by the root apex (Rangel et al., 2010). Generally, in citrate-releasing plant species, the multidrug and toxin extrusion (MATE) family protein, as an Al-activated citrate transporter, was suggested to be responsible for Al resistance. For example, in sorghum (*Sorghum bicolor*), *SbMATE* was expressed only in the root tips of the Al-resistant genotype in an Al-inducible way (Magalhaes et al., 2007). Similarly, in barley (*Hordeum vulgare*) *HvMATE* expression in the root apices correlated with Al-activated citrate exudation and Al resistance in a set of barley cultivars (Furukawa et al., 2007). However, in contrast to these plant species, in common bean the *MATE* gene was highly expressed by Al within 4 hours of treatment in both an Al-resistant (Quimbaya) and an Al-sensitive (VAX 1) genotype. The expression of *MATE* was a prerequisite for citrate exudation, but the build-up of Al resistance within 24 h in Quimbaya exclusively depended on the capacity to sustain the synthesis of citrate for maintaining the cytosolic citrate pool that enabled continuous exudation (Eticha et al., 2010; Rangel et al., 2010). In addition, the genotype-independent initial Al-induced inhibition of root elongation and subsequent recovery in the Al-resistant genotype was closely correlated with the expression of the 1-aminocyclopropane-1-carboxylic acid oxidase (*ACCO*) gene (Eticha et al., 2010). It has been speculated that the Al-induced inhibition of root growth is due to enhanced gene expression and enzyme activity of ACCO resulting in increased ethylene production in *Lotus japonicus* and *Medicago truncatula* (Sun et al., 2007). Thus, it appears that the *MATE* gene behaves like an Al sensor in common bean independent on the Al resistance of the genotype, and the *ACCO* gene as an indicator of Al-induced inhibition of root

elongation.

The combined Al toxicity and drought stress on root growth, with special emphasis on Al/drought interaction in the root apex of common bean has been well studied. Using polyethylene glycol (PEG) to simulate osmotic stress (OS) or drought stress, we found that OS enhances Al resistance by inhibiting Al accumulation in the root apices of the Al-sensitive genotype VAX 1. This alleviation of Al toxicity was related to the alteration of cell wall (CW) porosity resulting from PEG 6000-induced dehydration of the root apoplast. A biochemical and molecular regulation of the OS-induced change of CW porosity has been proposed (Yang et al., 2010). The plant CW is a composite structure consisting of a cellulose-hemicellulose framework embedded within a pectic polysaccharides and proteins matrix (Carpita and Gibeaut, 1993). This viscoelastic semi-solid component is a decisive factor for its resistance to external stress. Water loss from the wall matrix can result in serious disruption to polymer organization. One obvious effect is that polymers usually well separated in the hydrated wall are brought into close proximity to each other, thus causing polymer adhesion or cross-linking under water stress (Moore et al., 2008). It has been reported that several proteins play key roles in the adjustment of cell-wall structure, such as expansin, xyloglucan endotransglycosylase (XET) and glucanase (Wu and Cosgrove, 2000; Cosgrove, 2005). Therefore, the identification genes particularly involved in CW modification appears to be necessary for a better understanding of PEG-induced reduction of root-tip Al accumulation.

Common bean is a molecularly under-researched crop; extensive microarray-based transcriptomic studies are not yet possible owing to the lack of available gene and expressed sequence tag (EST) information. Thus, less comprehensive approaches such as suppression subtractive hybridization (SSH) libraries need to be taken, which do not *per se* allow the quantification of the expression of differentially expressed genes (Molina et al., 2008). One powerful technique for gene expression analysis is the serial analysis of gene expression (SAGE) developed by Velculescu et al. (1995). However, the short tag sequence of only 13-15 bp generated from SAGE was not always sufficient to unequivocally identify the gene from which the tag was derived. A single tag sequence usually corresponded to several different ESTs and genomic sequences, which required further analysis (Matsumura et al., 2003). SuperSAGE is an improved version of SAGE which overcomes the limitations of SAGE by producing 26 bp long fragments from defined position in cDNAs, providing sufficient sequence information to unambiguously characterize the mRNAs (Matsumura et al., 2003; Molina et al., 2008). This technique has been

successfully applied in several gene expression studies (Matsumura et al., 2003; Hamada et al., 2008; Molina et al., 2008; Gilardoni et al., 2010).

The main objectives of this study were: (a) to describe the interaction of Al toxicity and OS (PEG) in the Al-sensitive common bean genotype VAX 1 at the molecular level; and (b) to identify OS-induced genes in the bean root tips using SuperSAGE with particular emphasis on genes related to CW modification, in order to better understand the OS-induced changes of CW structure and thus reduction of Al accumulation in the root tips at the transcriptional level.

Materials and Methods

Plant materials and growing conditions

Seeds of the common bean (*Phaseolus vulgaris* L.) genotype VAX 1 (Al-sensitive) were germinated on filter paper sandwiched between sponges. After three days, uniform seedlings were transferred to a continuously aerated simplified nutrient solution containing 5 mM $CaCl_2$, 1 mM KCl, and 8 μM H_3BO_3 (Rangel et al., 2007). Plants were cultured in a growth chamber under controlled environmental conditions of a 16/8 h light/dark cycle, 27/25 °C day/night temperature, 70% relative air humidity, and a photon flux density of 230 μmol m^{-2} s^{-1} of photosynthetically active radiation at plant height. The pH of the solution was gradually lowered to 4.5 within two days. Then the plants were transferred into a solution (see above) without or with $AlCl_3$ (25 μM), PEG 6000 (150 g L^{-1}) and PEG 1000 (115 g L^{-1}) (Sigma-Aldrich Chemie GmbH, Steinheim, Germany), pH 4.5. Root tips (1-cm) were harvested for Al analysis or immediately frozen in liquid nitrogen in diethylpyrocarbonate (DEPC)-H_2O-treated Eppendorf vials for RNA isolation. The osmotic potentials (OPs) of both PEG 6000 (150 g L^{-1}) and PEG 1000 (115 g L^{-1}) solutions were -0.60 MPa, measured with a cryoscopic osmometer (Osmomat 030, Gonotec GmbH, Berlin, Germany).

Measurement of root-elongation rate

Two hours before the treatment was initiated, tap roots were marked 30 mm behind the root tip using a fine point permanent marker (Sharpie blue, Stanford) which did not affect root growth during the experimental period. Afterwards, the plants were transferred into a simplified nutrient solution (see above) without or with PEG in the absence or presence of Al. Root elongation was measured after the 24 h treatment period using a mm scale.

RNA isolation and construction of the SuperSAGE library

For construction of the SuperSAGE library, only PEG 6000 was used. After treating the plants with PEG 6000 for 24 h in a simplified nutrient solution (see above), the roots were rinsed with distilled water and five to six root tips (1 cm long) from each plant were harvested and shock-frozen in liquid nitrogen. Root tips of 10 plants per treatment were bulked and ground to powder in liquid nitrogen. Total RNA was isolated using the NucleoSpin RNA plant kit (MACHEREY-NAGEL GmbH and Co., KG, Düren, Germany)

following the manufacturer's protocol. From total RNA, poly(A)-RNA was purified with the Oligotex mRNA mini Kit (Qiagen) according to manufacturer's protocol.

SuperSAGE libraries were constructed by GenXPro GmbH (Frankfurt am Main, Germany) essentially as described by Matsumura et al. (2010). In order to avoid PCR bias during the amplification steps, GenXPro's "PCR-bias-proof technology" was employed to distinguish PCR copies from original tags. Sequencing was performed on an Illumina GA II machine (Illumina, Inc., San Diego, USA). For each library, 26 bp long tags were extracted from the sequences using the GXP-Tag sorter software provided by GenXPro GmbH (Frankfurt am Main, Germany). Sequencing artifacts were reduced according to Akmaev and Wang (2004).

Library comparisons were carried out using the DiscoverySpace 4.01 software (Canada's Michael Smith Genome Sciences Centre, available at http://www.bcgsc.ca/discoveryspace). Statistical analysis of differentially expressed tags was conducted using the probability (P)-value according to the description of Audic and Claverie (1997). The expression ratios of the 26 bp tags from control versus PEG 6000-treated roots were calculated as: Ratio $(R) = \log_2^{(PEG6000/control)}$, after normalizing to one million. Tags that are present zero times are replaced by 0.05, to allow calculation of the ratio.

Sequence homology alignments

Tags sequences were BLASTed (Altschul et al., 1990) against different public databases (Phaseolus_TIGR_PHVGI.release_3/PHVGI.052909; TIGR_Phaseolus_cocc_TiGR_PCGI. Release_1/PCGR. 052909; Glycine_MAX_TIGR_GMGI.release_14/GMGI.052909; Medicago_TIGR_MTGI.release_9/MTGI.071708; Lotus_TIGR_LJGI.release_5/LJGI. 052909; Refseq_plant_June09/ refseqPlantJune09.fna; All-plant-EST.fasta (plantGDB)).

Primer design for qRT-PCR

The ESTs from different organisms with high similarity to the sequences of candidate genes obtained from the SuperSAGE library were aligned, and the conserved regions were BLASTed against the *P. vulgaris* database. Finally the ESTs of *P. vulgaris* were aligned and the conserved region was used for primer design. Primers were designed using Primer3 software (Rozen and Skaletsky, 2000). The primers of the *β-tubulin*, *MATE* (multidrug and toxin extrusion) family protein and *ACCO* (1-aminocyclopropane-1-carboxylic acid

oxidase) genes were obtained from Eticha et al. (2010). The specifications of the primers of the genes studied in more detail are given in Tab. 1. For a complete list of all primers used see Supporting Information Table 1. The PCR efficiencies of the primer pairs were in the range of 90 – 110% as determined by dilution series of the cDNA template. Primer pairs with PCR efficiencies deviating from this range were discarded and new primers of the genes were designed to get more reliable quantification.

Table 1 List of main genes and specific primer pairs used for quantitative gene expression analysis

Candidate genes	Primer pairs (5'→3')*	Amplicon size (bp)	TC/GB Acc. No.
LTP (Protease inhibitor/seed storage/lipid transfer protein family protein)	(+) CCTCAGCAGCACAAGATGAG (-) TGACAGCAATCTGAGGGGTTG	147	CV542382
HRGP (Hydroxyproline-rich glycoprotein)	(+) CCTGTCTTGATGGTGAAGCA (-) TTCATTTGTTGCAGGCTGAC	114	CV543261
SUS (Sucrose synthase 2)	(+) GCATGGCCTCATGAAAGAGT (-) GAAAGCAGGCTGAACGAAAG	133	TC11609
XTHa (Xyloglucan endotransglycosylase precursor)	(+) ATATGTCATCGGAGGGTCCA (-) TTGGTAGGGTCGAACCAAAG	151	TC12227
AQP (Aquaporin)	(+) CCACATCACCATCCTCACTG (-) ATTGCCAAACCTCCTGTGAC	102	TC14630
BEG (Glucan endo-1, 3-beta-glucosidase precursor)	(+) ATGGAAGACTTGGCAACGAC (-) GCCTCTCAAAGCTCCAAGAA	122	TC11172
PRP (Proline-rich protein)	(+) GCAAGTGTTGTGCATTGCTT (-) TGGAAGCCAGAAGGAACTGT	160	TC12228
XTHb (Xyloglucan endotransglucosylase/hydrolase)	(+) TTTGACCAACCCATGAAGGT (-) GCATTCACTGAGGCTTCACA	153	CV542742
CYP701A (Cytochrome P450 monooxygenase CYP701A16)	(+) GGATGCAACATGGACAAGAA (-) AACCTGCACACACCCTCTTC	136	TC18728
MYB (MYB transcription factor MYB134)	(+) CCGATTCCGACAAAATGAAC (-) GCATCAGGTGTGTTCAGCTC	136	TC13287
P5CS (VuP5CS protein)	(+) GACAGTGCTGCTGTTTTCCA (-) AAACCCTCTACTCCCACAGGA	128	TC14708
bZIP (bZip transcription factor)	(+) AAACTGCCACTTCCCTCCTT (-) TCTCCTGTGCTTCCTTTCGT	127	TC17978
ACCO (ACC-oxidase) (Eticha et al., 2010)	(+) GAAGATGGCGCAAGAAGAAG (-) TGGAGCAAAGGTTCAAGGAG	105	AB002667
MATE (Citrate transporter family) (Eticha et al., 2010)	(+) CTGGATGCAGTTTCAAGAGAG (-) ACTCCAGCAGCTGCAAGTTC	138	CV535133
β-Tubulin (Eticha et al., 2010)	(+) CCGTTGTGGAGCCTTACAAT (-) GCTTGAGGGTCCTGAAACAA	117	CV530631

* (+) and (-) indicate forward and reverse primers, respectively.

First-strand cDNA synthesis and qRT-PCR

After isolating the RNA from 1-cm root tips of bean genotype VAX 1 (see above), first-strand cDNA was synthesized using RevertAid H-Minus first strand cDNA synthesis kit (Fermentas, www.fermentas.com) following the manufacturer's protocol. qRT-PCR was performed using the CFX96^{TM} Real Time System plus C1000^{TM} Thermal Cycler (www.bio-rad.com). The SYBR Green detection system was used with self-prepared SYBR Green master mix. The qRT-PCR reaction mix composed of $1 \times$ hot-start PCR buffer (DNA Cloning Service, Germany), 3.6 mM $MgCl_2$ (DNA Cloning Service, Germany), 200 µM each dNTP (dATP, dTTP dCTP dGTP) (Fermentas), $0.1 \times$ SYBR Green-I (Invitrogen), 0.75 U µL^{-1} DCSHot DNA Polymerase (DNA Cloning Service, Germany), 252 nM each forward and reverse primer (Biolegio), 2 ng µL^{-1} cDNA template and ultra-pure DNase/RNase-free distilled water (Invitrogen) in a final volume of 25 µL. The qRT-PCR cycling stages consist of initial denaturation at 95 ℃ (10 min), followed by 45 cycles of 95 ℃ (15 s), 60 ℃ (30 s), 72 ℃ (30 s), and a final melting curve stage of 95 ℃ (15 s), 60 ℃ (15 s) and 95 ℃ (15 s). Samples for qRT-PCR were run in three biological replicates and two technical replicates. Relative gene expression was calculated using the comparative ΔΔCT method according to Livak and Schmittgen (2001). For the normalization of gene expression, *β-tubulin* was used as an internal standard according to Eticha et al. (2010), and the control (non-treated) plants of bean genotype VAX 1 were used as reference sample.

Confirmation of SuperSAGE expression profiles via qRT-PCR

Parallel RNA extractions to the SuperSAGE library construction in 1-cm root tips from control (-PEG) and PEG 6000-treated plants were used. 46 differentially expressed genes according to SuperSAGE with putative role in the regulation of cell-wall properties and response to OS were selected and the primers were designed according to the method described above (Supporting Information Table S1). The expression of these genes in control and PEG 6000-treated 1-cm root tips of bean were confirmed by SYBR Green-based qRT-PCR.

Determination of Al

For the determination of Al, 1-cm root tips were digested in 500 µL ultra-pure HNO_3 (65%, v/v) by overnight shaking on a rotary shaker. The digestion was completed by heating the

samples in a water bath at 80 ℃ for 20 min. Then 1.5 mL ultra-pure deionised water was added after cooling the samples in an ice-water bath. Aluminium was measured with a Unicam 939 QZ graphite furnace atomic absorption spectrophotometer (GFAAS; Analytical Technologies Inc., Cambridge, UK) at a wavelength of 308.2 nm after appropriate dilution, and an injection volume of 20 μL.

Statistical analysis

A completely randomized design was used, with four to twelve replicates in each experiment. Statistical analysis was carried out using SAS 9.2. Means were compared using t or Tukey test depending on the number of treatments being compared. *, **, ***, and ns denote significant differences at $P < 0.05$, 0.01, 0.001, and not significant, respectively.

Results

Both PEG 6000 and PEG 1000 treatment induced the same extent of inhibition of root elongation (30%) of common bean at the same osmotic potential (OP) treatment level (Fig. 1A). Aluminium treatment strongly reduced root elongation (80%). Addition of PEG in the presence of Al significantly reduced the Al-induced inhibition of root elongation to 50% and 40% with PEG 1000 and 6000, respectively (Fig. 1A). The PEG-induced decrease in Al toxicity was related to a significant reduction of Al accumulation in the 1-cm root tips (PEG 6000 > PEG 1000, Fig. 1B).

The expressions of the citrate transporter *MATE* gene and the *ACCO* gene were clearly enhanced by increasing Al supply (Fig. 2A, B). The relative expression levels were significantly negatively correlated with root elongation as affected by Al supply (Fig. 2C, D) and positively correlated with the Al concentrations of the roots tips (Fig. 2E, F). This confirms the decisive role of root-tip Al accumulation in Al-induced inhibition of root elongation.

It thus appears that the expression of the *MATE* and *ACCO* genes are sensitive indicators of Al toxicity and Al accumulation, which could provide opportunities to further clarify the PEG-induced reduction of Al accumulation in the root tips. In contrast to Al stress, OS induced by PEG 1000 or PEG 6000 did not affect the regulation of both genes (Fig. 3). However, the Al treatment-induced up-regulation was significantly decreased by PEG treatment (PEG 6000 > PEG 1000) in agreement with the greater suppression of Al accumulation and Al stress by PEG 6000 (see Fig. 1).

The removal of PEG from the treatment solution rapidly allowed Al to accumulate in the root tips (Fig. 4A), and the expressions of *MATE* and *ACCO* genes were restored near to the level of the treatment with Al alone with the exception of *ACCO* in the PEG 1000-treated root tips (Fig. 4B, C).
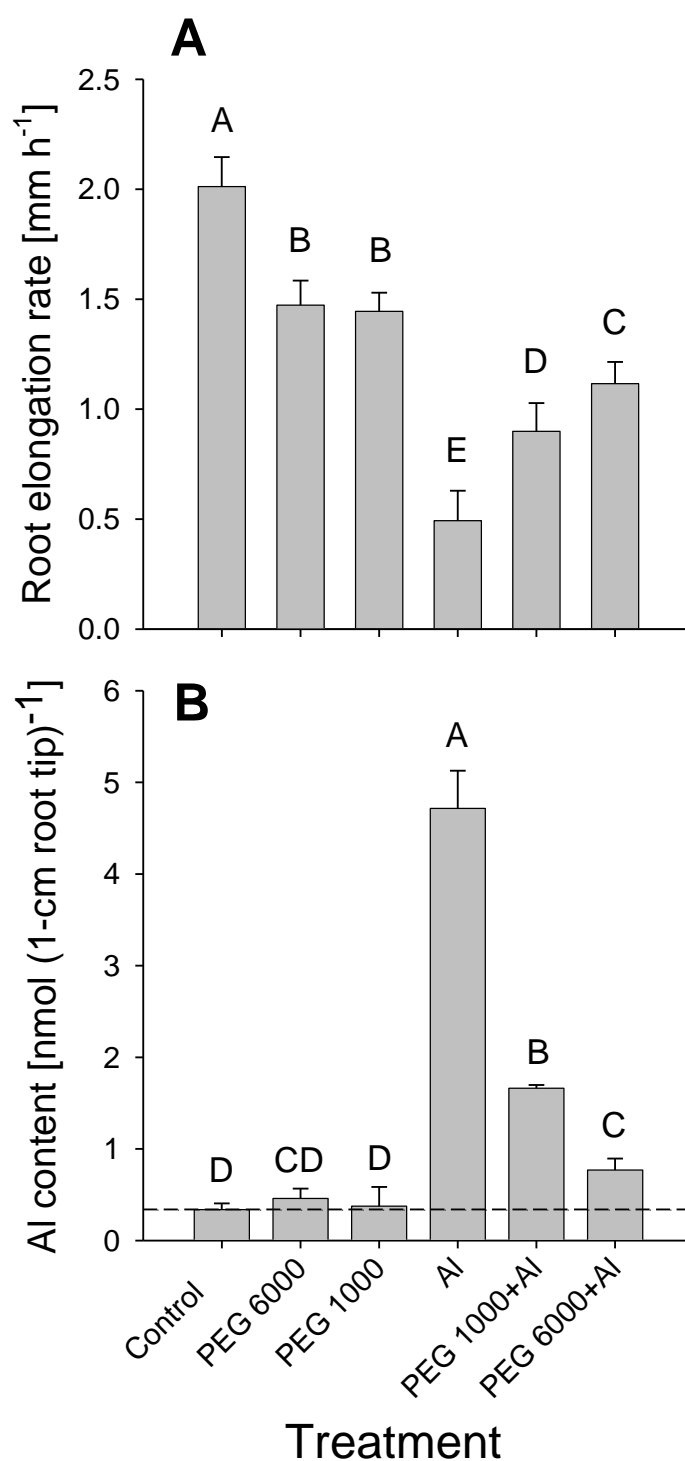
Figure 1 Root-elongation rate (A) and Al content (B) of 1-cm root tips of the common bean genotype VAX 1 under osmotic (0, -0.60 MPa OP) and Al (0, 25 μM Al) stresses. Plants were pre-cultured in a simplified nutrient solution containing 5 mM $CaCl_2$, 1 mM KCl, and 8 μM H_3BO_3 for 48 h for acclimation and pH adaptation, then treated without or with 25 μM Al in the absence or presence of PEG (150 g L^{-1} PEG 6000, 115 g L^{-1} PEG 1000) in the simplified nutrient solution for 24 h, pH 4.5. The background value (dashed line) in (B) represents the mean Al content of the root tips without Al treatment. Bars represent means ± SD, n = 12 for (A) and n = 4 for (B). Means with different capital letters are significantly different at $P < 0.05$ (Tukey test) for the comparison of treatments.
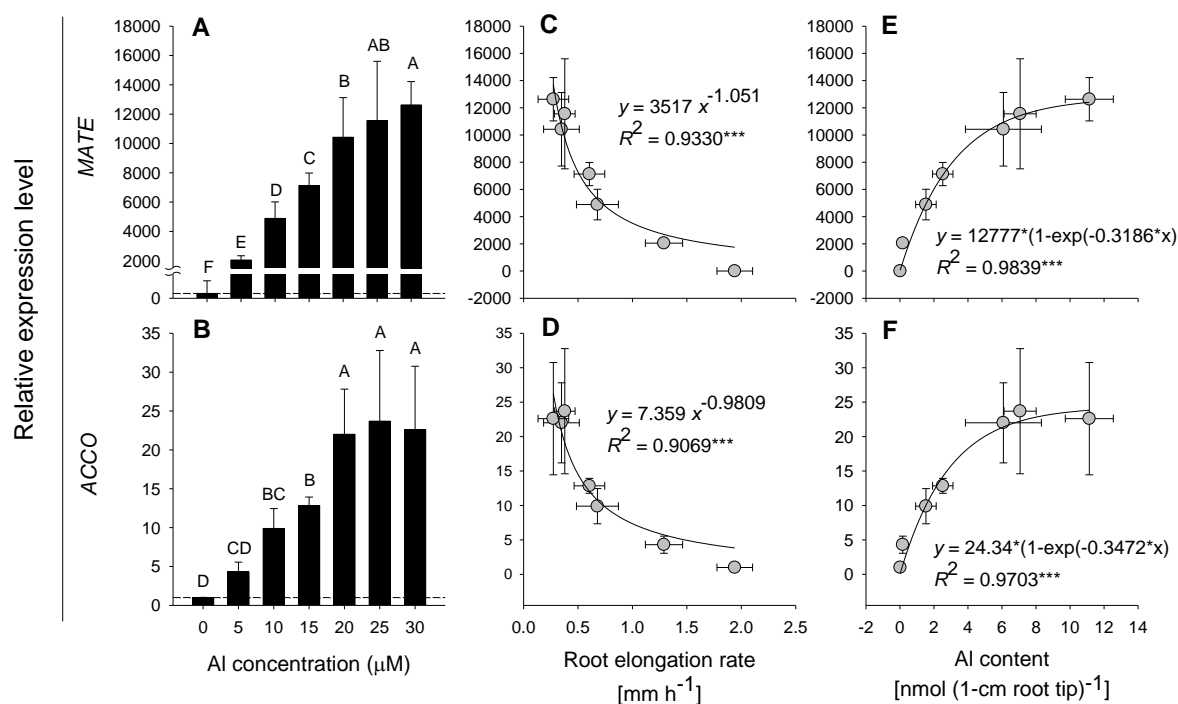
Figure 2 The effect of Al (0 - 30 μM) on the relative expression level of *MATE* and *ACCO* genes in 1-cm root tips of the common bean genotype VAX 1 and the correlation of the *MATE* and *ACCO* gene expression with root elongation rate and Al content. Plants were pre-cultured in a simplified nutrient solution containing 5 mM $CaCl_2$, 1 mM KCl, and 8 μM H_3BO_3 for 48 h for acclimation and pH adaptation, then treated with different concentrations of Al (0 - 30 μM) in the simplified nutrient solution for 24 h, pH 4.5. The background value (dashed line) in (A) and (B) represents the calibrated reference using untreated plants. qRT-PCR was performed using the *β-tubulin* gene as internal standard. Bars represent means $\pm$ SD, n = 4 for root elongation rate and Al content, n = 3 for gene expression. Means with different capital letters are significantly different at $P < 0.05$ (Tukey test) for the comparison of Al treatments. *** denote significant differences at $P < 0.001$.

The results clearly showed that particularly PEG-6000 reduced the Al accumulation of root tips and that the Al accumulation of the same roots tips is rapidly restored upon withdrawing PEG. In order to better understand the molecular basis of the PEG effect, two libraries from control (-PEG 6000) and PEG 6000-treated root tips were constructed using SuperSAGE. After excluding the singletons from the total sequenced 9,015,356 tags of 26 bp length in both libraries (data not shown), we analysed in total 8,960,486 tags, 3,913,099 (44%) from the root tips of the control and 5,047,387 (56%) from PEG-treated plants (Table 2). These tags represented 75,867 unique transcripts (UniTags) overall, 67,185 (89%) from the PEG 6000-treated and 68,969 (91%) from the control roots; among these, 9,819 UniTags were up- and 8,019 UniTags were down-regulated at P < 0.05 (Fig. 5A, Table 2). UniTags present at < 100, 100-1000 and > 1000 copies per million (copies * million^{-1})

were considered as low, mid and high abundant tags, respectively. The frequency distribution of the 68,969 UniTag in control library showed 0.2% low, 2.3% mid and 97.6% high-abundant tags, and the 67,185 UniTags in the PEG 6000 library showed 0.2% low, 2.4% mid and 97.5% high-abundant tags (Table 2). The annotation of the 75,867 UniTags matched 39,314 previously well characterized sequences from the public databases with a maximum of 5 mismatches (scores $\geq$ 42.1; about 52%). Of these, 28% matched to sequences from *P. vulgaris*, 6% to *Phaseolus coccineus*, 3% to *Glycine max*, 0.3% to *Medicago truncatula*, 0.2% to *Lotus japonicus*, and 15% to other species (Table 3).

Table 2 Features of SuperSAGE libraries from control and PEG 6000-treated root tips of common bean genotype VAX 1.

Library	Control	PEG 6000	Total
Sequenced tags	5,047,387 (56%)	3,913,099 (44%)	8,960,486 (100%)
Number of unique transcripts (UniTags)	68,969 (91%)	67,185 (89%)	75,867 (100%)
Abundance classes of UniTags[*]			
High-abundant: > 1,000 copies.million^{-1}	104 (0.2%)	98 (0.2%)	-
Mid-abundant: 100 - 1,000 copies.million^{-1}	1,578 (2.3%)	1,594 (2.4%)	-
Low-abundant: < 100 copies.million^{-1}	67,287 (97.6%)	65,493 (97.5%)	-
Total	68,969	67,185	-

[*] Values normalized to 1 million tags

Table 3 BLAST search results of the SuperSAGE Unitags in different EST databases.

EST database	Control	PEG 6000	Total
Phaseolus vulgaris	19,147 (28%)	18,291 (27%)	21,121 (28%)
Glycine max	2,116 (3%)	1,993 (3%)	2,223 (3%)
Phaseolus coccineus	4,066 (6%)	3,914 (6%)	4,338 (6%)
Medicago truncatula	195 (0.3%)	248 (0.4%)	248 (0.3%)
Lotus japonicus	125 (0.2%)	136 (0.2%)	136 (0.2%)
Other species	9,449 (14%)	9,542 (14%)	11,248 (15%)
Not matched	33,871 (49%)	33,061 (49%)	36,553 (48%)
Total	68,969	67,185	75,867
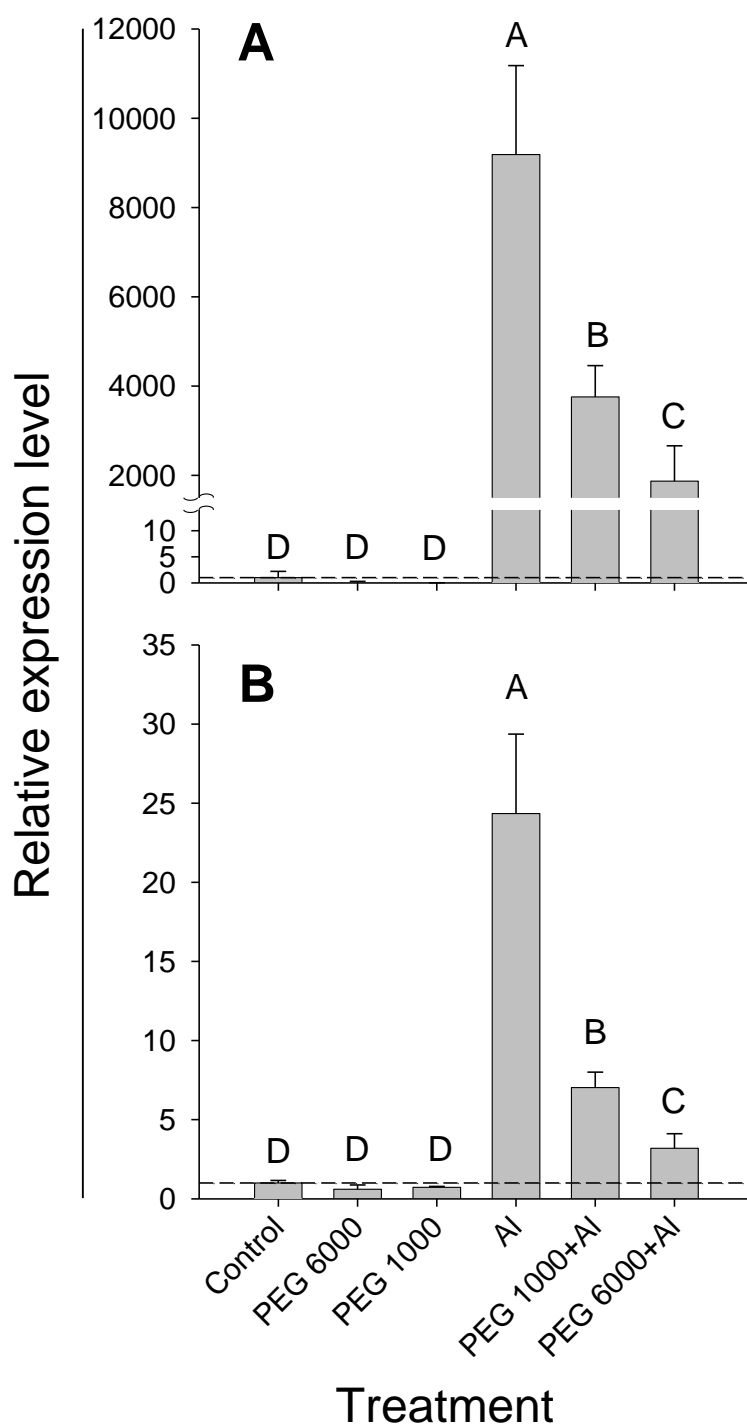
Figure 3 Relative expression level of *MATE* (A) and *ACCO* (B) genes in 1-cm root tips of common bean genotype VAX 1 under osmotic (0, -0.60 MPa OP) and Al (0, 25 μM Al) stress. Plants were pre-cultured in a simplified nutrient solution containing 5 mM $CaCl_2$, 1 mM KCl, and 8 μM H_3BO_3 for 48 h for acclimation and pH adaptation, then treated without or with 25 μM Al in the absence or presence of PEG (150 g L^{-1} PEG 6000, 115 g L^{-1} PEG 1000) in the simplified nutrient solution for 24 h, pH 4.5. The background value (dashed line) represents the calibrated reference using untreated plants. qRT-PCR was performed using the *β-tubulin* gene as internal standard. Bars represent means ± SD, n = 3. Means with different capital letters are significantly different at *P* < 0.05 (Tukey test) for the comparison of treatments.

Time		1	2	3	4	5	6	7
0 - 8 h	PEG 1000				*	*		
	PEG 6000						*	*
8 - 10 h	Al		*	*	*	*	*	*
	PEG 1000				*	*		
	PEG 6000						*	*
10 - 12 h	Al			*		*		*

Figure 4 Al content (A) and relative expression level of *MATE* (B) and *ACCO* (C) genes in 1-cm root tips of common bean genotype VAX 1 under osmotic (-0.60 MPa OP) and Al stress. Plants were pre-cultured in a simplified nutrient solution containing 5 mM $CaCl_2$, 1 mM KCl, and 8 μM H_3BO_3 for 48 h for acclimation and pH adaptation, then the plants were subjected to a series of Al (0, 25 μM), PEG 6000 (0, 150 g L^{-1}) and PEG 1000 (0, 115 g L^{-1}) treatment solutions. A detailed description of the different treatments are shown under figure with a tableDifferent numbers (1 - 7) represent different Al and PEG treatment combinations, and * indicate the presence of treatment. Briefly, the plants were pre-treated with either PEG 1000 or PEG 6000 for 8 h. They were then transferred for 2 h (8-10 h) to a solution containing Al and/or PEG or not. This treatment was then followed by a 2 h (10-12 h) recovery period from PEG stress in presence or absence of Al. The background value (dashed line) represents the calibrated reference using untreated plants. qRT-PCR was performed using the *β-tubulin* gene as internal standard. Bars represent means ± SD, n = 4 for (A) and n = 3 for (B, C). Means with different capital letters are significantly different at $P < 0.05$ (Tukey test) for the comparison of treatments.
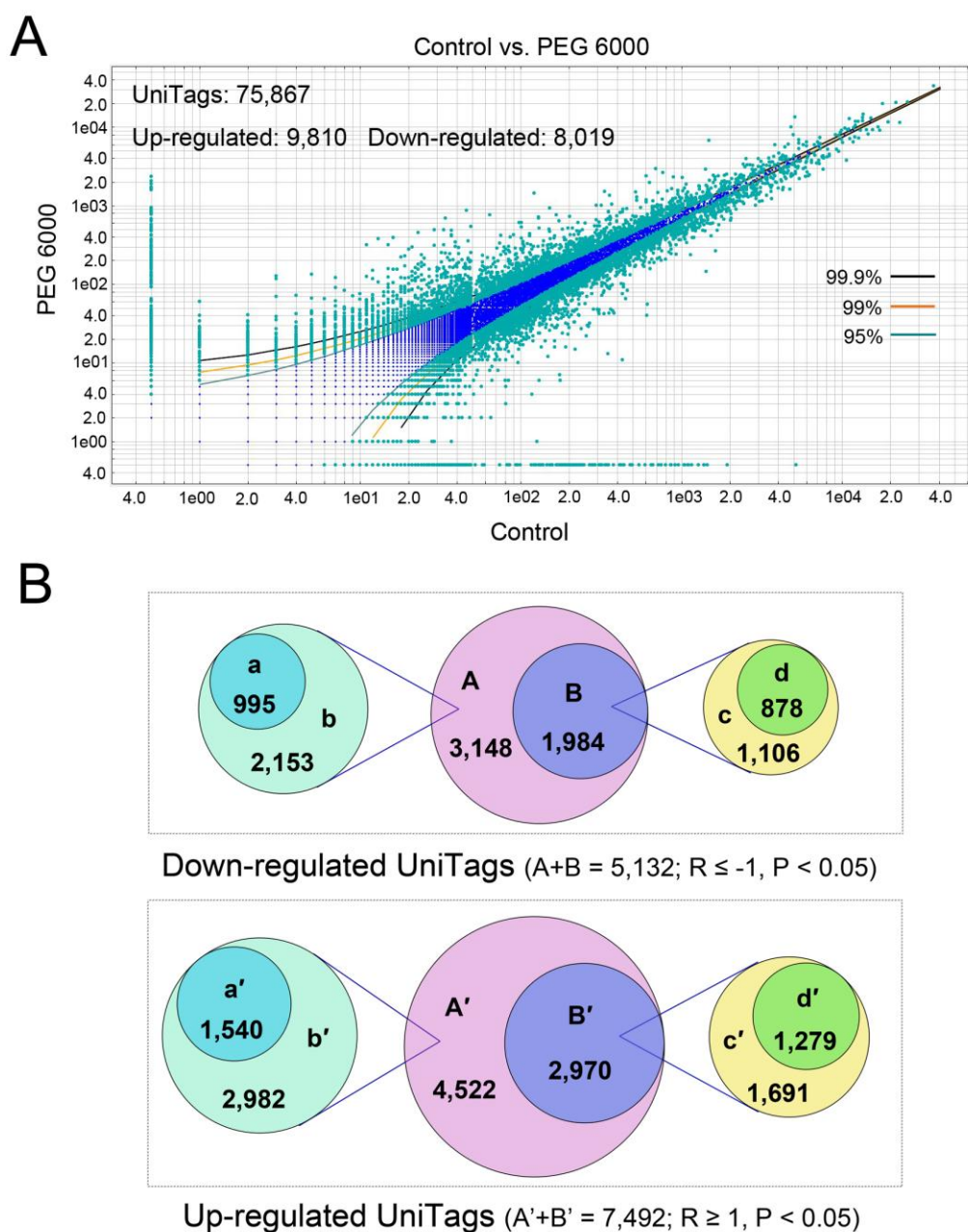
Figure 5 (A) Scatter plot showing the UniTags expressed in control and PEG 6000-treatment libraries. (B) Venn diagram showing down and up-regulated UniTags using rigorous threshold parameters ($|R| > 1$; $P < 0.05$) in root tips of common bean genotype VAX 1. In (A), lines represented as 99.9%, 99% and 95% demarcate UniTags that are significantly up- or down-regulated at P value lower than 0.001, 0.01 and 0.05, respectively. In (B), A/A': UniTags exclusively expressed in control/PEG 6000 libraries; B, B': in both libraries; a, d, a', d': no hit and b, c, b', c': hit to previously known public databases.

For further analysis of the PEG-induced differentially expressed genes, the significant differences in abundance of UniTags in control and PEG subjected roots were rigorously limited to a threshold $|R| \geq 1$ ($\geq$ 2-fold change) and $P < 0.05$. Based on this, a total of 12,624 UniTags (7,492, up-regulated; 5,132, down-regulated) were differentially expressed (Fig. 5B), and of these, 3,259 down-regulated UniTags (2,153 exclusively expressed in control and 1,106 expressed in both control and PEG treatment libraries) and 4,673 up-regulated UniTags (2,982 exclusively expressed in control and 1,691 in expressed in both control and PEG treatment libraries) hit to previously known sequences from *P. vulgaris*, *P. coccineus*, *G. max*, *M. truncatula*, *L. japonicus* and other organisms (Fig.5B). By assembling the same expressed sequence transcripts (ESTs) from the differentially expressed UniTags annotation in control and PEG 6000-treated roots, and the exclusion of the UniTags with more than six 3'-poly(A) in the 26 bp tags, finally a total of 611 up- and 728 down-regulated transcripts were obtained for the gene functional categorization (Fig. 6, Supporting Information Table S2). The gene functional categories of the differentially expressed transcripts were BLASTed against the non-redundant GeneBank and UniProt protein databases (http://www.uniprot.org/) by the gene ontology (GO) annotation (Supporting Information Table S2).

The unique transcripts were categorized and identified according to the functional category defined by KEGG PATHWAY and UniProt protein database (Fig. 6). About 47.5% of the up and 42.0% of the down-regulated transcripts had unknown functions or were unclassified. The metabolism categories (12.4%, up; 11.8%, down) were sub-classified into carbohydrate, energy, amino acid, lipid, nucleotide, secondary and other metabolic pathways. Functional categories equally up and down-regulated were transcription regulation (5.89%, up; 5.22%, down) and cytoskeleton (0.33%, up; 0.41%, down). Predominantly down-regulated transcripts by PEG were found in the categories of signal transduction, transport, stress/defence, cell-wall synthesis and organization, protein posttranslational modification, whereas transcripts in the categories of protein translation, processing and degradation, RNA processing and modification, replication and repair were more often up-regulated (Fig. 6). The differentially regulated UniTags with different functional categories were listed (Supporting Information Table S2).

Up-regulated transcripts (611)

Down-regulated transcripts (728)

Legend:
- Transcription regulation
- Signal transduction
- Transport
- Stress/defence
- Carbohydrate metabolism
- Energy metabolism
- Amino acid metabolism
- Lipid metabolism
- Nucleotide Metabolism
- Secondary metabolism
- Other metabolisms
- Cell wall synthesis and organization
- Protein translation, processing, and degradation
- Protein posttranslational modification
- RNA processing and modification
- Replication and Repair
- Cytoskeleton
- Unknown/unclassfied

Figure 6 Functional categories of differentially expressed transcripts in control and PEG 6000-treated root tips of common bean genotype VAX 1.

To validate the results generated from SuperSAGE, 46 differentially expressed genes (Supporting Information Table S1) according to SuperSAGE with putative role in the regulation of cell-wall properties and response to OS were selected and their expression tested by quantitative real-time PCR (qRT-PCR). A highly significant correlation ($R^2 = 0.71$, $P < 0.0001$) between SuperSAGE and qRT-PCR was found (Fig. 7).

Among the 46 genes, six genes each with suspected functions in PEG-induced cell-wall modification (*XTHa*, *XTHb*, *BEG*, *HRGP*, *PRP* and *LTP*) and osmotic-stress response (*bZIP*, *MYB*, *AQP*, *P5CS*, *SUS* and *CYP701A*) were selected for a more detailed gene expression study using qRT-PCR (Fig. 8). The results showed that among the CW-associated genes only *LTP* and *HRGP* were significantly up-regulated by PEG treatment, whereas *XTHa*, *XTHb*, *BEG*, and *PRP* were down-regulated. All OS-associated genes were significantly up-regulated with the exception of *CYP701A*. Removal of the PEG stress for 2 hours which allowed root elongation rate to recover (data not shown) and partly restored the Al accumulation capacity (see Fig. 4), did reverse the gene expression to the control level for *XTHa*, *BEG*, and *HRGP* among the cell wall-associated genes and

bZIP, *MYB*, and *P5CS* among the OS-associated genes. The *LTP*, *SUS*, and *AQP* genes remained up-regulated and *PRP*, *XTHb*, *CYP701A* down-regulated compared to the controls. These results were highly reproducible because similar results were found in another experiment where root tips were treated only for 10 h compared to 24 hours as in the current experiment (data not shown).
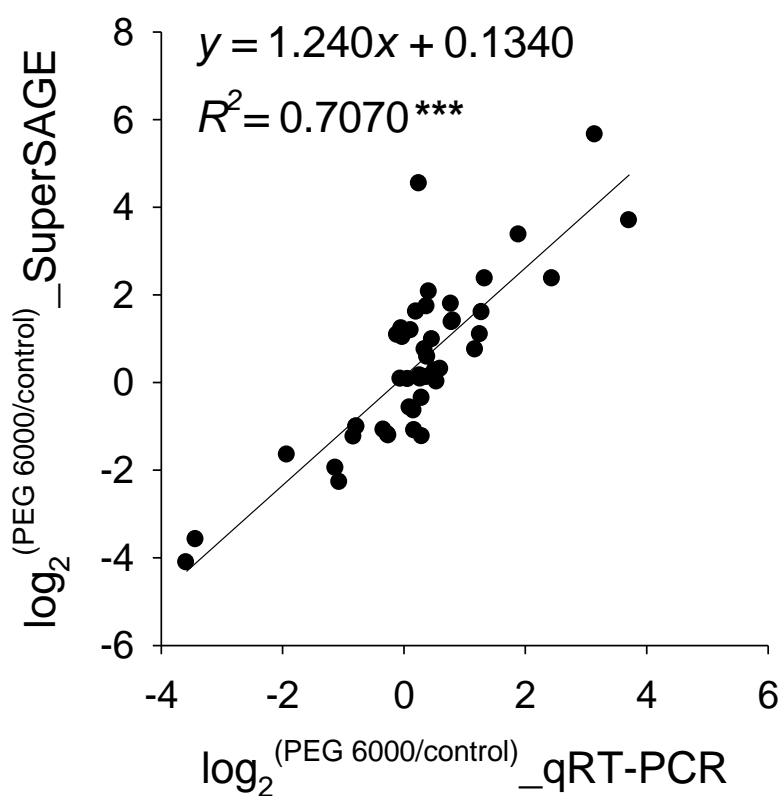
Figure 7 Validation of the PEG-induced expression of 46 genes selected from SuperSAGE in root tips of common bean genotype VAX 1 by qRT-PCR.
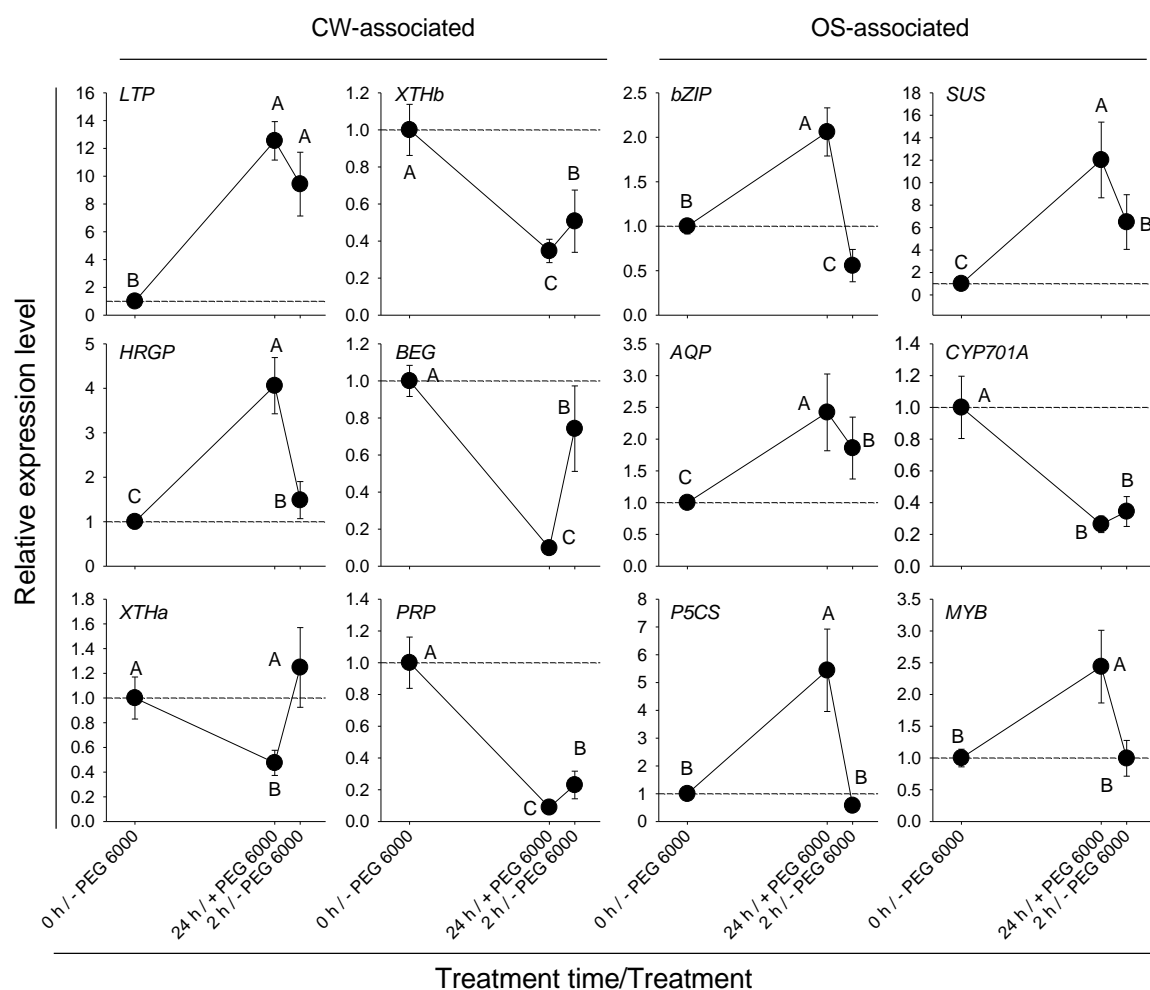
Figure 8 Relative expression level of CW- and OS-associated genes in 1-cm root tips of common bean genotype VAX 1 under OS (-0.60 MPa OP). Plants were pre-cultured in a simplified nutrient solution containing 5 mM $CaCl_2$, 1 mM KCl, and 8 μM H_3BO_3 for 48 h for acclimation and pH adaptation, then the plants were transferred into a simplified nutrient solution containing PEG 6000 (150 g L^{-1}) for 24 h; then the plants were allowed to recover in a simplified nutrient solution for 2 h. The background value (dashed line) presents the calibrated reference using untreated plants. qRT-PCR was performed using the *β-tubulin* gene as internal standard. Bars represent means ± SD, n = 3. Means with different capital letters are significantly different at $P < 0.05$ (Tukey test) for the comparison of treatment periods.

Discussion

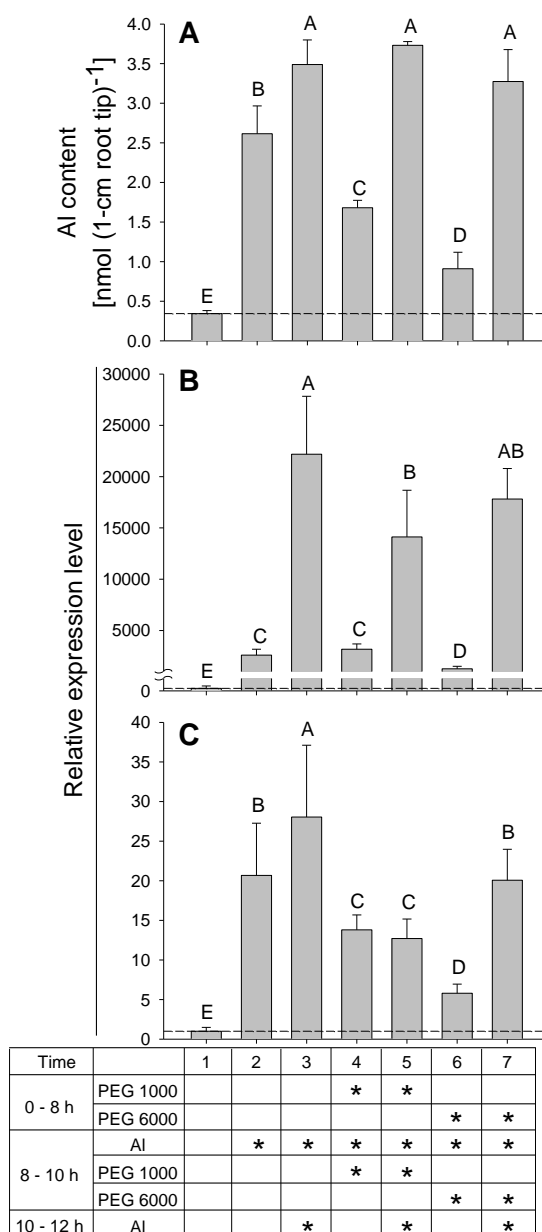In the CW of the root apex Al is primarily bound to the negatively charged carboxylic groups (COO⁻) provided by de-methylated pectin (Blamey et al., 1990; Horst, 1995; Horst et al., 2010). The exclusion of Al from the root tip apoplast is a prerequisite for the reduction of Al-induced inhibition of root elongation and thus Al resistance in common bean which is conferred by citrate exudation (Rangel et al., 2009; Horst et al., 2010). The role of Al exclusion from the root tip for Al resistance is corroborated by the current study demonstrating that the PEG (OS)-induced improvement of root growth under Al stress was related to a reduction of Al accumulation in the root tip (Fig. 1). The PEG (OS)-induced reduction of Al accumulation was due neither to enhanced citrate exudation, precipitation or complexation of Al^{3+} in the PEG treatment solution nor to reduction of CW negativity, but was attributed to the reduction of cell-wall porosity which limits the Al flux into the apoplast (Yang et al., 2010). This conclusion is based on the specificity of the exclusion for Al compared to La, Sr, and Rb and is consistent with their hydrated ionic radii ($Al^{3+} > La^{3+} > Sr^{2+} > Rb^+$) (Yang et al., 2010). In this study, a higher reduction of Al accumulation in PEG 6000 than in PEG 1000-treated plants was observed (Fig. 1). This differential change in Al accumulation is related to the molecular size and the estimated hydrodynamic radius (PEG 6000 > PEG1000) of the applied PEGs. The higher the hydrodynamic radius of the osmotic solute, the better was the exclusion from the apoplast and thus the higher level of dehydration of the apoplast (Kuga, 1981; Yang et al., 2010). The removal of PEG from the pre-treatment solution quickly allowed accumulation of Al in the root tip (Fig. 4A) indicating that the CW can rapidly recover from the shrinkage and structural alteration caused by OS independent of the osmotic solute used.

In agreement with the highly sensitivity reaction of the *MATE* and *ACCO* gene expression in response to Al in common bean reported by Eticha et al. (2010), a significant correlation among *MATE* and *ACCO* gene expression, root elongation and the Al concentration in the root tips of common bean was found (Fig. 2). PEG treatment alone had no effect on the expression of both genes (Fig. 3) providing opportunities to further clarify the PEG-induced reduction of Al accumulation in the root tips and Al-induced inhibition of root elongation using the expression of the *MATE* and *ACCO* genes as sensitive indicators of Al toxicity. As expected, the OS-induced exclusion of Al from the root apex and the improvement of root growth were accompanied by a decrease in gene expression of *MATE* and *ACCO* (Fig. 2) confirming that OS reduces Al injury.

In this study the results generated from SuperSAGE could be well confirmed by qRT-PCR in OS-treated bean root tips (Fig. 7), indicating the reliability of SuperSAGE. However, about 49% of the UniTags generated from SuperSAGE did not match with previously known genome and EST sequences found in public databases (Table 3). This may have hampered the identification of genes responding to OS in the root tips. Among the differentially expressed genes approximately 55% of the unitags matched to *P. vulgaris* EST databases (Table 3). The fact that nearly half of the tags generated by SuperSAGE did not match with previously known sequences could be attributed to the nature of the 26 bp tags. The 26 bp tag fragments were isolated from the NlaIII recognition site (5'-CATG-3') closest to the poly-A tail of the cDNA, which in most cases lie in the 3' untranslated region (3' UTR). Therefore, it appears that the 3' UTR of common bean transcripts are very specific that they did not match with previously known sequences.

Although SuperSAGE is a powerful tool for quantitative gene expression analysis as well as for the discovery of novel genes, the method may miss out some transcripts. Particularly, transcripts which do not have the NlaIII restriction site (5'-CATG-3'), and those which have the restriction site extremely closer to the poly-A tail cannot be recognized. Based on *in silico* sequence data analysis of Arabidopsis RefSeq database, Matsumura et al. (2010) reported that, within 35,286 genes, 2,000 genes (5.7%) did not have NlaIII restriction site. Similarly in common bean, some genes which lack the recognition site for the anchoring enzyme, NlaIII, might have been missed out.

Drought-induced genes were classified into two groups according to microarray analysis in *Arabidopsis* (Shinozaki et al., 2003). The first group code for proteins which probably function in stress tolerance, such as late embryogenesis abundant proteins, osmotin, key enzymes for osmolyte biosynthesis such as proline, water channels, sugar and proline transporters, and lipid-transfer proteins. It has been reported that dehydration induced the expression of osmoregulation-related genes such as Δ1-pyrroline-5-carboxylate synthase (*P5CS*), sucrose synthase (*SUS)* in the resurrection plant *Craterostigma plantagineum* (Kleines et al., 1999; Rodriguez et al., 2010), maize (*Zea mays*) (Zheng et al., 2004; Spollen et al., 2008) and *Arabidopsis* (Oono et al., 2003). Overexpression of the *P5CS* gene in various plants resulted in elevated proline production and improved OS tolerance (Bartels and Sunkar, 2005). Also, it was found that some water transport-related *AQPs* (aquaporin family protein) genes were up-regulated by drought in *Arabidopsis*, upland rice (*Oryza sativa*) and grapevine (*Vitis vinifera*) (Alexandersson et al., 2005, 2010; Lian et al., 2006; Vandeleur et al., 2009), which may trigger greater membrane water-permeability

facilitating water flux (Bartels and Sunkar, 2005).

The second group comprises genes coding for regulatory proteins involved in signal transduction and transcription factors such as *bZIP*, *MYB*, *MYC* and *DREB* (Shinozaki and Yamaguchi-Shinozaki, 2007). The *bZIP* and *MYB* genes are transcription factors involved in an ABA-dependent pathway mediating gene expression in plants during OS (Shinozaki and Yamaguchi-Shinozaki, 2007). Rodriguez-Uribe and O'Connell (2006) found that a root-specific *bZIP* transcription factor is responsive to water deficit in tepary bean (*Phaseolus acutifolius*) and common bean, which may allow the plant to maintain root elongation. More recently the *OsbZIP23* gene in rice and the *MYB96* gene in *Arabidopsis* were found to confer drought resistance (Xiang et al., 2008; Seo et al., 2009). In addition, the cytochrome P450s superfamily (CYP) may serve as mono-oxygenases involved in the biosynthesis of metabolites conferring abiotic stress tolerance (Schuler and Werck-Reichhart, 2003).

Based on this information, the OS-associated genes *SUS*, *P5CS*, *AQP*, *CYP701A*, *bZIP*, and *MYB* were selected to underpin the PEG-induced dehydration and rehydration in the root tips in the present study. All of these genes were significantly up-regulated by OS stress with the exception of *CYP701A*, while the removal of the PEG stress for only two hours rapidly reversed the gene expression to the control level for *P5CS*, *bZIP* and *MYB* (Fig. 8), suggesting a differentially response of gene expression to dehydration and rehydration in common bean. The quick reversal of *bZIP* and *MYB* genes expression after removal of the PEG stress may support the recovery of root elongation within two hours (data not shown) by mediating the expression of ABA-regulated genes, since it was reported that in maize the accumulation of ABA in the root tips is required for the maintenance of primary root elongation at low water potentials (Sharp et al., 2004). P5CS catalyzes the first committed and rate-limiting step for proline biosynthesis in plants (Kavi Kishor et al., 2005). Besides osmotic adjustment, proline also functions as a major constituent of CW structural proteins in plants (Nanjo et al., 1999). In *P5CS* antisense transgenic *Arabidopsis thaliana* plants proline (pro) and hydroxyproline (hyp) contents in hydrolysates of a purified CW fraction were specifically and significantly reduced indicating that proline deficiency affected the biosynthesis of CW matrix proteins, such as proline-rich proteins (PRPs) and hydroxyproline-rich glycoproteins (HRGPs) (Nanjo et al., 1999) which could provide mechanical support for cells under stressed conditions (Cosgrove, 1997). Therefore, the rapid reversal of *P5CS* gene expression after the removal of PEG stress may allow recovery of CW porosity by modifying the CW structural

properties. For further discussion of the OS-induced expression of *PRP* and *HRGP* genes see below in the discussion.

Among the OS-regulated genes, CW synthesis and organization-related genes were mostly down-regulated (Fig. 6) providing an opportunity to identify genes involved in the OS-induced alteration of CW porosity. Water loss in plant tissues reduces turgor pressure and so directly affects the extensibility of the plant CW. In maize, Sharp et al. (2004) reported that the extent of osmotic adjustment in root tip is insufficient to maintain turgor under severe water deficit. The maintenance of root elongation requires the enhancement of longitudinal CW extensibility under water stress (Sharp et al., 2004; Yamaguchi and Sharp, 2010). Some genes may play a role in CW extension during dehydration. For example, it was reported that *LTP* (lipid transfer proteins) are associated with hydrophobic wall compounds, causing non-hydrolytic disruption of the cell wall and subsequently facilitating wall extension in tobacco (Nieuwland et al., 2005). Our study showed that the expression of an *LTP* gene in the root tips of bean was significantly enhanced by OS (Fig. 8) suggesting that this gene may contribute to the maintenance of the root elongation of common bean under OS (Fig. 1).

Structural proteins are one of the main components of the growing plant CW. The CW structural proteins were classified according to their predominant amino acid composition, e.g. HRGP, glycine-rich protein, and PRP (Cosgrove, 1997). In our studies, we observed differential expression of genes encoding HPRG and PRP proteins in the root tips of common bean by OS (Fig. 8, Supporting Information Table S2). These proteins can rapidly be insolubilized in the CW during stress condition, such as upon wounding (Showalter, 1993; Cosgrove, 1997). In contrast, two proline-rich glycoproteins of 33 and 36 KDa (p33 and p36), similar to soybean PRP2, were highly accumulated in the soluble fraction of the cell walls in common bean in response to water deficit (Covarrubias et al., 1995; Battaglia et al., 2007). However, this does not exclude that higher amounts of proline-rich glycoproteins are tightly bound with the CW polymers in immobilized form, since only very low amounts of p33/p36 were detected in the soluble fraction of cell walls of well watered bean hypocotyls, while immunolocalization indicated that these proteins were abundantly localized in the cell corners of the cortex, epidermis, pith, vascular cells and phloem. However, we found that the expression of one *PRP* gene was significantly suppressed by OS and recovery of roots from OS could not rapidly restore the expression of this gene, which was in contrast with the *HRGP* gene (Fig. 8). The expression of a *HRGP* gene was significantly enhanced by OS, and withdrawing of OS rapidly restored the

expression of this gene (Fig. 8). The HRGP proteins are particularly abundant in dicots compared to other structural proteins (Showalter, 1993); thus the role of the *HRGP* gene appears to be important in the OS-induced modification of the CW in common bean. Once the HRGP is secreted into the wall, it will be rapidly insolubilized. The insolubilization of HRGP may be mediated by the water deficit-induced enhancement of hydrogen peroxide and catalyzed by a CW peroxidase. This response is thought to be an ultra-rapid stress-response reaction that serves to further strengthen the cell wall (Showalter, 1993; Zhu et al., 2007).

It has been reported that the pectin matrix is the decisive factor of CW porosity (Baron-Epel et al., 1988). Although the pectin content in the root tips of bean was reduced approximately by 25% due to PEG 6000-induced OS (Yang et al., 2010), this level of decrease of pectin content may not drastically alter CW porosity. It thus appears that the reduction of CW porosity may be largely due to the physical shrinkage of the CW and further enhanced by the deposition of other wall components, such as structural proteins as schematically depicted in Fig. 9A. The increased deposition of HRGP proteins in the wall may increase the cross-link between HRGP proteins and other wall components, such as pectin (Showalter, 1993), and further reinforce a cell-wall barrier, thus impeding Al uptake (Fig. 9B).

The shrinkage of the CW resulting from PEG 6000-induced dehydration of the apoplast causes adhesion and cross-linking of wall polymers through hydrogen bonding. This bonding will be enhanced by removal of water from the apoplast and is likely to cause an irreversible bonding between polymers resulting in altered biophysical CW properties (Fig. 9A; Moore et al., 2008; Yang et al., 2010), unless some CW loosening or modifying genes/enzymes were re-induced/activated. In *Arabidopsis*, water deficit consistently down-regulated the expression of genes involved in CW synthesis and modification (Bray, 2004). Similarly, also in common bean the number of down-regulated genes related to CW synthesis and organization under OS was two-fold higher than that of up-regulated genes (Fig. 6). Several CW proteins/enzymes are believed to play key roles in modifying the wall structure and controlling wall extension. These include expansin, xyloglucan endotransglucosylase/hydrolase (XTH), and glucanases (Wu and Cosgrove, 2000; Bray, 2004; Sharp et al., 2004; Moore et al., 2008).

The XTH proteins are a large family of CW proteins which have 33 members known in the *Arabidopsis* genome, and they are involved in controlling CW extensibility through the

cleavage and reformation of bonds between xyloglucan chains (Rose et al., 2002; Bray, 2004). Under soil moisture deficit, the genes encoding XTH were among the commonly down-regulated genes when 23 genes annotated in the *XTH* family were analyzed (Bray, 2004). In Chickpea (*Cicer arietinum*) Romo et al. (2005) found that the expression of the *CaXTH1* gene encoding the XTH protein was repressed by PEG treatment which inhibited epicotyl growth. The removal of PEG resulted in restoration of the normal expression level of this gene suggesting the involvement of XTH encoded by *CaXTH1* in cell-expansion. Spatial analysis of CW proteomics in maize primary roots indicated that the abundance of XTH proteins was significantly reduced by water deficit in the first three millimeters of the root apex (Zhu et al., 2007). In the present study, qRT-PCR results showed that the expressions of *XTHa* and *XTHb* genes in the root tips of common bean were significantly reduced by PEG-induced dehydration of the apoplast (Fig. 8). Withdrawal of PEG from the pre-treatment solution rapidly allowed the recovery of the expression level of the *XTHa* gene (Fig. 8), supporting the view that the *XTHa* gene may be involved in the CW modification during the recovery period of the apoplast from dehydration (Fig. 9B).

In addition, Glucan endo-1,3-beta-glucosidase (or beta-1,3-glucanase) (BEG) may also play an important role in the OS-induced wall modification and thus influencing Al accumulation that was observed in the present study (Fig. 9B). BEGs are abundant proteins found in all higher plants. They are known to be involved in pathogen defense as well as a wide range of normal developmental processes and can hydrolytically cleave the 1,3-β-linked glucans, a major component of the fungal cell wall (Minic and Jouanin, 2006). BEG belongs to the family of 17 plant glycoside hydrolases, and molecular studies suggested that this enzyme shares a common ancestry with beta-1,3-1,4-glucanase (Minic and Jouanin, 2006; Borad and Sriram, 2008). Although the function of many cell-wall enzymes has yet to be determined, a role of BEG in the OS-induced CW modification of common bean root tips in the present study is likely, since PEG-induced OS significantly reduced the *BEG* gene, but removal of PEG rapidly recovered its expression (Fig. 8). Wu et al. (2001) reported that the induction of BEG in the micropylar tissues of imbibed tomato (*Lycopersicon esculentum* Mill.) seeds can be inhibited by ABA. Therefore, the expression of the *BEG* gene may be repressed by the OS-induced accumulation of ABA in the root apex of plants. This is corroborated by the observation that water deficit increased the accumulation of ABA in the root apex of maize (Sharp et al., 2004; Yamaguchi and Sharp, 2010), which consequently reduced the abundance of BEG proteins in the root tips (Zhu et al., 2007).

In the present study, PEG treatment by itself inhibited root growth by 30% compared to the control, possibly by reducing CW expansion. While sole Al treatment inhibited root growth by 80%, combined Al and PEG treatment only resulted in 40% inhibition (See Fig. 1A). Therefore, the PEG-induced recovery from Al injury resulted from the reduced Al accumulation in the root tips of common bean as a consequence of PEG-induced reduction of CW porosity (Yang et al., 2010). The enhanced expresseion of the *HRGP* and reduced expression of the *XTH* and *BEG* genes may contribute to the reduction of CW porosity, but the main cause of the reduction of CW porosity by PEG is the osmotic stress-induced physical collapse of CW structure (presented in Fig. 9A). The main role of HRGP, XTH and BEG is the involvement in the recovery of CW porosity (Fig. 9B).

In conclusion, our results suggest that several CW modifying- and assembling-related genes such as *XTHs*, *BEG* and *HRGP* may play important roles in the PEG (OS)-induced changes of CW porosity leading to reduced Al accumulation in the root tips. There is a need for further research to determine the role of functional genes related to CW modification under conditions of water deficit.
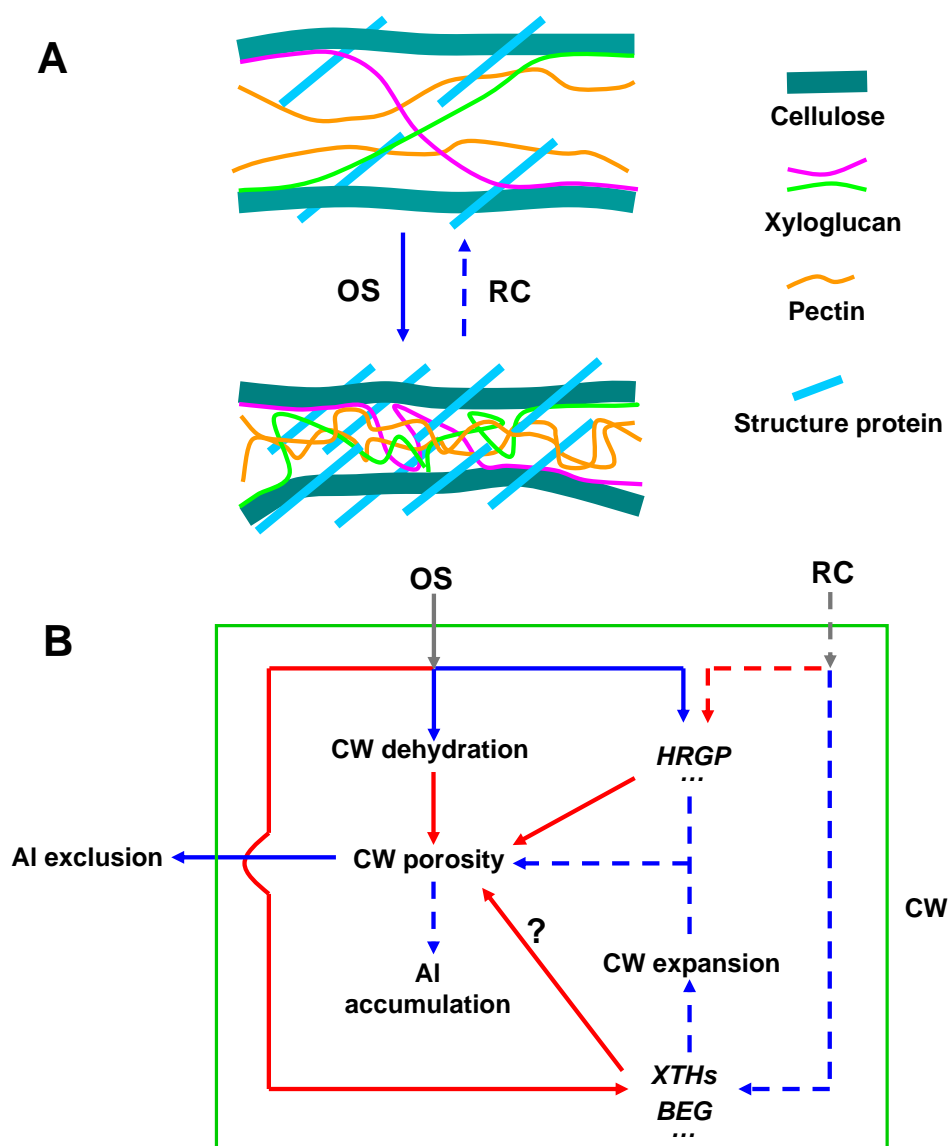
Figure 9 (A) A model representing the effect of osmotic stress (OS) on the cell wall (CW) structure of common bean plants. (B) Hypothesis for the possible role of CW modification-related genes or structure proteins in the OS-induced change in CW porosity and thus Al binding to the CW. In (B): the blue and red arrows denote up and down-regulated changes, respectively; the solid and dashed arrows indicate the effect of OS and recovery (RC), respectively. ? = uncertain; … = unidentified genes. Green line frame represent CW.

CHAPTER 3

Proteomic analysis of polyethylene glycol-induced osmotic stress in root tips of common bean (*Phaseolus vulgaris* L.)

Zhong-Bao Yang[1], Dejene Eticha[1], Hendrik Führs[1], Sébastien Gallien[2], Dimitri Heintz[3], Alain Van Dorsselaer[2], Idupulapati Madhusudana Rao[4], Walter Johannes Horst[1]

[1] Institute of Plant Nutrition, Leibniz Universität Hannover, Herrenhaeuser Str. 2, D-30419 Hannover, Germany

[2] Laboratoire de Spectrométrie de Masse Bio-organique, IPHC-DSA, Université de Strasbourg, CNRS, UMR7178, 25 rue Becquerel, 67087 Strasbourg, France

[3] Institut de Biologie Moléculaire des Plantes (IBMP), 28 rue Goethe, CNRS-UPR2357, Université de Strasbourg, 67083 Strasbourg, France

[4] International Center for Tropical Agriculture (CIAT), AA 6713, Cali, Colombia

(To be submitted)

Abstract

Previous work showed that PEG induced osmotic stress reduced cell-wall (CW) porosity limiting aluminium (Al) uptake by root tips of common bean (*Phaseolus vulgaris* L.). A subsequent transcriptomic study provided genes involved in CW adjustment to osmotic stress. In this study a proteomic approach was used to analyze osmotic stress-induced proteins to further improve our understanding of how osmotic stress affects Al accumulation. Analysis of total soluble proteins in root tips indicated that in total 22 proteins were differentially regulated by osmotic stress; these proteins were functionally categorized. 77% of the total expressed proteins were involved in metabolic pathways particularly of the carbohydrate and amino acid metabolism. An apoplastic proteomic analysis suggested that five proteins were reduced and seven proteins were increased by osmotic stress. Investigation of the total soluble phophoproteome highlighted dehydrin of which the phosphorylation state was increased but not its abundance under osmotic stress. This is supposed to play a major protective role in the osmotic stress-induced physical breakdown of the CW structure and thus the maintenance of the reversibility of CW extensibility during recovery from osmotic stress. The proteomic analysis provided novel insights into the complex mechanisms of osmotic stress-induced reduction of Al accumulation in the root tips of common bean and highlights a key role of CW structure modification.

Key words: apoplast, cell wall, common bean, phophoproteomics, proteomics, dehydrin, root tips

Introduction

Common bean (*Phaseolus vlugaris* L.) is the major food legume for human nutrition worldwide, and a major source of calories and protein particularly for people in undeveloped countries in the tropics (Graham, 1978; Rao, 2001). Under field conditions, common bean often experiences different abiotic stresses including drought, toxicities of aluminium (Al) and manganese, low soil fertility, and high temperatures (Thung and Rao, 1999; Singh, 2001; Ishitani et al., 2004). About 60% of common bean production in the world are grown in areas subjected to drought stress, and consequently results in a low level of average global yield production (Graham and Ranalli, 1997; Beebe et al., 2008).

In plants growing in dry soil, both shoot and root growth are hampered (Westgate and Boyerm 1985; Sharp et al., 1988) While an important feature of the root system response to soil drying is, the maintenance of root elongation at water potentials that are low enough to inhibit shoot growth completely (Sharp et al., 2004; Yamaguchi and Sharp, 2010), which facilitating water uptake from subsoil (Sponchiado et al., 1989; Serraj and Sinclair, 2002). Investigations on the spatial distribution of the response of root-elongation to drought indicated that the elongation was preferentially maintained at the root apex (Sharp et al., 2004; Yamaguchi and Sharp, 2010; Yamaguchi et al., 2010). Physiological studies on the response of the primary root growth of maize to water stress have demonstrated the involvement of three possible mechanisms: osmotic adjustment, modification of cell-wall (CW) extension properties and ABA accumulation (Sharp et al., 2004; Yamaguchi and Sharp, 2010). Water loss from the plant cells controls turgor pressure and so directly affects the extensibility of the plant CW (Moore et al., 2008). The effect of drought stress on CW structure and properties has been extensively studied in maize roots at physiological and molecular level (Wu and Cosgrove, 2000; Fan and Neumann, 2004; Sharp et al., 2004; Fan et al., 2006; Poroyko et al., 2007; Zhu et al., 2007; Spollen et al., 2008; Yamaguchi and Sharp, 2010).

Our previous physiological study demonstrated that the osmotic stress (OS, polyethylene glycol, PEG)-induced reduction of CW porosity enhanced Al resistance in common bean by the reduction of Al accumulation in the root tips (Yang et al., 2010), the main Al-sensitive root zone (Rangel et al., 2007). A transcriptomic analysis indicated that among the osmotic stress-regulated genes, CW synthesis and organization-related genes were mostly down-regulated, and the CW modification genes *XTH* (xyloglucan endotransglucosylase/hydrolase) and *BEG* (glucan endo-1,3-beta-glucosida or

beta-1,3-glucanase), and the structure protein hydroxyproline-rich glycoprotein (HRGP) were supposed to be involved in modification of CW porosity (Yang et al., 2011). However, transcriptomic profiling sometimes fails to unequivocally reveal the final functions of regulations of biological processes e.g. due to gene redundancy or post-translational modifications (Toorchi et al., 2009; Zörb et al., 2010). Post-translational modifications, such as phosphorylation and glycosylation, can result in a dramatic increase in proteome complexity without a concomitant increase in gene expression (Jensen, 2004; Rose et al., 2004; Jiang et al., 2007). Therefore, a proteomic and phosphoproteomic approach was performed in this study (i) to better understand the PEG-induced changes of osmotic stress and CW-related proteins in root tips of the common bean genotype VAX 1, and (ii) to further classify the potential mechanisms of CW proteins involved in the adjustment of wall porosity.

Materials and Methods

Plant materials and growing conditions

Seeds of common bean genotype VAX (Al-sensitive) were germinated on filter paper sandwiched between sponges. After three days, uniform seedlings were transferred to a continuously aerated simplified nutrient solution containing 5 mM $CaCl_2$, 1 mM KCl, and 8 μM H_3BO_3 (Rangel et al., 2007). Plants were cultured in a growth chamber under controlled environmental conditions at 16/8 h light/dark cycle, 27/25 ℃ day/night temperature, 70% relative air humidity, and a photon flux density of 230 μmol m^{-2} s^{-1} of photosynthetically active radiation at mid plant height. The pH of the nutrient solution was gradually lowered to 4.5 within two days. Then the plants were transferred into a simplified nutrient solution (see above) without or with $AlCl_3$, PEG 6000 (Sigma-Aldrich Chemie GmbH, Steinheim, Germany). 1-cm root tips were harvested and immediately frozen in liquid nitrogen in Eppendorf vials for protein extraction. The osmotic potential (OP) of PEG 6000 (150 g L^{-1}) solution was -0.60 MPa, measured with a cryoscopic osmometer (Osmomat 030, Gonotec GmbH, Berlin, Germany).

Measurement of root-elongation rate

Two hours before the treatment was initiated tap roots were marked three centimetres behind the root tip using a fine point permanent marker (Sharpie blue, Stanford) which did not affect root growth during the experimental period. Afterwards, the plants were transferred into a simplified nutrient solution (see above) without or with PEG in the absence or presence of Al. Root elongation was measured after the treatment period using mm scale.

Determination of cell-sap osmotic potential

The root-tip cell-sap was extracted and measured according to Tabuchi et al. (2004) with modifications. After treating the plants with PEG (0 and 150 g L^{-1}) for 24 h, 30 root tips of 1 cm length were excised and transferred into micro-filtration tubes with a membrane pore size of 0.45 μm (GHP Nanosep MF Centrifugal Device, Pall Life Sciences, Ann Arbor, USA) in a 1.5 mL plastic tube after removing the free solution on the surface of roots by brief centrifugation. Then the samples were immediately frozen in liquid nitrogen and stored at -80 ℃ until use. The root tips were thawed at room temperature, and then

centrifuged at 5,000 g for 10 min at 4 ℃. More than 50 μL cell sap was obtained from 30 root tips. The osmotic concentration of the cell sap was determined with a cryoscopic osmometer (Osmomat 030, Gonotec GmbH, Berlin, Germany), and the osmotic potential was calculated according to the van't Hoff equation (Nobel, 1991): $\pi = -nRT$, where π is the osmotic potential, R the gas constant, T the absolute temperature, and n the molar concentration.

Extraction of total soluble protein

Approximately 200 root tips of 1 cm length were harvested after treating the plants without or with 150 g L^{-1} PEG for 24 h, and ground with mortar and pestle in liquid nitrogen. The homogenized sample powder was suspended in 4 mL extraction buffer (500 mM Tris, 50 mM EDTA, 100 mM KCl, 700 mM sucrose, 25 mM sodium fluoride, 1 mM sodium molybdate, 50 mM sodium pyrophosphate, 2% v/v β-mercaptoethanol and protease inhibitor (1 tablet/10 ml aliquots, Sigma-Aldrich Chemie GmbH, Steinheim, Germany) and incubated for 10 min on ice. Afterwards, an equal volume of water-saturated phenol was added and incubated for another 10 min at room temperature on a rotary shaker. The aqueous and organic phases were separated by centrifugation for 10 min at 11,000 g and 4 ℃. The phenolic phase was re-extracted with an equal volume of extraction buffer and centrifuged again. Phenol phases were combined and supplemented with 5 volumes of 0.1 M ammonium acetate in methanol and incubated overnight at -20 ℃ for protein precipitation. After centrifugation at 11,000 g for 3 min at 4 ℃, precipitated proteins were washed three times with ammonium acetate in methanol and finally with acetone. Pellets were air-dried. Extracted proteins were redissolved in rehydration solution (see below) for 2-DE analysis. Protein concentration of extracts were determined in rehydration solution using the 2-D Quant Kit$^{©}$ (GE Healthcare, Munich, Germany) according to the manufacturer's instructions.

Extraction of apoplastic proteins

Apoplastic proteins were extracted from control (-PEG) and PEG-treated root tips of 1 cm length of bean genotype VAX 1 for 24 h, according to the methods described by Zhu et al. (2006). Approximately 2,000 root tips (1 cm length) were excised and transferred into 20 mM ice-cold K$_2$PO$_4$ solution (pH 6.0). The root tips were then rinsed twice with 0.01 M MES buffer and oriented vertically with the root apex at the top in a filter column with a membrane pore size of 0.45 μM (MACHEREY-NAGEL, Düren, Germany). The filter

column was placed into a vial and the whole assembly was held on ice. Twenty millilitres of ice-cold 0.01 M MES buffer (pH 5.5) containing 0.2 M KCl plus protease inhibitors (1 mM phenylmethylsulfonyl fluoride and 5 µL of protease inhibitor cocktail; Sigma, Germany) were added to the vial submerging the plant tissue. The whole assembly containing the root tips was vacuum infiltrated at -50 kPa for 15 min and for another 5 min without vacuum. The vial was removed, drained, and excess buffer was blotted away from the root tips through the bottom of the filter column. The filter column with root tips were then transferred to a new vial and centrifuged for 15 min at 1,000 *g*. All steps were conducted on ice or in a cold room at 4 ℃. Infiltration and centrifugation were then repeated twice. Apoplastic extracts of resulting three fractions were combined in Vivaspin 6 Centrifugal Concentrators (5,000 MWCO PES, VIVASCIENCE, UK) and centrifuged for 2 h at 5,000 *g*. Precipitation of apoplastic proteins was done as described in previous section.

In each fraction of apoplastic protein extracts, the activity of malate dehydrogenase (MDH), a commonly accepted marker for cytosolic contamination, was assayed according to Bergmeyer and Bernt (1974) and the protein yield was quantified according to the method of Bradford (1976).

Two dimensional isoelectric focusing (2D IEF) / sodium dodecyl sulphate-polyacrylamide gel electrophoresis (SDS-PAGE)

IEF/SDS-PAGE was carried out as described by Führs et al. (2008). Basically an IPGphor system (GE Healthcare, Munich, Germany) and immobiline DryStrip gels (18 cm) with a nonlinear pH gradient of 3-11 (for total soluble and apoplastic proteins) or 4-7 (for total soluble phosphoproteins) were used. Proteins (about 1,000 µg and 80 µg for total and apoplastic soluble proteins, respectively) were dissolved in rehydration solution (8 M urea, 2% w/v CHAPS, 0.5% v/v carrier ampholyte mixture (IPG bufferm pH 3-11 or 4-7 NL; GE Healthcare), 50 mM dithiothreitol, 12 µL/mL DeStreak (GE Healthcare) and a trace of bromophenol blue) and loaded onto individual gel strips. Focussing was done according to Werhahn and Braun (2002). Afterwards, the focused IPG strips were incubated with equilibration solution (50 mM Tris-HCl (pH 8.8), 6 M urea, 30% v/v glycerol, 2% w/v SDS and bromophenol blue) supplemented with (i) 1% w/v dithiothreitol and (ii) 2.5% w/v iodoacetamide each for 15 min. Then the strips were placed horizontally onto second dimension SDS gels and proteins were separated according to Schägger and von Jagow (1987). Afterwards, for total soluble and apoplastic proteins, 2-D gels were stained with

colloidal Coomassie-blue (CBB)-G250 according to Neuhoff et al. (1985, 1990).

For phosphoprotein detection, 2D gels were stained with a modified protocol using Pro-Q Diamond Phosphoprotein Stain (Pro-Q DPS; Molecular Probes) according to Agrawal and Thelen (2009). Following image acquisition gels stained with Pro-Q DPS-stained gels, the gels were stained with CBB-G250 to detect total proteins (Neuhoff et al., 1985; 1990). In each treatment of the independent experiment, three biologically independent replicates were performed.

Image acquisition, image analysis and statistical analysis

Image acquisition of coomassie-stained gels was done using an Epson Expression 1600 scanner (Epson, Mehrbusch, Germany) at 300 dpi. Resolutions were stored as TIFF files. Phosphoprotein detection on gels was done using a Typhoon^{TM} Variable Mode Imager using 532 nm excitation and 580 nm bandpass emission filter at 100 μm resolution. Images were stored as 16-bit TIFF files (Agrawal and Thelen, 2009). 2-D gel image analysis of coomassie and for phosphoproteins stained gels was carried out using ImageMaster^{TM} 2D Platinum Software 6.0 (GE Healthcare). To compensate the variability due to sample loading, gel staining and destaining, the spot volume was normalized as relative volume, dividing each spot volume value by the sum of the total spot volume of the corresponding gel. In this study, significantly changed proteins between control and treatment were defined as proteins which were more or less abundant by a factor of 1.5 or 0.67, respectively, with $P \leq 0.05$ (Student's t-test) unless otherwise specified.

Mass spectrometric analysis and data interpretation

After manually picking of protein spots with changed abundance each spot was dried under vacuum. In-gel digestion was performed with an automated protein digestion system, MassPREP Station (Micromass, Manchester, UK). The gel slices were washed three times in a mixture containing 25 mM NH_4HCO_3:acetonitrile (1:1, v/v). The cysteine residues were reduced by 50 μL of 10 mM dithiothreitol at 57 ℃ and alkylated by 50 μL of 55 mM iodacetamide. After dehydration with acetonitrile, the proteins were cleaved in the gel with 40 μL of 12.5 ng μL^{-1} of modified porcine trypsin (Promega, Madison, WI, USA) in 25 mM NH_4HCO_3 at room temperature for 14 h. The resulting tryptic peptides were extracted with 60% acetonitrile in 0.5% formic acid, followed by a second extraction with 100% (v/v) acetonitrile.

Nano-LC-MS/MS analysis of the resulting tryptic peptides was performed using an Agilent 1100 series HPLC-Chip/MS system (Agilent Technologies, Palo Alto, USA) coupled to an HCT Ultra ion trap (Bruker Daltonics, Bremen, Germany). Chromatographic separations were conducted on a chip containing a Zorbax 300SB-C18 (75 μm inner diameter×150 mm) column and a Zorbax 300SB-C18 (40 nL) enrichment column (Agilent Technologies).

HCT Ultra ion trap was externally calibrated with standard compounds. The general mass spectrometric parameters were as follows: capillary voltage, –1750 V; dry gas, 3.0 L min^{-1}; dry temperature, 300 ℃. The system was operated with automatic switching between MS and MS/MS modes. The MS scanning was performed in the standard-enhanced resolution mode at a scan rate of 8100 m/z s^{-1} with an aimed ion charge control of 100,000 in a maximal fill time of 200 ms and a total of four scans were averaged to obtain a MS spectrum. The three most abundant peptides and preferentially doubly charged ions were selected on each MS spectrum for further isolation and fragmentation. The MS/MS scanning was performed in the ultrascan resolution mode at a scan rate of 26,000 m/z s^{-1} with an aimed ion charge control of 300,000 and a total of six scans were averaged to obtain an MS/MS spectrum. The complete system was fully controlled by ChemStation Rev. B.01.03 (Agilent Technologies) and EsquireControl 6.1 Build 78 (Bruker Daltonics) softwares. Mass data collected during LC-MS/MS analyses were processed using the software tool DataAnalysis 3.4 Build 169 and converted into .mgf files. The MS/MS data were analyzed using the MASCOT 2.2.0. algorithm (Matrix Science, London, UK) to search against an in-house generated protein database composed of protein sequences of Viridiplantae downloaded from http://www.ncbi.nlm.nih.gov/sites/entrez (on 6 March 2008) concatenated with reversed copies of all sequences (23 478 588 entries). Spectra were searched with a mass tolerance of 0.5 Da for MS and MS/MS data, allowing a maximum of one missed cleavage by trypsin and with carbamidomethylation of cysteines, oxidation of methionines, and N-terminal acetylation of proteins specified as variable modifications. Protein identifications were validated when at least two peptides with high quality MS/MS spectra (Mascot ion score greater than 31) were detected. In the case of one-peptide hits, the score of the unique peptide must be greater (minimal 'difference score' of 6) than the 95% significance Mascot threshold (Mascot ion score >51). For the estimation of the false positive rate in protein identification, a target-decoy database search was performed (Elias and Gygi, 2007).

Protein identifications by MS only were carried out for one of the three gel replicates,

because gels obviously were very similar. Also, all analyses allowed to unambiguously identify proteins of the expected molecular mass range.

Statistical analysis

A completely randomized design was used, with four to twelve replicates in each experiment. If not mentioned otherwise, statistical analysis was carried out using SAS 9.2. Means were compared using t or Tukey test depending on the number of treatments being compared. *, **, *** and ns denote significant differences at $P < 0.05$, 0.01, 0.001, and not significant, respectively.

Results

Root elongation rate of bean genotype VAX 1 was inhibited by 31% by a 24-h exposure to 150 g L^{-1} PEG (pH 4.5) in the simplified nutrient solution (Fig. 1A). Since cell expansion is determined by osmotic potential as well as CW extensibility in the root cells and osmotic adjustment plays a major role in plant adaptation to osmotic stress (OS), the osmotic potential of the root cells was examined using an osmometer. The osmotic potential of the cell sap of the root tips was decreased by 24-h treatment with 150 g L^{-1} PEG from -0.55 to -0.96 MPa (Fig. 1B), suggesting osmotic adjustment of root cells by accumulating osmolytes facilitating water uptake into cells and thus adaptation to the PEG-induced osmotic stress.
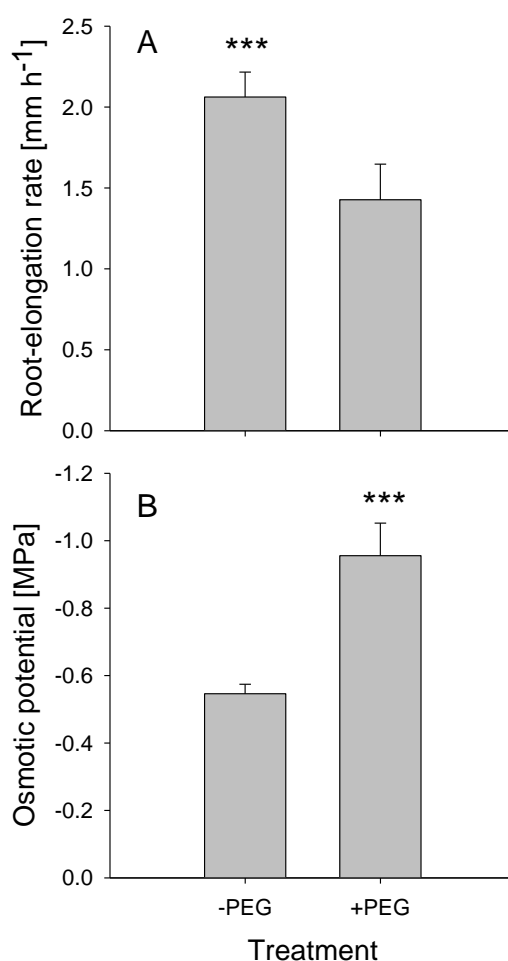
Figure 1 Root-elongation rate (A) and cell sap osmotic potential (B) of 1-cm root tips of the common bean genotype VAX 1 under osmotic stress (0, -0.60 MPa OP). Plants were pre-cultured in a simplified nutrient solution containing 5 mM $CaCl_2$, 1 mM KCl, and 8 μM H_3BO_3 for 48 h for acclimation and pH adaptation, and then treated without or with PEG (150 g L^{-1}) in the simplified nutrient solution for 24 h, pH 4.5. Bars represent means $\pm$ SD, n = 12 for (A) and n = 4 for (B). *** denote significant differences at $P < 0.001$.

To identify the proteins affected by short-term (24 h) PEG-induced osmotic stress, the total soluble proteins were extracted from control (- PEG) and PEG-treated root tips. A total of 716 spots were detected after 2D IEF/SDS PAGE and CBB staining. Using specific threshold parameters (see Materials and Methods section), twenty two proteins were identified exhibiting differential abundance due to the PEG treatment (Fig. 2). Nine of these proteins showed higher abundance in PEG-treated roots and thirteen proteins showed higher abundance in control (- PEG) roots (Fig. 2). Close-ups of gel regions containing proteins of differential abundance are shown in Fig. 3.

The twenty two differentially expressed proteins were analyzed by *de novo* peptide sequencing using ESI MS/MS and identified by sequence comparisons using the NCBI protein database (Table 1). The identified twenty two proteins were classified according to their proposed biological functions using the UniProt database (Table 1; Fig. 4). Among the nine increased proteins the functional categories carbohydrate metabolism, amino acid metabolism, protein processing, transcription and unknown were represented by 45%, 22%, 11%, 11% and 11%, respectively. Among the thirteen decreased proteins (showed in Table 1) the functional categories carbohydrate metabolism, amino acid metabolism, other metabolisms, stress response/defence and protein processing were represented by 38%, 31%, 15%, 8% and 8%, respectively. The functional classification of the identified increased and decreased proteins showed that most of the proteins (77%) were involved in pathways of the primary metabolism (acetoacetyl-CoA thiolase, fructokinase, myo-inositol 1-phosphate synthase, phosphoglycerate mutase, fructokinase-like protein, alcohol dehydrogenase Adh-1, enolase and NADPH-specific isocitrate dehydrogenase in carbohydrate metabolism; S-adenosylmethionine synthetase, D-3-phosphoglycerate dehydrogenase, methionine synthase in amino acid metabolism), showing the importance of the primary metabolism in the response and adaptation of root tips to PEG-induced OS.
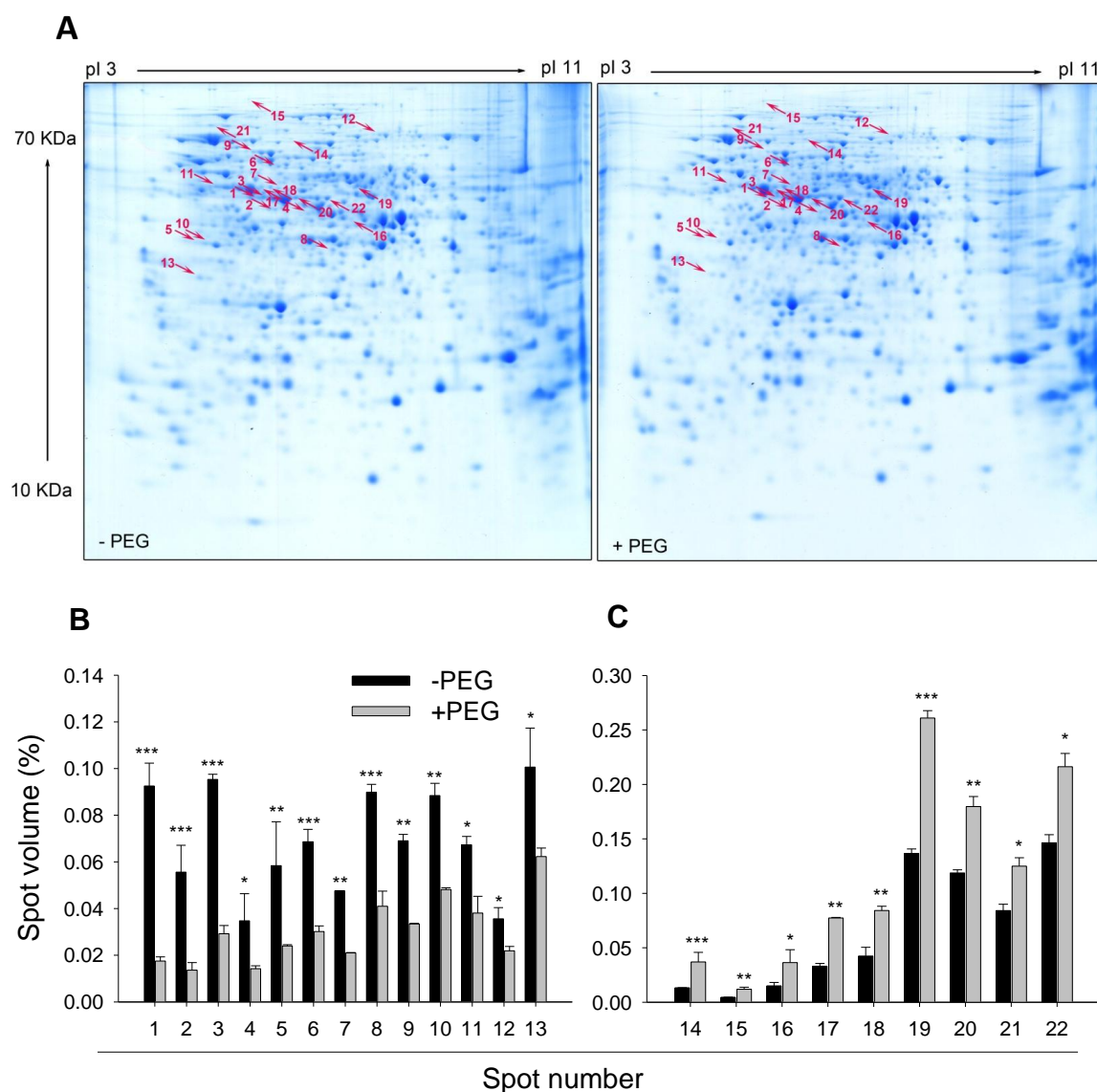
Figure 2 Representative Coomassie-stained 2D IEF/SDS–PAGE gels of the total soluble proteins (A) and the relative spot volumes of the 22 significantly decreased (B) and increased (C) protein spots in the control (-PEG) and PEG-treated root tips of common bean genotype VAX 1. Plants were pre-cultured in a simplified nutrient solution containing 5 mM $CaCl_2$, 1 mM KCl, and 8 μM H_3BO_3 for 48 h for acclimation and pH adaptation, and then treated without or with PEG (150 g L^{-1}) in the simplified nutrient solution for 24 h, pH 4.5. Proteins were extracted from the root tips, separated by 2D IEF/SDS–PAGE, and stained by CBB. Treatment-affected spots were marked by arrows and numbered consecutively. Three biological replications of each treatment were analyzed using the Image Master[TM] 2D PLATINUM Software 6.0. In (B) and (C), bars represent means ± SD, n = 3 and *, ** and *** denote significant treatment differences between means at $P < 0.05$, 0.01 and 0.001, respectively.
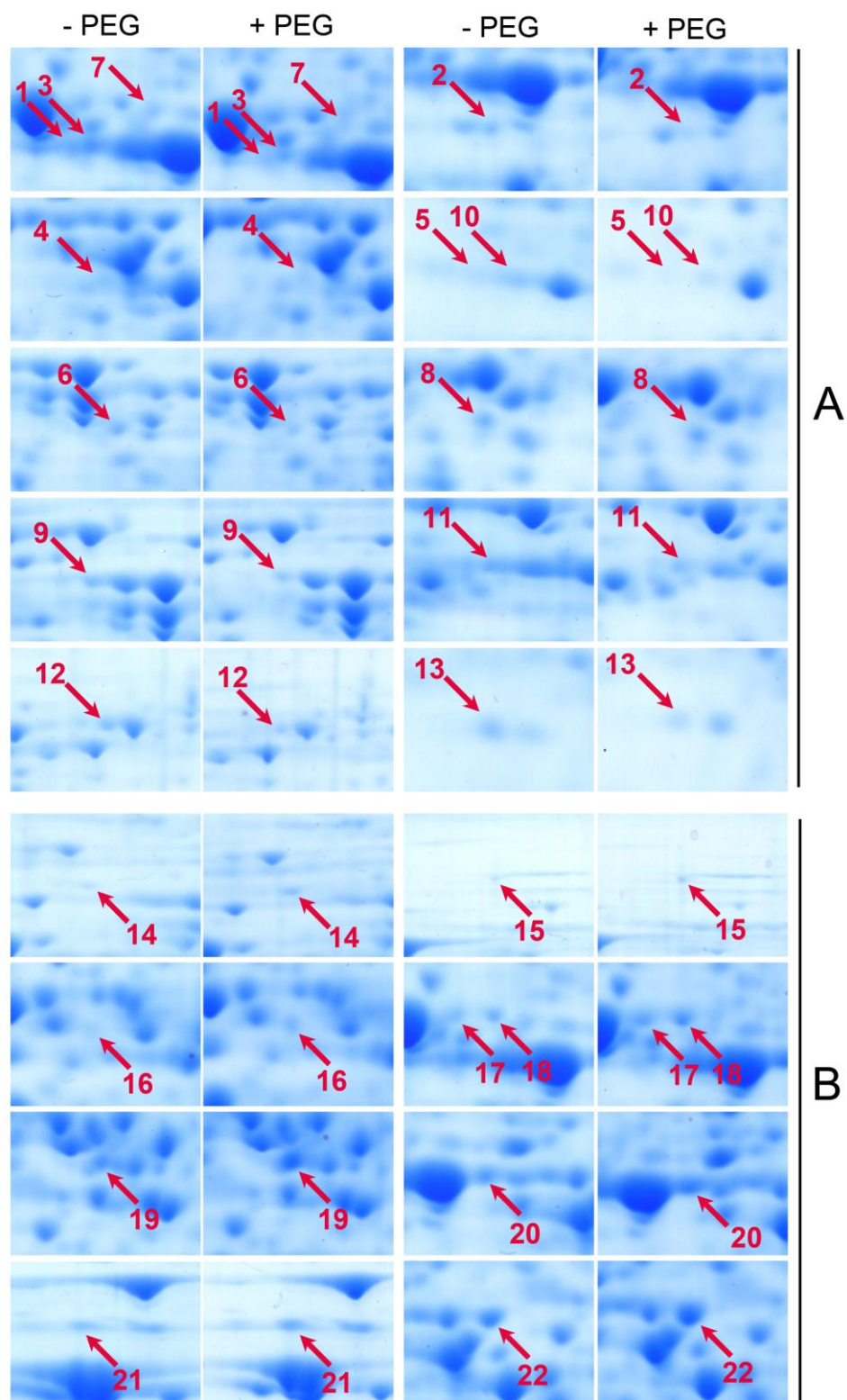
Figure 3 Close-ups of significantly decreased (A) and increased (B) protein spots in response to PEG in the root tips of common bean genotype VAX 1. The Coomassie-stained 2D IEF/SDS–PAGE gels of the total soluble proteins are shown in Fig. 2.

Table 1 The list of the 22 proteins with significantly different abundance in the root tips of common bean genotype VAX 1 in response to PEG. Plants were pre-cultured in a simplified nutrient solution containing 5 mM $CaCl_2$, 1 mM KCl, and 8 μM H_3BO_3 for 48 h for acclimation and pH adaptation, and then treated without or with PEG (150 g L^{-1}) in the simplified nutrient solution for 24 h, pH 4.5. These 22 protein spots were shown in the Coomassie-stained 2D IEF/SDS–PAGE gels of Fig. 2 and Fig. 3. Spot No.: corresponding to the spots number of Figure 2 and Figure 3. FC: fold change (the relative protein spot volume of +PEG treatment to the relative protein spot volume of -PEG treatment). The proteins were identified by nano LC-MS/MS and BLASTed in NCBI database. The protein functions were categoried based on the UniProt database and KEGG pathway.

Spot No.	Identity	MW (Da)	Acc. No.	FC
Carbohydrate metabolism				
4	Acetoacetyl-CoA thiolase (*Medicago sativa*)	41 659,8	ACX47470	0.410
5	Fructokinase (*Arachis hypogaea*)	20 047,7	ACF74294	0.411
7	Myo-inositol 1-phosphate synthase (*Phaseolus vulgaris*)	56 431,4	CAH68559	0.441
9	Phosphoglycerate mutase (*Solanum tuberosum*)	60 271,9	AAD24857	0.484
10	Fructokinase-like protein (*Cicer arietinum*)	26 092,1	CAD31714	0.544
16	Alcohol dehydrogenase Adh-1 (*Glycine max*)	34 407,4	AAC62469	2.425
7	Enolase (*Glycine max*)	47 701,9	AAS18240	2.341
18	Enolase (*Glycine max*)	47 701,9	AAS18240	1.986
22	NADPH-specific isocitrate dehydrogenase (*Glycine max*)	49 124,2	AAA33978	1.500
Amino acid metabolism				
1	S-adenosylmethionine synthetase (*Phaseolus lunatus*)	43 041,9	BAB83761	0.190
2	Methionine adenosyltransferase (*Pisum sativum*)	40 958,3	CAA57581	0.245
3	S-adenosylmethionine synthetase (*Phaseolus lunatus*)	43 041,9	BAB83761	0.307
6	D-3-phosphoglycerate dehydrogenase, putative (*Ricinus communis*)	63 086,7	EEF43612	0.440
20	S-adenosylmethionine synthetase (*Phaseolus lunatus*)	43 041,9	BAB83761	1.514
21	Methionine synthase (*Glycine max*)	84 266,4	AAQ08403	1.500
Other metabolisms				
12	1-deoxyxylulose 5-phosphate synthase (*Chrysanthemum x morifolium*)	71 701,7	BAE79547	0.615
13	Inorganic pyrophosphatase, putative (*Ricinus communis*)	33 895,5	EEF44062	0.619
Stress response/defence				
8	Chloroplast thylakoid-bound ascorbate peroxidase (*Vigna unguiculata*)	39 791,4	AAS55852	0.596
Protein processing				
11	Tubulin A (*Glycine max*)	49 552,7	AAX86047	0.566
19	26S proteasome regulatory particle triple-A ATPase subunit1 (*Oryza sativa* Japonica Group)	46 667,0	BAB17624	1.910
Transcription				
14	Pre-mRNA-splicing factor SLU7-A (*Arabidopsis lyrata* subsp. Lyrata)	61 961,8	EFH64697	2.794
Unknown				
15	ND	-	-	2.625

A

Legend:
- Carbohydrate Metabolism — 38%
- Amino Acid Metabolism — 31%
- Other metabolisms — 15%
- Stress response/defence — 8%
- Protein processing — 8%

B

Legend:
- Carbohydrate Metabolism — 45%
- Amino Acid Metabolism — 22%
- Protein processing — 11%
- Transcription — 11%
- Unknown — 11%
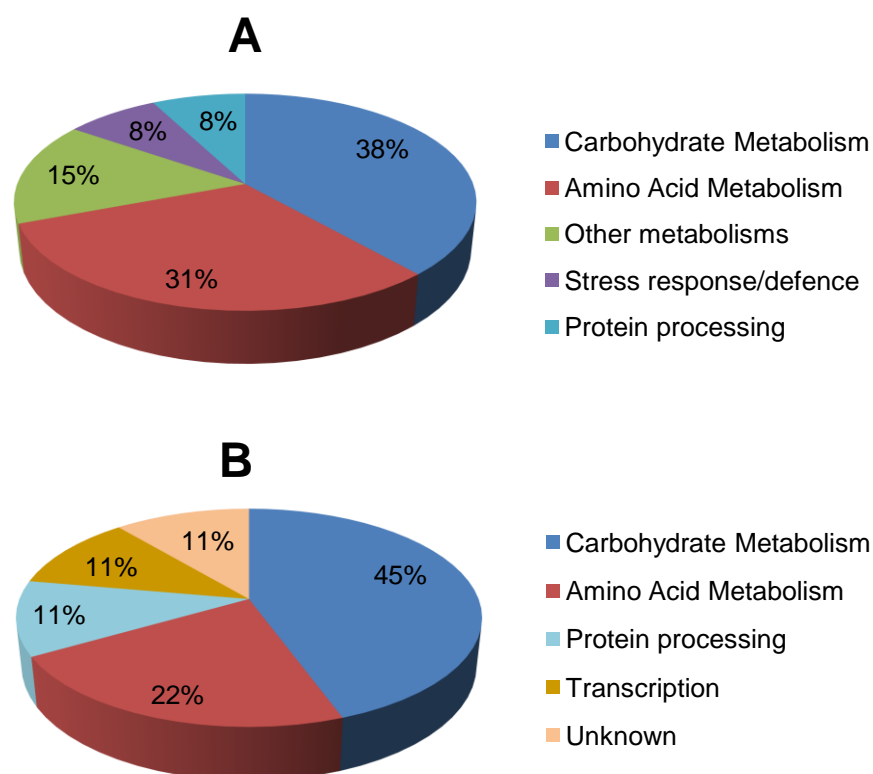
Figure 4 Functional categories of the 22 significantly decreased (A) and increased (B) proteins in response to PEG in the root tips of common bean genotype VAX 1. The identifications of these 22 proteins by nano LC-MS/MS are shown in Table 1.

To investigate the effect of OS on the regulation of CW proteins of root tips of common bean, soluble and ionically bound apoplastic proteins were extracted and analysed. First we tested the capability and efficiency of KCl as an extractant of CWPs from root tips of common bean. Different concentrations were tested for their effect on CWP yield and cytosolic protein contamination (CPC). The CPC was assessed by assay of malate dehydrogenase (MDH) activity (Table 2). Cell-wall proteins extracted with 0.1 M KCl did not show CPC in each of three sequential extractions, however, the protein yield was low. Infiltration with 0.4 M KCl yielded a great amount of protein, but also resulted in a high CPC in the first infiltration step (data not shown). Therefore, to obtain the maximum protein yield with minimum CPC, 0.2 M KCl was chosen for extracting CWPs from PEG-treated root tips of common bean. This KCl concentration of 0.2 M has been previously used to extract CWPs from the root elongation zone of maize (Zhu et al., 2006).

Compared to the residues of proteins (tightly, non-extractable apoplastic proteins and symplastic proteins), the MDH activity in the apoplastic and CW loosely bound proteins is low (Table 2), indicating only little contamination. PEG treatment (150 g L^{-1}) reduced the extracted apoplastic protein yield in the root tips (Table 2).

2D IEF/SDS PAGE and subsequent staining with CBB showed that individual proteins could be visualized in spite of the low amount of CW proteins (80 µg) loaded on each gel (Fig. 5). On average, a total of 171 spots was detected on gels containing proteins extracted from PEG-treated and control (- PEG) root tips. A total of thirteen proteins were significantly affected by PEG-induced OS. Of these, five and eight proteins showed lower and higher abundance in PEG-treated root tips, respectively (Fig. 5). ESI MS/MS analysis of these thirteen spots allowed the identification of eight proteins by BLAST search at the NCBI protein database (Tab. 3). Two of the proteins (fructokinase and pathogenesis-related protein 1) were reduced and six proteins (beta xylosidase, pectinacetylesterase precursor, serine hydroxymethyltransferase, serine carboxypeptidase and fructose-1,6-bisphosphate aldolase) increased in abundance by PEG-induced OS (Table 3). Close-ups of the gels are shown in Supplemental Fig. S1.

Table 2 Yield of 0.2 mM KCl-extractable apoplastic proteins and their MDH activity (indicator of cytosolic contamination) from 1-cm root tips of common bean genotype VAX 1 grown in absence and presence of PEG 6000 for 24 h. Root tips were three times consecutively infiltrated. The residue included tightly, non-extractable apoplastic proteins and symplastic proteins.

PEG treatment [g/L]	Infiltration step	Protein yield [ng (1-cm root tip)$^{-1}$]	MDH Activity [nmol min^{-1} (1-cm root tip)$^{-1}$]
0	I	33.68 ±5.45	0.10 ±0.02
	II	29.06 ±7.66	0.05 ±0.02
	III	28.86 ±7.34	0.06 ±0.03
	residue	251.19 ±119.23	0.94 ±0.54
150	I	21.39 ±3.01	0.05 ±0.01
	II	21.51 ±9.46	0.06 ±0.03
	III	19.60 ±7.16	0.04 ±0.02
	residue	379.68 ±212.15	0.58 ±0.10
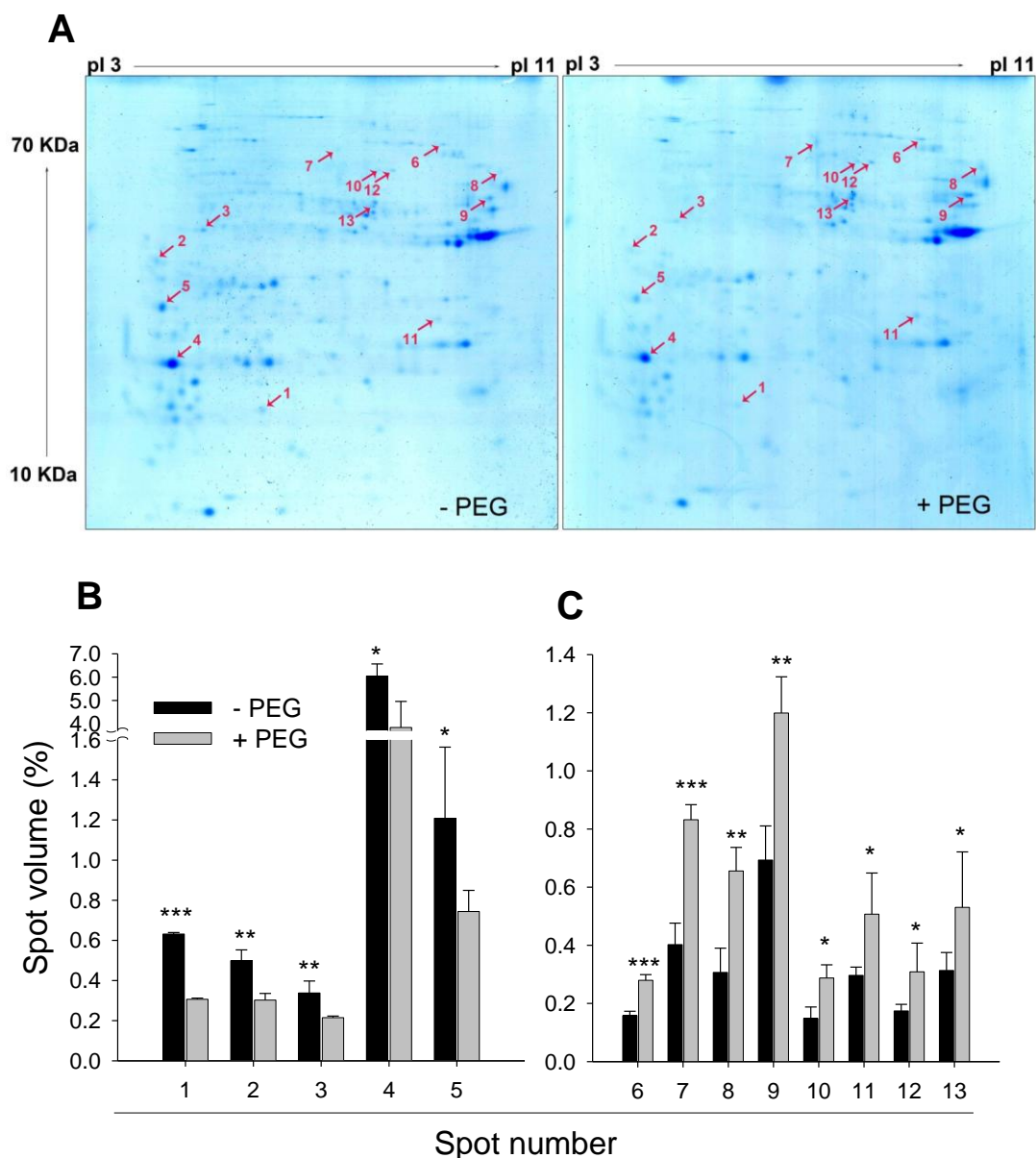
Figure 5 Representative Coomassie-stained 2D IEF/SDS–PAGE gel images of apoplastic proteins (A) and the relative volume of the 13 significantly decreased (B) and increased (C) apoplastic protein spots in control (-PEG) and PEG-treated root tips of common bean genotype VAX 1. Plants were pre-cultured in a simplified nutrient solution containing 5 mM $CaCl_2$, 1 mM KCl, and 8 μM H_3BO_3 for 48 h for acclimation and pH adaptation, and then treated without or with PEG (150 g L^{-1}) in the simplified nutrient solution for 24 h, pH 4.5. Apoplastic proteins were extracted from root tips, separated by 2D IEF/SDS–PAGE, and stained by CBB. Treatment-affected spots were marked by arrows and numbered consecutively. Three biological replications of each treatment were analysed using the Image Master^{TM} 2D PLATINUM Software 6.0. In (B) bars represent means ± SD, n = 3, and the symbol *, ** and *** denote significant treatment differences between means at $P < 0.05$, 0.01 and 0.001, respectively.

Table 3 List of thirteen apoplastic proteins with significantly different abundance in the root tips of common bean genotype VAX 1 in response to PEG. Plants were pre-cultured in a simplified nutrient solution containing 5 mM CaCl$_2$, 1 mM KCl, and 8 μM H$_3$BO$_3$ for 48 h for acclimation and pH adaptation, and then treated without or with PEG (150 g L^{-1}) in the simplified nutrient solution for 24 h, pH 4.5. These 13 protein spots were shown in the Coomassie-stained 2D IEF/SDS–PAGE gels of Fig. 5 and supplemental Fig. 1. Spot No. : corresponding to the spots number of Figure 5 and in supplemental Figure 1. FC: fold change (the relative protein spot volume of +PEG treatment to the relative protein spot volume of -PEG treatment). The proteins were identified by nano LC-MS/MS and BLASTed in NCBI database. ND: not detected.

Spot No.	Identity	MW (Da)	Acc. No.	FC
1	ND	-	-	0.486
2	ND	-	-	0.607
3	Fructokinase (*Arachis hypogaea*)	20 047,7	ACF74294	0.636
4	Pathogenesis-related protein 1 (PvPR1) (*Phaseolus vulgaris*)	16 511,4	CAA43637	0.635
5	ND	-	-	0.616
6	Beta xylosidase (*Fragaria* x *ananassa*)	83 468,2	AAS17751	1.768
7	ND	-	-	2.067
8	ND	-	-	2.136
9	Pectinacetylesterase precursor (*Vigna radiata* var. Radiata)	43 804,9	CAA67728	1.730
10	Serine hydroxymethyltransferase, putative (*Ricinus communis*)	51 889,9	XP_002522806	1.935
11	Serine carboxypeptidase, putative (*Ricinus communis*)	50 034,7	XP_002521402	1.709
12	Serine hydroxymethyltransferase (*Gossypium hirsutum*)	51 889,9	ACJ11726	1.771
13	Fructose-1,6-bisphosphate aldolase (*Pisum sativum*)	38 473,4	CAA61947	1.692

The PEG-induced changes of phosphorylated and de-phosphorylated proteins in root tips were examined by a phosphoproteomic approach using 2D IEF/SDS PAGE and Pro-Q DPS staining. Out of the identified ten significantly changed proteins, seven showed increased phosphorylation (glucose-6-phosphate isomerase, actin, dehydrin and lactoylglutathione lyase) and three proteins decreased phosphorylation (Ser/Thr-specific protein phosphatase 2A, regulatory subunit beta isoform, pyruvate kinase and branched-chain amino acid aminotransferase) by PEG-induced OS (Fig. 6; Table 4). Close-ups of three of these proteins with high abundance are shown in Fig. 6B and were identified as belonging to the same protein family, dehydrin. The close-ups of all differentially formed proteins in response to PEG treatment are presented in Supplemental Fig. S2.
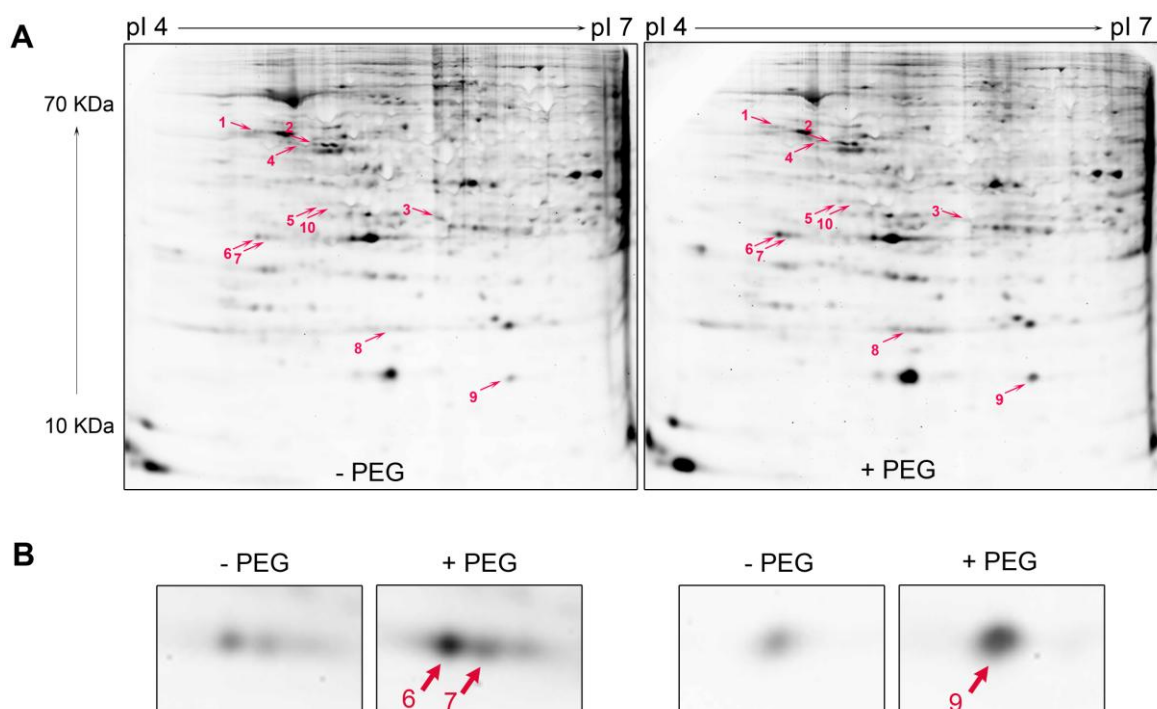
Fig. 6 Representative Pro-Q DPS-stained 2D IEF/SDS–PAGE gels of the total soluble proteins in the control (- PEG) and PEG-treated root tips of common bean genotype VAX 1 (A) and three magnified spots with high protein abundance (B). Plants were pre-cultured in a simplified nutrient solution containing 5 mM $CaCl_2$, 1 mM KCl, and 8 μM H_3BO_3 for 48 h for acclimation and pH adaptation, and then treated without or with PEG (150 g L^{-1}) in the simplified nutrient solution for 24 h, pH 4.5. Proteins were extracted from the root tips, separated by 2D IEF/SDS–PAGE, and stained by Pro-Q DPS. Treatment-affected spots were marked by arrows and numbered consecutively. Three biological replications of each treatment were analyzed using the Image Master^{TM} 2D PLATINUM Software 6.0.

Table 4 List of ten phosphoproteins with significantly different abundance in the root tips of common bean genotype VAX 1 in response to PEG. Plants were pre-cultured in a simplified nutrient solution containing 5 mM CaCl$_2$, 1 mM KCl, and 8 μM H$_3$BO$_3$ for 48 h for acclimation and pH adaptation, then treated without or with PEG (150 g L^{-1}) in the simplified nutrient solution for 24 h, pH 4.5. These 10 phosphoprotein spots are shown in the Pro-Q DPS-stained 2D IEF/SDS–PAGE gels of Fig. 6 and in supplemental Fig. 2. Spot No. : corresponding to spot number of Fig. 6 and supplemental Fig. 2. FC: fold change (the relative protein spot volume of +PEG treatment to the relative protein spot volume of -PEG treatment). The proteins were identified by nano LC-MS/MS and BLASTed in NCBI database.

Spot No.	Identity	MW (Da)	Acc. No.	FC
1	Ser/Thr specific protein phosphatase 2A A regulatory subunit beta isoform (*Medicago sativa* subsp. x varia)	65161.6	AAG29594	0.647
2	Pyruvate kinase (*Lactuca sativa*)	56174.9	ABS87384	0.481
3	Branched-chain amino acid aminotransferase, putative (*Ricinus communis*)	45159.9	XP_002530599	0.541
4	Glucose-6-phosphate isomerase (*Zea mays*)	68403.5	NP_001147983	1.837
5	Actin (*Phaseolus acutifolius*)	33121.3	AAZ95077	2.277
6	Dehydrin (*Phaseolus vulgaris*)	22955.6	AAB00554	2.048
7	Dehydrin (*Phaseolus vulgaris*)	22955.6	AAB00554	1.846
8	Lactoylglutathione lyase, putative / glyoxalase I, putative (*Arabidopsis thaliana*)	20830.4	NP_001030996	2.414
9	Dehydrin (*Phaseolus vulgaris*)	22955.6	AAB00554	2.438
10	Dehydrin (*Phaseolus vulgaris*)	22955.6	AAB00554	1.625

Discussion

Physiological osmotic adjustment and modification of cell-wall (CW) extensibility were suggested as two major mechanisms involved in the maintenance of root elongation during water deficit (Sharp et al., 2004; Yamaguchi and Sharp, 2010). In this study, functional categorization of total soluble proteins showed that the majority of the affected proteins were involved in primary metabolism (Fig. 4; Table 1), particularly carbohydrate (acetoacetyl-CoA thiolase, fructokinase, myo-inositol 1-phosphate synthase, phosphoglycerate mutase, fructokinase-like protein, alcohol dehydrogenase Adh-1, enolase and NADPH-specific isocitrate dehydrogenase) and amino acid (S-adenosylmethionine synthetase, D-3-phosphoglycerate dehydrogenase, methionine synthase) metabolism, confirming the important role of accumulation of carbohydrates and soluble amino acids involved in osmotic adjustment (Morgan, 1984). On the other hand, protein synthesis and modification of carbohydrates regulated by the proteins involved in metabolic pathways, may facilitate the adjustment of CW synthesis and extensibility, and thus the regulation of root elongation. Also, some proteins were supposed to play key roles in the protection against OS-induced severe physical destruction of CW integrity, such as dehydrin (Layton et al., 2010), which was highly significantly up-regulated by OS in this study. Therefore, based on the above information, the discussion below will particularly focus on the carbohydrate and amino acid metabolism and on CW-related proteins.

The osmotic adjustment in the growing root region in response to OS can in part result from increased net accumulation rates of osmotic solutes. Physiological factors influencing such accumulation rates are solute synthesis, uptake, catabolism and utilization. All of these represent adaptive responses contributing to growth maintenance (Sharp et al., 2004). It has been reported that OS increased sugar (e.g. fructose, glucose and sucrose) accumulation in roots of mung bean (*Vigna mungo*) seedlings (Itoh et al., 1987) and the tropical tree *Colophospermum mopane* (Johnson et al., 1996). Fructokinase specifically catalyzes the transfer of a phosphate group from ATP to fructose, thereby activating this sugar for further metabolic processes. In this study, OS-induced reduced abundance of fructokinase in the root tips of common bean (Fig. 2; Fig. 3; Table 1) may lead to fructose accumulation and in this sense may be regarded as part of osmotic adjustment. Indeed, also in soybean roots Toorchi et al. (2009) found by proteomic analysis that PEG-induced OS reduced the formation of a fructokinase 2 protein.

In Arabidopsis, Hummel et al. (2010) found that organic acids in addition to K^+ are main

contributors to osmotic adjustment under water deficit conditions. We previously reported that PEG-induced OS increased citrate, malate, cis-aconitate and fumarate contents in root tips of common bean (Yang et al., 2010) indicating a major role of the accumulation of these organic acids in osmotic adjustment. The isocitrate dehydrogenase is an enzyme that participates in the citric acid cycle. It catalyzes oxidative decarboxylation of isocitrate to alpha-ketoglutarate and requires either NAD^+ or $NADP^+$, producing NADH and NADPH, respectively. It was thought (Chen and Gadal, 1990) that citrate in the cytosol is first converted to isocitrate by the action of aconitase, and then to 2-oxoglutarate by the action of NADP-specific isocitrate dehydrogenase (NADP-ICDH). Subsequently, 2-oxoglutarate is utilized as carbon skeleton for the glutamine synthase/glutamate synthase pathway. Thus a decrease of NADP-ICDH activity was associated with the accumulation of citrate in the plant tissue (Sadka et al., 2000; Kihara et al., 2003). In contrast, in the present study it was found that osmotic stress increased the expression of NADPH-specific ICDH in root tips of common bean (Fig. 2; Fig. 3; Table 1) not supporting the hypothesis that increased accumulation of citrate in the cytosol is a consequence of reduced activity NADP–ICDH (Massonneau et al. 2001, Anoop et al., 2003, Rangel et al., 2010). However, on the other hand enhanced formation of NADPH-specific ICDH due to OS may increase the accumulation of citrate in root tips through increasing citric acid cycle turnover. Moreover, it may be involved in defense processes, since NADP-ICDH was shown to play an important role in cellular defense against stress-induced oxidative injury (Jo et al., 2002; Lee et al., 2002). Liu et al. (2010) found that an isolated cDNA encoding cytosolic NADP-dependent ICDH from maize conferred salt tolerance to Arabidopsis.

Phosphoglycerate mutase (PGM) is a glycolytic enzyme, which catalyzes the conversion of 3-phosphoglycerate to 2-phosphoglycerate. Ergen et al. (2009) found that the expression of the gene encoding PGM in leaves of wild durum wheat (*Triticum turgidum*) was promoted while in roots it was suppressed during dehydration. Mazarei et al. (2003) observed that an *AtPGM* gene in Arabidopsis was localized in the shoot and root meristems, of which the expression was down-regulated by ABA. However, the function of this protein in stress responses remains to be elucidated. *Myo*-inositol 1-phosphate synthase (MIPS) catalyzes the rate-limiting step in the synthesis of *myo*-inositol. It was reported that *mips1* mutants resulted in lowered *myo*-inositol levels and enhanced cell death in Arabidopsis (Meng et al., 2009; Donahue et al., 2010). Moreover, Donahue et al. (2010) provided evidence that *mips1* mutants had increased sensitivity to ABA and OS (salt and sorbitol treatment), which could be rescued by *myo*-inositol supplementation. The

OS-induced suppression of MIPS in this study (Fig. 2; Fig. 3; Table 1) suggests that the root tips of common bean suffered severe stress causing cell damage through lowered *myo*-inositol abundance. Enolase is responsible for the conversion of 2-phosphoglycerate to phosphoenolpyruvate, which is involved in glycolysis. Enolase was detected in the CWs of *Candida albicans*, *Arabidopsis thaliana*, *Medicago sativa*, and *Zea mays* (Chivasa et al., 2002; Pitarch et al., 2002; Watson et al., 2004; Zhu et al., 2006). Using immunolocalization, enolase was shown to be secreted to the cell wall or the extracellular space even though it lacked a signal peptide (Edwards et al., 1999). In this study, the abundance of enolase was enhanced by PEG treatment (Fig. 2; Fig. 3; Table 1). The role of overexpression of enolase under osmotic stress remains unclear.

Some proteins involved in amino acid biosynthesis were differentially affected in abundance by OS in this study, such as S-adenosylmethionine synthethase (methionine adenosyltransferase, SAMS), methionine synthase (MetS) and D-3-phosphoglycerate dehydrogenase (PHGDH) (Fig. 1; Fig. 2; Table 1). MetS catalyzes the final step in methionine biosynthesis and SAMS catalyzes the conversion of ATP and methionine into S-adenosylmethionine (SAM) (Ravanel et al., 1998). SAM serves as a cofactor in a variety of biochemical reactions in all living organisms. It acts as a methyl donor to proteins, lipids, polysaccharides, nucleic acids (Tabor and Tabor 1984), participates in cell-wall lignin-synthesis (Sederoff and Chang 1991), and mediates the biosynthesis of ethylene (Yang and Hoffman, 1984; Kende 1993). Also, SAM is believed to play a regulatory role in synthesis of methionine and other aspartate-derived amino acids (Peleman et al., 1989). Manavella et al. (2006) demonstrated that overexpression of the sunflower (*Helianthus annuus*) HD-Zip protein subfamily 1 member *Hahb-4* transcription factor in *Arabidopsis thaliana* improved desiccation tolerance via the repressing of of SAMS transcription and 1-aminocyclopropane-1-carboxylate oxidase, and subsequently suppressed the biosynthesis of ethylene. Ingram and Bartels (1996) reported that drought-caused alterations in the chemical composition and physical properties of the CW (e.g. CW extensibility) may involve genes encoding SAMS. Under non-stressed conditions, higher expression of *SAMS* genes correlated with the extent of lignification of tissues in Arabidopsis (Peleman et al., 1989). Lignification of CW by methylation of lignin monomers was described as one mechanism to avoid water loss under dehydration (Bhushan et al., 2007). Indeed, it has been reported that water deficit intensified the lignifications of root-tip cell-walls in maize (Fan et al., 2006) and soybean (Yamaguchi et al., 2009). Moreover, it has been suggested that cellular levels of SAM were regulated by MetS activity forming methionine, a

precursor of SAM (Ravanel et al., 1998, 2004). Therefore, the induction of MetS transcripts suggests an increased production of methionine and lignin methylation by SAM. Recent results confirmed that SAMS was involved in tolerance to abiotic stresses such as salinity stress (Sanchez-Aguayo et al., 2004; Jiang et al., 2007) and drought stress (Toorchi et al., 2009; Pandey et al., 2010). In this study PEG treatment led to increased abundance of a MetS (spot 21 in Fig. 1; Fig. 2 and Table 1) and SAMS (spot 20 in Fig. 1; Fig. 2 and Table 1), while the amount of another three SAMS proteins (spot 1, 2, 3 in Fig. 1; Fig. 2 and Table 1) in the root tips was repressed. The PEG-induced differential regulation of SMS proteins may be indicative for different isoforms of this protein. Under OS conditions the increase of SAMS may either improve lignification of root tips CW or increase biosynthesis of ethylene, while down-regulation of SMS may be caused by a changed demand for more methyl groups for lignin methylation (Bhushan et al., 2007). It has been reported that transcriptome and proteome levels of SAMS are down-regulated by OS (Seki et al., 2002; Yan et al., 2005; Jiang et al., 2007; Toorchi et al., 2009).

Sharp et al. (2004) suggested that in maize the extent of osmotic adjustment in the primary root tip, although substantial, was insufficient to maintain turgor comparable to well-watered levels in roots growing under severe drought. This was assessed directly by measuring the spatial distribution of turgor using a cell-pressure probe, which showed that turgor was reduced by over 50% throughout the root elongation zone of roots growing at a water potential of -1.6 MPa compared with well-watered control plants (Spollen and Sharp, 1991). Thus, enhancement of CW extensibility may contribute to the maintenance of root elongation in the apical region of water-stressed roots (Sharp et al., 2004; Yamaguchi and Sharp, 2010). Under multiple abiotic stress conditions, we recently found that osmotic stress-induced reduction of CW porosity could improve Al resistance by restricting Al accumulation in the apoplast of common bean root tips (Yang et al., 2010). Also by means of a transcriptome analysis we indentified some genes encoding proteins involved in CW modification (xyloglucan endotransglucosylase/hydrolase, XTH) and CW structure (hydroxyproline-rich glycoproteins, HRGPs), which were supposed to play major roles in PEG-mediated decrease of CW porosity (Yang et al., 2011). Several CW proteins/enzymes are believed to play roles in modifying the wall structure and controlling wall extension. These include expansin, XTH, and glucanases (Wu and Cosgrove, 2000; Bray, 2004; Sharp et al., 2004; Moore et al., 2008). Therefore, we aimed at identifying these proteins and to clarify their response to PEG treatment by extracting apoplastic and loosely ionically bound proteins in root tips of common bean and separating them by protein electrophoresis

techniques. Unlike what we expected, only a low protein yield was obtained by a fractional infiltration method. In addition, the extracted apoplastic protein yield in each infiltration step was reduced in PEG-treated roots (Table 2), further supporting that PEG-induced OS reduced CW porosity thereby reducing exchangeability of these proteins by extractants. Thus, proteins with high molecular weight could not be exchanges so that predominantly small molecular proteins were identified in this study. Although Zhu et al. (2007) identified a large amount of water deficit-induced CW proteins in maize using the same extraction procedures employed in the current study, the type I CW of common bean is different from type II CW of maize: the former contains higher pectic polysaccharides (Carpita and Gibeaut, 1993), which is the main factor determining CW porosity (Baron-Epel et al., 1988).

In spite of this, thirteen PEG-induced differentially affected proteins in the CW were obtained and eight of them were detected by MS analysis (Fig. 3; Table 3). The OS-induced reduction of fructokinase was also found in the CW fraction. It has been suggested that fructose formed from sucrose cleavage could be directly and rapidly converted into UDP-glucose via the hexose-phosphate pool (i.e. fructose-6-phosphate $\rightleftharpoons$ glucose-6- phosphate $\rightleftharpoons$ glucose-1- phosphate), and subsequently apoplastically provided for synthesis of CW polysaccharides (Konishi et al., 2004). Thus, it appears that a decrease of fructokinase may result in a reduction in CW polysaccharide content in root tips impeding root growth under OS, since fructokinase catalyzes the transfer of fructose into fuctose-6-phosphate. Similar conclusions have been drawn by Toorchi et al. (2009). Indeed, Odanaka et al. (2002) reported that suppression of the gene *Frk2* encoding fructose kinase inhibited root growth of tomato. In sum, fructokinase may play a role in regulation of the energy metabolism, (1) possibly by providing fructose-6-phosphate for glycolysis and/or (2) through conversion to UDP-glucose (UDPG) to support biosynthesis of CW material (Karni and Aarni, 2002).

Fructose-1,6-bisphosphate aldolase reversibly catalyzes the conversion of fructose-1,6-bisphosphate to glyceraldehyde-3-phosphate. The extracellular matrix proteome analysis revealed that fructose-1,6-bisphosphate aldolase was indeed a CW protein which was increased during dehydration stress in chickpea (*Cicer arietinum*) (Bhushan et al., 2007) and rice (*Oryza sativa*) (Pandey et al., 2010) corroborating results of this study showing that PEG-induced apoplastic dehydration increased the abundance of apoplastically localized fructose-1,6-bisphosphate aldolase in root tips of common bean (Fig. 5; Table 3). Enhanced synthesis of fructose-1,6-bisphosphate aldolase was also

reported as response to salt stress in rice (Abbasi and Komatsu 2004) and mangrove plant *Bruguiera gymnorhiza* (Tada and Kashimura, 2009). Enhanced formation of fructose-1,6-bisphosphate aldolase may increase the flow of carbon through the Calvin cycle and lead to C-skeleton production for subsequent increased carbon flux through glycolysis. These traits would also lead to osmolyte production and contribute to OS tolerance.

Pathogenesis-related proteins (PRs) are mainly involved in the defense against pathogenic constraints and in general adaptation to stressful environments. The CW was the major accumulation site of these PRs (Edreva, 2005). Up to now, the biochemical function of PR1 is not known. However, supression of PR 1 by OS (Fig.5; Table 3) in this study may reflect lower protection level and severe root-cell damage. Beta xylosidase was found in the stock of pathogen-degrading enzymes (Tezuka et al., 1993). A gene, *AtBLX1*, encoding beta xylosidase in Arabidopsis was proposed to be involved in secondary CW hemicellulose metabolism and plant development (Goujon et al., 2003). In contrast to our results showing PEG-mediated increased abundance of beta xylosidase in the CW of bean root tips (Fig. 5; Table 3), Zhu et al. (2007) found that water deficit reduced beta xylosidase in the apical 3-7 mm region of the maize primary roots. The exact function of beta xylosidase in response to osmotic/drought stress remains to be elucidated. In addition, the amount of pectin acetylesterase, serine hydroxymethyltransferase, and serine carboxypeptidase was enhanced by osmotic stress, but the role of them in OS is not yet known.

Phophoproteomics revealed that three proteins showed reduced and seven proteins increased phosphorylation by OS. Out of these, dehydrin underwent significantly enhanced phosphorylation by OS (Fig. 6; Table 4), while no PEG-effect in abundance of dehydrin by CBB-staining (data not shown) has been found indicating that the activation of dehydrin during OS by phosphorylation may play an important role in root responses to OS. Dehydrins are the second biggest group of late embryogenesis abundant proteins, which are well known to play crucial roles in cellular dehydration tolerance (Ingram and Bartels, 1996; Hundertmark and Hincha, 2008). A number of studies have demonstrated that dehydrin proteins play an important role in drought tolerance by preventing membrane denaturation and maintaining the integrity of the CW (Lopez et al., 2003; Collett et al., 2004; Vicré et al., 2004; Samarah et al., 2006; Hu et al., 2010). Dehydrins are known to undergo phosphorylation both *in vivo* and *in vitro* (Heyen et al., 2002; Jiang and Wang, 2004; Alsheikh et al., 2005; Brini et al., 2006; Röhrig et al., 2006). However, we are aware

that Pro-Q Diamond staining for phosphoproteins includes a risk of false positive identifications. Therefore, a mass spectrometral approach was employed to verify phosphorylation and to identify the phosphorylation site of this dehydrin. Unfortunately, we could not identify the phosphorylation site of dehydrin successfully by MS because the protein amount available was insufficient for the quantification. Thus, the confirmation of the phosphorylation of dehydrin awaits further work in the future.

Dehydrins were found to be localized in various subcellular sites including plasma membrane, cytoplasm and nucleus (Danyluk et al., 1998; Wisniewski et al., 1999; Carjuzaa et al., 2008). Recently, Layton et al. (2010) observed that dehydrin mainly accumulated near the CW of dried tissues in the desiccation-tolerant fern *Polypodium polypodioides*. The author supposed that the ability to avoid CW damage in some desiccation-tolerant species may be partially attributed to CW localization of dehydrins enabling reversible great CW deformation. Dehydrins are extremely hydrophilic proteins (Close et al., 1989), which can attract, sequester and localize water and may behave as a lubricant between either, the plant CW and cell membrane or between individual CW layers. It has been reported that dehydrins are highly specialized proteins that lack a fixed three-dimensional structure and have evolved to maintain their disordered character under conditions such as water deficit, in which unfolded states of several globular proteins would tend to collapse (Mouillon et al., 2008). However, the effect of phosphorylation on dehydrin structure is small and does not significantly enhance the response to osmotic stress induced by glycecol and PEG 4000 *in vitro* (Mouillon et al., 2008). In spite of this, the studies *in vitro* may not reflect the response of dehydrin structure to phosphorylation *in vivo*, since dehydrins may interact with other proteins *in vivo*. In addition the site of osmotic stress induced by glycerol and PEG 4000 is different from PEG 6000 because of the differences in molecular weight; the former solutes mainly induce OS in the cytoplasm while the latter mainly in the apoplast (Yang et al., 2010). Thus, it appears that the increased dehydrin formation could play an important role in the protection of CW against breakage and in the maintenance of the mechanical CW integrity. Our previous study (Yang et al., 2010) suggested that CW porosity was reduced by PEG-induced OS and quickly recovered after the removal of OS in root tips of common bean, which was concluded on the basis of the penetration of ions with different hydrated ionic radius ($Al^{3+} > La^{3+} > Sr^{2+} > Rb^+$) into the apoplast. Therefore, dehydrins may prevent CW from PEG-caused mechanical fracture, and consequently maintain the elastic extension (reversible stretching) properties of the CW and thus allow quick reversion of CW extension after removal of osmotic stress.

Importantly, the above hypothesis also provides the opportunity to further clarify the exact cellular localization of dehydrins in root tips of common bean prior to the analysis of phosphorylation sites of dehydrin, in order to better understand the potential roles of dehydrin in the reduction and rapid recovery of CW porosity during OS.

In conclusion, the large-scale proteomic analysis revealed the importance of carbohydrate and amino acid metabolism involved in the response of root tips to osmotic stress. The phosphoproteomics provided novel insights into the potential role of dehydrin as a CW structure moderator, which may participate in alteration of CW porosity by maintaining the integrity and reversible extension properties of the CW during OS. Future research is necessary to further clarify the cellular localization of dedydrin and its possible role in CW modification.

CHAPTER 4

Physiological and molecular analysis of the interaction between aluminum toxicity and drought stress in common bean (*Phaseolus vulgaris* L.)

Zhong-Bao Yang[1], Dejene Eticha[1], Alfonso Albacete[2], Idupulapati Madhusudana Rao[3], Thomas Roitsch[2], Walter Johannes Horst[1]

[1] Institute of Plant Nutrition, Leibniz Universität Hannover, Herrenhaeuser Str. 2, D-30419 Hannover, Germany

[2] Institute of Plant Science, Universität Graz, Schubertstrasse 51, A-8010 Graz, Austria

[3] International Center for Tropical Agriculture (CIAT), AA 6713, Cali, Colombia

(To be submitted)

Abstract

Aluminium (Al) toxicity and drought are two major factors limiting common bean (*Phaseolus vulgaris* L.) production in the tropics. In the present study short-term effects of combined Al toxicity and drought stress on root growth in an acid, Al-toxic soil were studied with special emphasis on Al/drought interaction in the root apex at the physiological and molecular level. The root elongation rate of Al-sensitive bean genotype VAX 1 was significantly inhibited by both increased Al supply and reduced soil moisture. Drought reduced Al toxicity as indicated by the reduction of Al-induced callose formation and lower expression level of a *MATE* gene in root tips. However, in contrast to PEG-induced reduction of Al injury in hydroponics, combined Al and drought stress in soil resulted in a more severe inhibition of root elongation than either stress alone. This finding is consistent with Al-enhanced drought-induced up-regulation of *ACCO* gene expression, Al-reduced drought-induced enhancement of ABA concentration and the expression of genes and transcription factors involved in ABA biosynthesis and gene regulation, and Al-stimulated synthesis of zeatin riboside in the root tips by Al. Six genes, each with possible role in the regulation of cell-wall properties and response to osmotic stress were (with only one exception) comparably affected by osmotic stress (PEG) and by drought stress in soil. Al remarkably reduced or further increased the expression of drought-affected genes in agreement with reduced drought resistance in presence of Al. Taken together, these results provide circumstantial evidence that drought alleviates Al toxicity, but Al renders the root apex more sensitive to drought particularly by impacting the gene regulatory network involved in ABA signal transduction and ABA signal cross-talk with other phytohormones that are necessary for maintaining root growth under drought.

Key words: abscisic acid, *ACCO*, aluminum, common bean, cytokinin, drought, ethylene, *MATE*, *NCED*, polyethylene glycol, root elongation, zeatin riboside

Introduction

Common bean (*Phaseolus vlugaris* L.) is the major food legume for human nutrition in the world, and a major source of calories and protein particularly in many developing Latin American and African countries (Graham, 1978; Rao, 2001). Bean production in the tropics is severely limited by two major abiotic stresses, drought and Al toxicity (Goldman et al., 1989; Ishitani et al., 2004). Generally, common bean has been regarded as an Al and drought-sensitive crop (Rao, 2001; Beebe et al., 2008).

Al resistance in common bean is related to lower Al accumulation in the root tips (Rangel et al., 2007). Under short-term Al exposure, Al accumulates primarily in the root apoplast (Wang et al., 2004; Rangel et al., 2009) where Al^{3+} strongly binds to the negatively charged binding sites (Blamey et al., 1990; Horst et al., 2010) provided by unmethylated pectin in the cell wall (CW) (Schmohl et al., 2000; Eticha et al., 2005a). Thus, a lower CW negativity reducing Al accumulation (Horst, 1995) and the detoxification of Al in the apoplast through root exudates play key roles in Al resistance. Excluding Al from the root apex by releasing organic acid anions such as citrate, malate and oxalate is the most studied mechanism of Al resistance (Ryan et al., 2001; Ma et al., 2001; Kochian et al., 2004; Ma, 2007; Ryan et al., 2007; Ryan and Delhaize, 2010). In common bean, Rangel et al. (2010) found that Al-activated exudation of citrate from root tips plays a major role in Al resistance. Further studies by Eticha et al. (2010) showed that the Al-induced expression of a *MATE* (multidrug and toxin extrusion family protein) gene in root apices is a prerequisite for citrate exudation and Al resistance in common bean, and a most sensitive indicator of Al injury. A role of MATE organic acid anion permeases for Al resistance has been reported in several plant species, such as sorghum (Magalhaes et al., *2007*), barley (Furukawa et al., 2007), wheat (Ryan et al., 2009) and Arabidopsis (Liu et al., 2009). Whereas the expression of the *MATE* gene did not differ between two common bean genotypes, Quimbaya (Al-resistant) and VAX 1 (Al-sensitive), the genotypic difference in Al-induced inhibition of root elongation was positively correlated with the expression of an *ACCO* (1-aminocyclopropane-1-carboxylic acid oxidase) gene in the root apex (Eticha et al., 2010). Enhanced *ACCO* gene expression may lead to an increase of ethylene production which may contribute to Al-induced inhibition of root elongation as observed in *Lotus japonicus* and *Medicago truncatula* (Sun et al., 2007). Since the expressions of the *MATE* and *ACCO* genes were significantly negatively correlated with Al-induced inhibition of root elongation and positively correlated with the Al contents in the root tips

of common bean (Yang et al., 2011), they can be regarded as sensitive indicators of Al toxicity and Al accumulation in the root tips.

The maintenance of root growth during water deficit facilitates water uptake from the subsoil (Sponchiado et al., 1989; Serraj and Sinclair, 2002). In maize, three possible mechanisms involved in the primary root growth maintenance under water deficit have been proposed i) osmotic adjustment; ii) modification of cell wall extension properties; and iii) the role of abscisic acid (ABA) accumulation (Sharp et al., 2004; Yamaguchi et al., 2010). Using SuperSAGE (serial analysis of gene expression) and quantitative real time polymerase chain reaction (qRT-PCR), our previous studies demonstrated that polyethylene glycol (PEG)-simulated drought stress up or down-regulated some genes involved in osmotic stress such as aquaporin (*AQP*), Δ1-pyrroline-5-carboxylate synthase (*P5CS*), sucrose synthase (*SUS)*, late embryogenesis abundant (*LEA*), KS-type dehydrin (*KS-DHN*) and cytochrome P450 monooxygenase CYP701A (*CYP701A*), cell-wall assembling or modifying genes such as xyloglucan endotransglucosylase/hydrolase (*XTH*), glucan endo-1,3-beta-glucosidase (*BEG*), proline-rich protein (*PRP*), hydroxyproline-rich glycoprotein (*HRGP*), lipid transfer protein (*LTP*), and the regulation of ABA-dependent drought stress such as transcription factors *bZIP* and *MYB* in the root tips of common bean (Yang et al., 2011). ABA is produced under water-deficit conditions and plays an important role in the response of plants to drought. The accumulation of ABA in the root tips has been shown to be required for the maintenance of maize primary root elongation at low water potentials (Sharp, 2002; Sharp et al., 2004; Yamaguchi and Sharp, 2010). Using the ABA-deficient mutant *vp5* and a chemical inhibitor of ABA biosynthesis to decrease endogenous ABA levels in seedlings growing at low water potentials, Sharp et al. (2004) reported that reduced ABA accumulation in maize primary roots was associated with more severe inhibition of root elongation. Under drought, ABA accumulated mainly towards the root apex (Saab et al., 1992) indicating that it was required for the maintenance of elongation in the distal elongation zone at low water potentials (Yamaguchi and Sharp, 2010). On the other hand, several studies have clearly shown that ABA can suppress ethylene production, and the maintenance of root elongation under water deficit conditions requires increased ABA levels to prevent excess ethylene production (Sharp et al., 2000; Spollen et al., 2000; Sharp, 2002; LeNoble et al., 2004), which can mediate the cytokinin (CK)-induced inhibition of root elongation (Bertell and Eliasson, 1992; Cary et al., 1995; Růžička et al., 2009).

It has been reported that cell elongation was maintained at low water potentials in the

apical 0-3 mm and 0-4 mm of the root in maize and soybean, respectively (Sharp et al., 2004; Yamaguchi et al., 2010). However, the root apex is the most Al-sensitive root zone (Horst et al., 1992; Delhaize and Ryan, 1995). In common bean, Rangel et al. (2007) found that the transition zone (1-2 mm) and the elongation zone are targets of Al injury. Excess Al will result in a rapid inhibition of root elongation and enhanced callose synthesis in the root tips, both are sensitive indicators of Al injury in roots (Horst et al., 1992; Delhaize and Ryan, 1995; Staß and Horst, 2009). Therefore, in dried acid soil, the Al-impeded root growth may strongly restrict the exploitation of water from the subsoil and thus the ability of the roots to withstand drought stress (Goldman et al., 1989). However, using different bean species, Butare et al. (2011) found that Al partially ameliorated the negative effects of water stress in *Phaseolus coccineus* genotypes, strongly in contrast to *Phaseolus acutifolius* and the Mesoamerican common bean genotypes in which combined stress led to a more severe inhibition of root development. Using PEG 6000 to simulate drought stress (Carpita et al., 1979; Jia et al., 2001; Fan and Neumann, 2004; Yang et al., 2010), we found that PEG 6000-induced osmotic stress can reduce Al-induced inhibition of root elongation by inhibiting Al accumulation in the root tip of common bean genotype VAX 1 (Yang et al., 2010). Also, the positive PEG effect on Al injury was confirmed by the expression of the *MATE* and *ACCO* genes, as sensitive indicators of Al toxicity (Yang et al., 2011). The PEG-suppressed Al accumulation in the root tips was suggested to be due to the osmotic stress-induced reduction of CW porosity, involving the regulation of the expression of the genes *XTH*, *BEG* and *HRGP* (Yang et al., 2011).

Although PEG 6000 can induce water deficit due to dehydration of the root apoplast (Yang et al., 2010), PEG treated hydroponic system and dried soil system are two completely different systems. Thus, the interaction between PEG-induced water deficit and Al toxicity in common bean may not reflect soil conditions. Therefore, the main objective of the present study was to determine the short-term effects of combined Al toxicity and drought stress on root growth in an acid, Al-toxic soil with special emphasis on Al/drought interaction in the root apex of the Al-sensitive common bean genotype VAX 1 at the physiological and molecular level.

Materials and Methods

Soil properties and preparation

The acid soil was obtained from Matazul farm (4"9'N 72"39'W) in the Llanos region of Colombia. Soil chemical characteristics are shown in Tab. 1. The soil pH was measured in 0.01 M $CaCl_2$ solution (pH_$CaCl_2$) or distilled water (pH_H_2O) with 1:3 soil:extract ratio (w/v). For the determination of soil exchangeable acidity, H^+ and Al^{3+} were determined by NaOH titration using 1% phenolphthalein and 0.1% methyl orange after extracting with 1 M KCl. For the measurement of the effective cation exchange capacity (ECEC), 2 g air-dried soil was weighed in a 30-mL centrifuge tube. 10 mL deionized water was added and the suspension shaken for 1 h. After centrifugation at 5,000 g the supernatant was discarded. The pellet was washed first with 20 mL 70% ethanol and then with 20 mL 10% ethylene glycol ($C_2H_6O_2$). After discarding the supernatant 10 mL 0.2 M $BaCl_2$/0.2 M NH_4Cl solution was added, shaken for a further 2 h, centrifuged and in the supernatant Ca, Mg, K, Na and Al were determined by inductively coupled plasma mass spectroscopy (ICP-MS) (7500cx, Agilent Technology, Santa Clara, California, USA). The ECEC was calculated by the formula: ECEC = Ca^{2+} + Mg^{2+} + Na^+ + K^+ + Al^{3+} representing exchangeable cations in centimoles of cation charge per kilogram soil ($cmol_c$ kg^{-1} soil). The Al saturation (%) of the soil was calculated as the ratio of exchangeable Al^{3+}/ECEC × 100. The soil water retention was determined and the water retention curve is shown in Supplemental Fig. S2. The soil water potential at different soil moisture used for the drought treatment in this study is shown in Supplemental Fig. S2.

For the soil treatment, first the soil was limed by adding 1.1 g $Ca(OH)_2$ per kg soil, well mixed and incubated at 25 ℃ for one week. Then different levels of Al ($AlCl_3.6H_2O$) (0, 0.5, 1.0, 1.5, 2.0, 2.5, 3.0 g kg^{-1} soil) were added to the limed soils, well mixed and incubated for two weeks. Finally the soil pH_H_2O was 6.5, 5.5, 5.0, 4.7, 4.3, 4.1 and 3.9, respectively, and the corresponding Al concentrations in the water extract were 0.4, 0.7, 1.0, 4.3, 40, 173 and 426 μM (see supplemental Fig. S1). The treated soil was air-dried and stored for future use.

Table 1 Chemical characteristics of an Oxisol collected from Matazul farm in the Llanos region of Colombia

Soil chemical characteristics	Oxisol
pH_CaCl$_2$	4.05
pH_H$_2$O	4.89
Exchangeable acidity (cmol$_c$/kg soil)	1.57
Exchangeable H$^+$ (cmol$_c$/kg soil)	0.33
Exchangeable Al (cmol$_c$/kg soil)	1.23
Total Al content (mg/kg soil)	111.0
ECEC (cmol$_c$/kg soil)	1.49
Al Saturation (%)	89.1

Plant materials and growing conditions

Seeds of common bean (*Phaseolus vulgaris* L.) genotype VAX 1 (Al-sensitive) were germinated for two or three days on filter paper sandwiched between sponges. For the soil experiments uniform seedlings were transferred into the soil with different levels of Al application and/or soil moisture in falcon vials (one plant per vial), covered with Al foil and kept in an upright position for 24 h. For the hydroponic experiments uniform seedlings were transferred to a continuously aerated simplified nutrient solution containing 5 mM CaCl$_2$, 1 mM KCl, and 8 μM H$_3$BO$_3$ (Rangel et al., 2007). The pH of the nutrient solution was gradually lowered to 4.5 within two days. Then the plants were transferred into a simplified nutrient solution (see above, pH 4.5) containing AlCl$_3$ (0, 25 μM Al) and PEG 6000 (0, 150 g L^{-1}) (Sigma-Aldrich Chemie GmbH, Steinheim, Germany) for 24 h. The osmotic potential (OP) of 150 g L^{-1} PEG 6000 was -0.60 MPa, measured with a cryoscopic osmometer (Osmomat 030, Gonotec GmbH, Berlin, Germany). Plants were cultured in a growth chamber under controlled environmental conditions of a 16/8 h light/dark cycle, 27/25 °C day/night temperature, 70% relative air humidity, and a photon flux density of 230 μmol m^{-2} s^{-1} of photosynthetically active radiation at plant height. One-cm root tips were harvested for Al analysis or immediately frozen in liquid nitrogen in Eppendorf vials for callose and phytohormone determination and RNA isolation.

Measurement of root elongation rate

Before transferring the plants into the soil or the nutrient solution, the tap roots were marked one (for soil) or three (for hydroponics) centimeter behind the primary root tip using a fine point permanent marker (Sharpie blue, Stanford) which did not affect root

growth during the experimental period. Root elongation was measured after treating the plants for 24 h using a mm scale.

RNA isolation and quantitative real time-PCR

After treating the plants in the soil with different Al supplies (0, 1.0, 2.0 g kg^{-1} soil) and soil moisture (-0.05, -0.14, -0.31 MPa SWP) for 24 h, the roots were rinsed with distilled water, and loosely adhering soil particles were removed with a brush. Primary root tips (1 cm long) from each plant were harvested and shock-frozen in liquid nitrogen. Nine root tips were bulked and ground to powder in liquid nitrogen. Total RNA was isolated using the NucleoSpin RNA plant kit (MACHEREY-NAGEL GmbH and Co., KG, Düren, Germany) following the manufacturer's protocol. After isolating the RNA from the root tips first-strand cDNA was synthesized using RevertAid H-Minus first strand cDNA synthesis kit (Fermentas, www.fermentas.com) following the manufacturer's protocol. Quantitative Real Time PCR (qRT-PCR) was performed using the CFX96^{TM} Real Time System plus C1000^{TM} Thermal Cycler (www.bio-rad.com). The SYBR Green detection system was used with self-prepared SYBR Green master mix. The qRT-PCR reaction mix composed of 1× hot-start PCR buffer (DNA Cloning Service, Germany), 3.6 mM MgCl$_2$ (DNA Cloning Service, Germany), 200 μM each dNTP (dATP, dTTP dCTP dGTP) (Fermentas), 0.1× SYBR Green-I (Invitrogen), 0.75 U μL^{-1} DCSHot DNA Polymerase (DNA Cloning Service, Germany), 252 nM each forward and reverse primer (Biolegio), 2 ng μL^{-1} cDNA template and ultra-pure DNase/RNase-free distilled water (Invitrogen) in a final volume of 25 μL. The qRT-PCR cycling stages consist of initial denaturation at 95 ℃ (10 min), followed by 45 cycles of 95 ℃ (15 s), 60 ℃ (30 s), 72 ℃ (30 s), and a final melting curve stage of 95 ℃ (15 s), 60 ℃ (15 s) and 95 ℃ (15 s). Samples for qRT-PCR were run in three biological replicates and two technical replicates. Relative gene expression was calculated using the comparative ΔΔCT method according to Livak and Schmittgen (2001). For the normalization of gene expression, *β-tubulin* was used as an internal standard according to Eticha et al. (2010), and the control (-0.05 MPa SWP in the absence of Al application) plants of bean genotype VAX 1 were used as reference sample.

Candidate gene selection and primer design for qRT-PCR

Candidate genes were selected either from our previous SuperSAGE library (Yang et al., 2011) or from a public database. The ESTs obtained from the *P. vulgaris* were aligned; otherwise the EST sequences from other legumes were gathered for sequence alignment.

The well conserved regions were used for primer design. Primers were designed using Primer3 software (Rozen and Skaletsky, 2000). The primers of *β-tubulin*, *MATE* and *ACCO* genes were obtained from Eticha et al. (2010). The specifications of the primers of the genes studied are given in Supplemental Table S1. The PCR efficiencies of the primer pairs were in the range of 90 – 110% as determined by dilution series of the cDNA template. Primer pairs with PCR efficiencies deviating from this range were discarded and new primers of the genes were designed to get more reliable quantification.

Determination of Al

For the determination of Al in roots, 1-cm root tips were digested in 500 μL ultra-pure HNO_3 (65%, v/v) by overnight shaking on a rotary shaker. The digestion was completed by heating the samples in a water bath at 80 °C for 20 min. Then 1.5 mL ultra-pure deionised water was added after cooling the samples in an ice-water bath. Aluminium was measured with a Unicam 939 QZ graphite furnace atomic absorption spectrophotometer (GFAAS; Analytical Technologies Inc., Cambridge, UK) at a wavelength of 308.2 nm after appropriate dilution, and an injection volume of 20 μL.

Determination of callose

Root tips of 1 cm length were excised from primary roots of three plants, collected in Eppendorf reaction vials, and instantly frozen in liquid N_2. The root tips were homogenized in 500 mL of 1 M NaOH with a mixer mill (MM 200; Retsch GmbH & Co. KG, Haan, Germany) at a speed of 20 cycles s^{-1} for 2 min. After homogenization, another 500 mL of 1 M NaOH was added, and callose was solubilized by heating in a water bath at 80 °C for 20 min. Callose was measured according to Kauss (1989), after addition of aniline blue reagent using a microplate fluorescence reader (FLx 800, Bio-Tek Instruments, Winooski, VT, USA) at excitation and emission wavelengths of 400 and 485 nm, respectively. Pachyman (1, 3-β-D-glucan) was used as a calibration standard, and thus, root callose content was expressed as pachyman equivalents (PE) per cm root tip.

Analysis of phytohormones

Different forms of CKs, IAA, ABA, JA and SA were extracted and purified according to Albacete et al. (2008) with some modifications. Primary root tips (1 cm long) were excised from common bean genotype VAX 1 and immediately frozen in liquid N_2. The root tips were ground to powder in liquid nitrogen. Afterwards, 1 mL of 80% (v/v) methanol was

added into each sample and vortexed. Then 4 μL of internal standard mix (5 μg mL^{-1}) composed of deuterium-labelled hormones ([^{2}H$_5$]Z, [^{2}H$_5$]ZR, [^{2}H$_5$]ZOG, [^{2}H$_5$]ZROG, [^{2}H$_6$]iP, [^{2}H$_5$]DHZ, [^{2}H$_5$]DHZR, [^{2}H$_6$]ABA, [^{2}H$_3$]IAA, and [^{2}H$_5$]JA, Olchemin Ltd, Olomouc, Czech Republic) was added, well mixed and incubated for 30 min at 4 °C. Afterwards, the samples were centrifuged at 20,000 g and 4 °C for 15 min. The supernatant was carefully pipetted into a syringe and passed through pre-equilibrated Chromafix C18 columns (Macherey-Nagel, Düren, Germany) with 80% (v/v) methanol. Samples were collected in 5 mL tubes on ice and 1 mL 80% (v/v) methanol was added and vortexed thoroughly. After centrifuging at 20,000 g and 4 °C for 15 min the filtration step was repeated. The collected samples were concentrated to dryness using a Thermo ISS110 centrifugal vacuum evaporator (Thermo Savant, Holbrook, NY, USA). The concentrated residue from each sample was re-dissolved in 500 μL 20% (v/v) methanol, sonicated for 8 min, filtrated through 0.22 μm syringe filters (Chromafil PES-20/25, Macherey-Nagel, Düren, Germany) and collected in 1.5 mL Eppendorf vials. The samples were immediately frozen for phytohormone measurement.

Analyses were carried out on a UPCL-MS/MS system consisting of a Thermo ACCELA UPLC (Thermo Scientific, Waltham, Massachusetts, USA) coupled to a thermostated HTCPAL autosampler (CTC Analytics, Zwingen, Switzerland), and connected to a Thermo TSQ Quantum Acces Max Mass Spectrometer (Thermo Scientific, Waltham, Massachusetts, USA) with a heated electrospray ionization (HESI) interface. Standards with known concentrations of each hormone (0.5, 0.1, 0.05, 0.01, 0.005 μg mL^{-1}) and the internal standards (0.01 μg mL^{-1}) were prepared in a 80% (v/v) methanol solution, and filtrated through 0.22 μm syringe filters (Chromafil PES-20/25, Macherey-Nagel, Düren, Germany). Ten μL of each standard or sample were injected onto a Thermo Hypersil Gold column (1.9 μm, 50 x 2.1 mm, Thermo Scientific, Waltham, Massachusetts, USA) eluted at a flow rate of 250 μL min^{-1}. Mobile phase A consisting of water/methanol/acetic acid (89.5/10/0.5, v/v/v) and mobile phase B consisting of methanol/acetic acid (99.5/0.5, v/v) were used for chromatographic separation. The elution consisted in 2 min of 95% A and a linear gradient from 5 to 100% of B in 8 min. 100% B was maintained 6 min and afterwards the column was equilibrated with the starting composition (95% A) for 8 min before each analytical run. The mass spectrometer was operated in the positive mode for all the hormones analyzed, except JA and SA that were measured in the negative mode. Capillary spray voltage was set to 4,000 V, the nebulizer gas (He) pressure to 40 psi with a flow rate of 8 L s^{-1} at a temperature of 250 °C, and the scan cycle time was 0.5 s from 100

to 600 m/z. The chromatogram of each hormone from both standards and samples was extracted, and the peak area quantified using the Thermo XCalibur software version 2.1.0.

Statistical analysis

A completely randomized design was used with four to twelve replicates in each experiment. Statistical analysis (ANOVA) was carried out using SAS 9.2. Means were compared using t or Tukey test depending on the number of treatments being compared. *, **, *** denote significant differences at $P < 0.05$, 0.01, 0.001, respectively.

Results

Application of AlCl$_3$ (0 - 3.0 g Al kg^{-1} soil) to the acid soil limed to pH 6.5 reduced the soil pH (H$_2$O) to 3.9 after incubation for two weeks, and the reduction of soil pH was correlated with an increase of Al concentration in the water extract (Supplemental Fig. S1). The root elongation rate of the common bean genotype VAX 1 was increasingly inhibited by the application of increasing Al rates (Fig. 1A). The supply of 1.0 and 2.0 g Al kg^{-1} soil reduced the root elongation rate by 29% and 52%, respectively, compared to the control (no Al). Decreasing soil water potential (SWP) from -0.05 to -0.87 MPa also drastically reduced root elongation. Medium to severe drought stess at -0.14 MPa and -0.31 MPa SWP inhibited root elongation rate by 45% and 68%, respectively, compared to the well-watered control (-0.05 MPa SWP).

Since a meaningful determination of Al contents of root tips in soil-grown plants is not possible, we evaluated the suitability of the callose content of root tips as indicator of Al injury in soils. In hydroponics, a significant negative correlation ($P < 0.001$) between Al contents and root elongation was observed (Fig. 2A). Aluminum induced callose formation in the root tips. The relationship between Al and callose contents could be described by a highly significant positive linear regression (Fig. 2B). Thus the root-tip callose content can be used as a sensitive indicator of Al-induced inhibition of root elongation rate in hydroponics (Fig. 2C). Similarly, in the soil-culture experiment addition of Al enhanced the root-tip callose contents (Fig. 2D). Thus callose content proved to be a sensitive indicator of Al injury (inhibition of root elongation) in the soil culture experiment also (Fig. 2E).

In order to verify whether Al-induced callose formation is also a reliable indicator of Al stress under combined Al and drought stress, we first conducted a hydroponic experiment using PEG 6000, which cannot penetrate into the root apoplast because of its high molecular weight (Carpita et al., 1979), to simulate drought stress. PEG at -0.60 MPa osmotic potential (OP) significantly reduced root elongation (Fig. 3A) but did not stimulate callose formation (Fig. 3C). 25 μM Al strongly inhibited root elongation (Fig. 3A) and increased root-tip Al (Fig. 3B) and callose contents (Fig. 3C). Combined PEG/Al stress alleviated the Al-induced inhibition of root elongation (Fig. 3A) by reducing the Al accumulation in the root tips (Fig. 3B). The PEG-caused alleviation of the Al stress is also clearly shown by reduced callose formation (Fig. 3C) suggesting a high sensitivity and specificity of callose formation for Al toxicity.
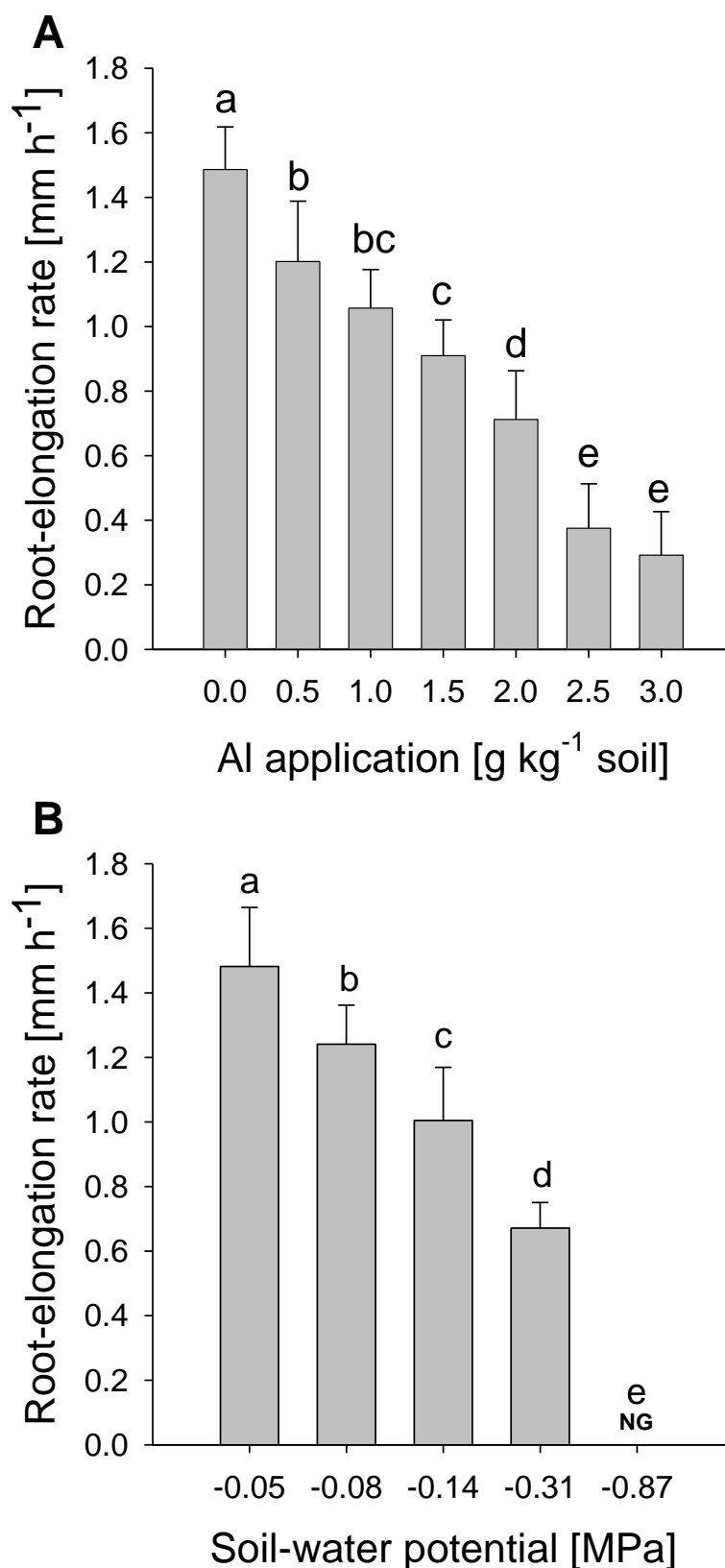
Figure 1 Root-elongation rate at different levels of Al supply under well-watered conditions (A) and at different levels of soil-water potentials in the absence of Al application (pH 6.5) (B). Two-day-old seedlings were grown in the soil for 24 h. Bars represent means ± SD, n = 12. Means with different letters are significantly different at $P < 0.05$ (Tukey test) for the comparison of treatments. NG = no growth.
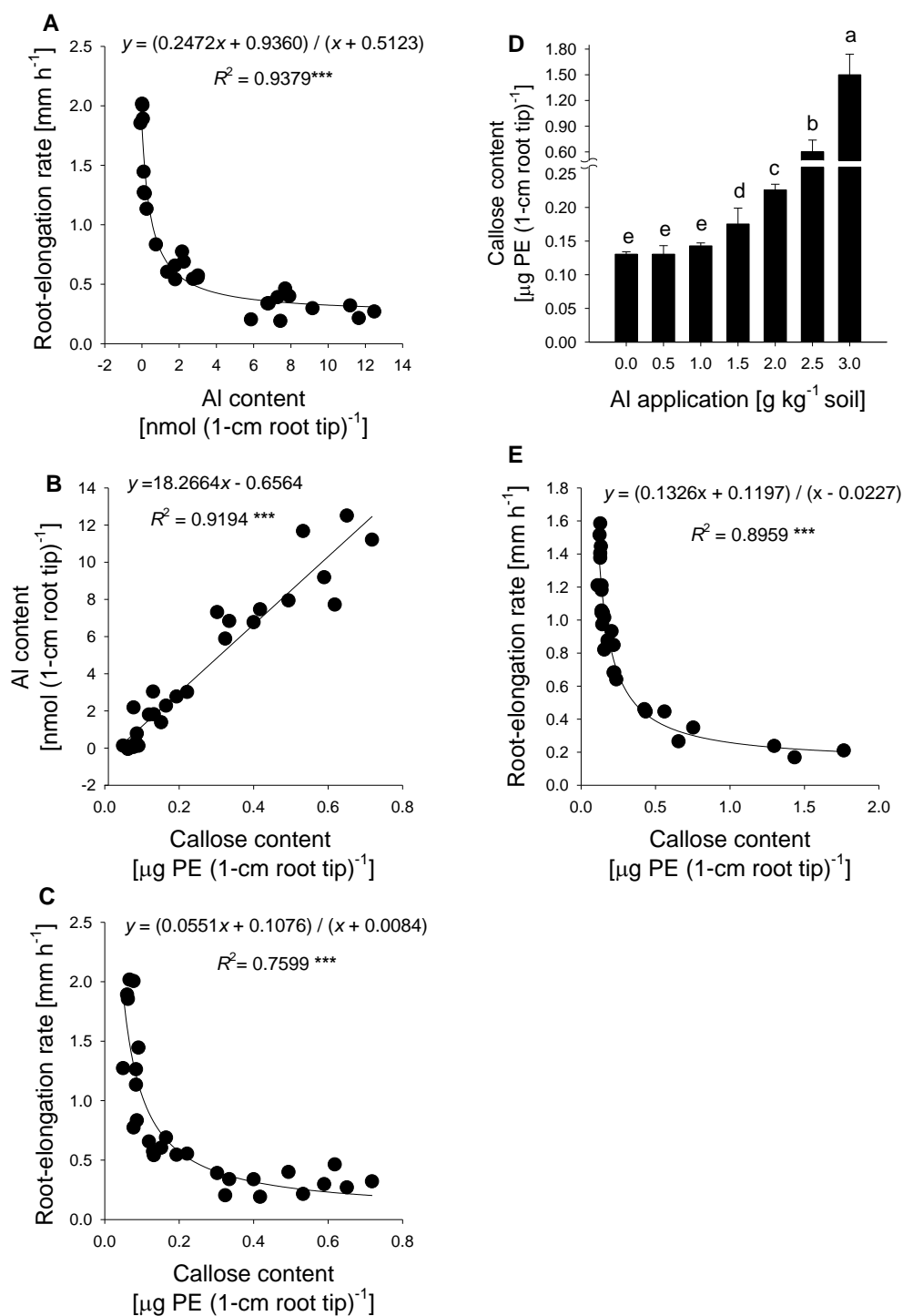
Figure 2 Correlations between root-elongation rate, Al and callose contents in the 1-cm root tips of common bean genotype VAX 1 in nutrient solution (A, B, C) or soil (E), and the effect of soil Al treatment on callose contents in the root tips (D). A, B, C: Plants were pre-cultured in simplified nutrient solution containing 5 mM $CaCl_2$, 1 mM KCl, and 8 μM H_3BO_3 for 48 h for acclimation and pH adaptation; then the plants were exposed to 25 μM Al in the simplified nutrient solution for 24 h, pH 4.5. D, E: Two-day-old seedlings were grown in well watered (-0.05 MPa SWP) soil with different levels of Al supply for 24 h. In D, bars represent means $\pm$ SD, n = 4, and means with different letters are significantly different at $P < 0.05$ (Tukey test) for the comparison of treatments. For the regression analysis, *** denote significant at $P < 0.001$.
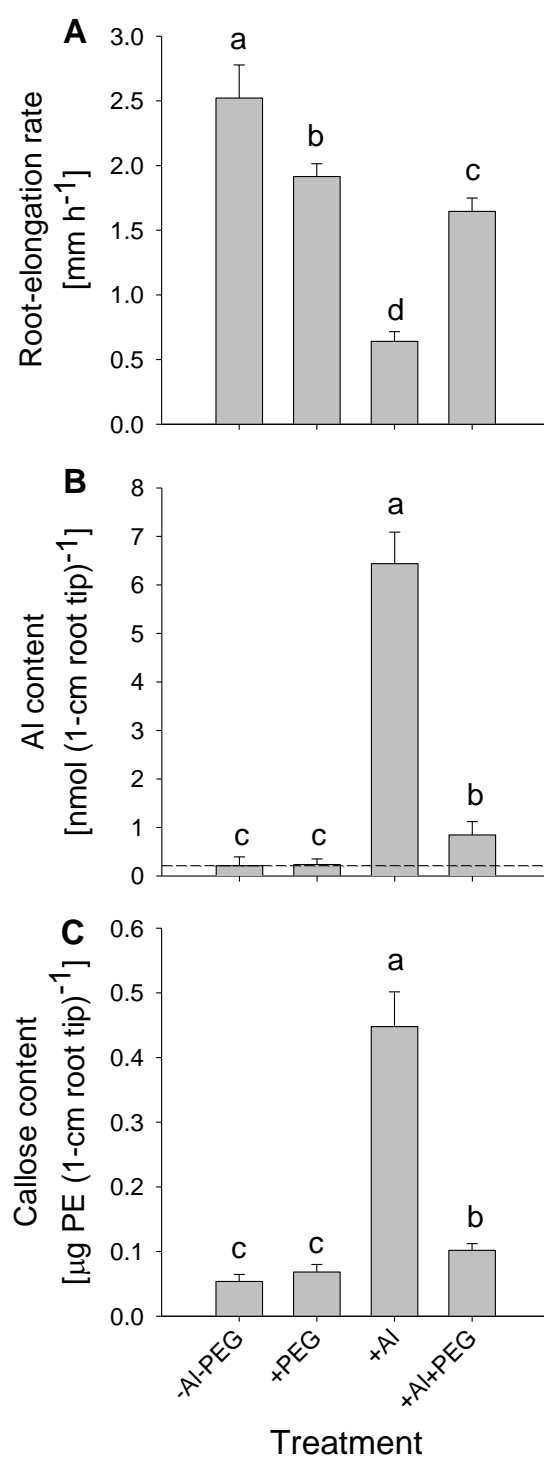
Figure 3 Root-elongation rate (A), Al (B) and callose (C) contents in 1-cm root tips of the common bean genotype VAX 1 under osmotic (0, -0.60 MPa OP) and Al stress (0, 25 μM Al). Plants were pre-cultured in a simplified nutrient solution containing 5 mM $CaCl_2$, 1 mM KCl, and 8 μM H_3BO_3 for 48 h for acclimation and pH adaptation, then treated without or with 25 μM Al in the absence or presence of PEG (150 g L^{-1} PEG 6000) in the simplified nutrient solution for 24 h, pH 4.5. The background value (dashed line) in (B) presents the mean Al content of the root tips without Al treatment. Bars represent means $\pm$ SD, n = 12 for (A) and n = 4 for (B, C). Means with different letters are significantly different at $P < 0.05$ (Tukey test) for the comparison of treatments.

Unlike the hydroponic experiment with PEG (see Fig. 3), in the soil experiment, combined drought (-0.31 MPa SWP) and Al stresses enhanced the inhibition of root elongation beyond the effects of the individual stresses (Fig. 4A, B) in spite of reduced Al stress as indicated by the significant reduction of callose formation in the root tips (Fig. 4C).
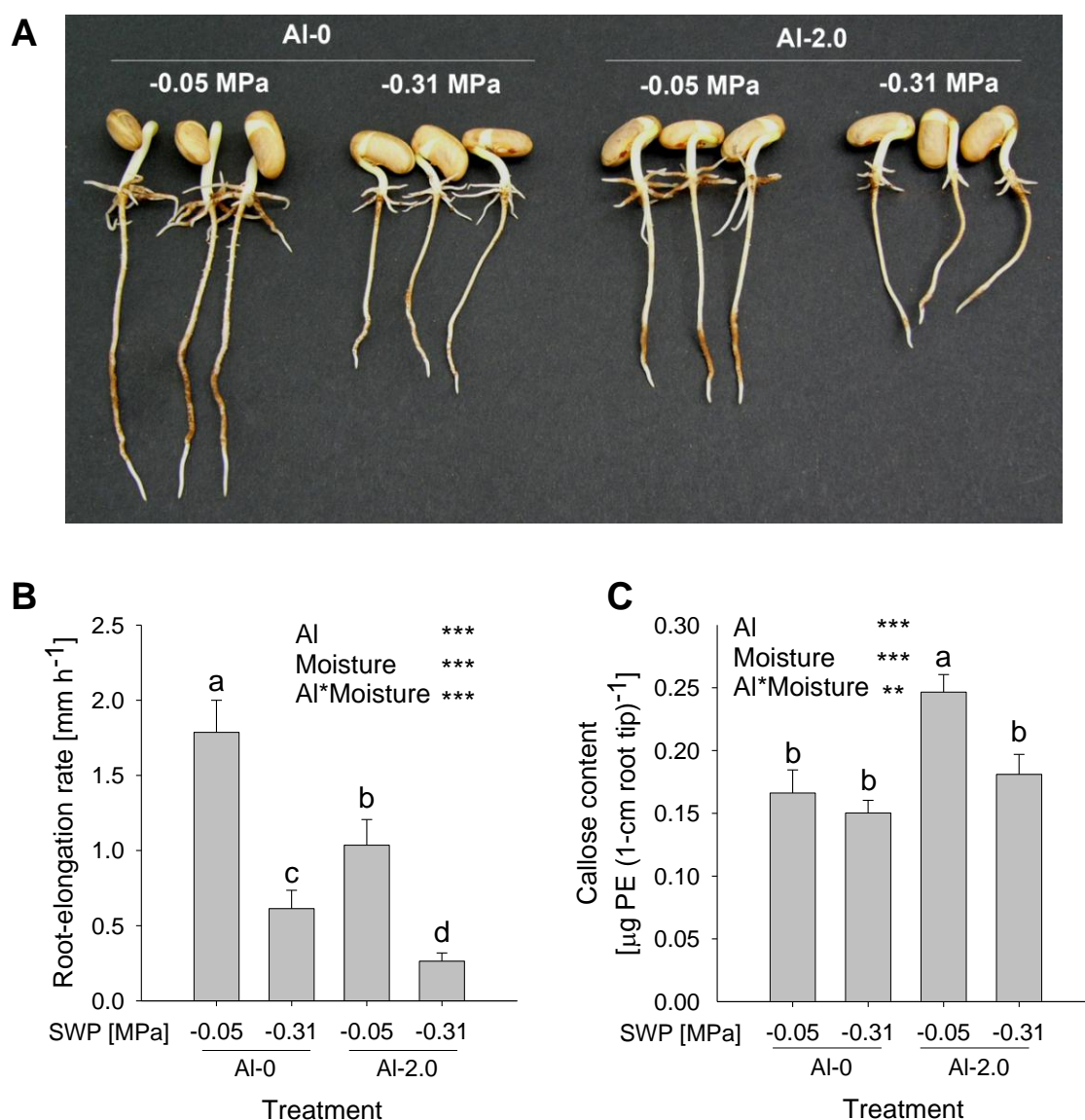
Figure 4 Seedling appearance (A), root-elongation rate (B) and callose contents in the 1-cm root tips (C) of the common bean genotype VAX 1 as affected by soil moisture and Al supply (g kg^{-1} soil). Two-day-old seedlings were grown in soil for 24 h. Bars represent means ± SD, n = 12 for (B) and n = 4 for (C). Means with different letters are significantly different at $P < 0.05$ (Tukey test) for the comparison of treatments. For the ANOVA, **, *** denote significant differences at $P < 0.01$, $P < 0.001$, respectively. SWP, soil-water potential.

To better understand the interaction between Al toxicity and drought in soil, both Al

supply and soil moisture, were varied in three rates in a factorial combination (0, 1.0 and 2.0 g Al and -0.05, -0.14, and -0.31 MPa SWP). The results confirmed that Al supply could enhance drought-induced inhibition of root elongation at all stress levels (Fig. 5A). Similar to osmotic stress, increasing drought stress reduced Al-induced root-tip callose formation confirming the amelioration of Al toxicity by drought (Fig. 5B). This observation is supported by the expression of a citrate transporter *MATE* gene which sensitively responds to Al treatment. Particularly the high Al supply strongly enhanced the expression of the *MATE* gene (Fig. 6A). High drought stress which only slightly stimulated the *MATE* gene expression, significantly suppressed the Al-induced gene expression confirming reduced Al stress as indicated by reduced callose formation (see above, Figs. 4 and 5). The *ACCO* gene sensitively responded to both Al and drought stresses (Fig. 6B). At all soil moisture levels, Al further enhanced the drought-induced up-regulated *ACCO* gene expression which is in agreement with the enhanced inhibition of root elongation at combined Al and drought stress factors (see above, Figs. 4 and 5).

From an analysis of PEG-induced changes in gene transcription in common bean root tips using SuperSAGE (Yang et al., 2011) we selected twelve genes with possible roles in the regulation of cell-wall properties and response to osmotic stress. In agreement with these results eleven of the selected genes were comparably affected osmotic stress (Yang et al., 2011) and by drought stress in soil (Fig. 7): six genes (*P5CS*, *SUS*, *HRGP*, *KS-DHN*, *PvLEA18* and *LTP*) were strongly up-regulated, one gene (*AQP*) was slightly up-regulated, while four genes (*BEG*, *PRP*, *XTHa* and *XTHb*) were down-regulated. Only the *CYP701A* gene was up-regulated by drought but down-regulated be osmotic (PEG) stress.

Aluminum stress alone (optimum soil moisture, -0.05 MPa SWP) also significantly affected the expression of most genes in the same direction as drought stress (Fig. 7). However, in most cases the effect was small compared to the drought effect. Exceptions were the *BEG*, *PRP* and *XTHa* genes which were affected by Al to the same degree as by decreasing soil moisture. Only the *BEG* gene expression was enhanced by Al but decreased by drought. The Al x soil moisture interaction was significant for all and highly significant for most genes. Al remarkably reduced the drought-enhanced expression of the *SUS*, *KS-DHN*, *PvLEA18* and *LTP* genes but further increased the expression of the *P5CS* and *HPRG* genes (only at the high Al supply).
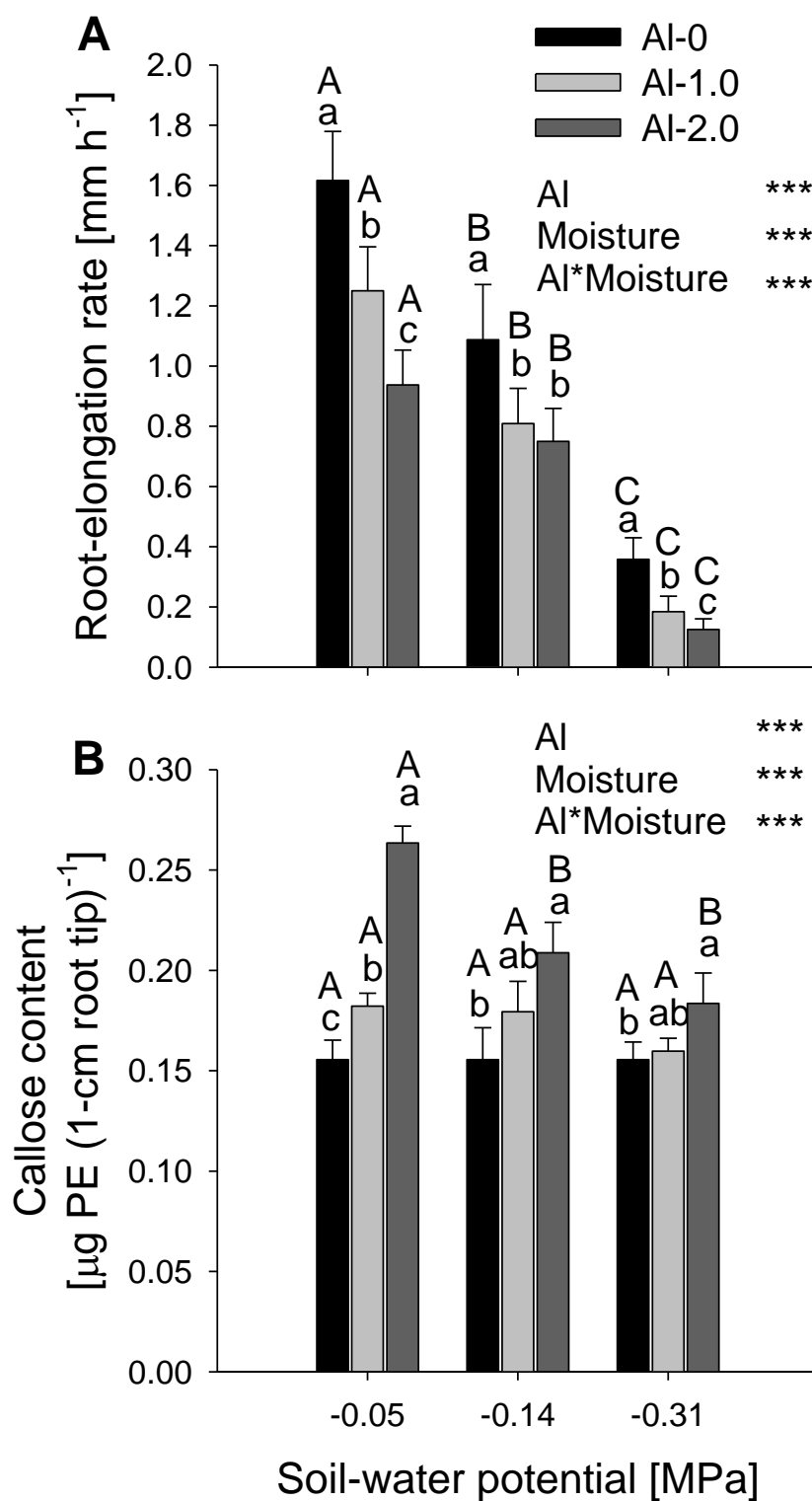
Figure 5 Root-elongation rate (A) and callose contents in the 1-cm root tips (B) of the common bean genotype VAX 1 as affected by soil moisture and Al supply (g kg^{-1} soil). Two-day-old seedlings were grown in soil for 24 h. Bars represent means ± SD, n = 12 for (A) and n = 4 for (B). Means with different small and capital letters are significantly different at $P < 0.05$ (Tukey test) for the comparison of Al treatments within soil moisture and comparison of soil-moisture treatments within Al treatments, respectively. For the ANOVA, *** denote significant differences at $P < 0.001$.
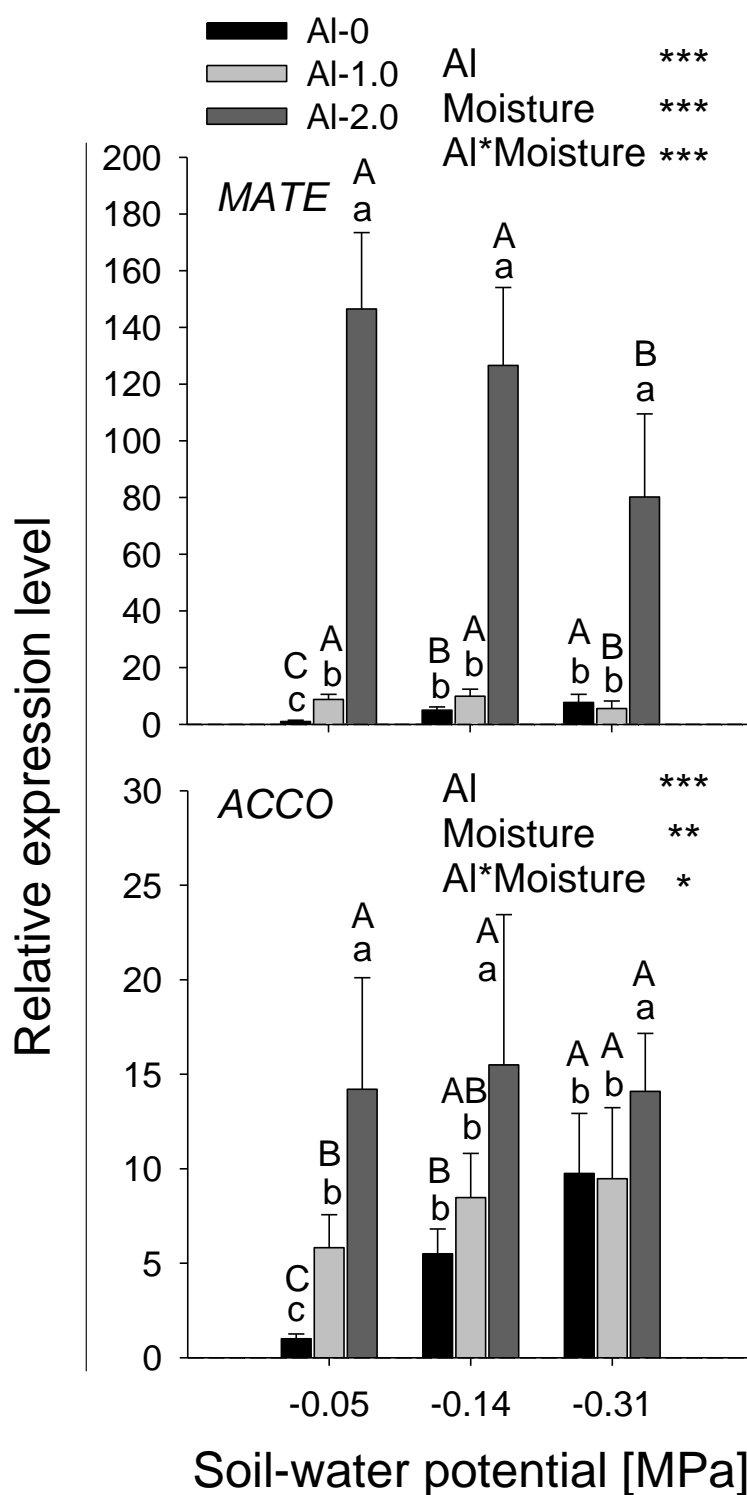
Figure 6 *MATE* and *ACCO* gene expression in the 1-cm root tips of the common bean genotype VAX 1 as affected by soil moisture and Al supply (g kg^{-1} soil). Two-day-old seedlings were grown in soil for 24 h. qRT-PCR was performed using the β-tubulin gene as internal standard. Bars represent means ± SD, n = 3. Means with different small and capital letters are significantly different at $P < 0.05$ (Tukey test) for the comparison of Al treatments within soil moisture and comparison of soil-moisture treatments within Al treatments, respectively. For the ANOVA, *, **, *** denote significant differences at $P < 0.05$, $P < 0.01$, $P < 0.001$, respectively.
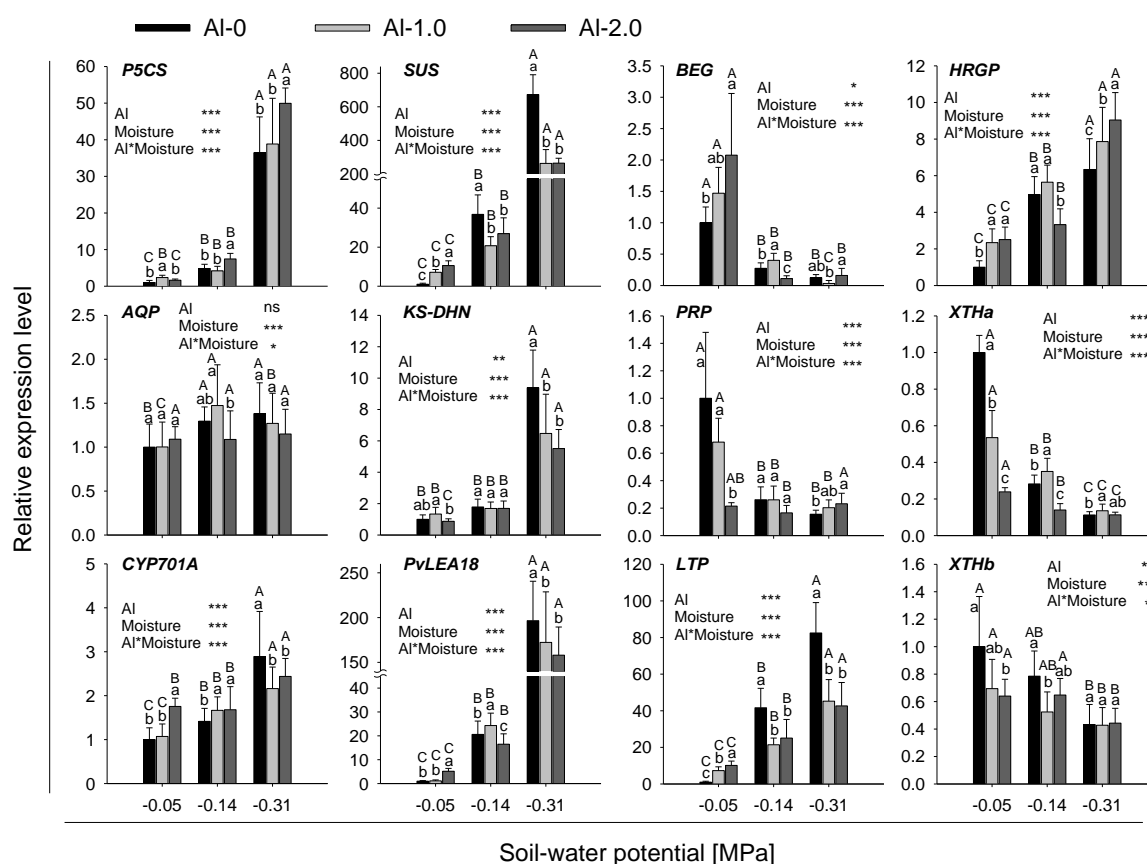
Figure 7 Cell-wall and osmotic stress-associated gene expression in 1-cm root tips of common bean genotype VAX 1 as affected by soil moisture and Al supply (g kg^{-1} soil). Two-day-old seedlings were grown in soil for 24 h. qRT-PCR was performed using the β-tubulin gene as internal standard. Bars represent means ± SD, n = 3. Means with different small and capital letters are significantly different at $P < 0.05$ (Tukey test) for the comparison of Al treatments within soil moisture and comparison of soil-moisture treatments within Al treatments, respectively. *** denote significant differences at $P < 0.001$. ns = not significant.

Drought stress significantly increased the expression of the genes *NCED* (9-cis-epoxycarotenoid dioxygenase), *ZEP* (zeaxanthin epoxidase), *AAO1* and *AAO2* (abscisic aldehyde oxidase) (Fig. 8B) involved in abscisic acid (ABA) biosynthesis (Fig. 8A). Al markedly affected only the *NCED* gene which was down-regulated at low soil moisture (significant Al × soil-moisture interaction) reversing the drought-enhanced expression of this gene (Fig. 8B). The expression of the two transcription factors *bZIP* and *MYB* (Fig. 8C) that are involved in the ABA-dependent gene regulation under drought stress (Fig. 8A, Shinozaki and Yamaguchi-Shinozaki, 1997) and selected from our previous analysis of PEG-induced genes expression in common bean root tips using SuperSAGE (Yang et al., 2011), was highly up-regulated by drought (Fig. 8B). In agreement with the *NCED* gene expression, Al stress in addition to drought stress reversed the drought-enhanced gene expression of both transcription factors (highly significant Al ×

soil-moisture interaction).
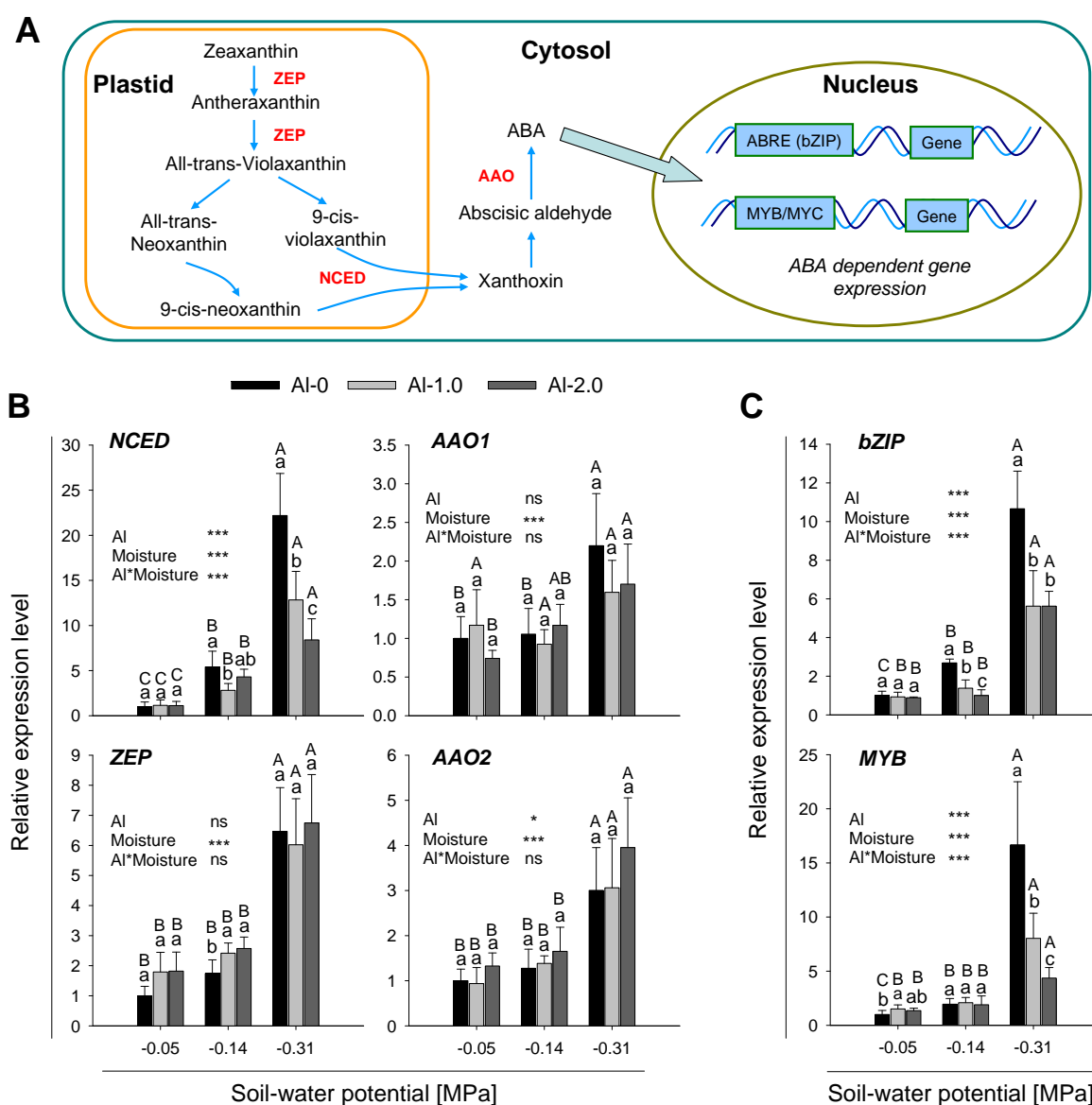
Figure 8 Schematic flow of ABA biosynthesis and ABA-dependent gene-regulation pathways (A) and the expression of genes coding for enzymes involved in the pathways as shown in A (B,C) in 1-cm root tips of the common bean genotype VAX 1 as affected by soil moisture and Al supply (g kg^{-1} soil). Two-day-old seedlings were grown in soil for 24 h. qRT-PCR was performed using the β-tubulin gene as internal standard. Bars represent means ± SD, n = 3. Means with different small and capital letters are significantly different at $P < 0.05$ (Tukey test) for the comparison of Al treatments within soil moisture and comparison of soil-moisture treatments within Al treatments, respectively. For the ANOVA, *, *** denote significant differences at $P < 0.05$, $P < 0.001$, respectively. ns = not significant. ZEP, zeaxanthin epoxidase; NCED, 9-cis-epoxycarotenoid dioxygenase; AAO, abscisic aldehyde oxidase; ABRE, ABA-responsive element.

The observed changes in the expression of genes related to ABA biosynthesis and of transcription factors mediating ABA-dependent gene regulation were fully supported by the determination of ABA concentrations in the root tips (Fig. 9). Drought stress alone

greatly increased the ABA concentration. Al supply alone only slightly decreased the ABA concentration in the root tips of well-watered plants. In combination with drought stress Al markedly suppressed the drought-enhanced ABA accumulation in the root tips (highly significant Al x drought interaction).
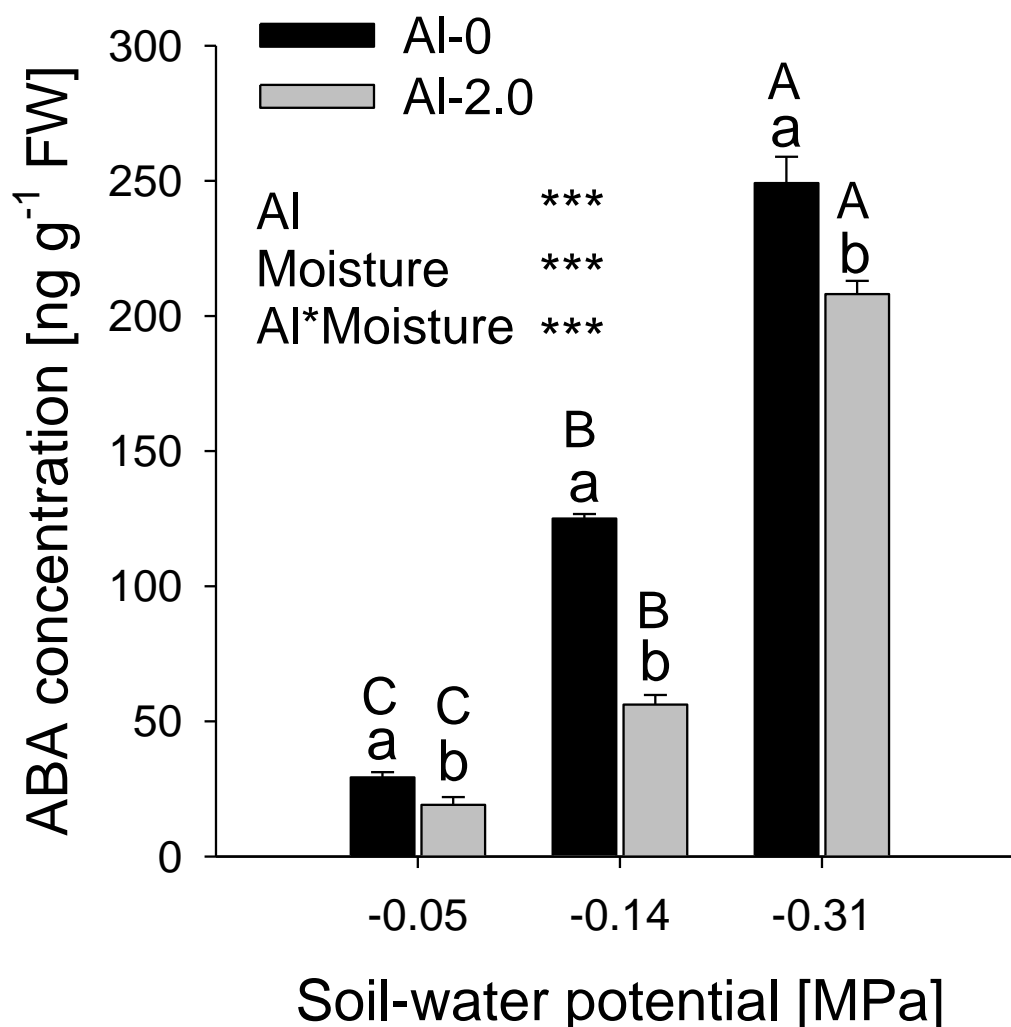
Figure 9 Abscisic acid (ABA) concentration in the 1-cm root tips of the common bean genotype VAX 1 as affected by soil moisture and Al supply (g kg^{-1} soil). Two-day-old seedlings were grown in soil for 24 h. Bars represent means ± SD, n = 3. Means with different small and capital letters are significantly different at $P < 0.05$ (Tukey test) for the comparison of Al treatments within soil moisture and comparison of soil-moisture treatments within Al treatments, respectively. For the ANOVA, *** denote significant differences at $P < 0.001$.

In addition to ABA, the concentrations of other phytohormones were analyzed in the root tips. No significant effects of either drought or Al were found on salicylic acid (SA) and jasmonic acid (JA) (Supplemental Fig. S3). Sole Al stress significantly increased, but combined Al and drought stress reversed the Al-enhanced indole-3-acetic acid (IAA)

116

concentration. However, drought stress significantly increased not only the biologically active zeatin-riboside (ZR) (Fig. 10) but also the trans-zeatin (tZ) (Supplemental Fig. S3) concentrations in the root tips. Among the cytokinin (CK) storage forms only the zeatin-O-glucoside (ZOG) concentration was strongly increased at the lowest soil moisture (Supplemental Fig. S3). In well-watered soil Al did not affect the CK concentrations. However, Al strongly enhanced the drought-increased ZR and ZOG concentrations in the root tips (Fig. 10; Supplemental Fig. S3).

The clear changes in CK concentration prompted the study in the root tips of common bean the expression of the genes *IPT* (adenosine-phosphate isopentenyl-transferase), *CYP735A* (cytochrome P450 monooxygenase 735A) involved in CK biosynthesis and *ZOGT* (zeatin-O-glucosyltransferase), *βGlc* (β-glucosidase) and *CKX* (cytokinin oxidase/dehydrogenase) involved in CK degradation (Fig. 11A). Both drought and Al treatment individually significantly increased the gene expression of all genes except *βGlc* (Fig. 11B). Under combined drought and Al stresses, Al treatment decreased the drought-enhanced expression of all *IPT* genes. The Al-enhanced expression of the *CYP735A, ZOGT*, and *CKX* genes in well-watered plants disappeared under reduced soil moisture maintaining the drought-stimulated expression level.
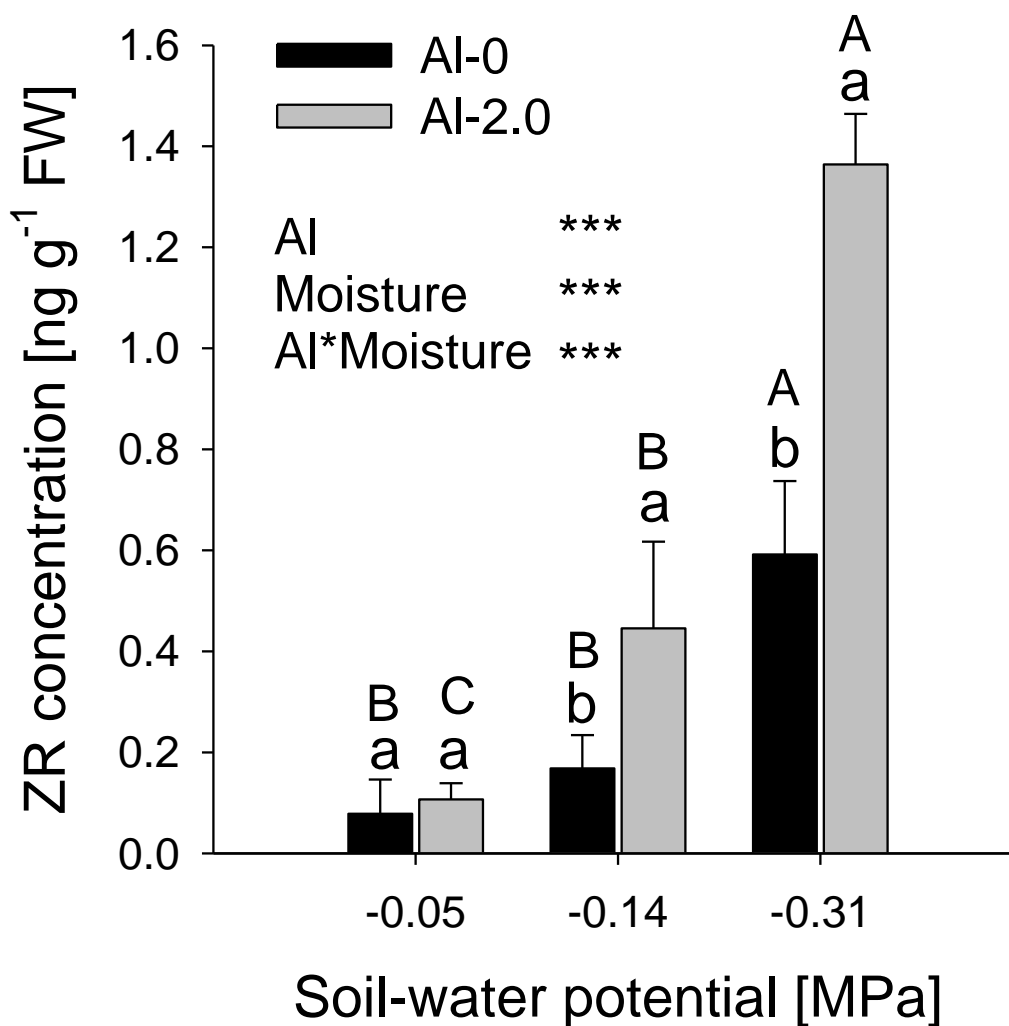
Figure 10 Zeatin riboside (ZR) concentration in the 1-cm root tips of the common bean genotype VAX 1 as affected by soil moisture and Al supply (g kg^{-1} soil). Two-day-old seedlings were grown in soil 24 h. Bars represent means ± SD, n = 3. Means with different small and capital letters are significantly different at $P < 0.05$ (Tukey test) for the comparison of Al treatments within soil moisture and comparison of soil-moisture treatments within Al treatments, respectively. For the ANOVA, *** denote significant differences at $P < 0.001$.

Figure 11 Schematic flow of CK biosynthesis pathways. Unknown genes are marked with ? (B) Expression of genes coding for enzymes involved in CKs biosynthesis as shown in A in the root tips of the common bean genotype VAX 1 as affected by soil moisture and Al supply (g kg^{-1} soil). Two-day-old seedlings were grown in soil for 24 h. qRT-PCR was performed using the β-tubulin gene as internal standard. Bars represent means ± SD, n = 3. Means with different small and capital letters are significantly different at $P < 0.05$ (Tukey test) for the comparison of Al treatments within soil moisture and comparison of soil-moisture treatments within Al treatments, respectively. For the ANOVA, *, **, *** denote significant differences at $P < 0.05$, $P < 0.01$, $P < 0.001$, respectively. ns = not significant. DMAPP, dimethylallyl diphosphate; iP, N^6-(Δ^2-isopentenyl)-adenine; tZ, *trans*-zeatin; cZ, *cis*-zeatin; DZ, dihydrozeatin; iPR, N^6-(Δ^2-isopentenyl)-adenine riboside; tZR, *trans*-zeatin riboside, cZR, *cis*-zeatin riboside; DZR, dihydrozeatin riboside; iPRDP, iP riboside 5'-diphosphate; iPRTP, iP riboside 5'-triphosphate; iPRMP, iP riboside 5'-moophosphate; tZRDP, tZR 5'-diphosphate; tZRTP, tZR 5'-triphosphate; tZRMP, tZR 5'-monophosphate; DZRMP, DZR 5'-monophosphate; cZRMP, cZR 5'-monophosphate; IPT, adenosine-phosphate isopentenyl-transferase, CYP735A, cytochrome P450 monooxygenase 735A; CKX, cytokinin oxidase/dehydrogenase; ZOGT, zeatin-O-glucosyltransferase; βGlc, β-glucosidase.

Discussion

The main and easily observed symptom of Al toxicity is the rapid inhibition of root growth (Horst et al., 1992; Delhaize and Ryan, 1995; Horst et al., 2010). Plant Al toxicity mainly depends on the soil pH, when the pH drops below 5, Al^{3+} will be released into the soil solution and becomes the main limiting factor of crop production on acid soils (Eswaran et al., 1997). This is supported by the present results: the lower the soil pH the higher the Al toxicity in common bean (Fig. 1). A positive correlation between Al-induced short-term inhibition of root elongation and Al accumulation was found in the root-tip apoplast of common bean (Rangel et al., 2009) indicating that the exclusion of Al from the root tip apoplast is crucial for Al resistance (Horst et al., 2010). Under short-term Al stress, Al accumulates mainly in the root apoplast of common bean (Rangel et al., 2009), where Al^{3+} strongly binds to the negatively charged binding sites (Blamey et al., 1990; Horst et al., 2010). However, under soil conditions, the Al content in the root tip could not reliably be analyzed because of the difficulty to remove soil from the root surface. Although it was suggested that titanium (Ti) can be used as an indicator of soil contamination of plant samples because it is abundant in soil but not in plants (Cook et al., 2009), laser ablation inductively coupled plasma mass spectrometry (LA-ICP-MS) analysis of root tips showed that titanium can also be absorbed into the root tissue (data not shown). Therefore, our efforts to analyze root Al in the soil-grown plants corrected for soil contamination on the basis of the Ti content failed in this study.

Induction of callose synthesis has been proved to be a sensitive indicator of Al injury in roots (Wissemeier et al., 1987; Staß and Horst, 2009), particularly in the root apex (Wissemeier and Horst 1995; Sivaguru et al., 2006) and has been used as a reliable parameter for the classification of genotypes of different plant species for Al resistance and adaptation to acid Al-toxic soils (Wissenmeier et al., 1992; Horst et al., 1997; Eticha et al. 2005b). In the present study, we confirmed that there was a significantly negatively correlation between the Al-induced inhibition of root elongation and the callose content in the root tips of the Al-sensitive bean genotype VAX 1 (Fig. 2B, E). Since, in addition, a significantly positive linear correlation between the Al-induced callose synthesis and Al concentration in the root tips existed (Fig. 2C) the induction of callose was used in this study as a sensitive and reliable indicator of Al accumulation in the root tips of soil-grown plants. In the present study, PEG 6000-induced osmotic stress reduced the Al content in root tips and thus enhanced the Al resistance in the bean genotype VAX 1 (Fig. 3A, B),

which support our previous results (Yang et al., 2010). The significant suppression of Al-induced callose production in the PEG 6000-treated root tips (Fig. 3C) further confirmed that callose content is a reliable indicator of Al accumulation in root tips and Al toxicity. In soil-grown plants drought reduced the Al-induced enhancement of callose production in the bean root tips (Fig. 4C, Fig. 5B) suggesting that drought in soils as well as PEG 6000 in hydroponics may share the same mechanism in reducing Al accumulation in the root tips and thus Al toxicity.

In contrast to PEG 6000 (Yang et al., 2011), drought also increased the expression of the *ACCO* gene (Fig. 6). Thus it appears that the expression of this gene is not specific to Al. Drought (-0.31 MPa SWP) resulted in a 10-fold up-regulation compared to the well-watered control (WW, no Al). This up-regulation was similar to the 15-fold up-regulation by Al (2.0 g Al kg^{-1} soil). In contrast to the *ACCO* gene, the expression of the *MATE* gene was rather specific for Al (140-fold increase) compared to drought (10-fold increase). Compared to hydroponics (Eticha et al., 2010; Yang et al., 2011) the Al-induced *MATE* gene expression was less in soil, which can mainly be attributed to a higher basic level of gene expression in the WW limed soil. Drought (-0.31 MPa SWP) significantly reduced the Al-induced expression of the *MATE* gene particularly at the high Al level (2.0 g kg^{-1} soil) (Fig. 6A), providing further evidence that drought reduces Al toxicity of common bean.

Although the decrease of callose formation and *MATE* gene expression strongly support the view that drought reduces Al toxicity of common bean in soil, Al supply aggravated the drought stress-induced inhibition of root elongation (Fig. 4A, B; Fig. 5A). This result is in contrast to the alleviation of Al-induced inhibition of root elongation by PEG 6000 (osmotic stress) in hydroponics (Fig. 3A; Yang et al., 2010). It thus appears that in soil, Al increases the susceptibility of roots to drought as proposed by Goldman et al. (1989) in soybean. The difference between the two experimental approaches may result from the possibility to adapt to osmotic stress (PEG 6000) in hydroponic culture allowing sufficient water uptake to resume root elongation, whereas in dried soil the adaptation to water deficit fails particularly in presence of Al.

Microarray analysis in Arabidopsis has revealed that the drought-induced genes can be classified into two groups (Shinozaki et al., 2003). The first group codes for proteins which probably function in stress tolerance, such as late embryogenesis abundant (LEA) proteins, osmotin, antifreeze proteins, mRNA-binding proteins, key enzymes for osmolyte

biosynthesis, water channel proteins, sugar and proline transporters, detoxification enzymes and lipid-transfer proteins. The second group comprises genes coding for regulatory proteins involved in signal transduction and transcription factors such as *bZIP*, *MYB*, *MYC* and *DREB* (Shinozaki and Yamaguchi-Shinozaki, 2007). Our previous study with common bean in hydroponics using PEG 6000 mimicking drought stress revealed that the osmotic stress-associated genes *P5CS*, *SUS*, *AQP*, *KS-DHN*, *PvLEA18* were significantly up-regulated while *CYP701A* was down-regulated in the root tips under stress (Yang et al., 2011). In the present study the same genes were comparably regulated, with the exception of the *CYP701A* gene which was up-regulated by drought stress in soil (Fig. 7) supporting the use of PEG-6000 in hydroponics in determining short-term drought stress responses of root apices at the molecular level.

The accumulation of ABA in the root tips is necessary to maintain the primary root elongation in maize at low water potentials (Sharp et al., 2004; Yamaguchi and Sharp, 2010). In the current study drought significantly increased the ABA concentration in the root tips of common bean (Fig. 9). Al significantly suppressed this drought-enhanced ABA accumulation suggesting reduced protection of root tips from drought causing aggravated inhibition of root elongation. Three genes encoding zeaxanthin epoxidase (ZEP), 9-cis-epoxycarotenoid dioxygenase (NCED) and abscisic aldehyde oxidase (AAO) involved in the ABA biosynthesis have been identified (Seo and Koshiba, 2002; Fig. 8A). It has been reported that drought increased the gene expression of *ZEP* in tobacco (*Nicotiana plumbaginifolia*) (Audran et al., 1998), tomato (*Solanum lycopersicum*) (Thompson et al., 2000), *NCED* in common bean (*P. vulgaris*) (Qin and Zeevaart, 1999), cowpea (*Vigna unguiculata*) (Iuchi et al., 2000), avocado (*Persea Americana*) (Chernys and Zeevaart, 2000) and barley (*Hordeum vulgare*) (Seiler et al., 2011), and *AAO* in *Arabidopsis thaliana* (Seo et al., 2000). Overexpression of *NCED* in tobacco (*N. plumbaginifolia*) and Arabidopsis resulted in an increase in the endogenous ABA level and an improvement of drought tolerance (Iuchi et al., 2001; Qin and Zeevaart, 2002). In this study, the expression of *NCED*, *ZEP*, *AAO1* and *AAO2* genes in the root tips of common bean were significantly up-regulated by drought (Fig. 8B). However, Al reversed the drought-enhanced expression only of the *NCED* gene (Fig. 8B) suggesting that *NCED* is the critical gene in the Al/drought interaction leading to the suppression of drought-induced ABA production in the root apex of common bean. Some hydroponic studies indicated that Al induces ABA production in the root tips of soybean (*Glycine max*), which was supposed to regulate Al resistance mechanisms (Shen et al., 2004; Hou et al., 2010). However, we

found that in common bean Al slightly but significantly reduced the ABA accumulation in the root tips, but had no effect on the expression of genes involved in ABA biosynthesis except *ZEP* which was enhanced by Al treatment (Fig. 8B).

ABA was shown to be involved in the regulation of many water deficit-induced genes (Bray, 1997), in which the ABA-responsive element (ABRE) and the MYB/MYC transcription factor play key roles (Shinozaki and Yamaguchi-Shinozaki, 1997; 2007). The ABRE elements contain a DNA-binding motif of the basic domain/leucine zipper (*bZIP* structure). When ABREs binds to the corresponding bZIP family transcription factors, it can lead to ABA-induced gene expression. Therefore, based on the above information, we speculated that Al might suppress drought-induced ABA-responsive genes expression via decreasing the regulation of ABA-dependent transcription factors such as bZIP and MYB, and thus reduce the drought tolerance of the root (Presented in Fig. 12). As expected, in this study, the expression of the two transcription factor genes, *bZIP* and *MYB*, were significantly enhanced by drought in the root tips of common bean (Fig. 8C), which was in agreement with the osmotic stress (PEG 6000)-induced expression of both genes in common bean (Yang et al., 2011). Consistent with the change in *NCED* gene expression and ABA accumulation in the root tips, Al reversed the drought-elevated gene expression of *bZIP* and *MYB* (Fig. 8C). A number of studies have demonstrated that the induction of bZIP and MYB transcription factors play a key role in drought-induced gene expression and drought tolerance. For example, Uno et al. (2000) reported that the ABA-mediated induction of the dehydration-responsive Arabidopsis gene, *rd29B*, via phosphorylation of a protein kinase requires two ABREs and two bZIP transcription factors (AREB1 and AREB2). Transgenic rice over-expressing *OsbZIP23* showed significantly improved tolerance to drought and sensitivity to ABA, while the *Osbzip23* mutant showed significantly decreased sensitivity to ABA and decreased drought tolerance (Xiang et al., 2008). Rodriguez-Uride and O'Connell (2006) found a root specific bZIP transcription factor responsive to water deficit in tepary bean (*Phaseolus acutifolius*) and common bean (*P. vulgaris*) which may allow the plant to maintain root elongation. The MYB and MYC elements were defined from the analysis of an Arabidopsis drought-inducible gene, *rd22*, involved in regulating the expression of ABA-induced genes in response to severe water-deficit stress (Abe et al., 1997). In Arabidopsis, Seo et al. (2009) observed that the R2R3-type MYB transcription factor, MYB96, regulated drought stress response by integrating ABA and auxin signals. The *MYB96*-overexpressing *A. thaliana myb96-ox* mutant exhibited enhanced drought resistance with reduced number of lateral roots,

whereas the *myb96-1* mutant was more susceptible to drought, suggesting that *MYB96* is a molecular link that mediates the ABA-auxin crosslink in the drought-stress response.

The accumulation of osmotically active compounds, such as sucrose and proline, has been considered as one of the crucial processes for osmotic adjustment in plant cellular adaptation to drought (Chaves et al., 2003). In the resurrection plant *C. plantagineum*, the sugar octulose was rapidly converted into sucrose during dehydration (Bianchi et al., 1991), and this sugar conversion was coupled with an increased expression of the Δ1-pyrroline-5-carboxylate synthase (*P5CS*), sucrose synthase (*SUS)* and sucrose-phosphate synthase (*SPS*) genes (Ingram et al., 1997; Rodriguez et al., 2010). Dehydration-induced enhanced expression of the *SUS* gene was also found in other species such as maize (Zheng et al., 2004; Spollen et al., 2008). SUS plays a major role in sucrose biosynthesis, which catalyses a reversible reaction UDPGlc + fructose $\rightleftharpoons$ sucrose + UDP. Whether the up-regulation of *SUS* contributes to the synthesis (Geigenberger and Stitt, 1993; Déjardin et al., 1997) or degradation (Heim et al., 1993) of sucrose is still not well known. But it appears that the physiological significance of a rapid cycling of sucrose for stressed-cells is an enhanced carbon partitioning in favour of sucrose accumulation for osmoregulation (Wang et al., 2000). P5CS is the enzyme which catalyzes conversion of pyrroline-5-carboxylic acid (P5C) to proline in plants (Kishor et al., 2005). Ooho et al. (2003) found that dehydration and rehydration rapidly up-regulated and repressed the gene expression of *P5CS* in Arabidopsis, respectively, which was supported by our previous study on PEG-induced osmotic stress in common bean (Yang et al., 2011). Overexpression of the *P5CS* gene in various plants resulted in elevated proline production and improved OS tolerance (reviewed by Bartels and Sunkar, 2005).

Aquaporins (AQPs) facilitate water transport through cellular membranes, and thus play major roles in water homeostasis (Alexandersson et al., 2010). Genes encoding AQPs show distinct responses to drought. For example, in *Arabidopsis* the transcripts of the plasma membrane intrinsic protein (PIP) (one subfamily of AQPs) were down-regulated by drought, with the exception of *AtPIP1*;*4*, *AtPIP2*;*5* (up-regulated) and *AtPIP2*;*6* (unaffected) (Alexandersson et al., 2005). Upon osmotic stress, *OsPIP1*;*3* was up-regulated in upland rice that has better drought resistance compared to lowland rice, in which *OsPIP1*;*3* did not show any change in expression (Lian et al., 2006). A positive response of the AQP gene to drought may trigger higher water permeability and facilitate water flux, while a negative response may result in decreased membrane permeability and allow cellular water conservation (Bartels and Sunkar, 2005).

Late embryogenesis-abundant (LEA) proteins are well known to play crucial roles in cellular dehydration tolerance (Ingram and Bartels, 1996; Hundertmark and Hincha, 2008). In common bean, it has been found that the expression of the *PvLEA18* gene was highly induced particularly in roots by water deficit (Colmenero-Flores et al., 1999). The *PvLEA18* gene was found to be up-regulated by PEG 6000 in root tips of common bean according to a transcriptomic study using SuperSAGE library (Yang et al., 2011) which was supported by the present study (Fig. 7).

The cytochrome P450s superfamily (CYP) is a large and diverse group of enzymes and may serve as monooxygenases involved in the biosynthesis of metabolites conferring abiotic stress tolerance (Schuler and Werck-Reichhart, 2003). In common bean, the expression of a *CYP701A* gene belonging to the *CYP* family and homologue to soybean (*G. max*) *CYP701A16* was up-regulated by drought (Fig. 7), but it was down-regulated by PEG-induced osmotic stress (Yang et al., 2011). The role of this gene in drought tolerance is not well understood. The different response of the *CYP701A* gene to drought and PEG stress may indicate that the response to drought and PEG may involve different molecular responses.

The modification of cell-wall extension properties has been shown to be one of the mechanisms of the response of maize primary root growth to water deficit (Sharp et al., 2004; Yamaguchi and Sharp, 2010). Thus, besides the osmotic stress-associated genes, in this study, six cell wall-associated genes (*BEG*, *HRGP*, *PRP*, *XTHa*, *XTHb* and *LTP*) were also selected from our transcriptomic analysis (SuperSAGE) of PEG-induced gene expression in common bean (Yang et al., 2011). The PEG 6000-induced reduction of Al accumulation has been related to the reduction of cell-wall porosity (Yang et al., 2010). In this study, quantitative Real-Time-PCR (qRT-PCR) analysis demonstrated that the differential expression of these six cell wall-associated genes by drought were similar with their response to PEG (Fig. 7; Yang et al., 2011). Thus, it appears that the drought-induced reduction of Al toxicity, which is indicated by the suppression of Al-enhanced callose production and *MATE* gene expression in the root tips (Fig.4, Fig. 5, Fig. 6), might also result from drought-induced alteration of cell-wall structure. Reduced expression of the *XTHa*, *XTHb* and *BEG* genes and increased expression of the *HRGP* gene might contribute to PEG-induced reduction of cell-wall porosity in common bean. XTH (xyloglucan endotransglucosylase/hydrolase) and BEG (Glucan endo-1, 3-beta-glucosidase) are two cell wall loosening enzymes involved in cleavage or degradation of cell-wall polymers (Rose et al., 2002; Bray, 2004; Minic and Jouanin, 2006). Nieuwland et al. (2005) reported

that *LTP* (lipid transfer proteins) enhanced cell-wall extension causing non-hydrolytic disruption of the cell wall in tobacco. Therefore, in this study with common bean, the increased expression of the *LTP* gene (Fig. 7) may contribute to the maintenance of root elongation of common bean under drought stress. Al treatment reduced the drought-enhanced expression of the *LTP* gene (Fig. 7) thus enhancing the inhibition of root elongation by combined drought/Al stresses by reducing cell-wall extensibility.

It has been reported that most genes encoding LEA proteins in Arabidopsis had ABRE elements in their promoters and were induced by ABA. Among these, two genes (*At2g23110*, *At2g23120*) belong to the *PvLEA18* group. Dehydrins (DHNs) is the second biggest group of LEA proteins (Hundertmark and Hincha, 2008). The EST of the *KS-DHN* gene in common bean has high sequence similarity to the *At1g54410* gene which belongs to the DHN group of LEA proteins and also can be induced by ABA (Hundertmark and Hincha, 2008). In tomato (*S. lycopersicum*), over-expression of the drought-induced *SlAREB1* gene up-regulated the genes encoding LTP and LEA proteins (Orellana et al., 2010). Moreover, Saftner and Wyse (1984) observed that ABA increased sucrose uptake in the roots of sugar beet (*Beta uldgaris*), and the ABA-insensitive (*abi8*) mutant showed a strong reduction of the expression of the *SUS* gene in Arabidopsis (Brocard-Gifford et al., 2004). In this study, the Al suppression of the drought-induced gene expression of *SUS*, *PvLEA18*, *KS-DHN* and *LTP* in the root tips of common bean (Fig. 7) was consistent with the reduction in expression of the *NCED* gene (Fig. 8B) involved in ABA biosynthesis and thus ABA accumulation (Fig. 9) and of the two transcription factors *bZIP* and *MYB* (Fig. 8C) involved in the regulation of ABA-dependent genes under drought stress.

Several studies have clearly shown that ABA can suppress ethylene production, and the maintenance of root elongation under water-deficit conditions requires increased ABA levels to prevent excess ethylene production (Sharp et al., 2000; Spollen et al., 2000; Sharp, 2002; LeNoble et al., 2004). Cytokinin (CK) stimulates ethylene biosynthesis (Chae et al., 2003) and ethylene mediated the CK-induced inhibition of root elongation as observed in pea (*Pisum sativum*) (Bertell and Eliasson, 1992), Arabidopsis (Cary et al., 1995; Růžička et al., 2009) and common bean (Massot et al., 2002). It was reported that ethylene and CKs strongly inhibit root growth (Werner et al., 2001; Stepanova et al., 2007; Swarup et al., 2007). Up to now, little evidence exists on the direct effect of ABA on CKs. However, Jelić and Bogdanović (1988) reported that ABA inhibited the CK-stimulated synthesis of chlorophyll in the light in *Pinus nigra.* Ding et al. (2008) found that ABA could suppress CK activation of cell division in the roots of *Medicago truncatula*. Vysotskaya et al. (2009)

supposed that ABA could regulate shoot CK concentrations via mediating the activity of cytokinin oxidase/dehydrogenase (CKX) involved in the CK biosynthesis; Takei et al. (2004) observed that ABA treatment highly reduced the expression of the CK biosynthesis genes *CYP735A1* and *CYP735A2* in Arabidopsis. Therefore, the cross-talk between these phytohormones revealed a potential regulatory mechanism of Al-reduced drought resistance in common bean (presented in Fig. 12): the Al-suppressed drought-induced ABA accumulation in the root tips may promote CK production, subsequently stimulate synthesis of ethylene, and thus enhance inhibition of root elongation. Furthermore, we also observed that Al enhanced the drought-induced expression of the *ACCO* gene (Fig. 6) in agreement with the enhanced inhibition of root elongation at combined Al and drought stresses (Fig. 5A). It is well known that ACCO catalyzes the last step in the biosynthesis of ethylene in plants (Wang et al., 2002).

According to the above speculation, we further analysed the concentrations of other phytohormones in the root tips of common bean, such as different forms of CKs, IAA, SA and JA (Supplemental Fig. S3). Of these phytohormones, drought only significantly increased the concentrations in the root apices of the biologically active CK forms, particularly zeatin riboside (ZR) (Fig. 10) and *trans*-zeatin (tZ) (Supplemental Fig. S3). Al greatly enhanced the drought effect on the concentrations of ZR and of zeatin-O-glucoside (ZOG) which is the major CK storage form (Supplemental Fig. S3). Although the specific role of ZR in root elongation is not yet known, its increased accumulation in the root tips (Fig. 10) particularly under combined drought/Al stress may be involved in the aggravated inhibition of root elongation (Skoog and Miller, 1957; Cary et al., 1995; Werner et al., 2001). Moreover, we found that there was no Al effect on the SA synthesis in the root tips of bean, though Yang et al. (2003) observed that SA induced Al resistance by modulation of citrate exudation from roots of *Cassia tora*. The difference may depend on the species or the Al stress conditions. However, we found that sole Al treatment increased the IAA concentration in the root tips of bean while subsequently was suppressed by drought (Supplemental Fig. S3), which may support the results that drought reduced Al toxicity.

The genes *IPT* (adenosine-phosphate isopentenyl-transferase), *CYP735A* (cytochrome P450 monooxygenase 735A), *CKX*, *ZOGT* (zeatin-O-glucosyltransferase) and *βGlc* (β-glucosidase) encoding the proteins involved in the biosynthesis of CKs have been identified (Sakakibara, 2006; Kudo et al., 2010; Fig. 11A). Transgenic studies have demonstrated that these genes affect root growth by changing the CKs level in the root tissues. For example, using a transactivation system overexpression of the *IPT* gene in

Arabidopsis (Kuderová et al., 2008) enhanced the levels of biologically active CKs and inhibited primary root elongation. Over-expression of the *ZOGT* gene in maize (Pineda Rodo et al., 2008), the *CKX* gene in Arabidopsis (Werner et al., 2010) and tobacco (Werner et al., 2001; Werner et al., 2010) resulted in enhanced root growth and branching. It appears that not only the primary root but also the lateral root growth is seriously inhibited by CKs. In the current study, the inhibition of both primary and lateral root growth in common bean by drought and Al (Al plus drought > drought > Al > control) is clearly shown in Fig. 4A. Werner et al. (2010) reported that the root-specific reduction of CK by overexpression of the *CKX* gene strongly enhanced drought resistance in Arabidopsis and tobacco. In the present study, both drought and Al treatment significantly increased the expression levels of the *IPT*, *CYP735A*, *ZOGT* and *CKX* genes but not of the *βGlc* gene which catalyze the de-glycosylation of CKs (Fig. 11A) in the root tips of common bean (Fig. 11B). However, although drought reduced Al toxicity as described above, it did not reduce the Al-induced gene expression of *CYP735A*, *ZOGT* and *CKX* (Fig. 11B), suggesting that the *CYP735A* and *ZOGT* genes play key roles in Al-enhanced drought-induced ZR and ZOG accumulation, respectively, in the root tips of common bean (Fig. 10; Supplemental Fig. S3). The maintenance of the expression of the ZOGT and CKX genes, responsible for the glycosylation and degradation of CKs, respectively (Fig. 11A), may play a role in the rescue of the roots from ZR-induced growth inhibition by degradation or deactivation and maintenance of optimal levels of CKs (Werner et al., 2001). No Al effect on CK concentrations was found in the root tips (Fig. 11B), although Al alone significantly increased the expression of most CK biosynthetic genes indicating that the synthesized CKs were transported from the root tips to other plant organs. It was reported that CKs transported to the shoot function as a long-distance regulatory signal (Kudo et al., 2010) contributing to maintaining shoot growth (Werner et al., 2001) under Al stress.

In conclusion, taken together the results from this study suggest that low soil moisture leading to drought stress alleviates Al toxicity based on less Al-induced callose formation and lower expression of a *MATE* gene in the root tips of the Al-sensitive bean genotype VAX 1. However, Al treatment increased the susceptibility of the root apex to drought by aggravating drought-induced inhibition of root elongation resulting from the disruption of the gene regulatory network involved in the ABA signal transduction and the ABA signal cross-talk with other phytohormones that are necessary for maintaining root growth under drought stress.
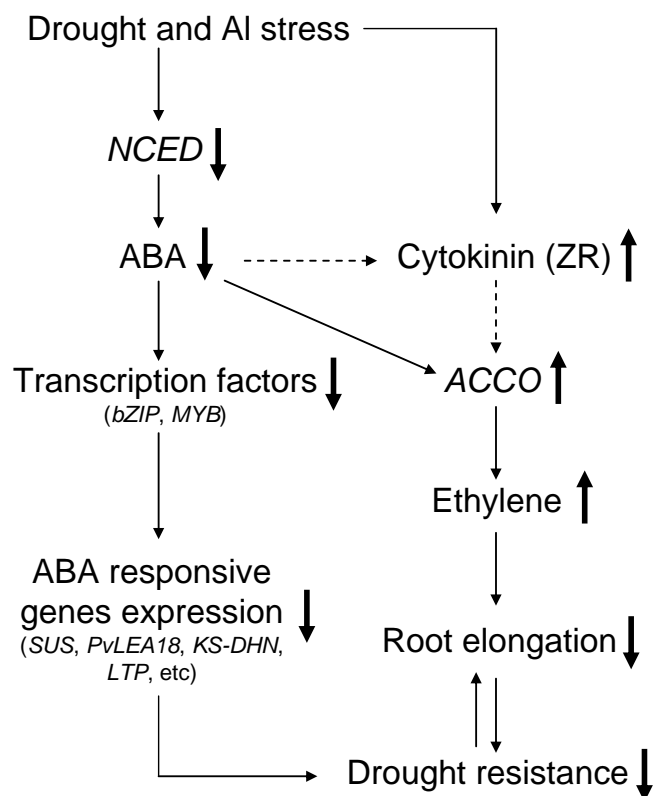
Figure 12 Schematic representation of the potential regulatory mechanisms of combined drought and Al stress in common bean. The thick arrows indicate the up- and down-regulated changes. The thin dashed arrows indicate the potential connections. For further explanations see the related discussion

GENERAL DISCUSSION

Much progress has been made during recent years in the physiological and molecular understanding of the response of plants roots to the individual aluminium and drought stress (see reviews, Kochian et al., 2004; Ma, 2007; Ryan and Delhaize, 2010; Horst et al., 2010; Ryan et al., 2011; Wu and Cosgrove, 2000; Sharp et al., 2004; Moore et al., 2008; Yamaguchi and Sharp, 2010). Generally, the inhibition of root elongation is thought to be the primary symptom of Al toxicity and the root apex is the most Al-sensitive root zone (Kochian et al., 2004; Horst et al., 2010; Ryan et al., 2010). In common bean, Rangel et al. (2007) found that the response of root elongation to Al in the genotypes Quimbaya (Al-resistant) and VAX 1 (Al-sensitive) was characterized by a similar initial period (4 h) of Al sensitivity followed by a contrasting recovery period (8 - 25 h), and both the transition zone (TZ, 1-2 mm) and elongation zone (EZ, 2-10 mm) are targets of Al injury. Mechanisms of Al resistance have been established in common bean to be related to a lower Al accumulation in the root tip resulting from the Al-induced citrate exudation from the root apex (Rangel et al., 2009; 2010). However, in contrast to Al, the traits for evaluation of drought resistance have not yet been established. In plants growing in dry soil, both shoot and root growth is hampered (Westgate and Boyer, 1985; Sharp et al., 1988), while an important feature of the root response to drought is the ability of some roots to continue elongation under water deficit conditions that may have completely inhibited shoot growth (Sharp et al., 2004). The maintenance of root growth during water deficit facilitates water uptake from the subsoil (Sponchiado et al., 1989; Serraj and Sinclair, 2002). However, in acid soils under low soil-moisture conditions (dry spells), Al toxicity may strongly restrict the roots to exploit water from the subsoil. This hypothesis was strongly supported by our studies performed in acid, Al-toxic soil under low moisture (see Chapter 4), but not in PEG-simulated drought (osmotic) stress conditions in hydroponics (see Chapter 1 and 2). The current studies provide better comprehensive understanding and a set of novel insights into the physiological and molecular mechanisms of Al and drought resistance, and are important to clarify the opportunities and constraints in breeding for adaptation to multiple abiotic stresses.

PEG-simulated drought (osmotic) stress improves aluminium resistance in common bean

In common bean, a positive relationship between Al-induced short-term inhibition of root

elongation and Al accumulation in the root tip apoplast was found (Rangel et al., 2009). Our present study indicated that PEG ameliorated Al-inhibited root elongation by reducing Al accumulation in the root tips (Fig. 1 in Chapter 1), suggesting that PEG improved Al resistance of common bean. The PEG-induced reduction of Al accumulation in the root tips was not due to complexing or precipitating Al in the treatment solution because PEG did not affect the concentration of mononuclear phytotoxic Al in the treatment (+Al+PEG) solution (see Materials and methods in Chapter 1). The apoplast of the root apex has been proposed to be the primary site of Al injury and plays an important role in Al resistance (Horst, 1995; Horst et al., 2010). The density of the negative charge carried by the CW is determined by the pectin content and the degree of methylation of pectin which thus determines the Al binding capacity of roots (Schmohl et al., 2000; Eticha et al., 2005; Yang et al, 2008). About 80% of the total Al in the root tips of common bean was bound in the CW (Rangel et al., 2009). Our study with common bean showed that PEG did not reduce Al accumulation by decreasing the CW negativity since no PEG effect on the unmethylated pectin content of root apices was found (Fig. 4 in Chapter 1).

Citrate exudation contributes to Al resistance of common bean by excluding Al from the root apex (Rangel et al., 2010). Further studies by Eticha et al. (2010) indicated that the expression of a *MATE* gene was crucial for Al-induced citrate exudation and thus Al resistance. However, in contrast to sorghum (Magalhaes et al., 2007) and barley (Furukawa et al., 2007), where the expression level of the *SbMATE* and *HvMATE* genes decided on the genotypic variation in Al resistance the expression of the *MATE* gene in common bean can not explain genotypic differences in Al resistance. The expression of the *MATE* gene only was a prerequisite for citrate exudation, genotypic Al resistance in common bean mainly depended on the capacity to sustain the synthesis of citrate for maintaining the cytosolic citrate pool that enabled exudation (Eticha et al., 2010; Rangel et al., 2010). The present study demonstrated that Al stress significantly increased citrate exudation from root apices during the early Al injury period (3 – 9 h), but the exudation was reduced with time because of the reduction of citrate content in the root apex (Fig. 2 and Fig. 3 in Chapter 1), confirming that the citrate exudation was related to the synthesis of citrate in the root apex (Rangel et al., 2010). However, no positive effect of PEG on Al-induced citrate exudation from root apex was found (Fig. 3 in Chapter 1) though PEG enhanced the Al-suppressed citrate content in the root apical tissues (Fig. 2 in Chapter 1). Considering that the removal of PEG from the treatment solution rapidly restored the Al accumulation capacity of the root apices (Fig. 5 in Chapter 1), the contribution of citrate exudation in reducing the Al

binding capacity in presence of PEG cannot be unequivocally ruled out. On the other hand, PEG did not induce citrate exudation from the root apex, although it highly increased the citrate content in the root apical tissues (Fig. 2 in Chapter 1). Thus, the lack of citrate exudation under PEG stress may largely depend on the lack of the *MATE* gene expression (Fig. 3 in Chapter 2).

Eticha et al. (2010) observed that the initial Al-induced inhibition of root elongation was correlated with the expression of an *ACCO* gene in both bean genotypes, Quimbaya (Al-resistant) and VAX 1 (Al-sensitive). It has been speculated that the Al-induced inhibition of root growth is due to enhanced gene expression and enzyme activity of ACCO resulting in increased ethylene production in *Lotus japonicus* and *Medicago truncatula* (Sun et al., 2007). In this study, a significant correlation among *MATE* and *ACCO* gene expression, root elongation and the Al concentration in the root tips of common bean was found (Fig. 2 in Chapter 2), and PEG treatment alone had no effect on the expression of both genes (Fig. 3 in Chapter 2) providing opportunities to further clarify the PEG-induced reduction of Al accumulation in the root tips and Al-induced inhibition of root elongation using the expression of the *MATE* and *ACCO* genes as sensitive indicators of Al toxicity. As expected, the OS-induced exclusion of Al from the root apex and the improvement of root growth were accompanied by a decrease in gene expression of *MATE* and *ACCO* (Fig. 3 in Chapter 2) confirming that OS reduces Al injury.

Water is the most abundant component of the CW making up about two thirds of the wall mass in growing tissues (Cosgrove, 1997). Loss of water from the wall matrix can result in serious disruption to polymer organization (Moore et al., 2008). One obvious effect is that polymers usually well separated in the hydrated wall are brought in close proximity to each other, thus causing polymer adhesion or cross-linking under water stress (Fig. 9A in Chapter 2; Moore et al., 2008). In the present study, the findings that the removal of PEG from the treatment solution quickly (within 15 min) recovered the Al accumulation in the intact root tips (*in vivo*, Fig. 5 in Chapter 1) but not in the isolated ethanol-insoluble CW (*in vitro*, Fig. 8A in Chapter 1) prompted us to further explore the potential involvement of CW structure alteration in PEG-induced reduction of Al accumulation. Using La, Sr and Rb as a tracer of Al, Ca and K, respectively, we found that in comparison with La, Sr, and Rb, the strong reduction of cation accumulation in the root apex and isolated CWs by osmotic stress appears to be specific to Al (Fig. 5, Fig. 7, Fig. 8 and Fig. 9 in Chapter 1). The specificity of cation accumulation might be related to the hydrated ionic radius of the cations: Al^{3+} (0.475 nm) > La^{3+} (0.452 nm) > Sr^{2+} (0.412 nm)

$= Ca^{2+}$ (0.412 nm) $> K^+$ (0.331 nm) $> Rb^+$ (0.329 nm) (Nightingale, 1959). Since the pore size of the CW controls the apoplastic transport of water, ions, metabolites and proteins (Carpita et al., 1979; Brett and Waldron, 1996; Cosgrove, 2005), the differences between the ions in Al accumulation of the PEG-exposed root apices and isolated CWs may suggest that PEG (osmotic stress) affects CW porosity. After physically destroying the structure of the CW isolated from PEG-treated root tips, Al binding to the CW was almost restored (Fig. 10 in Chapter 1). In addition, the extent of water loss from the apoplast and consequently shrinkage of the root structure appeared to be dependent of the molecular size of the applied PEG: PEG 6000 > PEG 3000 >> PEG 1000 (Fig. 6 and Fig. S2 in Chapter 1). The higher the hydrodynamic radius the better the exclusion from the apoplast and consequently the dehydration of the apoplast.

Potential roles of genes/proteins related to modification of CW structure in PEG-induced reduction of aluminium accumulation in the root apex

Since the restoration of the Al accumulation capacity of the CWs after the cessation of the PEG stress could only be observed in living root apices (Fig. 5 in Chapter 1) but not in ethanol-insoluble CW material isolated from root apices pre-treated with PEG (Fig. 8A in Chapter 2), a role of enzymes mediating the suppression of Al accumulation has to be postulated. Several CW proteins/enzymes are believed to play important roles in modifying the wall network and thus, possibly, the CW's ability to extend, such as expansin, xyloglucan endotransglycosylase (XET), glucanase (Wu and Cosgrove, 2000). Therefore, the identification of genes/proteins particularly involved in CW modification appeared to be necessary for a better understanding of PEG-induced reduction of root-tip Al accumulation.

First, we conducted the trancriptomic analysis of PEG-stressed root tips using SuperSAGE and confirmed the reliability of this technique by qRT-PCR using 46 differentially expressed genes (Fig. 7 in Chapter 2). Total 611 up- and 728 down-regulated genes in PEG-treated root tips were identified (Fig. 6 and Table S2 in Chapter 2). Among these osmotic stress-regulated genes, CW synthesis and organization-related genes were mostly down-regulated (Fig. 6 in Chapter 2) providing an opportunity to identify genes involved in the OS-induced alteration of CW porosity. Similarly, in *Arabidopsis*, Bray (2004) found that water deficit consistently down-regulated the expression of genes involved in CW synthesis and modification. Structural proteins such as HRGP, glycine-rich protein, and proline-rich proteins are main components of the growing plant CW, and they

can rapidly be insolubilized in the CW during stress condition, such as upon wounding (Showalter, 1993; Cosgrove, 1997). The HRGP proteins are particularly abundant in dicots compared to other structural proteins (Showalter, 1993). In the present study, we found that the expression of a *HRGP* gene was significantly enhanced by OS, and withdrawing of OS rapidly restored the expression of this gene (Fig. 8 in Chapter 2). Thus the role of the *HRGP* gene appears to be important in the OS-induced modification of the CW in common bean. Once the HRGP is secreted into the CW, it will be rapidly insolubilized. The insolubilization of HRGP may be mediated by water deficit-induced enhancement of formation of hydrogen peroxide catalyzed by a CW peroxidase. This response is thought to be an ultra-rapid stress-response reaction that serves to further strengthen the cell wall (Showalter, 1993; Zhu et al., 2007). Osmotic stress-induced physical shrinkage of the CW and thus resulting in a reduction of CW porosity may be further enhanced by the deposition of other CW components, such as structural proteins as schematically depicted in Fig. 9A (Chapter 2). The increased deposition of HRGP proteins in the CW may increase the cross-link between HRGP proteins and other CW components, such as pectins (Showalter, 1993), which was the decisive factor of CW porosity (Baron-Epel et al., 1988), and further reinforce a cell-wall barrier for Al transport into and in the apoplast (Fig. 9B in Chapter 2).

The shrinkage of the CW resulting from PEG 6000-induced dehydration of the apoplast causes adhesion and cross-linking of wall polymers through hydrogen bonding. This bonding will be enhanced by removal of water from the apoplast and is likely to cause an irreversible bonding between polymers resulting in altered biophysical CW properties (Fig. 9A in Chapter 2; Moore et al., 2008), unless some CW loosening or modifying proteins/enzymes were re-induced/activated. The enzyme XTH has been supposed to play key roles in the response to water deficit by modifying the CW structure and extensibility through the cleavage and reformation of bonds between xyloglucan chains (Rose et al., 2002; Wu and Cosgrove, 2000; Bray, 2004; Sharp et al., 2004; Moore et al., 2008). Transcriptomic and proteomics studies have demonstrated that several *XTH* genes were down-regulated by water deficit (Bray, 2004; Zhu et al., 2007). In the present study, qRT-PCR results showed that the expressions of *XTHa* and *XTHb* genes in the root tips of common bean were significantly reduced by PEG-induced dehydration of the apoplast (Fig. 8 in Chapter 2). Withdrawal of PEG from the pre-treatment solution rapidly allowed the recovery of the expression level of the *XTHa* gene (Fig. 8 in Chapter 2), supporting the view that the *XTHa* gene may be involved in the CW modification during the recovery of the apoplast from dehydration (Fig. 9B in Chapter 2). Similar results were found in the

PEG-induced expression of the *CaXTH1* gene in Chickpea (*Cicer arietinum*) (Romo et al., 2005).

Besides the *XTH* and *HRGP* genes, the *BEG* gene may also play a important role of in the OS-induced CW modification and thus influencing Al accumulation in the root tips in the present study (Fig. 9B in Chapter 2), since PEG-induced OS significantly reduced the expression of the *BEG* gene, and removal of PEG rapidly restored its expression (Fig. 8 in Chapter 2). BEGs belongs to the family of 17 plant glycoside hydrolases, and molecular studies suggested that this enzyme shares a common ancestry with beta-1,3-1,4-glucanase (Minic and Jouanin, 2006; Borad and Sriram, 2008) an abundant protein in all higher plants. They are known to be involved in pathogen defense as well as a wide range of normal developmental processes, They can hydrolytically cleave the 1,3-β-linked glucans, a major component of the fungal CW (Minic and Jouanin, 2006). Although the functions of this enzyme in plant CW modification have not yet been established, a potential role in the OS-induced reduction of CW porosity cannot be ruled out.

In this study, large scale proteomic analysis was not successful in identifying OS-induced proteins involved in CW structure modification in the root tips of common bean as expected. The separation of overlapping protein spots, the recovery of sufficient amounts of proteins and the establishment of an extraction method for CW proteins are still challenges for future proteomics studies. In spite of this, one protein called dehydrin, which has been supposed to play important roles in avoiding irreversible disruption of the CW structure during drought stress (Layton et al., 2010), was significantly increased by OS in the present study (Fig. 6 and Table 4 in Chapter 3). Dehydrins are highly specialized proteins that lack a fixed three-dimensional structure and have evolved to maintain their disordered character under conditions such as water deficit, in which unfolded states of several globular proteins would tend to collapse (Mouillon et al., 2008). Therefore, the OS-elevated abundance of dehydrins in the root tips of common bean may protect the CW from irreversible disruption by PEG-caused CW dehydration, maintain the elastic extension (reversible stretching) properties of the CW, and thus allow the quickly recovery of CW extensibility and Al accumulation of the root tips after the removal of osmotic stress. Future research is necessary to clarify the cell localization of deydrin and its possible role in CW modification.

The interaction between aluminium toxicity and PEG-simulated drought stress in hydroponics is different from the aluminium/drought interaction in soil

PEG-simulated drought strongly reduced Al accumulation and thus enhanced the Al-inhibited root elongation (Fig. 1 in Chapter 1; Fig. 1 in Chapter 2, Fig. 3A, B in Chapter 4). However, in contrast, in dried acidic soils, combined Al toxicity and drought stress resulted in more severe inhibition of root elongation beyond the effects of the individual stresses (Fig. 4A, B, Fig. 5A in Chapter 4). The enhanced inhibition of root elongation was not due to the increased Al toxicity in the root tips. In contrast, a significant reduction of callose formation (Fig. 4C, Fig. 5B in Chapter 4) and *MATE* gene expression (Fig. 6A in Chapter 4) in the root tips strongly suggest amelioration of Al stress. However, obviously the residual Al effect indicated by still slightly higher callose formation and expression of the *MATE* gene (Fig. 6A in Chapter 4) was sufficient to interact with the drought resistance of the root apex leading to enhanced inhibition of root elongation. This Al toxicity-enhanced inhibition of root growth under drought may restrict water uptake of the root from deeper soil layers and thus impede withstanding drought (Fig. 1, this chapter).

It is well known that ABA is produced under water-deficit conditions and plays an important role in the response of plants to drought. The accumulation of ABA in the root tips has been shown to be required for the maintenance of maize primary root elongation at low water potentials (Sharp, 2002; Sharp et al., 2004; Yamaguchi and Sharp, 2010). The main contribution of ABA to drought resistance is the involvement in the regulation of drought-induced genes (Bray, 1997; 2002): the transcription factor bZIP and MYB are responsible for the down-stream regulation of ABA-dependent genes after the reception of the ABA signal (Shinozaki and Yamaguchi-Shinozaki, 1997; 2007). In the present study, we found that the drought-induced ABA accumulation (Fig. 9 in Chapter 4) and the expression of the *NCED* gene (Fig. 8B in Chapter 4) involved in ABA biosynthesis in the root tips were suppressed by Al. Subsequently the drought-induced up-regulation of the transcription factors *bZIP and MYB* (Fig. 8C in Chapter 4) and the ABA-dependent genes *SUS*, *PvLEA18*, *KS-DHN* and *LTP* (Fig. 7 in Chapter 4) were also reversed. This series of negative response to additional Al stress may impair the positive role of ABA involved in the maintenance of root elongation under drought, and thus led to greater susceptibility of roots to drought under additional Al stress (Fig. 12 in Chapter 4).

Besides ABA, other phytohormones such as CKs, IAA, SA and JA were also determined in this study (Supplemental Fig. S3 in Chapter 4). It was reported that CKs inhibited root elongation and branching (Skoog and Miller, 1957; Cary et al., 1995; Werner et al., 2001), and that CKs-induced inhibition of root elongation is mediated largely by the production of ethylene (Bertell and Eliasson, 1992; Cary et al., 1995; Růžička et al., 2009). Also, several studies have shown that ABA can suppress ethylene production, and the maintenance of root elongation under water deficit conditions requires the increased levels of ABA to prevent excess ethylene production (Sharp et al., 2000; Spollen et al., 2000; Sharp, 2002; LeNoble et al., 2004). The evidence of a direct effect of ABA on CK is less. However, Jelić and Bogdanović (1988) reported that ABA inhibited the CK-stimulated synthesis of chlorophyll in the light in *Pinus nigra*; Ding et al. (2008) found that ABA could suppress CK activation of cell division in the root cortex of *Medicago truncatula*; Vysotskaya et al. (2009) supposed that ABA could regulate shoot CK concentrations via mediating the enzyme activity of CKX; Takei et al. (2004) observed that ABA treatment highly reduced the CKs biosynthetic genes *CYP735A1* and *CYP735A2* in Arabidopsis. Therefore, the potential role of ABA in regulating CKs synthesis can not be ruled out. In the present study, the combined Al and drought stress significantly increased in the root tips of common bean the drought-enhanced concentration of ZR, a biologically active form of CKs (Fig. 10 in Chapter 4) and the expression of the *ACCO* gene (Fig. 6 in Chapter 4) involved in the biosynthesis of ethylene. Therefore, the cross-talk between photohormones appears to be involved in the enhanced inhibition of root elongation. The Al aggravated drought-induced inhibition of root elongation may partly be due to reduced ABA levels, promoted CK production and subsequently stimulated synthesis of ethylene in the root tips of common bean. The impeded root elongation will restrict the roots to explore water from deeper soil layers and thus reduced drought resistance (Fig. 12 in Chapter 4).

The difference between the two experimental approaches (PEG-simulated drought and dried acidic soil) may result from the possibility to adapt to osmotic stress (PEG-6000) in hydroculture allowing sufficient water uptake to resume root elongation, whereas in dried soil the adaptation fails particularly in presence of Al (Fig. 1, this chapter).
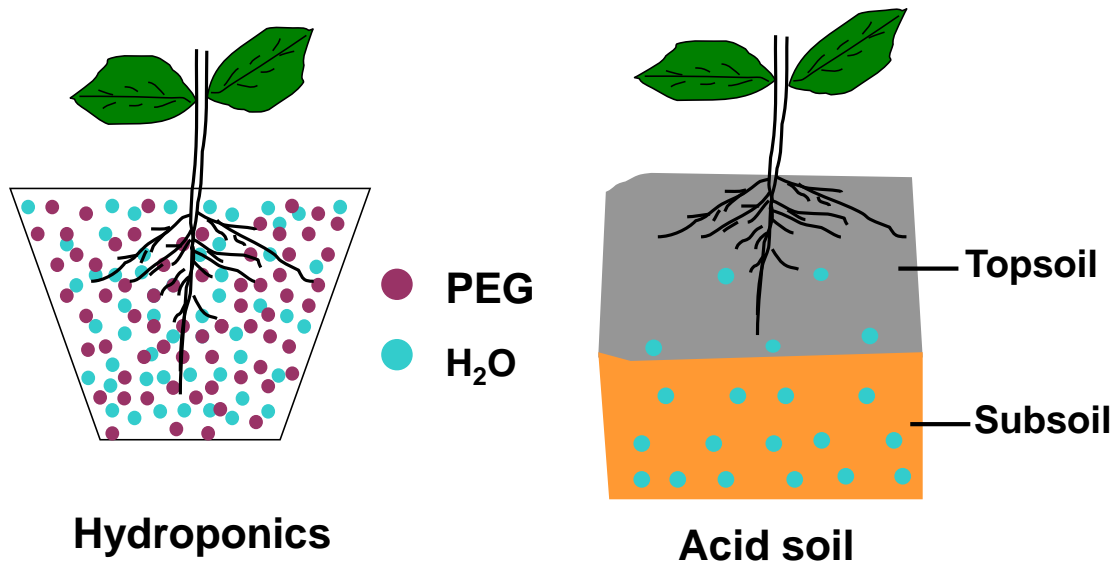
Figure 1 The hypothesized comparison of the two different experimental approaches used to induce combined Al and drought stress (PEG solution and low soil moisture in an acid soil).

In conclusion, PEG-simulated drought (osmotic) stress-inhibited Al accumulation in root apices and thus reduced Al-induced inhibition of root elongation is related to the reduction of CW porosity resulting from PEG 6000-induced dehydration of the root apoplast. The PEG-induced decrease of CW porosity was mediated by genes related to CW assembling and modification such as *XTH*, *BEG* and *HRGP*, and DHN may protect the CW from the osmotic stress-induced physical distortion and maintain the capability to restore CW extension. The interaction between Al toxicity and PEG-simulated drought in hydroponics is different from soil conditions. In the soil although drought reduced Al toxicity, the combined Al and drought stress increased the susceptibility of root tips to drought. This aggravated drought-induced inhibition of root elongation in soil results from the disruption of the gene regulatory networks involved in the ABA signal transduction and the ABA signal cross-talk with other phytohormones necessary for maintaining root elongation under drought.

OUTLOOK

The present study clearly showed that in common bean PEG-induced drought (osmotic) stress reduced Al accumulation in the root tips resulting in less inhibition of root elongation. Lower Al accumulation in PEG-treated root tips could be related to the reduction of CW porosity as a result of PEG-induced dehydration of the apoplast. The PEG-induced decrease of CW porosity was mediated by genes related to CW assembling and modification such as *XTH*, *BEG* and *HRGP*, and by dehydrin (DHN) which may protect the CW from the osmotic stress-induced physical breakage and contribute to maintain the capacity for restoration of CW extensibility. The interaction between Al toxicity and PEG-simulated drought was different from in the conditions in an acid, Al toxic soil, where although drought reduced Al toxicity, combined Al and drought stress increased the susceptibility of the root tips to drought indicated by aggravating drought-induced inhibition of root elongation. The Al-induced enhanced drought sensitivity of the root apex resulted from the disruption of the gene regulatory network involved in ABA signal transduction and the ABA signal cross-talk with other phytohormones such as CKs and ethylene, necessary for maintaining root growth under drought.

However, the majority of the conclusions are based on circumstantial evidence, particularly the potential role of the *XTH*, *BEG* and *HRGP* genes in the modification of CW porosity, of the DHN protein in CW protection against physical breakage during PEG-induced osmotic stress, of the role of regulation of ABA-dependent genes and ABA signal transduction and cross-talk in the maintenance of root elongation during drought stress. Therefore, the confirmation of these hypotheses is necessary in the future, to clearly understand the relationship of Al toxicity and drought in common bean and thus breeding for the adaptation to these combined abiotic stresses.

The genes/proteins involved in cell-wall modification

The present study suggest that the PEG-inhibited Al accumulation resulted from the reduction of CW porosity, and that the *XTH*, *BEG* and *HRGP* genes are involved in adjusting CW porosity. However, the exact role and mode of action in modifying CW porosity of the enzymes coded by these genes is still widely unknown. Own additional studies (not reported) may facilitate to better focus future work aiming at better understand the role of CW modification genes in the alteration of wall porosity: (i) The spatial growth analysis of the effect of PEG on roots have demonstrated that the elongation of the root

apical zone (0-2 mm from the root apex) was maintained during PEG-stress, while the elongation in the elongation zone (2-10 mm from the root apex) (Rangel et al., 2007) was strongly inhibited by PEG (Fig. 1, this chapter); (ii) Al binding in the isolated CWs of PEG-pretreated root tips showed that the root apical zone (0-2 mm from the root apex) maintained a comparatively higher level of Al binding in the isolated CWs, whereas PEG strongly decreased the Al binding the CWs in the EZ (2-12 mm from the root apex) (Fig. 2, this chapter); (iii) A kinetic study indicated that the PEG pre-treatment time significantly affected the Al binding in the CWs: the longer duration of the PEG stress the higher the reduction of Al binding (Fig. 3, this chapter). All these physiological results drive us to further investigate the potential involvement of *XTH*, *BEG* and *HRGP* gene in the modification of CW porosity and thus Al accumulation in the root tips at the spatial and temporal levels in the future.
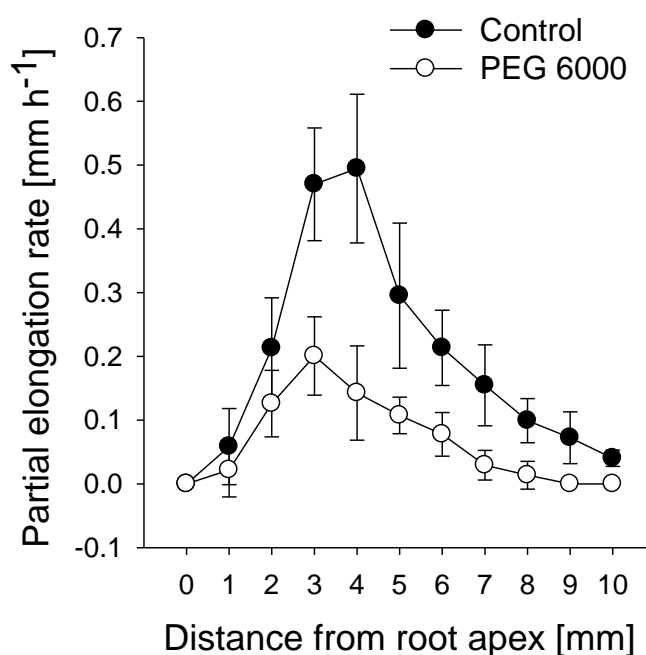
Figure 1 Effect of osmotic stress (-0.60 MPa OP) on the partial-elongation rate of apical 1-cm root segments in common bean genotype VAX 1. Plants were pre-cultured in a simplified nutrient solution containing 5 mM $CaCl_2$, 1 mM KCl, and 8 μM H_3BO_3 for 48 h for acclimation and pH adaptation, then treated without or with PEG 6000 (150 g L^{-1}) in the simplified nutrient solution for 4 h, pH 4.5. Bars represent means $\pm$SD, n = 9.
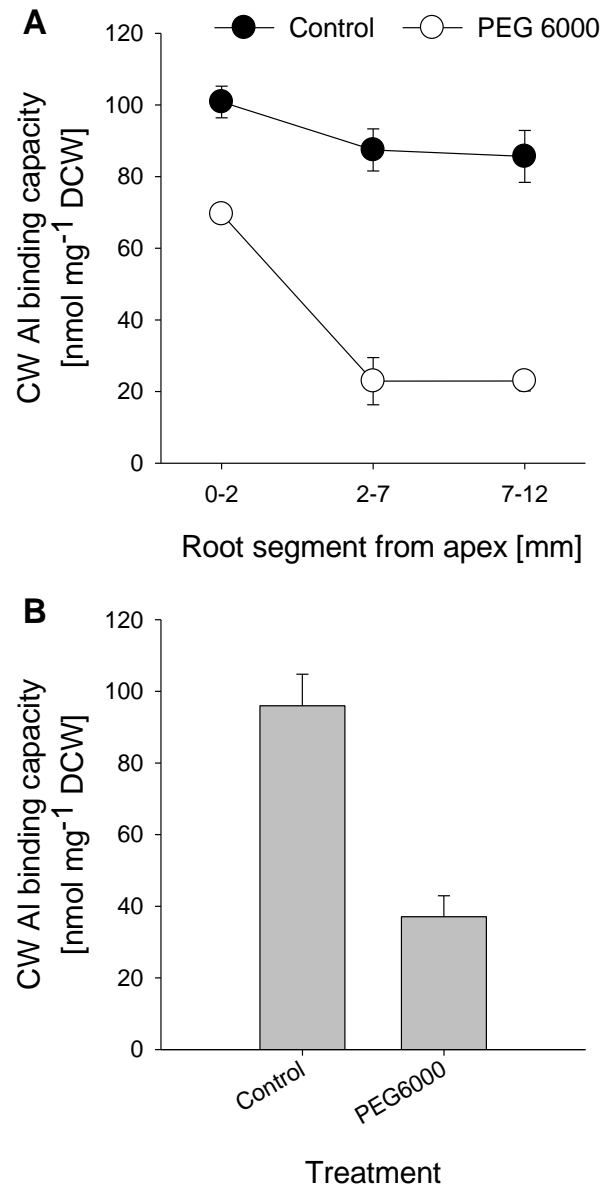
Figure 2 Al^{3+} binding of cell-walls isolated from segments 0-2, 2-7, 7-12 (A), and 0-12 mm (B) from the root apex of the Al-sensitive common bean genotype VAX 1. Plants were pre-treated without or with 150 g L^{-1} PEG for 24 h in a simplified solution (pH 4.5) containing 5 mM $CaCl_2$, 1mM KCl and 8 μM H_3BO_3. Then root segments were harvested for each sample and cell-wall material isolated according to Method A described in materials and methods of Chapter 1. Then the isolated cell-wall material (approximately 3 mg) was treated with 1 mL 300 μM Al for 30 min, pH 4.3. Bars represent means $\pm$SD, n = 4.
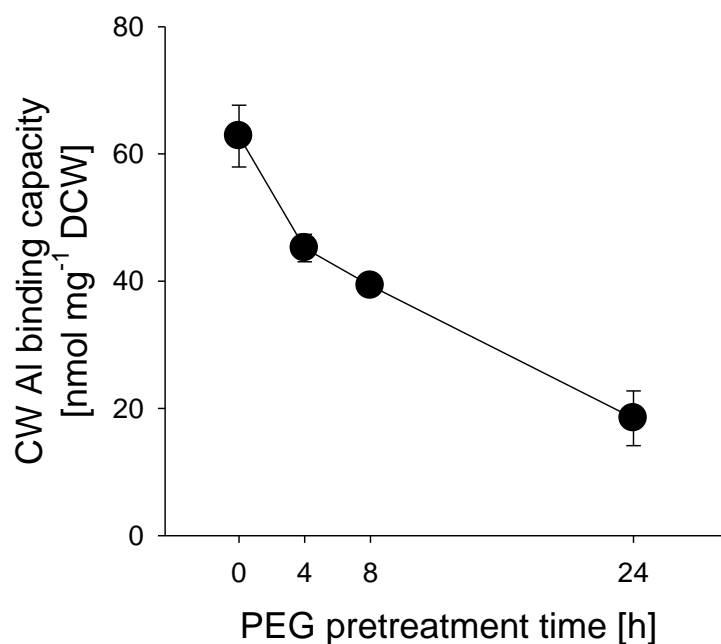
Figure 3 Al^{3+} binding of cell-wall material isolated from of 1-cm root tips of Al-sensitive common bean genotype (VAX 1). Plants were pre-treated with 150 g L^{-1} PEG for 0, 4, 8 and 24 h in a simplified solution (pH 4.5) containing 5 mM $CaCl_2$, 1 mM KCl and 8 μM H_3BO_3. Then root tips (1 cm long) were harvested for each sample and cell-wall material isolated according to Method A described in materials and methods of Chapter 1. Then the isolated cell-wall material was treated with 1 mL 300 μM Al for 30 min, pH 4.3. Bars represent means $\pm$ SD, n = 4.

Transcriptomic profiling cannot always explain the regulation of biological processes due to protein isoforms or post-translational regulation (Toorchi et al., 2009; Zörb et al., 2010). The combination of proteomics, biochemical assays and transcriptomics may be more successful in clarifying the molecular mechanism of CW modifications leading to alteration of CW porosity. Modification and improvement of the methods of the extraction of CW proteins are necessary in the future, since the methods used in the present study did not yield satisfactory results in the light of our objectives.

Moreover, although the interaction between Al toxicity and drought stress in the root tips of common bean were similar between PEG treatment in hydroponics and low moisture in soil with regard to the expression of genes involved in adjustment of the osmotic potential and CW modification, a more in-depth comparative characterization of common and differential features of stress adaptation is required in the future.

Finally, reverse genetic approaches using gene transformation, gene silencing or mutants are necessary. However, these techniques are still hardly applicable to common bean, presently.

The involvement of ABA crosstalk in the individual and combined drought and aluminium responses

In the present study, the response of the phytohormones ABA, CKs and the gene expression of *ACCO* involved in ethylene production to combined Al and drought stress provide new clues for the further investigation of the potential involvement of ABA-crosstalk. Several studies have clearly shown that ABA can suppress ethylene production, and the maintenance of root elongation under water deficit conditions requires increased ABA levels to prevent excess ethylene production (Sharp et al., 2000; Spollen et al., 2000; Sharp, 2002; LeNoble et al., 2004). Furthermore, ethylene can mediate the CK-induced inhibition of root elongation (Bertell and Eliasson, 1992; Cary et al., 1995; Růžička et al., 2009) by the overexpression or mutation of genes involved in the phytohormone biosynthesis and signal transduction pathways. Therefore, the information provided by the present study may facilitate the design of future studies aiming at clarifying the mechanisms involved in the Al and drought interaction.

Opportunities in breeding for adaptation to combined Al toxicity and drought

Using different bean species, Butare et al. (2011) found that Al partially ameliorated the negative effects of water stress in *Phaseolus coccineus* genotypes, strongly in contrast to *Phaseolus acutifolius* and the Mesoamerican common bean genotypes (such as VAX 1, the genotype used in this study) where combined stress led to a more severe inhibition of root development strongly supporting our present study in soil. Therefore, it appears promising to use interspecific crosses with *Phaseolus coccineus* to improve combined drought tolerance and Al resistance of common bean.

REFERENCES

Abbasi FM, Komatsu S (2004) A proteomic approach to analyze salt-responsive proteins in rice leaf sheath. *Proteomics* **4:** 2072-2081

Abe H, Yamaguchi-Shinozaki K, Urao T, Iwasaki T, Hosokawa D, Shinozaki K (1997) Role of Arabidopsis MYC and MYB homologs in drought- and ABA-regulated gene expression. *The Plant Cell* **9:** 1859–1868

Agrawal GK, Thelen JJ (2009) A high-resolution two dimensional gel- and Pro-Q DPS-based proteomics workflow for phosphoprotein identification and quantitative profiling. In Marjo de Graauw (ed.), *Phospho-Proteomics, Methods and Protocols*, 527: 3-19. Humana Press, New York, NY DOI: 10.1007/978-1-60327-834-8_1

Ahmed AER, Labavitch JM (1977) A simplified method for accurate determination of cell wall uronide content. *Journal of Food Biochemistry* **1:** 361–365.

Akmaev VR, Wang CJ (2004) Correction of sequence-based artifacts in serial analysis of gene expression. *Bioinformatics* **20:** 1254-1263

Albacete A, Ghanem ME, Martínez-Andújar C, Acosta M, Sánchez-Bravo J, Martínez V, Lutts S, Dodd IC, Pérez-Alfocea F (2008) Hormonal changes in relation to biomass partitioning and shoot growth impairment in salinised tomato (*Solanum lycopersicum* L.) plants. *Journal of Experimental Botany* **59:** 4119–4131

Alexandersson E, Danielson JA, Råde J, Moparthi VK, Fontes M, Kjellbom P, Johanson U (2010) Transcriptional regulation of aquaporins in accessions of Arabidopsis in response to drought stress. *The Plant Journal* **61:** 650–660

Alexandersson E, Fraysse L, Sjovall-Larsen S, Gustavsson S, Fellert M, Karlsson M, Johanson U, Kjellbom P (2005) Whole gene family expression and drought stress regulation of aquaporins. *Plant Molecular Biology* **59**: 469–484

Alsheikh MK, Svensson JT, Randall SK (2005) Phosphorylation regulated ion-binding is a property shared by the acidic subclass dehydrins. *Plant, Cell and Environment* **28:** 1114–1122

Altschul SF, Gish W, Miller W, Myers EW, Lipman DJ (1990) Basic local alignment search tool. *Journal of Molecular Biology* **215:** 403–410

Anoop VM, Basu U, McCammon MT, McAlister HL, Taylor GJ (2003) Modulation of citrate metabolism alters aluminum tolerance in yeast and transgenic canola overexpressing a mitochondrial citrate synthase. *Plant Physiology* **132:** 2205–2217

Audic S, Claverie J (1997) The significance of digital gene expression profiles. *Genome Research* **7:** 986–995

Audran C, Borel C, Frey A, Sotta B, Meyer C, Simonneau T, Marion-Poll A (1998) Expression studies of the zeaxanthin epoxidase gene in *Nicotiana plumbaginifolia*. *Plant Physiology* **118:** 1021–1028

Barceló J, Poschenrieder C (2002) Fast root growth responses, root exudates, and internal detoxification as clues to the mechanisms of aluminium toxicity and resistance: a review. *Environmental and Experimental Botany* **48:** 75–92

Baron-Epel O, Gharyal PK, Schindler M (1988) Pectins as mediators of wall porosity in soybean cells. *Planta* **175:** 389–395

Bartels D, Sunkar R (2005) Drought and salt tolerance in plants. *Critical Reviews in*

Plant Sciences **24:** 23–58

Battaglia M, Solórzano RM, Hernández M, Cuéllar-Ortiz S, García-Gómez B, Márquez J, Covarrubias AA (2007) Proline-rich cell wall proteins accumulate in growing regions and phloem tissue in response to water deficit in common bean seedlings. *Planta* **225:** 1121–1133

Bauchot AD, Hallett IC, Redgwell RJ, Lallu N (1999) Cell wall properties of kiwifruit affected by low temperature breakdown. *Postharvest Biology and Technology* **16:** 245–255

Beebe S, Rao IM, Cajiao C, Grajales M (2008) Selection for drought resistance in common bean also improves yield in phosphorus limited and favourable environments. *Crop Science* **48:** 582–592

Bergmeyer Hu, Bernt E (1974) Malate dehydrogenase. In: Bergmeyer HU. eds. *Methoden der enzymatischen Analyse*, Band I. Weinheim: Verlag Chemie, 649-653

Bertell G, Eliasson L (1992) Cytokinin effects on root growth and possible interactions with ethylene and indole-3-acetic acid. *Physiologia Plantarum* **84:** 255–261

Bhushan D, Pandey A, Choudhary MK, Datta A, Chakraborty S, Chakraborty N (2007) Comparative proteomics analysis of differentially expressed proteins in chickpea extracellular matrix during dehydration stress. *Molecular and Cellular Proteomics* **6:** 1868-1884

Bianchi G, Gamba A, Murelli C, Salamini F, Bartels D (1991) Novel carbohydrate metabolism in the resurrection plant *Craterostigma plantagineum. The Plant Journal* **1:** 355–359

Blamey FPC (2001) The role of the root cell wall in aluminum toxicity. *In:* Plant Nutrient Acquisition: New Perspectives. Ae N, Arihara J, Okada K, Srinivasan A, (eds). Springer Verlag, Tokyo, Japan, pp 201-226

Blamey FPC, Edmeades DC, Wheeler DM (1990) Role of root cation-exchange capacity in differential aluminium tolerance of *Lotus* species. *Journal of Plant Nutrition* **13:** 729–744

Blumenkrantz N, Asboe-Hansen G (1973) New method for quantitative determination of uronic acids. *Analytical Biochemistry* **54:** 484–489

Borad V, Sriram S (2008) Pathogenesis-related proteins for the plant protection. *Asian Journal of Experimental Sciences* **22:** 189–196

Bordenave M (1996) Analysis of pectin methyl esterases. In: Linskens H, Jackson J. eds. *Plant cell wall analysis*. Berlin: Springer, 165–180

Boyer JS (2009) Cell wall biosynthesis and the molecular mechanism of plant enlargement. *Functional Plant Biology* **36:** 383–394

Bradford MM (1976) A rapid and sensitive method for the quantitation of microgram quantities of protein utilizing the principle of protein-dye binding. *Analytical Biochemistry* **72:** 248-254

Bray EA (1997) Plant responses to water deficit. *Trends in Plant Science* **2:** 48–54

Bray EA (2002) Abscisic acid regulation of gene expression during water deficit stress in the era of the Arabidopsis genome. *Plant, Cell and Environment* **25:** 153–161

Bray EA (2004) Genes commonly regulated by water-deficit stress in *Arabidopsis thaliana. Journal of Experimental Botany* **55:** 2331–2341

Brett C, Waldron K (1996) Physiology and biochemistry of the plant cell wall. Chapman and Hall, London.

Brini F, Hanin M, Lumbreras V, Irar S, Pages M, Masmoudi K (2006) Functional characterization of DHN-5, a dehydrin showing a differential phosphorylation pattern in two Tunisian durum wheat (*Triticum durum* Desf.) varieties with marked difference in salt and drought tolerance. *Plant Science* **172:** 20–28

Brocard-Gifford I, Lynch TJ, Garcia ME, Malhotra B, Finkelstein RR (2004) The *Arabidopsis thaliana ABSCISIC ACID-INSENSITIVE8* encodes a novel protein mediating abscisic acid and sugar responses essential for growth. *The Plant Cell* **16:** 406-421

Broughton WJ, Hernández G, Blair M, Beebe S, Gepts P, Vanderleyden J (2003) Beans (*Phaseolus* spp.) – model food legumes. *Plant and soil* **252**, 55–128

Butare L, Rao I, Lepoivre P, Polania J, Cajiao C, Cuasquer J, Beebe S (2011) New genetic sources of resistance in the genus *Phaseolus* to individual and combined stress factors of aluminium toxicity and progressive soil drying. *Euphytica* (Revised manuscript submitted)

Carjuzaa P, Castellión M, Distéfano AJ, del Vas M, Maldonado S (2008) Detection and subcellular localization of dehydrin-like proteins in quinoa (*Chenopodium quinoa* Willd.) embryos. *Protoplasma* **233:** 149-156

Carpita N, Sabularse D. Montezinos D, Delmer DP (1979) Determination of the pore size of cell walls of living plant cells. *Science* **205:** 1144–1147

Carpita NC, Gibeaut DM (1993) Structural models of primary cell walls in flowering plants: consistency of molecular structure with the physical properties of the walls during growth. *The Plant Journal* **3:** 1-30

Cary AJ, Liu W, Howell SH (1995) Cytokinin action is coupled to ethylene in its effects on the inhibition of root and hypocotyl elongation in *Arabidopsis thaliana* seedlings. *Plant Physiology* **107:** 1075-1082

Castro, A. J., Carapito, C., Zorn, N., Magné C, Leize E, Van Dorsselaer A, Clément C (2005) Proteomic analysis of grapevine (*Vitis vinifera* L.) tissues subjected to herbicide stress. *Journal of Experimental Botany* **56:** 2783–2795

Chae HS, Faure F, Kieber JJ (2003) The *eto1*, *eto2*, and *eto3* mutations and cytokinin treatment increase ethylene biosynthesis in Arabidopsis by increasing the stability of ACS protein. *The Plant Cell* **15:** 545-559

Chang YC, Yamamoto Y, Matsumoto H (1999) Accumulation of aluminium in the cell wall pectin in cultured tobacco (*Nicotiana tabacum* L.) cells treated with a combination of aluminium and iron. *Plant, Cell and Environment* **22:** 1009–1017

Chaves MM, Maroco JP, Pereira JS (2003) Understanding plant responses to drought — from genes to the whole plant. *Functional Plant Biology* **30:** 239–264

Chazen O, Neumann PM (1994) Hydraulic signals from the roots and rapid cell-wall hardening in growing maize (*zea mays* L.) leaves are primary responses to polyethylene glycol-induced water deficits. *Plant Physiology* **104:** 1385-1392

Chen RD, Gadal P (1990) Do the mitochondria provide the 2-oxoglutarate needed for glutamate synthesis in higher plant chloroplasts? *Plant Physiology and Biochemistry* **28:** 141–145

Chernys J, Zeevaart JAD (2000) Characterization of the 9-cis-epoxycarotenoid

dioxygenase gene family and the regulation of abscisic acid biosynthesis in avocado. *Plant Physiology* **124:** 343–353

Chesson A, Gardner PT, Wood TJ (1997) Cell wall porosity and available surface area of wheat straw and wheat grain fractions. *Journal of the Science of Food and Agriculture* **75:** 289–295

Chivasa S, Ndimba BK, Simon WJ, Robertson D, Yu XL, Knox JP, Bolwell P, Slabas AR (2002) Proteomic analysis of the *Arabidopsis thaliana* cell wall. *Electrophoresis* **23:** 1754–1765

CIAT (1992) Constraints to and opportunities for improving bean production. A planning document 1993–98 and an achieving document 1987–92. CIAT, Cali, Colombia

Close TJ, Kortt AA, Chandler PM (1989) A cDNA-based comparison of dehydration-induced proteins (dehydrins) in barley and corn. *Plant Molecular Biology* **13:** 95–108

Collet L, Horst WJ (2001) Characterisation of maize cultivars in their adaptation to acid soils on the single plant level. In: Horst WJ, Schenk MK, Bürckert A, *et al. eds. Plant nutrition: food security and sustainability of agro-ecosystems through basic and applied research*. Dordrecht: Kluwer Academic Publishers, 86–87

Collett H, Shen A, Gardner M, Farrant JM, Denby KJ, Illing N. 2004. Towards transcript profi ling of desiccation tolerance in *Xerophyta humilis*: Construction of a normalized 11 k *X. humilis* cDNA set and microarray expression analysis of 424 cDNAs in response to dehydration. *Physiologia Plantarum* **122:** 39–53

Colmenero-Flores JM, Moreno LP, Smith CE, Covarrubias AA (1999) Pvlea-18, a member of a new late-embryogenesis-abundant protein family that accumulates during water stress and in the growing regions of well-irrigated bean seedlings. *Plant Physiology* **120:** 93–104

Cook LL, McGonigle TP, Inouye RS (2009) Titanium as an indicator of residual soil on arid-land plants. *Journal of Environmental Quality* **38:** 188–199

Cosgrove DJ (1997) Assembly and enlargement of the primary cell wall in plants. *Annual Review of Cell and Developmental Biology* **13:** 171–201

Cosgrove DJ (2005) Growth of the plant cell wall. *Nature Reviews Molecular Cell Biology* **6:** 850–861

Covarrubias AA, Ayala JW, Reyes JL, Hernández M, Garciarrubio A. 1995. Cell-wall proteins induced by water deficit in bean (*Phaseolus vulgaris* L) seedlings. *Plant Physiology* **107:** 1119–1128

Cushman JC, Bohnert HJ (2000) Genomic approaches to plant stress tolerance. *Current Opinion in Plant Biology* **3:** 117–124

Danyluk J, Perron A, Houde M, Limin A, Fowler B, Benhamou N, Sarhan F (1998) Accumulation of an acidic dehydrin in the vicinity of the plasma membrane during cold acclimation of wheat. *The Plant Cell* **10:** 623–638

de la Fuente JM, Raminrez-Rodriguez V, Cabrera-Ponce JL, Herrera-Estrella L (1997) Aluminum tolerance in transgenic plants by alteration of citrate synthesis. *Science* **276:** 1566–1568

Déjardin A, Rochat C, Maugenest S, Boutin JP (1997) Purification, characterization and physiological role of sucrose synthase in the pea seed coat (*Pisum sativum* L.). *Planta* **201:** 128–137

Delhaize E, Craig S, Beaton CD, Bennet RJ, Jagadish VC, Randall PJ (1993) Aluminum tolerance in wheat (*Triticum aestivum* L.) (I. Uptake and distribution of aluminum in root apices). *Plant Physiology* **103:** 685–693

Delhaize E, Gruber BD, Ryan PR (2007) The roles of organic anion permeases in aluminium resistance and mineral nutrition. *FEBS Letters* **581:** 2255–2262

Delhaize E, Ryan PR (1995) Aluminum toxicity and tolerance in plants. *Plant Physiology* **107:** 315–321

Delhaize E, Ryan PR, Hebb DM, Yamamoto Y, Sasaki T, Matsumoto H (2004) Engineering high-level aluminum tolerance in barley with the *ALMT1* gene. *Proceedings of the National Academy of Sciences of the United States of America* **101:** 15249–15254

Ding Y, Kalo P, Yendrek C, Sun J, Liang Y, Marsh JF, Harris JM, Oldroyd GE (2008) Abscisic acid coordinates nod factor and cytokinin signaling during the regulation of nodulation in *Medicago truncatula*. *The Plant Cell* **20:** 2681–2695

Donahue JL, Alford SR, Torabinejad J, Kerwin RE, Nourbakhsh A, Ray WK, Hernick M, Huang X, Lyons BM, Hein PP, Gillaspy GE (2010) The *Arabidopsis thaliana Myo-inositol 1-phosphate synthase1* gene is required for Myo-inositol synthesis and suppression of cell death. *The Plant Cell* **22:** 888–903

Edreva A (2005) Pathogenesis-related proteins: research progress in the last 15 years. *General and Applied Plant Physiology* **31:** 105–124

Edwards SR, Braley R, Chaffin WL (1999) Enolase is present in the cell wall of *Saccharomyces cerevisiae*. *FEMS Microbiology Letters* **177:** 211–216

Ergen NZ, Thimmapuram J, Bohnert HJ, Budak H (2009) Transcriptome pathways unique to dehydration tolerant relatives of modern wheat. *Functional and Integrative Genomics* **9:** 377–396

Eswaran H, Reich P, Beinroth F (1997) Global distribution of soils with acidity. In: Moniz AC, Furlani AMC, Schaffert RE, Fageria NK, Rosolem CA, Cantarella H, *ed. Plant-soil interactions at low pH*. Brazil, 159–164

Eticha D, Staß A, Horst WJ (2005a) Cell-wall pectin and its degree of methylation in the maize root-apex: significance for genotypic differences in aluminium resistance. *Plant, Cell and Environment* **28:** 1410–1420

Eticha D, Thé C, Welcker C, Narro L, Staß A, Horst WJ (2005b) Aluminium-induced callose formation in root apices: inheritance and selection trait for adaptation of tropical maize to acid soils. *Field Crop Research* **93:** 252–263

Eticha D, Zahn M, Bremer M, Yang Z, Rangel AF, Rao IM, Horst WJ (2010) Transcriptomic analysis reveals differential gene expression in response to aluminium in common bean (*Phaseolus vulgaris*) genotypes. *Annals of Botany* **105:** 1119–1128

Fan L, Linker R, Gepstein S, Tanimoto E, Yamamoto R, Neumann PM (2006) Progressive inhibition by water deficit of cell wall extensibility and growth along the elongation zone of maize roots is related to increased lignin metabolism and progressive stelar accumulation of wall phenolics. *Plant Physiology* **140:** 603–612

Fan L, Neumann PM (2004) The spatially variable inhibition by water deficit of maize root growth correlates with altered profiles of proton flux and cell wall pH. *Plant Physiology* **135:** 2291–2300

Fleischer A, O′Neill MA, Ehwald R (1999) The pore size of non-graminaceous plant cell

walls is rapidly decreased by borate ester cross-linking of the pectic polysaccharide rhamnogalacturonan II. *Plant Physiology* **121:** 829–838

Foy CD (1974) Effects of aluminum on plant growth. Pages 601-642 in E. W. Carson, ed. *The Plant Root and Its Environment*. Uni- versity Press of Virginia, Charlottesville.

Fry SC (1988) The growing plant cell wall: chemical and metabolic analysis. Longman, New York, USA

Führs H, Hartwig M, Molina LE, Heintz D, Van Dorsselaer A, Braun HP, Horst WJ (2008) Early manganese-toxicity response in *Vigna unguiculata* L. – a proteomic and transcriptomic study. *Proteomics* **8:** 149–159

Furukawa J, Yamaji N, Wang H, Mitani N, Murata Y, Sato K, Katsuhara M, Takeda K, Ma JF (2007) An aluminum-activated citrate transporter in barley. *Plant and Cell Physiology* **48:** 1081–1091

Geigenberger P, Stitt M (1993) Sucrose synthase catalyses a readily reversible reaction in vivo in developing potato tubers and other plant tissues. *Planta* **189:** 329–339

Gerendás J (2007) Significance of polyamines for pectin methylesterase activity and the ion dynamics in the apoplast. In: Sattelmacher B, Horst W. eds. *The apoplast of higher plants: compartment of storage, transport, and reactions*. Dordrecht: Kluwer Academic Publishers, 67–83

Gilardoni PA, Schuck S, Jüngling R, Rotter B, Baldwin IT, Bonaventure G (2010) SuperSAGE analysis of the *Nicotiana attenuate* transcriptome after fatty acid-amino acid elicitation (FAC): identification of early mediators of insect responses. *BMC Plant Biology* **10:** 66

Goldman IL, Carter Jr TE, Patterson RP (1989) A detrimental interaction of subsoil aluminum and drought stress on the leaf water status of soybean. *Agronomy Journal* **81:** 461–463

Goujon T, Minic Z, El Amrani A, Lerouxel O, Aletti E, Lapierre C, Joseleau JP, Jouanin L (2003) *AtBXL1*, a novel higher plant (*Arabidopsis thaliana*) putative beta-xylosidase gene, is involved in secondary cell wall metabolism and plant development. *The Plant Journal* **33:** 677–690

Graham PH (1978) Some problems and potentials of field beans (*Phaseolus vulgaris* L.) in Latin America. *Field Crops Research* **1**: 295–317

Graham PH, Ranalli P (1997) Common bean (*Phaseolus vulgaris* L.). *Field Crops Research* **53:** 131–146

Hamada H, Matsumura H, Tomita R, Terauchi R, Suzuki K, Kobayashi K (2008) SuperSAGE revealed different classes of early resistance response genes in *Capsicum chinense* plants harboring L3-resistance gene infected with *Pepper mild mottle virus*. *Journal of General Plant Pathology* **74:** 313–321

Heim U, Weber H, Bäumlein H, Wobus U (1993) A sucrose-synthase gene of *Vicia faba* L.: expression pattern in developing seeds in relation to starch synthesis and metabolic regulation. *Planta* **191:** 394–401

Heyen BJ, Alsheikh MK, Smith EA, Torvik CF, Seals DF, Randall SK (2002) The calcium-binding activity of a vacuole-associated, dehydrin-like protein is regulated by phosphorylation. *Plant Physiology* **130:** 675-687

Hoekenga OA, Maron LG, Piñeros MA, et al. 2006. *AtALMT1*, which encodes a malate transporter, is identified as one of several genes critical for aluminum tolerance in

Arabidopsis. *Proceedings of the National Academy of Sciences of the United States of America* **103**: 9738–9743

Hohl M, Schopfer P (1991) Water relations of growing maize coleoptiles: comparison between mannitol and polyethylene glycol 6000 as external osmotica for adjusting turgor pressure. *Plant Physiology* **95:** 716–722

Horst WJ (1995) The role of the apoplast in aluminium toxicity and resistance of higher plants: a review. *Journal of Plant Nutrition and Soil Science* **158**: 419–428

Horst WJ, Asher CJ, Cakmak J, Szulkiewicz P, Wissemeier AH (1992) Short-term responses of soybean roots to aluminium. *Journal of Plant Physiology* **140:** 174–178

Horst WJ, Kollmeier M, Schmohl N, et al (2007) Significance of the root apoplast for aluminium toxicity and resistance of maize. In: Sattelmacher B, Horst W. eds. *The apoplast of higher plants: compartment of storage, transport, and reactions*. Dordrecht: Kluwer Academic Publishers, 49–66

Horst WJ, Püschel A-K,Schmohl N (1997) Induction of callose formation is a sensitive marker for genotypic aluminium sensitivity in maize. *Plant and Soil* **192:** 23–30

Horst WJ, Schmohl N, Kollmeier M, Baluska F, Sivaguru M (1999) Does aluminium affect root growth of maize through interaction with the cell wall – plasma membrane – cytoskeleton continuum? *Plant and Soil* **215:** 163–174

Horst WJ, Wang Y, Eticha D (2010) The role of the root apoplast in aluminium-induced inhibition of root elongation and in aluminium resistance of plants: a review. *Annals of Botany* **106:** 185-197

Hou N, You J, Pang J, Xu M, Chen G, Yang ZM (2010) The accumulation and transport of abscisic acid in soybean (*Glycine max* L.) under aluminum stress. *Plant and Soil* **330:** 127–137

Hu L, Wang Z, Du H, Huang B (2010) Differential accumulation of dehydrins in response to water stress for hybrid and common bermudagrass genotypes differing in drought tolerance. *Journal of Plant Physiology* **167:** 103–109

Hummel I, Pantin F, Sulpice R, Piques M, Rolland G, Dauzat M, Christophe A, Pervent M, Bouteillé M, Stitt M, Gibon Y, Muller B (2010) Arabidopsis plants acclimate to water deficit at low cost through changes of carbon usage: an integrated perspective using growth, metabolite, enzyme, and gene expression analysis. *Plant Physiology* **154:** 357–372

Hundertmark M, Hincha DK (2008) LEA (late embryogenesis abundant) proteins and their encoding genes in *Arabidopsis thaliana*. *BMC Genomics* **9:** 118

Ingram J, Bartels D (1996) The molecular basis of dehydration tolerance in plants. *Annual Review of Plant Physiology and Plant Molecular Biology* **47:** 377–403

Ingram J, Chandler JW, Gallagher L, Salamini F, Bartels D (1997) Analysis of cDNA clones encoding sucrose-phosphate synthase in relation to sugar interconversions associated with dehydration in the resurrection plant *Craterostigma plantagineum Hochst*. *Plant Physiology* **115:** 113–121

Iraki NM, Bressan RA, Hasegawa PM, Carpita NC. (1989a) Alteration of the physical and chemical structure of the primary cell wall of growth-limited plant cells adapted to osmotic stress. *Plant Physiology* **91:** 39–47

Iraki NM, Singh N, Bressan RA, Carpita NC (1989b) Cell walls of tobacco cells and changes in composition associated with reduced growth upon adaptation to water and

saline stress. *Plant Physiology* **91:** 48–53

Ishikawa S, Wagatsuma T (1998) Plasma membrane permeability of root-tip cells following temporary exposure to Al ions is a rapid measure of Al tolerance among plant species. *Plant and Cell Physiology* **39:** 516–525

Ishitani M, Rao I, Wenzl P, Beebe S, Tohme J (2004) Integration of genomics approach with traditional breeding towards improving abiotic stress adaptation: drought and aluminum toxicity as case studies. *Field Crops Research* **90:** 35–45

Itoh K, Nakahara K, Ishikawa H, Ohta E, Sakata M (1987) Osmotic adjustment and osmotic constituents in roots of mung bean seedlings. *Plant and Cell Physiology* **28:** 397–403

Iuchi S, Kobayashi M, Taji T, Naramoto M, Seki M, Kato T, Tabata S, Kakubari Y, Yamaguchi-Shinozaki K, Shinozaki K (2001) Regulation of drought tolerance by gene manipulation of 9- cisepoxycarotenoid dioxygenase, a key enzyme in abscisic acid biosynthesis in Arabidopsis. *The Plant Journal* **27:** 325–333

Iuchi S, Kobayashi M, Yamaguchi-Shinozaki K, Shinozaki K (2000) A stress-inducible gene for 9-cisepoxycarotenoid dioxygenase involved in abscisic acid biosynthesis under water stress in drought-tolerant cowpea. *Plant Physiology* **123:** 553–562

Jacomini E, Bertani A, Mapelli S (1988) Accumulation of polyethylene glycol 6000 and its effects on water content and carbohydrate level in water-stresses tomato plant. *Canadian Journal of Botany* **66:** 970–973

Janes BE (1974) The effect of molecular size concentration in nutrient solution and exposure time on the amount and distribution of polyethylene glycol. *Plant Physiology* **54:** 226–229

Jarvis MC (1992) Control of thickness of collenchyma cell walls by pectins. *Planta* **187:** 218–220

Jelić G, Bogdanović M (1988) Antagonism between abscisic acid and cytokinin in chlorophyll synthesis in pine seedlings. *Plant Science* **61:** 197–202

Jensen ON (2004) Modification-specific proteomics: characterization of post-translational modifications by mass spectrometry. *Current Opinion in Chemical Biology* **8:** 33–41

Jia W, Zhang J, Liang J (2001) Initiation and regulation of water deficit-induced abscisic acid accumulation in maize leaves and roots: Cellular volume and water relations. *Journal of Experimental Botany* **52:** 295–300

Jiang X, Wang Y (2004) Beta-elimination coupled with tandem mass spectrometry for the identification of in vivo and in vitro phosphorylation sites in maize dehydrin DHN1 protein. *Biochemistry* **43:** 15567–15576

Jiang Y, Yang B, Harris NS, Deyholos MK (2007) Comparative proteomic analysis of NaCl stress-responsive proteins in Arabidopsis roots. *Journal of Experimental Botany* **58:** 3591–3607

Jo SH, Lee SH, Chun HS, Lee SM, Koh HJ, Lee SE, Chun JS, Park JW, Hun TL (2002) Cellular defence against UVB-induced phototoxicity by cytosolic NADP-dependent isocitrate dehydrogenase. *Biochemical and Biophysical Research Communications* **292:** 542–549

Johnson JM, Pritchard J, Gorham J, Tomos AD (1996) Growth, water relations and solute accumulation in osmotically stressed seedlings of the tropical tree *Colophospermum mopane*. *Tree Physiology* **16:** 713–718

Karni, L. and B. Aarni (2002) Fructokinase and hexokinase from pollen grains of bell pepper (*Capsicum annuum* L.): possible role in pollen germination under conditions of high temperature and CO_2 enrichment. *Annals of Botany* **90:** 607–612

Kauss H (1989) Fluorometric measurement of callose and other 1,3-β-glucans. In *Modern Methods of Plant Analysis* (eds H.-F. Linskens and J.F. Jackson), pp. 127–137. Springer Verlag, Berlin, Germany

Kavi Kishor PB, Sangam S, Amrutha RN, Sri Laxmi P, Naidu KR, Rao KRSS, Rao S, Reddy KJ, Theriappan P, Sreenivasulu N (2005) Regulation of proline biosynthesis, degradation, uptake and transport in higher plants: Its implications in plant growth and abiotic stress tolerance. *Current Science* **88:** 424–438

Kende H (1993) Ethylene biosynthesis. *Annual Review of Plant Physiology and Plant Molecular Biology* **44:** 283–307

Kerven GL, Edwards DG, Asher CJ, Hallman PS, Kobot S (1989) Aluminium determination in soil solution. II. Short-term colorimetric procedure for the measurement of inorganic monomeric aluminium in the presence of organic acid ligands. *Australian Journal of Soil Research* **27:** 91–102

Kihara T, Ohno T, Koyama H, Sawafuji T, Hara T (2003) Characterization of NADP-isocitrate dehydrogenase expression in a carrot mutant cell line with enhanced citrate excretion. *Plant and Soil* **248:** 145–153

Kinraide TB, Ryan PR, Kochian LV (1992) Interactive effects of Al, h, and other cations on root elongation considered in terms of cell-surface electrical potential. *Plant Physiology* **99:** 1461–1468

Kishor PBK, Sangam S, Amrutha RN, Laxmi PS, Naidu KR, Rao KRSS, Rao S, Reddy KJ, Theriappan P, Sreenivasulu N (2005) Regulation of proline biosynthesis, degradation, uptake and transport in higher plants: Its implications in plant growth and abiotic stress tolerance. *Current Science* **88:** 424–438

Kleines M, Elster RC, Rodrigo MJ, Blervacq AS, Salamini F, Bartels D (1999) Isolation and expression analysis of two stress-responsive sucrose-synthase genes from the resurrection plant *Craterostigma plantagineum* (Hochst.). *Planta* **209:** 13–24

Klimashevskii EL, Dedov VM (1975) Localization of growth inhibiting action of aluminum ions in elongating cell walls. *Fiziologiia Rastenii* **22:** 1183–1190

Kochian LV (1995) Cellular mechanisms of aluminum toxicity and resistance in plants. *Annual Review of Plant Physiology and Plant Molecular Biology* **46:** 237–260

Kochian LV, Hoekenga OA, Pineros MA (2004) How do crop plants tolerate acid soils? Mechanisms of aluminum tolerance and phosphorous efficiency. *Annual Review of Plant Biology* **55:** 459–493

Kochian LV, Pi ñeros MA, Hoekenga OA (2005) The physiology, genetics and molecular biology of plant aluminum resistance and toxicity. *Plant and Soil* **274:** 175–195

Kollmeier M, Dietrich P, Bauer CS, Horst WJ, Hedrich R (2001) Aluminum activates a citrate-permeable anion channel in the aluminum sensitive zone of the maize root apex. A comparison between an aluminum-sensitive and an aluminum-resistant cultivar. *Plant Physiology* **126:** 397–410

Kollmeier M, Horst WJ (2001) Aluminium-induced exudation of citrate from the root tip of *Zea mays* (L.): are differential impacts of Al on citrate metabolism involved in genotypical differences? In: Horst WJ, Schenk MK, Bu¨rckert A, *et al.* eds. *Plant*

nutrition: food security and sustainability of agro-ecosystems through basic and applied research. Dordrecht: Kluwer Academic Publishers, 492–493

Konishi T, Ohmiya Y, Hayashi T (2004) Evidence that sucrose loaded into the phloem of a poplar leaf is used directly by sucrose synthase associated with various beta-glucan synthases in the stem. *Plant Physiology* **134:** 1146–1152

Kuderová A, Urbánková I, Válková M, Malbeck J, Brzobohatý B, Némethová D, Hejátko J (2008) Effects of conditional IPT-dependent cytokinin overproduction on root architecture of Arabidopsis seedlings. *Plant Cell Physiology* **49:** 570–582

Kudo T, Kiba T, Sakakibara H (2010) Metabolism and long-distance translocation of cytokinins. *Journal of Integrative Plant Biology* **52:** 53–60

Kuga S (1981) Pore size distribution analysis of gel substances by size exclusion chromatography. *Journal of Chromatography* **206:** 449–461

Lawlor DW (1970) Absorption of polyethylene glycols by plants and their effects on plant growth. *New Phytologist* **69:** 501–504

Layton BE, Boyd MB, Tripepi MS, Bitonti BM, Dollahon MNR, Balsamo RA (2010) Dehydration-induced expression of a 31-kda dehydrin in *polypodium polypodioides* (polypodiaceae) may enable large, reversible deformation of cell walls. *American Journal of Botany* **97:** 535–544

Lee SM, Koh HJ, Park DC, Song BJ, Huh TL, Park JW (2002) Cytosolic NADP-dependent isocitrate dehydrogenase status modulates oxidative damage to cells. *Free Radical Biology and Medicine* **32:** 1185–1196

LeNoble ME, Spollen WG, Sharp RE (2004) Maintenance of shoot growth by ABA: genetic assessment of the role of ethylene suppression. *Journal of Experimental Botany* **55:** 237–245

Leucci MR, Lenucci MS, Piro G, Dalessandro G (2008) Water stress and cell wall polysaccharides in the apical root zone of wheat cultivars varying in drought tolerance. *Journal of Plant Physiology* **165**: 1168–1180

Lian HL, Yu X, Lane D, Sun WN, Tang ZC, Su WA (2006) Upland rice and lowland rice exhibited different PIP expression under water deficit and ABA treatment. *Cell Research* **16:** 651–660

Liang BM, Sharp RE, Baskin TI (1997) Regulation of growth anisotropy in well-watered and water-stressed maize roots. I. Spatial distribution of longitudinal, radial and tangential expansion rates. *Plant Physiology* **115:** 101–111

Ligaba A, Katsuhara M, Ryan PR, Shibasaka M, Matsumoto H (2006) The *BnALMT1* and *BnALMT2* genes from rape encode aluminum-activated malate transporters that enhance the aluminum resistance of plant cells. *Plant Physiology* **142:** 1294–1303

Liu J, Magalhaes JV, Shaff J, Kochian LV (2009) Aluminum-activated citrate and malate transporters from the MATE and ALMT families function independently to confer Arabidopsis aluminum tolerance. *The Plant Journal* **57:** 389–399

Liu Y, Shi Y, Song Y, Wang T, Li Y (2010) Characterization of a stress-induced NADP-isocitrate dehydrogenase gene in maize confers salt tolerance in Arabidopsis. *Journal of Plant Biology* **53:** 107–112

Livak KJ, Schmittgen TD (2001) Analysis of relative gene expression data using real-time quantitative PCR and the $2^{-\Delta\Delta CT}$ method. *Methods* **25:** 402–408

Lopez CG, Banowetz GM, Peterson CJ, Kronstad WE (2003) Dehydrin expression and drought tolerance in seven wheat cultivars. *Crop Science* **43:** 577–582

Ma JF (2007) Syndrome of aluminum toxicity and diversity of aluminum resistance in higher plants. *International Review of Cytology* **264:** 225–252

Ma JF, Ryan PR, Delhaize E (2001) Aluminium tolerance in plants and the complexing role of organic acids. *Trends in Plant Science* **6:** 273–278

Ma JF, Shen RF, Nagao S, Tanimoto E (2004) Aluminum targets elongating cells by reducing cell wall extensibility in wheat roots. *Plant and Cell Physiology* **45:** 583–589

Magalhaes JV, Liu J, Guimarães CT, Lana UG, Alves VM, Wang YH, Schaffert RE, Hoekenga OA, Piñeros MA, Shaff JE, Klein PE, Carneiro NP, Coelho CM, Trick HN, Kochian LV (2007) A gene in the multidrug and toxic compound extrusion (MATE) family confers aluminum tolerance in sorghum. *Nature Genetics* **39:** 1156–1161

Manavella PA, Arce AL, Dezar CA, Bitton F, Renou JP, Crespi M, Chan RL (2006) Cross-talk between ethylene and drought signalling pathways is mediated by the sunflower Hahb-4 transcription factor. *The Plant Journal* **48:** 125–137

Maron LG, Kirst M, Mao C, Milner MJ, Menossi M, Kochian LV (2008) Transcriptional profiling of aluminum toxicity and tolerance responses in maize roots. *New Phytologist* **179:** 116–128

Massonneau AS, Langlade N, Leon S, Smutny J, Vogt E, Neumann G, Martinoia E (2001) Metabolic changes associated with cluster root development in white lupin (*Lupinus albus* L.): relationship between organic acid excretion, sucrose metabolism and energy status. *Planta* **213:** 534–542

Massot N, Nicander B, Barceló J, Poschenrieder Ch, Tillberg E (2002) A rapid increase in cytokinin levels and enhanced ethylene evolution precede Al^{3+}-induced inhibition of root growth in bean seedlings (*Phaseolus vulgaris* L.). *Plant Growth Regulation* **37:** 105–112

Matsumura H, Reich S, Ito A, Saitoh H, Kamoun S, Winter P, Kahl G, Reuter M, Kruger DH, Terauchi R (2003) Gene expression analysis of plant host pathogen interactions by SuperSAGE. *Proceedings of the National Academy of Sciences of the United States of America* **100:** 15718–15723

Matsumura H, Yoshida K, Luo S, Kimura E, Fujibe T, Albertyn Z, Barrero RA, Krüger DH, Kahl G, Schroth GP, Terauchi R (2010) High-throughput SuperSAGE for digital gene expression analysis of multiple samples using next generation sequencing. *PLoS One* **5:** e12010

Mazarei M, Lennon KA, Puthoff DP, Rodermel SR, Baum TJ (2003) Expression of an Arabidopsis phosphoglycerate mutase homologue is localized to apical meristems, regulated by hormones, and induced by sedentary plant-parasitic nematodes. *Plant Molecular Biology* **53:** 513-530

McKenna BA, Kopittke PM, Wehr JB, Blamey FP, Menzies NW. 2010. Metal ion effects on hydraulic conductivity of bacterial cellulose-pectin composites used as plant cell wall analogs. *Physiologia Plantarum* **138:** 205–214

Meng PH, Raynaud C, Tcherkez G, Blanchet S, Massoud K, Domenichini S, Henry Y, Soubigou-Taconnat L, Lelarge-Trouverie C, Saindrenan P, Renou JP, Bergounioux C (2009) Crosstalks between myo-inositol metabolism, programmed cell death and basal immunity in Arabidopsis. *PLoS One* **4:** e7364

Miklas PN, Kelly JD, Beebe SE, Blair MW (2006) Common bean breeding for resistance against biotic and abiotic stresses: From classical to MAS breeding. *Euphytica* **147:** 105–131

Minic Z, Jouanin L (2006) Plant glycoside hydrolases involved in cell wall polysaccharide degradation. *Plant Physiology and Biochemistry* **44:** 435–449

Miyasaka SC, Buta JG, Howell RK, Foy CD (1991) Mechanisms of aluminum tolerance in snapbeans. Root exudation of citric acid. *Plant Physiology* **96:** 737–743

Molina C, Rotter B, Horres R, Udupa SM, Besser B, Bellarmino L, Baum M, Matsumura H, Terauchi R, Kahl G (2008) SuperSAGE: the drought stress responsive transcriptome of chickpea roots. *BMC Genomics* **9:** 553–581

Moore JP, Vicré-Gibouin M, Farrant JM, Driouich A (2008) Adaptations of higher plant cell walls to water loss: drought vs desiccation. *Physiologia Plantarum* **134:** 237–245

Morgan JM (1984) Osmoregulation and water stress in higher plants. *Annual Review of Plant Physiology* **35:** 299–319

Mouillon JM, Eriksson SK, Harryson P (2008) Mimicking the plant cell interior under water stress by macromolecular crowding: disordered dehydrin proteins are highly resistant to structural collapse. *Plant Physiology* **148:** 1925–1937

Mugai EN, Agong SG, Matsumoto H (2000) Aluminium tolerance mechanisms in *Phaseolus vulgaris* L.: citrate synthase activity and TTC reduction are well correlated with citrate secretion. *Soil Science and Plant Nutrition* **46:** 939–950

Nanjo T, Kobayashi M, Yoshiba Y, Sanada Y, Wada K, Tsukaya H, Kakubari Y, Yamaguchi-Shinozaki K, Shinozaki K (1999) Biological functions of proline in morphogenesis and osmotolerance revealed in antisense transgenic *Arabidopsis thaliana*. *The Plant Journal* **18:** 185–193

Neuhoff V, Stamm R, Eibl H (1985) Clear background and highly sensitive protein staining with Coomassie Blue dyes in polyacrylamide gels: A systematic analysis. *Electrophoresis* **6:** 427–448

Neuhoff V, Stamm R, Pardowitz I, Arold N, Ehrhardt W, Taube D (1990) Essential problems in quantification of proteins following colloidal staining with coomassie brilliant blue dyes in polyacrylamide gels, and their solution. *Electrophoresis* **11:** 101–117

Nieuwland J, Feron R, Huisman BA, Fasolino A, Hilbers CW, Derksen J, Mariani C (2005) Lipid transfer proteins enhance cell wall extension in tobacco. *The Plant Cell* **17:** 2009–2019

Nightingale Jr ER (1959) Phenomenological theory of ion solvation. Effective radii of hydrated ions. *The Journal of Physical Chemistry* **63:** 1381–1387

Nobel PS (1991) Physicochemical Environmental Plant Physiology. Academic Press, New York, NY, ISBN 0125200250

Odanaka S, Bennett AB, Kanayama Y (2002) Distinct physiological roles of fructokinase isozymes revealed by gene-specific suppression of *Frk1* and *Frk2* expression in tomato. *Plant Physiology* **129:** 1119–1126

Ogawa A, Yamauchi A (2006) Root osmotic adjustment under osmotic stress in maize seedlings 2. Mode of accumulation of several solutes for osmotic adjustment in the root. *Plant Production Science* **9:** 39–46

Oono Y, Seki M, Nanjo T, Narusaka M, Fujita M, Satoh R, Satou M, Sakurai T, Ishida J, Akiyama K, Iida K, Maruyama K, Satoh S, Yamaguchi-Shinozaki K, Shinozaki K (2003) Monitoring expression profiles of *Arabidopsis* gene expression during rehydration process after dehydration using *ca.* 7000 full-length cDNA microarray. *The Plant Journal* **34:** 868–887

Orellana S, Yañez M, Espinoza A, Verdugo I, González E, Ruiz-Lara S, Casaretto JA (2010) The transcription factor SlAREB1 confers drought, salt stress tolerance and regulates biotic and abiotic stress-related genes in tomato. *Plant, Cell and Environment* **33:** 2191–2208

Pandey A, Rajamani U, Verma J, Subba P, Chakraborty N, Datta A, Chakraborty S, Chakraborty N (2010) Identification of extracellular matrix proteins of rice (*Oryza sativa* L.) involved in dehydration-responsive network: a proteomic approach. *Journal of Proteome Research* **9:** 3443–3464

Peleman J, Boerjan W, Engler G, Seurinck J, Botterman J, Alliotte T, Van Montagu M, Inzé D (1989) Strong cellular preference in the expression of a housekeeping gene of Arabidopsis thaliana encoding S-adenosylmethionine synthetase. *The Plant Cell* **1:** 81-93

Pineda Rodo A, Brugière N, Vankova R, Malbeck J, Olson JM, Haines SC, Martin RC, Habben JE, Mok DW, Mok MC (2008) Over-expression of a zeatin O-glucosylation gene in maize leads to growth retardation and tasselseed formation. *Journal of Experimental Botany* **59:** 2673–2686

Pitarch A, Sanchez M, Nombela C, Gil C (2002) Sequential fractionation and two-dimensional analysis unravels the complexity of the dimorphic fungi *Candida albicans* cell wall proteome. *Molecular and Cellular Proteomicss* **1:** 967–982

Poroyko V, Spollen WG, Hejlek LG, Hernandez AG, LeNoble ME, Davis G, Nguyen HT, Springer GK, Sharp RE, Bohnert HJ (2007) Comparing regional transcript profiles from maize primary roots under well-watered and low water potential conditions. *Journal of Experimental Botany* **58:** 279–289

Premachandra GS, Hahn DT, Rhodes D and Joly RJ (1995) Leaf water relations and solute accumulation in two grain sorghum lines exhibiting contrasting drought tolerance. *Journal of experimental botany* **46:** 1833–1841

Pritchard J, Hetherington PR, Fry SC, Tomos AD (1993) Xyloglucan endotransglycosylase activity, microfibril orientation and the profiles of cell wall properties along growing regions of maize roots. *Journal of Experimental Botany* **44:** 1281–1289

Qin X, Zeevaart JA (2002) Overexpression of a 9- cisepoxycarotenoid dioxygenase gene in *Nicotiana plumbaginifolia* increases abscisic acid and phaseic acid levels and enhances drought tolerance. *Plant Physiology* **128:** 544–551

Qin X, Zeevaart JAD (1999) The 9-cis-epoxycarotenoid cleavage reaction is the key regulatory step of abscisic acid biosynthesis in water-stressed bean. *Proceedings of the National Academy of Sciences of the United States of America* **96:** 15354–15361

Rangel AF, Mobin M, Rao IM, Horst WJ (2005) Proton toxicity interferes with the screening of common bean (*Phaseolus vulgaris* L.) genotypes for aluminium resistance in nutrient solution. *Journal of Plant Nutrition and Soil Science* **168:** 607–616

Rangel AF, Rao IM, Braun H-P, Horst WJ (2010) Aluminium resistance in common bean (*Phaseolus vulgaris*) involves induction and maintenance of citrate exudation from

root apices. *Physiologia Plantarum* **138:** 176–190

Rangel AF, Rao IM, Horst WJ (2007) Spatial aluminium sensitivity of root apices of two common bean (*Phaseolus vulgari*s L.) genotypes with contrasting aluminium resistance. *Journal of Experimental Botany* **58:** 3895–3904

Rangel AF, Rao IM, Horst WJ (2009) Intracellular distribution and binding state of aluminum in root apices of two common bean (*Phaseolus vulgaris*) genotypes in relation to Al toxicity. *Physiologia Plantarum* **135:** 162–173

Rao IM (2001) Role of physiology in improving crop adaptation to abiotic stresses in the tropics: The case of common bean and tropical forages. In: Pessarakli M, *ed. Handbook of Plant and Crop Physiology*, New York: Marcel Dekker, 583–613

Rao IM, Zeigler RS, Vera R, Sarkarung S (1993) Selection and breeding for acid-soil tolerance in crops. *BioScience* **43:** 454–465

Ravanel S, Gakière B, Job D, Douce R (1998) The specific features of methionine biosynthesis and metabolism in plants. *Proceedings of the National Academy of Sciences of the United States of America* **95:** 7805–7812

Ren Z, Zheng Z, Chinnusamy V, Zhu J, Cui X, Lida K, Zhu J-K (2010) RAS1, a quantitative trait locus for salt tolerance and ABA sensitivity in *Arabidopsis*. *Proceedings of the National Academy of Sciences of the United States of America* **107:** 5669–5674

Rengel Z, Reid RJ (1997) Uptake of Al across the plasma membrane of plant cells. *Plant and Soil* **192:** 31–35

Rodriguez MC, Edsgärd D, Hussain SS, Alquezar D, Rasmussen M, Gilbert T, Nielsen BH, Bartels D, Mundy J (2010) Transcriptomes of the desiccation-tolerant resurrection plant *Craterostigma plantagineum. The Plant journal* **63:** 212–228

Rodriguez-Uribe L, O'Connell MA (2006) A root-specific bZIP transcription factor is responsive to water deficit stress in tepary bean (*Phaseolus acutifolius*) and common bean (*P. vulgaris*). *Journal of Experimental Botany* **57:** 1391–1398

Rohrig H, Schmidt J, Colby T, Brautigam A, Hufnagel P, Bartels D (2006) Desiccation of the resurrection plant Craterostigma plantagineum induces dynamic changes in protein phosphorylation. *Plant, Cell and Environment* **29:** 1606–1617

Romo S, Jiménez T, Labrador E, Dopico B (2005) The gene for a xyloglucan endotransglucosylase/hydrolase from *Cicer arietinum* is strongly expressed in elongating tissues. *Plant Physiology and Biochemistry* **43:** 169–176

Rose JK, Braam J, Fry SC, Nishitani K (2002) The XTH family of enzymes involved in xyloglucan endotransglucosylation and endohydrolysis: current perspectives and a new unifying nomenclature. *Plant and Cell Physiology* **43:** 1421–1435

Rose JKC, Bashir S, Giovannoni JJ, Jahn MM, Saravanan RS (2004) Tackling the plant proteome: practical approaches, hurdles and experimental tools. *The Plant Journal* **39:** 715–733

Rozen S, Skaletsky H (2000) Primer3 on the WWW for general users and for biologist programmers. In: Krawetz S, Misener S, eds. *Bioinformatics methods and protocols*. Totowa, NJ: Humana Press, 365–386

Růžička K, Šimášková M, Duclercq J, Petrášek J, Zažímalová E, Simon S, Friml J, Van Montagu MC, Benková E (2009) Cytokinin regulates root meristem activity via modulation of the polar auxin transport. *Proceedings of the National Academy of*

Sciences of the United States of America **106:** 4284–4289

Ryan PR, Delhaize E (2010) The convergent evolution of aluminium resistance in plants exploits a convenient currency. *Functional Plant Biology* **37:** 275–284

Ryan PR, Delhaize E, Jones DL (2001) Function and mechanism of organic anion exudation from plant roots. *Annual Review of Plant Biology* **52:** 527–560

Ryan PR, DiTomaso JM, Kochian LV (1993) Aluminium toxicity in roots: an investigation of spatial sensitivity and the role of the root cap. *Journal of Experimental Botany* **44:** 437–446

Ryan PR, Raman H, Gupta S, Horst WJ, Delhaize E (2009) A second mechanism for aluminum resistance in wheat relies on the constitutive efflux of citrate from roots. *Plant Physiology* **149:** 340–351

Ryan PR, Tyerman SD, Sasaki T, Furuichi T, Yamamoto Y, Zhang WH, Delhaize E (2011) The identification of aluminium-resistance genes provides opportunities for enhancing crop production on acid soils. *Journal of Experimental Botany* **62:** 9–20

Saab IN, Sharp RE, Pritchard J (1992) Effect of inhibition of abscisic acid accumulation on the spatial distribution of elongation in the primary root and mesocotyl of maize at low water potentials. *Plant Physiology* **99:** 26–33

Sadka A, Dahan E, Or E and Cohen L (2000) NADP(+)-isocitrate dehydrogenase gene expression and isozyme activity during citrus fruit development. *Plant Science* **158:** 173–181

Saftner RA, Wyse RE (1984) Effect of plant hormones on sucrose uptake by sugar beet root tissue discs. *Plant Physiology* **74:** 951–955

Sakakibara H (2006) Cytokinins: activity, biosynthesis, and translocation. *Annual Review of Plant Biology* **57:** 431–449

Samarah NH, Mullen RE, Cianzio SR, Scott P (2006) Dehydrin-like proteins in soybean seeds in response to drought stress during seed filling. *Crop Science* **46:** 2141–2150

Sanchez-Aguayo I, Rodriguez-Galan JM, Garcia R, Torreblanca J, Pardo JM (2004) Salt stress enhances xylem development and expression of S-adenosyl-L-methionine synthase in lignifying tissues of tomato plants. *Planta* **220:** 278–285

Sasaki T, Yamamoto Y, Ezaki E, Katsuhara M, Ahn SJ, Ryan PR, Delhaize E, Matsumoto H (2004) A wheat gene encoding an aluminum-activated malate transporter. *The Plant Journal* **37:** 645–653

Schmohl N, Horst WJ (2000) Cell wall pectin content modulates aluminium sensitivity of *Zea mays* (L.) cell grown in suspension culture. *Plant, Cell and Environment* **23:** 735–742

Schmohl N, Pilling J, Fisahn J, Horst WJ (2000) Pectin methylesterase modulates aluminium sensitivity in *Zea mays* and *Solanum tuberosum*. *Physiologia Plantarum* **109:** 419–427

Schuler MA, Werck-Reichhart D (2003) Functional genomics of P450s. *Annual Review of Plant Biology* **54:** 629–667

Seiler C, Harshavardhan VT, Rajesh K, Reddy PS, Strickert M, Rolletschek H, Scholz U, Wobus U, Sreenivasulu N (2011) ABA biosynthesis and degradation contributing to ABA homeostasis during barley seed development under control and terminal drought-stress conditions. *Journal of Experimental Botany* **doi:**

10.1093/jxb/erq446

Seki M, Narusaka M, Ishida J, Nanjo T, Fujita M, Oono Y, Kamiya A, Nakajima M, Enju A, Sakurai T, Satou M, Akiyama K, Taji T, Yamaguchi-Shinozaki K, Carninci P, Kawai J, Hayashizaki Y, Shinozaki K (2002) Monitoring the expression profiles of 7000 Arabidopsis genes under drought, cold, and high-salinity stresses using a full-length cDNA microarray. *The Plant Journal* **31:** 279–292

Seo M, Koiwai H, Akaba S, Komano T, Oritani T, Kamiya Y, Koshiba T (2000) Abscisic aldehyde oxidase in leaves of *Arabidopsis thaliana. The Plant Journal* **23:** 481–488

Seo M, Koshiba T (2002) Complex regulation of ABA biosynthesis in plants. *Trends in Plant Science* **7:** 41–48

Seo PJ, Xiang F, Qiao M, Park JY, Lee YN, Kim SG, Lee YH, Park WJ, Park CM (2009) The MYB96 transcription factor mediates abscisic acid signaling during drought stress response in Arabidopsis. *Plant Physiology* **151:** 275–289

Serraj R, Sinclair TR (2002) Osmolyte accumulation: can it really help increase crop yield under drought conditions? *Plant, Cell and Environment* **25:** 333–341

Sharp RE (2002) Interaction with ethylene: changing views on the role of ABA in root and shoot growth responses to water stress. *Plant, Cell and Environment* **25:** 211–222

Sharp RE, Davies WJ (1989) Regulation of growth and development of plants growing with a restricted supply of water. In: Jones HG, Flowers TL, Jones MB, eds. *Plants under stress.* Cambridge: Cambridge University Press, 71–93

Sharp RE, LeNoble ME, Else MA, Thorne ET, Gherardi F (2000) Endogenous ABA maintains shoot growth in tomato independently of effects on plant water balance: evidence for an interaction with ethylene. *Journal of Experimental Botany* **51:** 1575–1584

Sharp RE, Poroyko V, Hejlek LG, Spollen WG, Springer GK, Bohnert HJ, Nguyen HT (2004) Root growth maintenance during water deficits: physiology to functional genomics. *Journal of Experimental Botany* **55:** 2343–2351

Sharp RE, Silk WK, Hsiao TC (1988) Growth of the maize primary root at low water potentials: I. Spatial distribution of expansive growth. *Plant Physiology* **87:** 50–57

Shen H, Ligaba A, Yamaguchi M, Osawa H, Shibata K, Yan X, Matsumoto H (2004) Effect of K-252a and abscisic acid on the efflux of citrate from soybean roots. *Journal of Experimental Botany* **55:** 663-671

Shen H, Yan X, Wang X, Zheng S (2002) Exudation of citrate in common bean in response to aluminum stress. *Journal of Plant Nutrition* **25:** 1921–1932

Shevchenko A, Sunyaev S, Loboda A, Shevchenko A, Bork P, Ens W, Standing KG (2001) Charting the proteomes of organisms with unsequenced genomes by MALDI-quadrupole time-of-flight mass spectrometry and BLAST homology searching. *Analytical Chemistry* **73:** 1917–1926

Shinozaki K, Yamaguchi-Shinozaki K (1997) Gene expression and signal transduction in water-stress response. *Plant Physiology* **115:** 327–334

Shinozaki K, Yamaguchi-Shinozaki K (2007) Gene networks involved in drought stress response and tolerance. *Journal of Experimental Botany* **58:** 221–227

Shinozaki K, Yamaguchi-Shinozaki K, Seki M (2003) Regulatory network of gene

expression in the drought and cold stress responses. *Current Opinion in Plant Biology* **6:** 410–417

Showalter AM (1993) Structure and function of plant cell wall proteins. *The Plant Cell* **5:** 9–23

Singh SP (2001) Broadening the genetic base of common bean cultivars: a review. *Crop Science* **41:** 1659–1675

Sivaguru M, Horst WJ (1998) The distal part of the transition zone is the most aluminum-sensitive apical root zone of maize. *Plant Physiology* **116:** 155–163

Sivaguru M, Horst WJ, Eticha D, Matsumoto H (2006) Aluminum inhibits apoplastic flow of high-molecular weight solutes in root apices of *Zea mays* L. *Journal of Plant Nutrition and Soil Science* **169:** 679–690

Skoog F, Miller CO (1957) Chemical regulation of growth and organ formation in plant tissue cultured in vitro. *Symposia of the Society for Experimental Biology* **11:** 118–131

Spollen WG, LeNoble ME, Samuels TD, Bernstein N, Sharp RE (2000) Abscisic acid accumulation maintains maize primary root elongation at low water potentials by restricting ethylene production. *Plant Physiology* **122:** 967–976

Spollen WG, Sharp RE (1991) Spatial distribution of turgor and root growth at low water potentials. *Plant Physiology* **96:** 438–443

Spollen WG, Tao W, Valliyodan B, Chen K, Hejlek LG, Kim JJ, Lenoble ME, Zhu J, Bohnert HJ, Henderson D, Schachtman DP, Davis GE, Springer GK, Sharp RE, Nguyen HT (2008) Spatial distribution of transcript changes in the maize primary root elongation zone at low water potential. *BMC Plant Biology* **8:** 32

Sponchiado BN, White JW, Castillo JA and Jones PG (1989) Root growth of four common bean cultivars in relation to drought tolerance in environments with contrasting soil types. *Experimental Agriculture* **25:** 249–257

Staß A, Horst WJ (2009) Callose in abiotic stress. In: Bacic A, Fincher GB, Stone BA. *eds. Chemistry, biochemistry, and biology of (1→3)-β-glucans and related polysaccharides*. Burlington, MA: Academic Press, 499–524

Stepanova AN, Yun J, Likhacheva AV, Alonso JM (2007) Multilevel interactions between ethylene and auxin in Arabidopsis roots. *The Plant Cell* **19:** 2169–2185

Sun P, Tian QY, Chen J, Zhang WH (2010) Aluminium-induced inhibition of root elongation in Arabidopsis is mediated by ethylene and auxin. *Journal of Experimental Botany* **61:** 347–356

Sun P, Tian QY, Zhao MG, Dai XY, Huang JH, Li LH, Zhang WH (2007) Aluminum-induced ethylene production is associated with inhibition of root elongation in *Lotus japonicus* L. *Plant and Cell Physiology* **48:** 1229–1235

Swarup R, Perry P, Hagenbeek D, Van Der Straeten D, Beemster GT, Sandberg G, Bhalerao R, Ljung K, Bennett MJ (2007) Ethylene upregulates auxin biosynthesis in Arabidopsis seedlings to enhance inhibition of root cell elongation. *The Plant Cell* **19:** 2186–2196

Tabor CW, Tabor H (1984) Methionine adenosyltransferase (S-adenosylmethionine synthetase) and S-adenosylmethionine decarboxylase. *Advances in Enzymology and Related Areas of Molecular Biology* **56:** 251–282

Tabuchi A, Kikui S, Matsumoto H (2004) Differential effects of aluminium on osmotic

potential and sugar accumulation in the root cells of Al-resistant and Al-sensitive wheat. *Physiologia Plantarum* **120:** 106–112

Tabuchi A, Matsumoto H (2001) Changes in cell-wall properties of wheat (*Triticum aestivum*) roots during aluminum-induced growth inhibition. *Physiologia Plantarum* **112:** 353–358

Tada Y, Kashimura T (2009) Proteomic analysis of salt-responsive proteins in the mangrove plant, *Bruguiera gymnorhiza*. *Plant and Cell Physiology* **50:** 439–446

Takei K, Yamaya T, Sakakibara H (2004) Arabidopsis CYP735A1 and CYP735A2 encode cytokinin hydroxylases that catalyze the biosynthesis of trans-Zeatin. *The Journal of Biological Chemistry* **279:** 41866–41872

Taylor GJ, McDonald-Stephens JL, Hunter DB, Bertsch PM, Elmore D, Rengel Z, Reid RJ (2000) Direct measurement of aluminum uptake and. distribution in single cells of *Chara coralline*. *Plant Physiology* **123:** 987–996

Tezuka K, Hayashi M, Ishihara H, Onozaki K, Nishimura M, Takahashi N (1993) Occurrence of heterogeneity of Nlinked oligosaccharides attached to sycamore (*Acer pseudoplatanus* L.) laccase after excretion. *Biochemistry and Molecular Biology International* **29:** 395–402

Thompson AJ, Jackson AC, Parker RA, Morpeth DR, Burbidge A, Taylor IB (2000) Abscisic acid biosynthesis in tomato: regulation of zeaxanthin epoxidase and 9-cis-epoxycarotenoid dioxygenase mRNAs by light/dark cycles, water stress and abscisic acid. *Plant Molecular Biology* **42:** 833–845

Thung M, Rao IM (1999) Integrated management of abiotic stresses. In: Singh SP *ed. Common Bean Improvement in the Twenty-First Century*, Dordrecht: Kluwer Academic Publishers, 331–370

Toorchi M, Yukawa K, Nouri MZ, Komatsu S (2009) Proteomics approach for identifying osmotic-stress-related proteins in soybean roots. *Peptides* **30:** 2108–2117

Uno Y, Furihata T, Abe H, Yoshida R, Shinozaki K, Yamaguchi-Shinozaki K (2000) Arabidopsis basic leucine zipper transcription factors involved in an abscisic acid-dependent signal transduction pathway under drought and high-salinity conditions. *Proceedings of the National Academy of Sciences of the United States of America* **97:** 11632–11637

Van HL, Kuraishi S, Sakurai N (1994) Aluminum-induced rapid root inhibition and changes in cell-wall components of squash seedlings. *Plant Physiology* **106:** 971–976

Van Volkenburgh E, Boyer JS (1985) Inhibitory effects of water deficit on maize leaf elongation. *Plant Physiology* **77:** 190–194

Vandeleur RK, Mayo G, Shelden MC, Gilliham M, Kaiser BN, Tyerman SD (2009) The role of plasma membrane intrinsic protein aquaporins in water transport through roots: diurnal and drought stress responses reveal different strategies between isohydric and anisohydric cultivars of grapevine. *Plant Physiology* **149:** 445–460

Velculescu V, Zhang L, Vogelstein B, Kinzler K (1995) Serial analysis of gene expression. *Science* **270:** 484–487

Vicré M, Farrant JM, Driouich A (2004) Insights into the cellular mechanisms of desiccation tolerance among angiosperm resurrection plant species. *Plant, Cell and Environment* **27:** 1329–1340

Voetberg GS, Sharp RE (1991) Growth of the maize primary root at low water potentials.

III. Role of increased proline deposition in osmotic adjustment. *Plant Physiology* **96:** 1125–1130

von Uexküll HR, Mutert E (1995) Global extent, development and economic impact of acid soils. *Plant and Soil* **171:** 1–15

Vysotskaya LB, Korobova AV, Veselov SY, Dodd IC, Kudoyarova GR (2009) ABA mediation of shoot cytokinin oxidase activity: assessing its impacts on cytokinin status and biomass allocation of nutrient-deprived durum wheat. *Functional Plant Biology* **36:** 66–72

Wagatsuma T, Ishikawa S, Obata H, Tawaraya K, Katohda S (1995) Plasma membrane of younger and outer cells is the primary specific site for aluminium toxicity in roots. *Plant and Soil* **171:** 105–112

Wakabayashi K, Hoson T, Kamisaka S (1997) Changes in amounts and molecular mass distribution of cell wall polysaccharides of wheat (*Triticum aestivum* L.) coleoptiles under water stress. *Journal of Plant Physiology* **151:** 33–40

Wang HL, Lee PD, Chen WL, Huang DJ, Su JC (2000) Osmotic stress-induced changes of sucrose metabolism in cultured sweet potato cells. *Journal of Experimental Botany* **51:** 1991–1999

Wang KLC, Li H, Ecker JR (2002) Ethylene biosynthesis and signaling networks. *The Plant Cell* **14:** S131–S151

Wang Y, Stass A, Horst WJ (2004) Apoplastic binding of aluminum is involved in silicon-induced amelioration of aluminum toxicity in maize. *Plant Physiology* **136:** 3762–3770

Watson BS, Lei Z, Dixon RA, Sumner LW (2004) Proteomics of *Medicago sativa* cell walls. *Phytochemistry* **65:** 1709–1720

Wehr JB, Menzies NW, Blamey FPC (2004) Inhibition of cell-wall autolysis and pectin degradation by cations. *Plant Physiology and Biochemistry* **42:** 485–492

Welcker C, Théc C, Andréau B, De Leon C, Parentoni SN, Bernal J, Félicité J, Zonkeng C, Salazar F, Narro L, Charcosset A, Horst WJ (2005) Heterosis and combining ability for maize adaptation to tropical acid soils: Implications for future breeding strategies. *Crop Science* **45:** 2405–2413

Werhahn W, Braun HP (2002) Biochemical dissection of the mitochondrial proteome from Arabidopsis thaliana by three-dimensional gel electrophoresis. *Electrophoresis* **23:** 640–646

Werner T, Motyka V, Strnad M, Schmülling T (2001) Regulation of plant growth by cytokinin. *Proceedings of the National Academy of Sciences of the United States of America* **98:** 10487–10492

Werner T, Nehnevajova E, Köllmer I, Novák O, Strnad M, Krämer U, Schmülling T (2010) Root-specific reduction of cytokinin causes enhanced root growth, drought tolerance, and leaf mineral enrichment in Arabidopsis and tobacco. *The Plant Cell* **22:** 3905–3920

Westgate ME, Boyer JS (1985) Osmotic adjustment and the inhibition of leaf, root, stem and silk growth at low water potentials in maize. *Planta* **164:** 540–549.

Wisniewski M, Webb R, Balsamo R, Close TJ, Yu XM, Griffith M (1999) Purification, immunolocalization, cryoprotective, and antifreeze activity of PCA60: a dehydrin from peach (*Prunus persica*). *Physiologia Plantarum* **105:** 600–608

Wissemeier AH, Diening A, Hergenröder A, Horst WJ, Mix-Wagner G (1992) Callose formation as parameter for assessing genotypical plant tolerance of aluminium and manganese. *Plant and Soil* **146:** 67–75

Wissemeier AH, Horst WJ (1995) Effect of calcium supply on aluminium-induced callose formation, its distribution and persistence in roots of soybean (*Glycine max* (L.) Merr.). *Journal of Plant Physiology* **145:** 470–476

Wissemeier AH, Klotz F, Horst WJ (1987) Aluminium induced callose synthesis in roots of soybean (*Glycine max* L.). *Journal of Plant Physiology* **129:** 487–492

Wojciechowski CL, Fall F (1996) A continuous fluorometric assay for pectin methylesterase. *Analytical Biochemistry* **137:** 103–108

Wu CT, Leubner-Metzger G, Meins F Jr, Bradford KJ (2001) Class I beta-1,3-glucanase and chitinase are expressed in the micropylar endosperm of tomato seeds prior to radicle emergence. *Plant Physiology* **126:** 1299–1313

Wu Y, Cosgrove DJ (2000) Adaptation of roots to low water potentials by changes in cell wall extensibility and cell wall proteins. *Journal of Experimental Botany* **51:** 1543–1553

Wu Y, Sharp RE, Durachko DM, Cosgrove DJ (1996) Growth maintenance of the maize primary root at low water potentials involves increases in cell wall extension properties, expansin activity and wall susceptibility to expansins. *Plant Physiology* **111:** 765–772

Wu Y, Spollen WG, Sharp RE, Hetherington PR, Fry SC (1994) Root growth maintenance at low water potentials: increased activity of xyloglucan endotransglycosylase and its possible regulation by abscisic acid. *Plant Physiology* **106:** 607–615

Xiang Y, Tang N, Du H, Ye H, Xiong L (2008) Characterization of OsbZIP23 as a key player of the basic leucine zipper transcription factor family for conferring abscisic acid sensitivity and salinity and drought tolerance in rice. *Plant Physiology* **148:** 1938–1952

Yamaguchi M, Sharp RE (2010) Complexity and coordination of root growth at low water potentials: recent advances from transcriptomic and proteomic analyses. *Plant, Cell and Environment* **33:** 590–603

Yamaguchi M, Valliyodan B, Zhang J, Lenoble ME, Yu O, Rogers EE, Nguyen HT, Sharp RE (2010) Regulation of growth response to water stress in the soybean primary root. I. Proteomic analysis reveals region-specific regulation of phenylpropanoid metabolism and control of free iron in the elongation zone. *Plant, Cell and Environment* **33:** 223–243

Yan S, Tang Z, Su W, Sun W (2005) Proteomic analysis of salt stress-responsive proteins in rice root. *Proteomics* **5:** 235–244

Yang JL, Li YY, Zhang YJ, Zhang SS, Wu YR, Wu P, Zheng SJ (2008) Cell wall polysaccharides are specifically involved in the exclusion of aluminum from the rice root apex. *Plant Physiology* **146:** 602–611

Yang JL, Zhu XF, Peng YX, Zheng C, Li GX, Liu Y, Shi YZ, Zheng SJ (2011) Cell wall hemicellulose contributes significantly to aluminum adsorption and root growth in Arabidopsis. *Plant Physiology* **155:** 1885–1892

Yang SF, Hoffman NE. (1984) Ethylene biosynthesis and its regulation in higher plants, *Annual Review of Plant Physiology* **35:** 155–189

Yang Z, Sivaguru M, HorstW, Matsumoto H (2000) Aluminium tolerance is achieved by exudation of citric acid from roots of soybean (*Glycine max*). *Physiologia Plantarum*

110: 72–77

Yang ZB, Eticha D, Rao IM, Horst WJ (2010) Alteration of cell-wall porosity is involved in osmotic stress-induced enhancement of aluminium resistance in common bean (*Phaseolus vulgaris* L.). *Journal of Experimental Botany* **61:** 3245–3258

Yang ZB, Eticha D, Rotter B, Rao IM, Horst WJ (2011) Physiological and molecular analysis of polyethylene glycol-induced reduction of aluminium accumulation in the root tips of common bean (*Phaseolus vulgaris* L.). New Phytol (in press)

Yang ZB, You JF, Xu MY, Yang ZM. 2009. Interaction between aluminum toxicity and manganese toxicity in soybean (*Glycine max*). *Plant and Soil* **319**, 277–289.

Yang ZM, Wang J, Wang SH, Xu LL (2003) Salicylic acid-induced aluminum tolerance by modulation of citrate efflux from roots of *Cassia tora* L. *Planta* **217:** 168–174

Yaniv Z, Werker E (1983) Absorption and secretion of polyethylene glycol by *Solanaceous* plants. *Journal of Experimental Botany* **34:** 1577–1584

Zhang G, Taylor GJ (1989) Kinetics of aluminum uptake by excised roots of aluminum-tolerant and aluminum-sensitive cultivars of *Triticum aestivum* L. *Plant Physiology* **91:** 1094–1099

Zhang G, Taylor GJ (1990) Kinetics of aluminum uptake in *Triticum aestivum* L. Identity of the linear phase of Al uptake by excised roots of aluminum-tolerant and aluminum-sensitive cultivars. *Plant Physiology* **94:** 577–584

Zhao XJ, Sucoff E, Stadelmann EJ (1987) Al^{3+} and Ca^{2+} Alteration of Membrane Permeability of Quercus rubra Root Cortex Cells. *Plant Physiology* **83:** 159–162

Zheng J, Zhao J, Tao Y, Wang J, Liu Y, Fu J, Jin Y, Gao P, Zhang J, Bai Y, Wang G (2004) Isolation and analysis of water stress induced genes in maize seedlings by subtractive PCR and cDNA macroarray. *Plant Molecular Biology* **55:** 807–823

Zheng SJ, Ma JF, Matsumoto H (1998) High aluminum resistance in buckwheat: I. Al-induced specific secretion of oxalic acid from root tips. *Plant Physiology* **117:** 745–751

Zhu J, Alvarez S, Marsh EL, Lenoble ME, Cho IJ, Sivaguru M, Chen S, Nguyen HT, Wu Y, Schachtman DP, Sharp RE (2007) Cell wall proteome in the maize primary root elongation zone. II. Region-specific changes in water soluble and lightly ionically bound proteins under water deficit. *Plant Physiology* **145:** 1533–1548

Zhu J, Chen S, Alvarez S, Asirvatham VS, Schachtman DP, Wu Y, Sharp RE (2006) Cell wall proteome in the maize primary root elongation zone. I. Extraction and identification of water-soluble and lightly ionically bound proteins. *Plant Physiology* **140:** 311–325

Zörb C, Schmitt S, Mühling KH (2010) Proteomic changes in maize roots after short-term adjustment to saline growth conditions. *Proteomics* **10:** 4441–4449

SUPPLEMENTAL DATA

The Interaction between Aluminium Toxicity and Drought Stress in Common Bean (*Phaseolus vulgaris* L.):

Physiological and Molecular Aspects

SUPPLEMENTAL DATA FOR CHAPTER 1

Alteration of cell-wall porosity is involved in osmotic stress-induced enhancement of aluminium resistance in common bean (*Phaseolus vulgaris* **L.**)

Zhong-Bao Yang[1], Dejene Eticha[1], Idupulapati Madhusudana Rao[2], Walter Johannes Horst[1]

[1] Institute of Plant Nutrition, Leibniz Universität Hannover, Herrenhaeuser Str. 2, D-30419 Hannover, Germany
[2] International Center for Tropical Agriculture (CIAT), AA 6713, Cali, Colombia
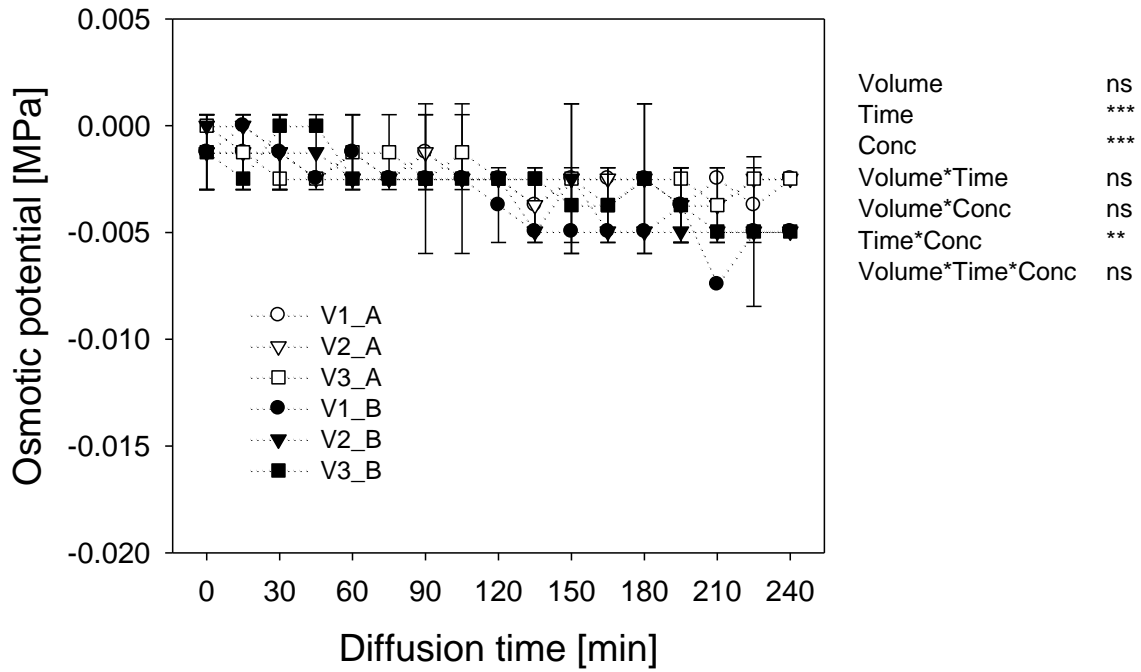
Supplemental Figure S1 Diffusion of low molecular weight PEG through DMT. PEG 6000 was incubated in DMT in 1.0 (V1), 1.5 (V2) or 2.0 (V3) L distilled water. A = original solution, B = 10 x concentrated solution. For the ANOVA, **, *** denote significant differences at $P < 0.01$, $P < 0.001$, respectively; ns = not significant (F test).
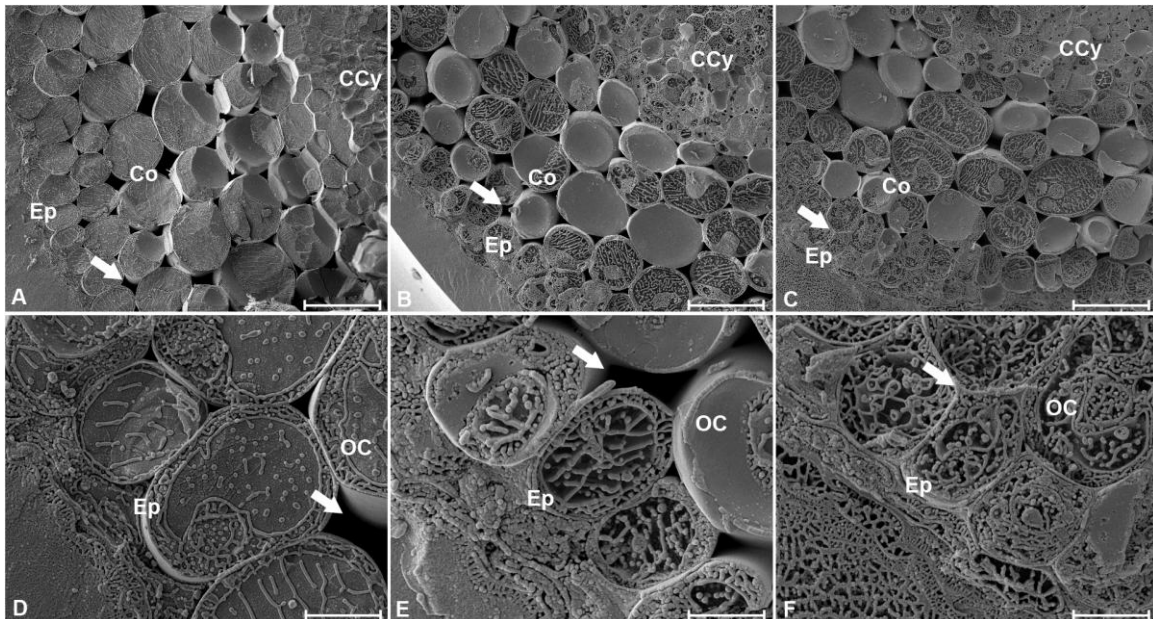
Supplemental Figure S2 Freeze-fracture scanning electron micrographs of root-tip cross-sections (1-5 mm from the root apex) of common bean genotype VAX 1 grown for 4 h in the presence of different molecular weight PEG. Upper row show root cross-section segments from the epidermis (Ep) through the cortex (Co) to the central cylinder (CCy), lower row pictures show the epidermis and one outer cortical cell layer (OC). Arrows indicate the presence (A, B, D, E,) or absence (C, F) of intercellular spaces between the epidermis and the outer cortical cell layer. A, D: control; B, E: PEG 1000; C, F: PEG 6000. Scale bars correspond to 40 μm in A, B and C, 10 μm in D, E and F.

SUPPLEMENTAL DATA FOR CHAPTER 2

Physiological and molecular analysis of polyethylene glycol-induced reduction of aluminium accumulation in the root tips of common bean (*Phaseolus vulgaris* L.)

Zhong-Bao Yang[1], Dejene Eticha[1], Björn Rotter[2], Idupulapati Madhusudana Rao[3], Walter Johannes Horst[1]

[1] Institute of Plant Nutrition, Leibniz Universität Hannover, Herrenhaeuser Str. 2, D-30419 Hannover, Germany

[2] GenXPro GmbH, Altenhöferallee 3, 60438 Frankfurt am Main, Germany

[3] International Center for Tropical Agriculture (CIAT), AA 6713, Cali, Colombia

Supplemental Table S1 List of genes and specific primer pairs used for confirmation of SuperSAGE data by qRT-PCR.

Candidate genes	TC/GB Acc. No.	Primer set		Amplicon size (bp)
		Forward primer (5'→3')	Reverse primer (5'→3')	
Protease inhibitor/seed storage/lipid transfer protein (LTP) family protein	CV542382	CCTCAGCAGCACAAGATGAG	TGACAGCAATCTGAGGGTTG	147
Hydroxyproline-rich glycoprotein	CV543261	CCTGTCTTGATGGTGAAGCA	TTCATTTGTTGCAGGCTGAC	114
40S ribosomal S4 protein	FG230265	AGGCACTCCCTTGATTTGTG	TGGGGCACTAGTTTCCTTTG	156
Major intrinsic protein NIP5;1	GO355339	CGTTGCAGCAGGAAATTACA	GCTGAACTAGCGACGGAAAC	154
Type IIIa membrane protein cp-wap13	TC8398	CCCTTCTGGAAAGGACATCA	GAAAGGATATCCACGGACGA	134
Beta-D-glucosidase	TC8422	ACCCTGCCACTGAAGTTGTC	ACTTGGACCAGGCTCAGGTA	155
Cytosolic fructose-1,6-bisphosphatase	TC8689	TTGATTGTGGGGGTTTCCATT	CGTGCAAGAGCTTCCATACA	140
Pip1 protein	TC9631	ATCCAAGAGCCTTAGCAGCA	GGTGAACAGTTCCCTGAGGA	107
Malate dehydrogenase	TC9663	CCTTGTCAATGGCCTATGCT	ATTCTTCCCAAGCCTCACCT	149
Xyloglucan endotransglycosylase/hydrolase XTH-39	TC10134	AGGATGGCTACACCCACTTG	CAACTTGATCGAGGCACTGA	152
Sucrose synthase 2	TC11609	GCATGGCCTCATGAAAGAGT	GAAAGCAGGCTGAACGAAAG	133
Xyloglucan endotransglycosylase precursor	TC12227	ATATGTCATCGGAGGGTCCA	TTGGTAGGGTCGAACCAAAG	151
Hydroxyproline-rich glycoprotein	TC12406	GCACCATTCACCACAAATCA	ACCGGGTCTGAATCACAAAC	160
Extensin	TC14119	TGGCAGTCAAAATCAGCAAC	CGATTTGCCTCACAAAACAA	111
Aquaporin	TC14630	CCACATCACCATCCTCACTG	ATTGCCAAACCTCCTGTGAC	102
Histone H2B	TC16175	TGGGCATCATGAACAGTTTC	TCTGGATTTCCCTTGAGGTG	111
Glycoside hydrolase family 1 protein	TC16408	TGCAATCTTTGGTAGGGAGTC	GCTAGGCCTTGCTTCACTTAAC	146
Phosphoenolpyruvate carboxylase	TC17381	GTGGAGGCAGTATTGGTCGT	CCCTGCTCAGTAGACCGAAG	100
Galactose-1-phosphate uridylyltransferase	TC19294	AGTGAGAAAAGACGCGGTGT	CTATGCAGAAGGGGCACTGT	128
Arabinofuranosidase/xylosidase homolog	TC19595	GCTGACGTCATCTTTGGTCA	GACGCATGTCCATGTTTGTC	106
Sucrose synthase	TC19787	AGTCTCCGTGAGAGGCTTGA	TCGAACTCAGCAATGACCTG	125
MYB transcription factor MYB136	TC20058	AGCCCAGATTTTGAGGATCA	TCCAAGTGATGGGAAAAGGA	155
Beta-carotene hydroxylase	TC20154	GGACCATTCGAGCTTAACGA	ATGTAGGCCATTCCGAACAC	149
KS-type dehydrin SLTI629	TC23304	CATAGCAGTGAGGGCTGTGA	CAAAGCAGTGGGGTTACACA	157
BHLH transcription factor like protein	TC279534	TCAGTGAACGGATGAAGCTG	ACTTGACGCTGCAATGACTG	115
Non-specific lipid-transfer protein	TC326494	ACCAGGAACTGGATCCACAG	AGAGGCCAATGGATTAACGA	152

Glucan endo-1,3-beta-glucosidase precursor ((1->3)-beta- glucan endohydrolase) ((1->3)-beta-glucanase)	TC11172	ATGGAAGACTTGGCAACGAC	GCCTCTCAAAGCTCCAAGAA	122
Proline-rich protein	TC12228	GCAAGTGTTGTGCATTGCTT	TGGAAGCCAGAAGGAACTGT	160
Aquaporin PIP2-7	TC17405	GTGCTATCTGTGGCACTGGA	ATCTCAGCACCCAAAGCAGT	121
PvLEA-18	TC17584	ACCAAAGACTGGTCGAGGTG	GGCAGTGTAGGAGGTGGTGT	141
Xyloglucan endotransglucosylase/hydrolase	CV542742	TTTGACCAACCCATGAAGGT	GCATTCACTGAGGCTTCACA	153
Nodulin-26	TC9759	GGAGGCAACATCACCTTTCT	ACACCAAAGCGTTACCCACT	154
MYB transcription factor MYB133	TC10101	GCAGCAAATCCCTCACTGAT	TCACCTTCTTGCTCCCACTT	131
bZIP transcription factor bZIP68	TC12512	CTTCCAAGACCTTGCAGGAG	GGAAGCACTGCTGTGAGACA	130
Dehydrin	TC13043	GAGGTGATCGTCACCGAGTT	CCTCCTCGCTTGAAGAGCTA	133
Dehydration responsive element-binding protein 3	TC19609	TACAGACTCCGAGGCGACTT	GCCAGGCTCTGACAAATAGC	125
Extensin	CV543796	ATAAGCTCCGAATGGGGAAG	AATCGGGTCTGAATCACGAG	160
Fasciclin-like AGP 12	TC9226	ACCTGGAATCCACCAAAGTG	TCCTCGGACTTGAGTTTGGA	139
Root nodule extensin	TC13862	CCCACCCTCCTTACACTCCT	GGTGGAGGTGATGCGTAGAT	124
Extensin-like protein	TC14611	CATCCTCTTCTTTGCCCTTG	GGAACCACCTGAAGGACTTG	100
Cytochrome P450 monooxygenase CYP701A16	TC18728	GGATGCAACATGGACAAGAA	AACCTGCACACACCCTCTTC	136
MYB transcription factor MYB134	TC13287	CCGATTCCGACAAAATGAAC	GCATCAGGTGTGTTCAGCTC	136
Hydroxyproline-rich glycoprotein precursor	TC14600	GCGTAGTGTCCCTCATGGTT	TTGCTTCCGTTGTTTTCCTT	107
Protease inhibitor	TC15317	TTTCAAGGGACCATGTGTGA	GAAGCATCTACGACGGAAGC	100
Alpha-expansin	TC17940	CTCAAGATTACAGGTCAAAGAACCT	CATCTGCAAATGCTTGCTGT	158
VuP5CS protein	TC14708	GACAGTGCTGCTGTTTTCCA	AAACCCTCTACTCCCACAGGA	128

Supplemental Table S2 Up- and down-regulated transcripts in control and PEG 6000-treated root tips of bean genotype VAX 1.

TC/GB Acc. No.	UniProt ID	Anotation	database	Identity	Normalized counts (counts million^{-1})		*p*-value	R
					- PEG 6000	+ PEG 6000		
Up-regulated transcripts								
Transcription regulation								
AW705917	Q9LSH5	Similarity to NAM	GMGI.052909	24	0.00	2.30	5.0E-04	5.52
TC10101	Q0PJI6	MYB transcription factor MYB133	PHVGI.052909	26	0.20	4.60	3.4E-06	4.54
TC304010	A2Q5K3	Helix-loop-helix DNA-binding	GMGI.052909	26	0.00	1.02	3.2E-02	4.35
TC286086	A2Q1B8	Homeobox domain, ZF-HD class; ZF-HD homeobox protein Cys/His-rich dimerisation region; Homeodomain-like	GMGI.052909	26	0.20	1.53	3.0E-02	2.95
CV539143	Q6NPP4	Calmodulin-binding transcription activator 2	PHVGI.052909	26	0.40	2.81	3.1E-03	2.83
TC18148	Q2HU72	Steroid nuclear receptor, ligand-binding	PHVGI.052909	26	1.59	8.94	4.8E-07	2.50
TC299353	A5BFL4	Putative uncharacterized protein	GMGI.052909	26	0.40	2.04	2.4E-02	2.37
TC297444	Q7X8E9	Calcium-dependent protein kinase substrate protein putative	GMGI.052909	22	0.40	2.04	2.4E-02	2.37
TC304387	Q9M886	LOB domain-containing protein 41	GMGI.052909	21	1.98	9.97	3.3E-07	2.33
TC9220	O22058	Plastid RNA polymerase sigma-subunit precursor	PHVGI.052909	26	1.19	5.62	2.0E-04	2.24
TC9168	O82396	Putative bHLH transcription factor	PHVGI.052909	26	2.18	8.69	1.6E-05	2.00
CA908825	Q0WNN4	Calmodulin-binding transcription activator 2	allTIGR_Plant_2007	24	16.05	63.63	9.6E-32	1.99
TC8775	Q8W0W5	Repressor protein	PHVGI.052909	26	3.96	13.80	3.7E-07	1.80
TC317299	Q10QA8	Somatic embryogenesis related protein putative expressed	GMGI.052909	21	4.16	13.29	2.1E-06	1.68
FE709146	Q9ZSQ0	Ethylene response sensor	PHVGI.052909	25	31.90	98.39	9.6E-37	1.63
TC18023 or TC13287	Q0PJG1 or Q0PJG5	MYB transcription factor MYB156 or MYB transcription factor MYB134	PHVGI.052909	26	4.56	13.80	3.0E-06	1.60
TC14903	A4GGD7	DNA-directed RNA polymerase subunit alpha	PHVGI.052909	26	1.19	3.58	1.9E-02	1.59
TC8613	Q7F8R0	KH domain-containing protein-like	PHVGI.052909	26	2.38	6.90	1.4E-03	1.54
TC9099	Q8S8F2	LRR and BTB/POZ domain-containing protein FBL11	PHVGI.052909	26	1.19	3.32	3.2E-02	1.48
TC307119	Q2HSV7	DNA-binding SAP; Zinc finger, MIZ-type; Zinc finger, FYVE/PHD-type	GMGI.052909	23	1.19	3.32	3.2E-02	1.48
TC17231	A7LHF5	WRKY5	PHVGI.052909	26	1.19	3.32	3.2E-02	1.48
TC279534	Q0WL61	BHLH transcription factor like protein	GMGI.052909	26	2.77	7.16	2.8E-03	1.37
CO985878	Q10PC4	Zinc finger, C2H2 type family protein, expressed	GMGI.052909	22	1.98	5.11	1.2E-02	1.37
TC9770	Q01IQ1	H0115B09.1 protein	PHVGI.052909	26	4.56	11.76	1.3E-04	1.37
TC18844	A2Q3L5	Zinc finger, CCCH-type	PHVGI.052909	26	18.03	46.51	2.1E-14	1.37
CV535841	Q9ZW96	LOB domain-containing protein 40	PHVGI.052909	22	2.38	5.88	9.1E-03	1.31
TC10776	Q9FMT4	Uncharacterized protein At5g14170	PHVGI.052909	26	3.17	7.67	3.4E-03	1.27
TC15853	Q7XJS4	At2g17410 protein	PHVGI.052909	26	2.58	6.13	9.9E-03	1.25
CV535953	Q2HTN6	Helix-loop-helix DNA-binding	PHVGI.052909	26	2.18	4.86	3.1E-02	1.16
TC18417	O82199	Putative CCCH-type zinc finger protein	PHVGI.052909	26	2.18	4.86	3.1E-02	1.16

CV538765	Q2HVE6	Zinc finger C2H2-type	PHVGI.052909	26	3.96	8.69	4.5E-03	1.13
TC20058	Q0PJI5	MYB transcription factor MYB136	PHVGI.052909	26	2.18	4.60	4.8E-02	1.08
TC13404	Q0PJH7	MYB transcription factor MYB177	PHVGI.052909	25	9.71	20.44	2.9E-05	1.07
TC12009	Q9LXT3	Transcriptional coactivator-like protein	PHVGI.052909	26	150.77	311.77	1.2E-57	1.05
TC19912	Q9ZNU9	Zinc finger A20 and AN1 domain-containing stress-associated protein 3	PHVGI.052909	26	212.59	435.97	2.1E-78	1.04
TC15183	Q5MJ54	AT-rich element binding factor 2	PHVGI.052909	26	3.17	6.39	2.7E-02	1.01
Signal transduction								
CV539969	Q2HRH3	Gibberellin regulated protein	PHVGI.052909	26	0.00	2.30	5.0E-04	5.52
TC318591	Q9ZQX6	Ethylene overproducer 1-like protein 1	GMGI.052909	24	0.00	1.28	1.4E-02	4.68
TC294213	Q42384	PP1/PP2A phosphatases pleiotropic regulator PRL1	GMGI.052909	24	0.00	1.02	3.2E-02	4.35
TC9591	Q677H6	ADP-ribosylation factor	PHVGI.052909	23	0.20	2.30	3.3E-03	3.54
TC9424	O64737	Hookless1-like protein	PHVGI.052909	26	0.59	3.58	1.4E-03	2.59
TC9180	Q39845	Small GTP-binding protein	PHVGI.052909	26	25.76	133.14	1.6E-80	2.37
TC10971	O64511-2	Isoform 2 of O64511	PHVGI.052909	26	0.40	2.04	2.4E-02	2.37
TC9735	Q8H6T7	Calmodulin-binding protein 60-D	PHVGI.052909	26	37.45	171.48	6.5E-94	2.20
TC293669	O64737	Hookless1-like protein	GMGI.052909	26	0.79	3.32	7.0E-03	2.07
TC17728	Q93YA8	Calcium binding protein	PHVGI.052909	26	6.14	15.84	8.5E-06	1.37
TC13805	O81059	Putative calmodulin	PHVGI.052909	26	1.39	3.58	3.6E-02	1.37
TC10201	Q9MAH1	TPR repeat-containing thioredoxin TTL1	PHVGI.052909	26	19.42	39.87	1.4E-08	1.04
Transport								
DT750927	Q94AA1-2	Isoform 2 of Q94AA1	allTIGR_Plant_2009	21	0.00	2.04	1.2E-03	5.35
TC26582	Q9M206	Transport protein subunit-like	PHVGI.052909	24	0.00	1.53	6.1E-03	4.94
TC12737	Q8LEF6	Non-intrinsic ABC protein 14 chloroplast precursor	PHVGI.052909	26	0.00	1.28	1.4E-02	4.68
TC25238	O04834	GTP-binding protein SAR1A	PHVGI.052909	24	0.00	1.28	1.4E-02	4.68
TC300789	Q84ND6	Cation diffusion facilitator 8	GMGI.052909	24	0.00	1.28	1.4E-02	4.68
TC14207	A4GG90	ATP synthase subunit beta	PHVGI.052909	25	0.20	1.79	1.5E-02	3.17
TC9592	Q9FG39	Ankyrin-like protein	PHVGI.052909	22	0.20	1.53	3.0E-02	2.95
TC28658	Q2PF04	Putative transporter-like protein	PHVGI.052909	24	0.20	1.53	3.0E-02	2.95
TC9884	A6Y950	Vacuolar H+-ATPase B subunit	PHVGI.052909	26	0.40	2.56	6.2E-03	2.69
TC14630	O81186	Aquaporin	PHVGI.052909	26	0.40	2.04	2.4E-02	2.37
TC12593	A5C3N9	Putative uncharacterized protein	PHVGI.052909	26	0.99	5.11	2.5E-04	2.37
TC19524	Q5W274	Pleiotropic drug resistance protein 3	PHVGI.052909	26	1.19	5.62	2.0E-04	2.24
CA911708	Q93YU5	Probable exocyst complex component 4	allTIGR_Plant_2007	26	16.05	71.04	7.8E-39	2.15
TC19957	P53393	Low affinity sulfate transporter 3	PHVGI.052909	26	0.59	2.30	3.2E-02	1.95
TC9631	Q39822	Pip1 protein	PHVGI.052909	26	209.02	726.53	8.9E-300	1.80
TC11810	Q39436	SIEP1L protein precursor	PHVGI.052909	26	6.54	19.17	7.0E-08	1.55
TC17437	A3RLB0	Plastid phosphate translocator	PHVGI.052909	26	15.85	43.19	1.5E-14	1.45
TC13136	Q5QMA9	Amino acid transporter-like protein	PHVGI.052909	26	9.31	24.79	1.1E-08	1.41

CV541023	Q9SIT6	ABC transporter G family member 5	PHVGI.052909	26	13.08	34.50	2.1E-11	1.40
TC14787	A9PJK2	Putative uncharacterized protein	PHVGI.052909	26	91.73	237.41	3.2E-67	1.37
TC16070	A3FA63	Aquaporin PIP1;1	PHVGI.052909	25	7.13	18.40	1.6E-06	1.37
FD787951	A7X2N3	Putative sulfate transporter	PHVGI.052909	26	1.78	4.60	1.7E-02	1.37
TC9391	Q9SH30	Putative copper-transporting ATPase 3	PHVGI.052909	26	10.30	26.07	1.8E-08	1.34
CV539606	Q9LH74	Gb|AAD30575.1	PHVGI.052909	26	19.02	47.28	8.1E-14	1.31
TC11479	Q7XJQ3	Putative peptide/amino acid transporter	PHVGI.052909	26	1.78	4.34	2.7E-02	1.28
TC112927		Biopterin transport-related protein BT1	MTGI.071708	21	1.78	4.34	2.7E-02	1.28
TC17827	O64455	Ca2+/H+ exchanger	PHVGI.052909	26	27.94	66.44	1.6E-17	1.25
GO355339	A9YTW6	Major intrinsic protein NIP5;1	PHVGI.052909	22	4.95	11.24	8.2E-04	1.18
TC16055	Q6S9Z3	Allantoin permease	PCGI.052909	26	2.18	4.60	4.8E-02	1.08
TC12483	A2Q3F3	Transport protein particle (TRAPP) component, Bet3	PHVGI.052909	26	13.27	27.86	1.2E-06	1.07
TC277893	Q6DNG7	Acyl CoA:diacylglycerol acyltransferase	GMGI.052909	26	4.36	8.94	7.3E-03	1.04
TC10547	Q39852	Putative ATP synthase subunit	PHVGI.052909	26	3.37	6.90	1.9E-02	1.03
Stress/defense								
TC50881	O82514	Adenylate kinase 1	LJGI.052909	26	0.00	3.07	4.2E-05	5.94
TC292046	Q39804	BiP isoform B	GMGI.052909	26	0.00	2.56	2.2E-04	5.68
TC16118	Q0PGJ6	Aldo-keto reductase	PHVGI.052909	26	0.00	2.30	5.0E-04	5.52
TC129931	Q8VWQ1	Dehydration-induced protein RD22-like protein	allTIGR_Plant_2009	22	0.00	1.53	6.1E-03	4.94
TC13823	Q76FR9	12-oxophytodienoic acid 10, 11-reductase	PHVGI.052909	26	0.00	1.28	1.4E-02	4.68
DV865383		Phosphoribulokinase, chloroplast precursor	allTIGR_Plant_2007	22	0.00	1.28	1.4E-02	4.68
FE898880	A2Q2Z0	SAM (And some other nucleotide) binding motif	PHVGI.052909	26	0.00	1.28	1.4E-02	4.68
FG232409	Q9LUV2	Putative protein Pop3	PHVGI.052909	26	0.00	1.02	3.2E-02	4.35
TC281883	Q8LEH1	Ripening-related protein-like	GMGI.052909	25	0.00	1.02	3.2E-02	4.35
FG233588	Q75NI2	Type 1 metallothionein	PHVGI.052909	26	1.19	14.06	3.0E-14	3.56
TC12563	Q9FNV7	Auxin-repressed protein	PHVGI.052909	26	0.59	4.60	9.0E-05	2.95
TC17061	Q9FQD6	Glutathione S-transferase GST 22	PHVGI.052909	26	1.39	10.48	2.7E-09	2.92
TC335266	Q9SKP5	Expressed protein	GMGI.052909	25	0.40	2.56	6.2E-03	2.69
TC12962	Q9FQE9	Glutathione S-transferase GST 9	PHVGI.052909	26	0.79	4.86	1.6E-04	2.62
TC17840	A3QRM3	Senescence-associated nodulin 1A	PHVGI.052909	26	0.40	2.04	2.4E-02	2.37
TC14708	Q9AYM4	VuP5CS protein	PHVGI.052909	26	0.59	3.07	5.0E-03	2.37
TC24424	A0FK57	Gibberellin 2-oxidase 2	allTIGR_Plant_2009	22	4.56	23.00	6.0E-15	2.34
TC19423	Q02921	Early nodulin 93	PCGI.052909	23	40.02	186.55	1.7E-103	2.22
TC13350	Q9MB25	S1-1 protein	PHVGI.052909	26	0.40	1.79	4.5E-02	2.17
TC17529	Q9SWS4	Ripening related protein	PHVGI.052909	22	0.40	1.79	4.5E-02	2.17
TC10571	A2Q6G3	TIR; AAA ATPase	PHVGI.052909	26	0.40	1.79	4.5E-02	2.17
TC9828	Q6UK15	Al-induced protein	PHVGI.052909	26	60.23	271.14	2.6E-145	2.17
TC15361	A8IXV9	Dehydration-responsive protein-related	PHVGI.052909	26	7.53	33.22	6.1E-19	2.14

TC11842	Q2HTH4	PAP fibrillin	PHVGI.052909	26	1.19	5.11	6.6E-04	2.10
TC9246	Q6U1L7	Bax inhibitor	PHVGI.052909	26	19.42	81.78	1.4E-42	2.07
TC15517	Q3IA99	Disease resistance protein	PHVGI.052909	21	1.39	5.62	5.0E-04	2.02
TC15917	Q9FPJ7	At2g27680	PHVGI.052909	26	0.59	2.30	3.2E-02	1.95
EH791107	Q9ZVC6	At2g27140	PHVGI.052909		11.69	42.42	6.0E-20	1.86
CV542752	Q8S8Z5	Syringolide-induced protein B13-1-1	PHVGI.052909	26	0.79	2.81	2.3E-02	1.83
TC16661	Q9SBS1	Ran GTPase activating protein	PHVGI.052909	26	0.79	2.81	2.3E-02	1.83
TC11510	Q93YW0	Protein EXECUTER 1, chloroplast precursor	PHVGI.052909	26	5.75	19.93	1.0E-09	1.79
TC18065	P93169	Early light-induced protein	PHVGI.052909	26	32.29	109.12	3.6E-45	1.76
FD793188	Q6K840	Putative quinone oxidoreductase	PHVGI.052909	26	16.84	47.02	3.1E-16	1.48
FG228988	A5BSD9	Putative uncharacterized protein	PHVGI.052909	26	40.22	109.63	1.5E-34	1.45
FG233023	Q7NFL3	Chaperone protein	PHVGI.052909	26	9.71	25.81	5.6E-09	1.41
TC17584	O24439	PvLEA-18	PHVGI.052909	26	287.87	760.27	6.6E-218	1.40
TC9660	Q308N9	Salt-tolerance protein	PHVGI.052909	26	2.18	5.62	8.3E-03	1.37
GE129592	Q9ZQ48	Putative D-amino acid dehydrogenase	GMGI.052909	26	1.39	3.58	3.6E-02	1.37
TC18146	O82444	Peroxisomal targeting sequence 1 receptor	PHVGI.052909	26	11.89	30.41	2.3E-20	1.36
TC15692	Q75NH9	Type 2 metallothionein	PHVGI.052909	26	120.66	308.45	4.3E-85	1.35
TC16338	Q07CZ3	Glyceraldehyde-3-dehydrogenase C subunit	PHVGI.052909	26	37.84	96.09	2.1E-27	1.34
TC12488	Q9LJ66	Oxylase-like protein	PHVGI.052909		12.28	31.18	6.8E-10	1.34
TC14099	P05478	18.5 kDa class I heat shock protein	PHVGI.052909	26	9.11	23.00	1.3E-07	1.34
TC140	Q8H1S6	Putative spliceosomal protein	PCGI.052909	26	1.59	3.83	3.9E-02	1.27
CV529754	P92947	Monodehydroascorbate reductase chloroplast precursor	PHVGI.052909	26	61.22	143.88	2.6E-35	1.23
TC14765	A5C6J1	Putative uncharacterized protein	PHVGI.052909	26	2.18	5.11	2.0E-02	1.23
TC15904	Q9M338	Reductase-like protein	PHVGI.052909	26	9.71	22.49	1.4E-06	1.21
TC19667	Q6Z4A1	Putative PS60	PCGI.052909	22	4.36	9.97	1.5E-03	1.19
TC17411	Q84QD7	Avr9/Cf-9 rapidly elicited protein 276	PHVGI.052909	26	10.70	23.77	1.9E-06	1.15
TC13986	P42744	NEDD8-activating enzyme E1 regulatory subunit	PHVGI.052909	26	11.29	24.53	2.2E-06	1.12
TC286579	Q43872	Peroxidase 64 precursor	GMGI.052909	23	13.67	29.13	4.3E-07	1.09
TC16700	Q949S4	Putative uncharacterized protein At1g14340	PHVGI.052909	26	2.77	5.88	2.4E-02	1.08
TC9391	Q8LAS8	S-formylglutathione hydrolase	PCGI.052909	26	2.18	4.60	4.8E-02	1.08
TC17091	Q9LUV2	Putative protein Pop3	PHVGI.052909	26	10.30	21.72	1.6E-05	1.08
TC17220	A5BBL4	Putative uncharacterized protein	PHVGI.052909	26	2.58	5.37	3.5E-02	1.06
Carbonhydrate metabolism								
TC8875	Q5W1H9	Myo-inositol 1-phosphate synthase	PCGI.052909	22	0.00	5.62	1.1E-08	6.81
TC9241	Q9STQ7	Pyrophosphate-dependent phosphofructo-1-kinase	PHVGI.052909	26	0.00	1.53	6.1E-03	4.94
TC11539	Q8W3P8	ABA-glucosyltransferase	PHVGI.052909	26	0.00	1.02	3.2E-02	4.35
TC10042	UPI0000162F42	inositol monophosphatase family protein	PHVGI.052909	26	0.00	1.02	3.2E-02	4.35
TC11609	O24301	Sucrose synthase 2	PHVGI.052909	26	1.59	20.44	1.1E-20	3.69

TC16748	A9PF71	Putative uncharacterized protein	PHVGI.052909	26	2.18	14.31	2.0E-11	2.72
FE707662	Q2MGQ0	Carbohydrate kinase, Pfk	PHVGI.052909	26	1.19	6.13	5.7E-05	2.37
TC15107	Q9SAC6	Alpha-glucan water dikinase 1 chloroplast precursor	PHVGI.052909	26	9.51	41.91	1.8E-23	2.14
TC8689	A8VYM8	Cytosolic fructose-1,6-bisphosphatase	PHVGI.052909	26	5.55	23.26	3.8E-13	2.07
TC17381	Q6Q2Z9	Phosphoenolpyruvate carboxylase	PHVGI.052909	26	2.77	9.20	5.6E-05	1.73
NP7938786	Q9XIS6	granule-bound starch synthase I	PHVGI.052909	26	1.98	5.37	7.4E-03	1.44
TC17943	Q9ZQZ7	Putative glycosylation enzyme	PHVGI.052909	26	2.18	5.88	5.2E-03	1.43
TC9623	Q8L9F5	Putative dTDP-glucose 4-6-dehydratase	PHVGI.052909	26	379.21	1003.30	1.2E-288	1.40
TC11031	O22111	6-phosphogluconate dehydrogenase, decarboxylating	PHVGI.052909	26	8.12	18.14	2.8E-05	1.16
TC19787	Q8GTA3	Sucrose synthase	PHVGI.052909	26	254.39	542.54	8.2E-106	1.09
TC15968	A8E1U7	Inositol 1,3,4-trisphosphate 5/6-kinase	PHVGI.052909	26	8.72	18.40	7.1E-05	1.08
TC9512	Q94K13	Putative D-ribulose-5-phosphate 3-epimerase	PHVGI.052909	26	37.84	78.45	8.2E-16	1.05
Energy metabolism								
TC17130	A3AYZ5	Putative uncharacterized protein	PHVGI.052909	25	0.00	2.30	5.0E-04	5.52
TC8979	P81760	Thylakoid lumenal 17.4 kDa protein chloroplast precursor	PHVGI.052909	26	0.00	1.28	1.4E-02	4.68
TC19958	O22769	NADH-ubiquinone oxidoreductase 24 kDa subunit mitochondrial precursor	PCGI.052909	25	0.00	1.28	1.4E-02	4.68
TC14290	Q9XFX1	Cytochrome P450	PHVGI.052909	26	0.00	1.02	3.2E-02	4.35
TC15397	Q9MBA1	Chlorophyllide a oxygenase chloroplast precursor	PHVGI.052909	26	0.00	1.02	3.2E-02	4.35
TC13074	Q8LGA9	Putative uncharacterized protein	PHVGI.052909	24	1.19	10.99	1.7E-10	3.21
TC13003	Q9SE03	Copper chaperone homolog CCH	PHVGI.052909	26	0.40	2.56	6.2E-03	2.69
TC14517	P46269	Cytochrome b-c1 complex subunit 8	PHVGI.052909	25	0.40	2.04	2.4E-02	2.37
TC11944	Q03943	Membrane-associated 30 kDa protein chloroplast precursor	PHVGI.052909	26	0.59	2.56	1.7E-02	2.10
CA901201	Q2HV82	E-class P450, group I	allTIGR_Plant_2007	26	9.51	40.38	5.5E-22	2.09
TC17629	Q9MUE2	S-adenosyl-L-methionine Mg-protoporphyrin IX methyltranserase	PHVGI.052909	26	0.59	2.30	3.2E-02	1.95
FE690386	Q5CD58	NADH-ubiquinone oxidoreductase chain 3	PHVGI.052909	26	21.60	80.50	2.0E-37	1.90
TC19033	Q1ELT8	Red chlorophyll catabolite reductase	PHVGI.052909	22	1.78	6.13	8.1E-04	1.78
TC16664	A9PIV1	Putative uncharacterized protein	PHVGI.052909	22	2.18	6.39	2.0E-03	1.55
TC9078	P51134	Cytochrome b-c1 complex subunit Rieske-4 mitochondrial precursor	PHVGI.052909	26	6.74	19.68	5.1E-08	1.55
FK009542	Q10DW5	Cytochrome b561 family protein expressed	GMGI.052909	26	1.39	3.58	3.6E-02	1.37
FE703827	Q8GUS1	NADPH:P450 reductase	PHVGI.052909	26	7.93	19.42	2.3E-06	1.29
TC19643	O65808	Magnesium chelatase subunit	PHVGI.052909	26	2.38	5.62	1.4E-02	1.24
FE696369	Q07A02	Sulfoquinovosyldiacylglycerol synthase type 2	PHVGI.052909	26	1.98	4.60	2.9E-02	1.22
TC16349	Q9XI73	F7A19.23 protein	PHVGI.052909	26	1.78	4.09	4.2E-02	1.20
CV532732	P14226	Oxygen-evolving enhancer protein 1, chloroplast precursor	PHVGI.052909	26	2.58	5.88	1.5E-02	1.19
TC17971	Q9SKE5	Putative photomorphogenesis repressor protein	PHVGI.052909	26	2.38	5.37	2.2E-02	1.17
TC19401	Q0PWS5	Chloroplast pigment-binding protein CP26	PHVGI.052909	26	4.56	9.71	3.6E-03	1.09
TC344013	P49161	Apocytochrome f precursor	GMGI.052909	26	5.94	12.01	2.3E-03	1.01
Amino acid metabolism								

TC12876	Q9SNY8	Branched-chain amino acid aminotransferase	allTIGR_Plant_2009	21	0.00	2.04	1.2E-03	5.35
TC22519	A9PL11	Plastid serine hydroxymethyltransferase	PHVGI.052909	24	0.00	1.53	6.1E-03	4.94
TA4282_3885	Q8W2G3	Alanine:glyoxylate aminotransferase-like protein	allTIGR_Plant_2007	25	0.00	1.53	6.1E-03	4.94
CB542177	O49383	Putative uncharacterized protein F10N7.100	PHVGI.052909	26	0.00	1.02	3.2E-02	4.35
TC9537	Q9FQE3	Glutathione S-transferase GST 15	PHVGI.052909	26	11.69	57.50	1.8E-34	2.30
TC13205	A2Q3J8	Glutamine amidotransferase, class I, active site	PHVGI.052909	26	21.00	89.70	3.9E-47	2.09
TC8497	A7XTY5	Dual-targeted glutathione reductase	PHVGI.052909	25	9.11	38.08	1.5E-20	2.06
TC102194	Q75HP7	Serine hydroxymethyltransferase	allTIGR_Plant_2009	21	0.59	2.30	3.2E-02	1.95
TC8658	Q4ZJF7	Tyrosine aminotransferase	PHVGI.052909	26	1.39	5.11	1.5E-03	1.88
TC19010	Q8L7P0	Phosphoserine aminotransferase	PHVGI.052909	26	178.11	568.35	1.7E-212	1.67
TC10562	Q9SM55	Asparagine synthetase	PHVGI.052909	26	9.71	25.81	5.6E-09	1.41
TC9912	A5Z1N7	4-hydroxyphenylpyruvate dioxygenase	PHVGI.052909	26	15.45	37.06	1.5E-10	1.26
Lipid metabolism								
CV542382	A9XNQ0	Protease inhibitor/seed storage/lipid transfer protein (LTP) family protein	PHVGI.052909	26	0.59	29.90	3.7E-38	5.65
EV194378	Q3ED51	Uncharacterized protein At1g28580.2	allTIGR_Plant_2009	21	0.00	1.53	6.1E-03	4.94
CV534689	Q71LW1	Phospholipase A1	PHVGI.052909	26	3.96	31.18	1.7E-25	2.98
TC16316	Q6PV95	Beta-carotene hydroxylase	PHVGI.052909	26	0.20	1.53	3.0E-02	2.95
TC13448	A9P5P3	Acyl ACP-thioesterase	PHVGI.052909	26	0.79	3.07	1.3E-02	1.95
TC17109	Q2HT24	Phosphatidate cytidylyltransferase	PHVGI.052909	26	30.71	109.38	6.0E-48	1.83
TC20154 or TC8507	Q6PV95 or Q8HQQ0	Beta-carotene hydroxylase or Aspartate aminotransferase	PHVGI.052909	26	9.71	29.64	5.3E-12	1.61
TC16022	Q9LTI7	Oxysterol-binding protein	PHVGI.052909	26	27.34	68.74	9.3E-20	1.33
TC14891	A1YNA0	Acyl-[acyl-carrier protein] desaturase	PHVGI.052909	26	24.57	57.75	4.0E-15	1.23
Secondary metabolism								
TC10519	P37115	Trans-cinnamate 4-monooxygenase	PCGI.052909	26	0.00	6.90	1.7E-10	7.11
TC15260	Q2YHM9	Caffeoyl-CoA O-methyltransferase	PHVGI.052909	22	2.97	6.90	7.5E-03	1.22
TC19405	Q0EDG6	Flavonol synthase	PHVGI.052909	26	6.74	15.33	8.9E-05	1.19
TC8645	O48602	2'-hydroxydihydrodaidzein reductase	PHVGI.052909	26	538.89	1098.36	5.5E-172	1.03
Other metabolisms								
TC17265	Q4JR83	Pyridoxal kinase	PHVGI.052909	26	0.99	3.32	1.6E-02	1.75
TC11968	A5AD21	Putative uncharacterized protein	PHVGI.052909	26	4.56	12.01	8.1E-05	1.40
TC9421	Q6EJC9	1-deoxy-D-xylulose 5-phosphate synthase	PHVGI.052909	26	10.70	28.11	1.7E-09	1.39
TC8800	Q9FEP0	LYTB-like protein precursor	PHVGI.052909	26	17.24	42.17	3.5E-12	1.29
TC13462	Q9LU48	Acid phosphatase	PHVGI.052909	26	14.07	33.22	2.2E-09	1.24
TC15665	A5HK00	O-methyltransferase	PHVGI.052909	26	2.18	4.86	3.1E-02	1.16
EC997013	Q9M442	Putative imbibition protein	PHVGI.052909	26	41.21	85.35	4.9E-17	1.05
Cell wall synthesis, organization								
TC14727	A2V885	Hydroxyproline-rich glycoprotein like protein	PHVGI.052909	22	0.00	1.28	1.4E-02	4.68
CX048769	Q9LEC9	Alpha-glucosidase	allTIGR_Plant_2009	22	0.00	1.28	1.4E-02	4.68

CV543261	A9YWR1	Hydroxyproline-rich glycoprotein	PHVGI.052909	26	0.40	4.09	9.0E-05	3.37
TC696	Q96558	UDP-glucose 6-dehydrogenase	PCGI.052909	26	0.20	1.53	3.0E-02	2.95
TC326558	Q5IFH7	Triterpene UDP-glucosyl transferase UGT71G1	GMGI.052909	26	0.99	5.62	7.0E-05	2.50
CN848234	Q658E4	Putative pectin-glucuronyltransferase	allTIGR_Plant_2007	21	0.40	2.04	2.4E-02	2.37
CB542664	Q1M0P2	UDP-glucuronic acid decarboxylase 1	allTIGR_Plant_2007	25	15.45	69.00	5.0E-38	2.16
FE695949	Q9XEG1	Putative callose synthase catalytic subunit	PHVGI.052909	26	4.36	17.38	9.0E-10	2.00
CX709760	Q9C617	Wall-associated kinase putative	GMGI.052909	22	1.78	5.88	1.4E-03	1.72
EV277253	Q8H021	Germin-like protein 3-1	GMGI.052909	24	4.75	15.33	3.0E-07	1.69
TC17182	Q1EP15	Glycoside hydrolase family 17 protein	PHVGI.052909	26	1.78	4.86	1.1E-02	1.45
TC298585	A0MMD6	Xyloglucan endotransglycosylase 1	GMGI.052909	22	1.78	4.60	1.7E-02	1.37
TC19966	A2TEI8	Xyloglucan endotransglycosylase/hydrolase XTH-25	PHVGI.052909	26	165.43	404.28	7.2E-103	1.29
TC14119	O04216	Extensin	PHVGI.052909	26	121.85	284.68	2.0E-67	1.22
TC302078	Q2A9T1	Pectinesterase family protein	GMGI.052909	22	2.38	5.11	3.3E-02	1.10
TC12264	Q9M373	Arabinogalactan peptide 20 precursor	PHVGI.052909	26	8.12	16.61	2.7E-04	1.03
TC19595	A1IIC0	Arabinofuranosidase/xylosidase homolog	PHVGI.052909	26	74.30	151.29	6.5E-28	1.03
GD534191	A0ZNK0	Pectin methylesterase 2	PCGI.052909	22	4.16	8.43	1.0E-02	1.02
Replication and Repair								
TC19910	Q9M0V3	DNA damage-binding protein 1a	PHVGI.052909	26	0.20	2.56	1.6E-03	3.69
TC17173	Q84ND9	PolI-like DNA polymerase	PHVGI.052909	26	3.37	18.40	7.1E-13	2.45
TC302358	A2X647	Putative uncharacterized protein	GMGI.052909	21	0.59	2.56	1.7E-02	2.10
TC298127	A6N174	Nucleoside-triphosphatase/ nucleotide binding protein	GMGI.052909	26	18.62	39.61	4.0E-09	1.09
Cytoskeleton								
TC31998	P49231	Profilin-1	PHVGI.052909	22	0.00	1.53	6.1E-03	4.94
FE694967	Q9FJX6	Formin-like protein 6 precursor	PHVGI.052909	26	3.57	7.92	6.0E-03	1.15
Protein translation,processing, and degradation								
TC31294	Q3HRW1	60S ribosomal protein L13a-like protein	allTIGR_Plant_2009	22	0.00	4.86	1.3E-07	6.60
DR453381	Q7X9K1	Ribosomal Pr 117	allTIGR_Plant_2009	26	0.00	2.04	1.2E-03	5.35
TC19188	Q0WM96	Ubiquitin-conjugating enzyme E2-like protein	PHVGI.052909	24	0.00	1.79	2.6E-03	5.16
BF009941	Q8W4H7	T6D22.2	allTIGR_Plant_2007	25	0.00	1.79	2.6E-03	5.16
TC9088	Q96499	60S ribosomal protein L44	PCGI.052909	21	0.20	6.39	1.4E-08	5.01
TC9038	Q8S8Z6	Syringolide-induced protein 13-1-1	PHVGI.052909	26	0.00	1.53	6.1E-03	4.94
TC8319	Q05462	60S ribosomal protein L27	PCGI.052909	25	0.00	1.53	6.1E-03	4.94
TC6278	Q3HVK7	Glycoprotein-like protein	PCGI.052909	22	0.00	1.28	1.4E-02	4.68
TC17076	A7P1Z0	Ubiquitin carrier protein	PHVGI.052909	25	0.00	1.28	1.4E-02	4.68
TC16355	Q9SWS9	Ribosomal protein S26	PCGI.052909	26	0.00	1.28	1.4E-02	4.68
TC22892	Q9FY64	40S ribosomal protein S15-4	PHVGI.052909	24	0.00	1.28	1.4E-02	4.68
TC30812	A5AWN5	Putative uncharacterized protein	PHVGI.052909	24	0.00	1.28	1.4E-02	4.68
TC8296	Q9ZSP3	Chaperone GrpE type 2	PCGI.052909	24	0.00	1.02	3.2E-02	4.35

177

TC11869	A8MQW0	Uncharacterized protein At2g22990.5	PHVGI.052909	22	0.00	1.02	3.2E-02	4.35
TC24489	Q9M5L1	40S ribosomal protein S16	PHVGI.052909	25	0.00	1.02	3.2E-02	4.35
FE684646	Q2R068	Peptide chain release factor 1 putative expressed	PHVGI.052909	26	0.00	1.02	3.2E-02	4.35
TC11098	Q9LF41	Ubiquitin-fusion degradation protein-like	PHVGI.052909	25	0.20	2.81	7.5E-04	3.83
TC10622	Q6RW44	Ly200 protein	PCGI.052909	21	0.40	5.37	2.3E-06	3.76
TC161	O65819	Histone H2B.3	PCGI.052909	26	0.20	2.30	3.3E-03	3.54
TC15421	Q6SPR2	Ribosomal protein L37	PHVGI.052909	25	0.20	2.04	7.0E-03	3.37
TC93858	Q9AT34	40S ribosomal protein S15a	allTIGR_Plant_2009	23	0.59	5.88	2.7E-06	3.31
TC288355	Q9SII9	Putative ubiquitin-like protein	GMGI.052909	22	25.56	177.10	2.0E-128	2.79
TC27358	Q6SPR2	Ribosomal protein L37	PHVGI.052909	23	0.59	3.58	1.4E-03	2.59
TC10204	O48879	Ribosomal protein L22	PHVGI.052909	26	14.86	86.63	1.6E-57	2.54
TC18675	Q8H6S8	Translation initiation factor	PHVGI.052909	26	0.99	5.62	7.0E-05	2.50
TC14888	Q41440	Mitochondrial processing peptidase	PHVGI.052909	22	1.78	8.94	1.4E-06	2.33
TC40175	A7Q1X4	Ubiquitin carboxyl-terminal hydrolase	allTIGR_Plant_2009	21	15.65	76.15	9.6E-45	2.28
GD541242	O49160	Eukaryotic translation initiation factor 3 subunit C	PCGI.052909	26	0.79	3.83	2.1E-03	2.27
CB541883	P60040	60S ribosomal protein L7-2	allTIGR_Plant_2007	26	1.19	5.37	3.6E-04	2.17
TC10895	O80360	50S ribosomal protein L3, chloroplast precursor	PHVGI.052909	26	1.59	7.16	3.6E-05	2.17
TC17214		Chloroplast tRNA-Ala, tRNA-Ile, 16S rRNA, tRNA-Val, rps12, rps7, ndhB genes, partial	PHVGI.052909	26	0.59	2.56	1.7E-02	2.10
FE705165	Q56X76	DEAD-box ATP-dependent RNA helicase 39	PHVGI.052909	26	0.59	2.56	1.7E-02	2.10
TC9077	P34811	Elongation factor G, chloroplast precursor	PHVGI.052909	26	0.59	2.56	1.7E-02	2.10
TC12423	Q65XC5	Putative uncharacterized protein OJ1187_E11.14	PCGI.052909	22	7.92	32.97	6.4E-18	2.06
TC12699	A8MS83	Uncharacterized protein At3g55280.3	PHVGI.052909	26	67.96	240.47	1.5E-102	1.82
FD789315	A6N048	60S ribosomal protein l2	PHVGI.052909	25	12.68	42.93	8.7E-19	1.76
CV541748	Q9SPL2	E3 ubiquitin-protein ligase CIP8	PHVGI.052909	26	12.09	38.84	3.4E-16	1.68
TC9217	Q4A197	Histone H1 subtype 7	PHVGI.052909	26	2.38	7.16	8.4E-04	1.59
TC15003	Q9FSZ9	Putative extracellular dermal glycoprotein	PHVGI.052909	26	3.57	10.22	1.1E-04	1.52
TC17791	Q6SPR3	Ribosomal protein S6	PHVGI.052909	26	2.18	6.13	3.2E-03	1.49
TC13036	A7KWH0	U-box domain containing protein	PHVGI.052909	26	1.19	3.32	3.2E-02	1.48
TC11528	Q9M5P4	Chloroplastic group IIB intron splicing facilitator CRS2 chloroplast precursor	PHVGI.052909	26	1.78	4.86	1.1E-02	1.45
TC11093	Q9FV50	Methionine aminopeptidase 1D, chloroplast/mitochondrial precursor	PHVGI.052909	22	6.34	16.87	2.5E-06	1.41
TC8275	P25803	Vignain precursor	PHVGI.052909	26	5.35	14.06	2.1E-05	1.39
TC13235	A9PBI3	Putative uncharacterized protein	PHVGI.052909	26	4.56	11.76	1.3E-04	1.37
TC8436	Q8GTE3	Ribosomal protein S3a	PHVGI.052909	26	30.91	77.94	2.7E-22	1.33
TC18311	Q9LHS4	RAN binding protein 16-like	PHVGI.052909	26	10.90	27.34	1.0E-08	1.33
TC18084	Q67XZ5	Putative ribosome recycling factor	PHVGI.052909	26	3.57	8.94	1.1E-03	1.33
TC12110	Q5IH79	HAT-like transposase	PHVGI.052909	26	18.43	45.74	2.1E-13	1.31
TC2464		18S ribosomal RNA gene	PCGI.052909	26	1.98	4.86	1.9E-02	1.29
TC20478	A2Q664	Ribosomal protein S6	PCGI.052909	22	1.78	4.34	2.7E-02	1.28

TC8305	Q9FXD5	F12A21.16	PHVGI.052909	26	2.58	6.13	9.9E-03	1.25
TC15423	Q8GY84	DEAD-box ATP-dependent RNA helicase 10	PHVGI.052909	26	32.69	75.64	8.1E-19	1.21
TC14389	Q38HS8	Ribosomal protein L23 family protein	PHVGI.052909	26	37.45	82.03	2.4E-18	1.13
FE897027	A2YFN5	Putative uncharacterized protein	PHVGI.052909	26	3.17	6.90	1.2E-02	1.12
TC11722	Q8L7B2	Serine carboxypeptidase-like 20 precursor	PHVGI.052909	26	31.90	66.19	1.3E-13	1.05
Nucleotide Metabolism								
TC18425	Q9STG6	DUTP pyrophosphatase-like protein	PHVGI.052909	26	26.94	87.65	4.4E-35	1.70
CV541552	A8MQM6	Uncharacterized protein At1g06190.2	PHVGI.052909	26	4.75	11.24	5.1E-04	1.24
TC119551	P34788	40S ribosomal protein S18	MTGI.071708	26	9.31	18.91	1.1E-04	1.02
Protein posttranslational modification								
TC16107	Q67YK2	Putative uncharacterized protein At1g20650	PHVGI.052909	26	0.00	1.02	3.2E-02	4.35
FE689283 TC11639	Q8GSL0	Phosphoenolpyruvate carboxylase kinase	PHVGI.052909	26	0.20	3.58	7.6E-05	4.17
TC11726	Q9FG32	Protein phosphatase 2C-like	PHVGI.052909	26	0.20	1.53	3.0E-02	2.95
TC13826	Q42806	Pyruvate kinase cytosolic isozyme	PHVGI.052909	22	0.79	5.37	4.2E-05	2.76
TC10417	P49599	Protein phosphatase 2C PPH1	PHVGI.052909	26	0.59	3.32	2.6E-03	2.48
TC24027	Q93X44	Protein tyrosine phosphatase	PHVGI.052909	24	2.97	12.01	3.1E-07	2.01
TC293367	Q8L3Y5	Receptor-like kinase RHG1	GMGI.052909	21	2.77	9.46	3.3E-05	1.77
TC9300	Q39836	Guanine nucleotide-binding protein subunit beta-like protein	PHVGI.052909	26	21.40	72.32	1.6E-30	1.76
TC15711	P93050	AtPK2324	PHVGI.052909	26	2.58	8.69	7.8E-05	1.75
TC14161	Q338A3	Expressed protein	PHVGI.052909	26	9.51	31.94	3.1E-14	1.75
TC8945	Q9LQN6	Probable protein phosphatase 2C POLTERGEIST-LIKE 5	PHVGI.052909	26	4.95	16.10	1.3E-07	1.70
TC8595	Q9SUK9	Probable protein phosphatase 2C 55	PHVGI.052909	26	0.79	2.56	4.0E-02	1.69
TC13423	Q45HK2	Serine/threonine protein kinase	PHVGI.052909	26	8.12	23.26	5.1E-09	1.52
TC14388	Q5SMM1	Diadenosine tetraphosphatase and related serine/threonine protein phosphatases-like	PHVGI.052909	26	0.99	2.81	4.6E-02	1.50
TC8891	Q8LSN3	Phytochrome-associated serine/threonine protein phosphatase or Serine/threonine protein phosphatase	PHVGI.052909	26	1.19	3.32	3.2E-02	1.48
TC12442	Q94BM7	Putative phytochrome A supressor spa1 protein	PHVGI.052909	26	3.17	7.41	5.3E-03	1.23
TA4025_3885	Q93X44	Protein tyrosine phosphatase	allTIGR_Plant_2007	26	4.56	9.97	2.4E-03	1.13
TC19415	P51568	Serine/threonine-protein kinase AFC3	PHVGI.052909	26	14.66	31.94	6.0E-08	1.12
TC281121	A5AKP8	Putative uncharacterized protein	GMGI.052909	22	5.94	12.52	1.1E-03	1.08
TC13246	Q5XWQ1	Serine/threonine protein kinase-like	PHVGI.052909	26	25.95	53.41	4.5E-11	1.04
TC37473	P55964	Pyruvate kinase isozyme G, chloroplast	LJGI.052909	23	2.77	5.62	3.6E-02	1.02
RNA processing and modification								
TC15924	Q93XX8	H/ACA ribonucleoprotein complex subunit 3-like protein	PHVGI.052909	25	0.00	29.64	1.6E-42	9.21
TC14175	Q9FMP4	Pre-mRNA branch site p14-like protein	PHVGI.052909	25	0.00	2.30	5.0E-04	5.52
TC9328	A2Y0Q3	Putative uncharacterized protein	PHVGI.052909	26	0.00	1.53	6.1E-03	4.94
TC304197	Q0WLH7	Putative uncharacterized protein At4g17610	GMGI.052909	26	0.00	1.02	3.2E-02	4.35
TC12797	A9P877	Putative uncharacterized protein	PHVGI.052909	26	18.43	53.41	3.8E-19	1.54

TC5819	Q9FJY5	Genomic DNA chromosome 5 TAC clone:K1F13	PCGI.052909	26	1.78	4.09	4.2E-02	1.20
TC19516	A6N081	Regulator of ribonuclease activity a	PHVGI.052909	26	14.26	31.94	2.5E-08	1.16
TC13228	Q9LY83	TRNA synthase-like protein	PHVGI.052909	26	4.56	9.97	2.4E-03	1.13
TC369	A9PCH9	Putative uncharacterized protein	PCGI.052909	26	8.92	19.42	2.4E-05	1.12
Unknown/unclassfied								
FG228882		Unknown	PHVGI.052909	22	0.00	4.34	6.7E-07	6.44
TC4893		Unknown	PCGI.052909	24	0.00	2.81	9.6E-05	5.81
NP9541233		Hypothetical protein	allTIGR_Plant_2009	24	0.00	2.81	9.6E-05	5.81
TC15748	Q8L9T8	Putative uncharacterized protein	PHVGI.052909	26	0.00	2.56	2.2E-04	5.68
TC294320	A9PG50	Putative uncharacterized protein	GMGI.052909	25	0.00	2.30	5.0E-04	5.52
TC12326	Q9LRR6	Similarity to RNA-binding protein	PHVGI.052909	26	0.00	2.04	1.2E-03	5.35
TC279139	Q9LLM2	MTD2	GMGI.052909	22	0.00	2.04	1.2E-03	5.35
TC18466	Q8VYL9	Putative uncharacterized protein At3g16310	PHVGI.052909	26	0.00	1.79	2.6E-03	5.16
CV540512	A5C505	Putative uncharacterized protein	PHVGI.052909	25	0.00	1.79	2.6E-03	5.16
TC326535	A7QYF2	Chromosome undetermined scaffold_245	GMGI.052909	22	0.00	1.79	2.6E-03	5.16
FG232512		Unknown	PHVGI.052909	26	0.00	1.53	6.1E-03	4.94
GD599130		Unknown	PCGI.052909	26	0.00	1.53	6.1E-03	4.94
TC18912		Unknown	PHVGI.052909	26	0.20	5.88	6.7E-08	4.89
TC9752	A5BTC6	Putative uncharacterized protein	PHVGI.052909	26	0.40	10.48	4.8E-13	4.72
TC20160	Q56Y76	Putative uncharacterized protein At1g50910	PHVGI.052909	26	0.00	1.28	1.4E-02	4.68
TC15994		Unknown	PHVGI.052909	26	0.00	1.28	1.4E-02	4.68
CB542963	Q9SLF4	Putative uncharacterized protein At2g16630	PHVGI.052909	26	0.00	1.28	1.4E-02	4.68
CV530964	Q01JI6	H0818E04.20 protein	PHVGI.052909	26	0.00	1.28	1.4E-02	4.68
FE684307	Q9AYM8	CPRD2 protein	PHVGI.052909	26	0.00	1.28	1.4E-02	4.68
TC548	A0BN49	Chromosome undetermined scaffold_118	PCGI.052909	21	0.00	1.28	1.4E-02	4.68
TC329065	A9PJA1	Putative uncharacterized protein	GMGI.052909	26	0.00	1.28	1.4E-02	4.68
CB544151		Unknown	PHVGI.052909	25	0.00	1.02	3.2E-02	4.35
TC12085	O04584	F19K23.12 protein	PHVGI.052909	26	0.00	1.02	3.2E-02	4.35
TC2855		Unknown	PCGI.052909	22	0.00	1.02	3.2E-02	4.35
TC9247	Q85X39	ORF53c	PCGI.052909	26	0.00	1.02	3.2E-02	4.35
GD596590		Unknown	PCGI.052909	24	0.00	1.02	3.2E-02	4.35
TC7072		Unknown	PCGI.052909	26	0.00	1.02	3.2E-02	4.35
TC4753	A7PV16	Chromosome chr4 scaffold_32	PCGI.052909	26	0.00	1.02	3.2E-02	4.35
TC1206	A7R5M8	Chromosome undetermined scaffold_1007	PCGI.052909	26	0.00	1.02	3.2E-02	4.35
TC19150	Q8LAW1	Putative uncharacterized protein	PHVGI.052909	25	0.00	1.02	3.2E-02	4.35
CA915881	A7NYN9	Chromosome chr6 scaffold_3	PCGI.052909	26	0.00	1.02	3.2E-02	4.35
TC323906	A7P0R0	Chromosome chr19 scaffold_4	GMGI.052909	22	0.00	1.02	3.2E-02	4.35
TC282391	A7PAA7	Chromosome chr14 scaffold_9	GMGI.052909	22	0.00	1.02	3.2E-02	4.35

TC300331	A5B9W5	Putative uncharacterized protein	GMGI.052909	22	0.00	1.02	3.2E-02	4.35
BM271448	A7NZN2	Chromosome chr6 scaffold_3	GMGI.052909	22	0.00	1.02	3.2E-02	4.35
TC117646	A7P7N3	Chromosome chr9 scaffold_7	MTGI.071708	22	0.00	1.02	3.2E-02	4.35
TC126794	Q9LVF1	Emb|CAB45066.1	MTGI.071708	22	0.00	1.02	3.2E-02	4.35
TC2280		Unknown	PCGI.052909	22	0.40	6.90	2.5E-08	4.12
TC1908		Unknown	PCGI.052909	24	1.39	24.02	4.6E-26	4.11
TC10784	A2ZFP6	Putative uncharacterized protein	PHVGI.052909	26	0.20	3.32	1.6E-04	4.07
BI973486	Q01I88	H0311C03.6 protein	GMGI.052909	24	0.20	2.81	7.5E-04	3.83
TC18317	Q8GUY7	Putative uncharacterized protein T26B15.6	PHVGI.052909	26	0.20	2.56	1.6E-03	3.69
TC9528	A0MDJ6	Putative uncharacterized protein	PHVGI.052909	26	0.20	2.56	1.6E-03	3.69
TC13475	Q2V4P4	Uncharacterized protein At1g09060.3	PHVGI.052909	26	3.96	50.34	1.3E-48	3.67
TC19745		Unknown	PHVGI.052909	26	0.20	2.30	3.3E-03	3.54
FD794806		Unknown	PHVGI.052909	26	0.20	2.30	3.3E-03	3.54
TC13132	O49971	Fimbrin-like protein AtFim2	PHVGI.052909	26	0.99	11.24	1.7E-11	3.50
CA916567		Unknown	PCGI.052909	22	0.20	2.04	7.0E-03	3.37
TC15747		Unknown	PHVGI.052909	26	0.59	6.13	1.3E-06	3.37
TC9362	O82347	Expressed protein	PHVGI.052909	26	0.59	5.88	2.7E-06	3.31
TC7370		Unknown	PCGI.052909	26	0.99	9.20	5.2E-09	3.22
TC11086	Q5S4Y8	Putative uncharacterized protein	PHVGI.052909	26	0.20	1.79	1.5E-02	3.17
TC118296	A7P609	Chromosome chr4 scaffold_6	MTGI.071708	21	0.20	1.79	1.5E-02	3.17
TC17741	A7R0U9	Chromosome undetermined scaffold_324	allTIGR_Plant_2009	21	0.20	1.79	1.5E-02	3.17
TC11915	O22044	Similar to YGR200c	PHVGI.052909	26	0.40	3.58	3.8E-04	3.17
TC12272	Q9LS48	Gb|AAC98059.1	PHVGI.052909	26	0.40	3.32	7.7E-04	3.07
GD594860		Unknown	PCGI.052909	26	0.40	3.32	7.7E-04	3.07
GD649510		Unknown	PCGI.052909	26	4.36	35.52	2.6E-29	3.03
TC12521	Q680W5	Putative uncharacterized protein At1g64140	PHVGI.052909	26	3.17	24.79	1.7E-20	2.97
TC12611	A7QGS6	Chromosome chr16 scaffold_94	PHVGI.052909	26	0.40	3.07	1.6E-03	2.95
FD796850	Q1S5K7	Putative uncharacterized protein	PHVGI.052909	26	0.20	1.53	3.0E-02	2.95
CV539190	Q94CC0	Uncharacterized protein At5g49945 precursor	PHVGI.052909	24	0.20	1.53	3.0E-02	2.95
GD333653		Unknown	PCGI.052909	22	0.20	1.53	3.0E-02	2.95
GD506124		Unknown	PCGI.052909	21	0.20	1.53	3.0E-02	2.95
TC2596	Q9ZW37	Expressed protein	PCGI.052909	26	0.20	1.53	3.0E-02	2.95
TC332634		Unknown	GMGI.052909	22	0.59	4.60	9.0E-05	2.95
GD412145			PCGI.052909	26	2.38	17.12	4.8E-14	2.85
TC17112	A9P7W9	Putative uncharacterized protein	PHVGI.052909	26	15.45	108.35	8.6E-80	2.81
CV537474		Unknown	PHVGI.052909	26	4.36	30.41	1.8E-23	2.80
CB544152		Unknown	PHVGI.052909	26	4.56	31.43	4.6E-24	2.79
TC18010	Q500X1	At4g32175	PHVGI.052909	26	2.97	20.19	7.7E-16	2.76

TC10841	Q2HW10	Wiscott-Aldrich syndrome, C-terminal	PHVGI.052909	26	1.39	9.20	7.8E-08	2.73
GD560312		Unknown	PCGI.052909	26	2.77	18.14	4.3E-14	2.71
CV537688		Unknown	PHVGI.052909	26	6.34	41.40	2.7E-30	2.71
TC14351	A7PZ23	Chromosome chr4 scaffold_39	PHVGI.052909	26	0.40	2.56	6.2E-03	2.69
TC18211	Q6V8P1	Putative senescence-associated protein SAG102	PHVGI.052909	26	0.40	2.56	6.2E-03	2.69
DW109650		Unknown	allTIGR_Plant_2009	21	0.59	3.83	7.0E-04	2.69
TC19921	Q9AVH2	Putative senescence-associated protein	PHVGI.052909	26	14.07	89.44	1.4E-62	2.67
TC16190	A9PFB0	Putative uncharacterized protein	PHVGI.052909	26	17.83	112.70	3.9E-78	2.66
TC18527	Q84VV0	At3g58830	PHVGI.052909	26	1.78	11.24	4.6E-09	2.66
CB541288		Unknown	PHVGI.052909	26	2.97	18.14	1.4E-13	2.61
CV534010		Unknown	PHVGI.052909	26	65.78	397.38	2.8E-263	2.59
EC599359		Probable cysteine-rich antifungal protein At2g26020 precursor	allTIGR_Plant_2007	22	17.04	102.73	2.4E-69	2.59
TC11568	Q2I307	Pollen-specific protein	PHVGI.052909	26	302.33	1776.09	0.0E+00	2.55
TC15102		Unknown	PCGI.052909	25	0.40	2.30	1.2E-02	2.54
TC12443	Q9M236	Putative uncharacterized protein T18D12_110	PHVGI.052909	26	0.79	4.60	3.0E-04	2.54
TA42910_3847		Hypothetical protein 6F11	allTIGR_Plant_2007	24	0.59	3.32	2.6E-03	2.48
TC19225		Unknown	PHVGI.052909	26	42.20	223.86	1.2E-136	2.41
TC1935	A7PB69	Chromosome chr16 scaffold_10	PCGI.052909	22	4.16	21.72	1.6E-14	2.38
GD539207		Unknown	PCGI.052909	24	0.59	3.07	5.0E-03	2.37
TC11838	A5B426	Putative uncharacterized protein	PHVGI.052909	25	0.40	2.04	2.4E-02	2.37
TC333669		Unknown	GMGI.052909	24	0.40	2.04	2.4E-02	2.37
TC13330	A5C924	Putative uncharacterized protein	PHVGI.052909	26	0.59	3.07	5.0E-03	2.37
TC3710		Unknown	PCGI.052909	22	0.59	3.07	5.0E-03	2.37
TC329903	UPI000034EDB9	MADS-box protein-related	allTIGR_Plant_2009	22	2.97	14.82	4.9E-10	2.32
TC9613		Unknown	PCGI.052909	21	2.18	10.48	2.6E-07	2.27
FE695348	Q9SUZ8	Putative uncharacterized protein F4F15.170	PHVGI.052909	26	0.59	2.81	9.4E-03	2.24
GD321209		Unknown	PCGI.052909	26	0.59	2.81	9.4E-03	2.24
FD792763		Unknown	PHVGI.052909	26	0.40	1.79	4.5E-02	2.17
TC15388		Unknown	PHVGI.052909	26	0.40	1.79	4.5E-02	2.17
		Unknown	refseqPlantJune09.fna.all.fas	22	0.40	1.79	4.5E-02	2.17
GD621125		Unknown	PCGI.052909	24	0.40	1.79	4.5E-02	2.17
TC344913		Unknown	GMGI.052909	22	0.40	1.79	4.5E-02	2.17
DB984828	A7Q6A9	Chromosome chr11 scaffold_56	GMGI.052909	23	0.40	1.79	4.5E-02	2.17
TC292803	Q39448	Specific tissue protein 2	GMGI.052909	26	0.40	1.79	4.5E-02	2.17
FE698282		Unknown	PHVGI.052909	26	1.98	8.94	3.7E-06	2.17
TC131788		Unknown	allTIGR_Plant_2009	21	3.57	15.59	1.5E-09	2.13
TC19508		Unknown	PHVGI.052909	26	0.59	2.56	1.7E-02	2.10

TC13352	Q3HRX2	Meloidogyne-induced giant cell protein-like protein	PHVGI.052909	26	5.15	21.47	3.5E-12	2.06
CA916034		Unknown	PCGI.052909	24	2.77	11.50	4.1E-07	2.05
CV540459		Unknown	PHVGI.052909	26	0.99	4.09	2.9E-03	2.05
TC12455	Q3SC80	ACI112	PHVGI.052909	26	0.99	4.09	2.9E-03	2.05
TC15886	Q9LLM2	MTD2	PHVGI.052909	26	0.99	4.09	2.9E-03	2.05
EC982314		Unkown	allTIGR_Plant_2009	21	2.18	8.94	9.0E-06	2.04
TC18200		Unkown	PHVGI.052909	26	4.95	20.19	2.5E-11	2.03
FD787265	A7PNV8	Chromosome chr8 scaffold_23	PHVGI.052909	26	1.78	7.16	8.8E-05	2.00
TC15863		Unkown	PHVGI.052909	26	1.98	7.92	3.7E-05	2.00
TC13185		Unknown	PCGI.052909	26	21.40	85.35	2.9E-42	2.00
CV531813	Q9SZK4	Putative uncharacterized protein F20D10.160	PHVGI.052909	26	0.59	2.30	3.2E-02	1.95
TC15268		Unknown	PHVGI.052909	26	1.19	4.60	2.1E-03	1.95
EY727849		Unknown	allTIGR_Plant_2009	21	5.75	22.23	8.3E-12	1.95
TC12359	Q10QA5	Hydrolase alpha/beta fold family protein expressed	PHVGI.052909	26	0.59	2.30	3.2E-02	1.95
GD404931		Unknown	PCGI.052909	26	0.59	2.30	3.2E-02	1.95
TC18151	Q8RV74	Leaf senescence protein-like	PHVGI.052909	26	72.91	270.12	1.1E-120	1.89
GD360653		Unknown	PCGI.052909	26	1.39	5.11	1.5E-03	1.88
TC9669		Unknown	PCGI.052909	26	1.39	5.11	1.5E-03	1.88
TC18925	Q8VWF1	Putative uncharacterized protein At4g34660	PHVGI.052909	26	23.58	86.63	1.4E-39	1.88
CV544018	A2YTE9	Putative uncharacterized protein	PHVGI.052909	26	6.54	24.02	4.6E-12	1.88
TC358517		Unknown	allTIGR_Plant_2009	21	3.76	13.80	1.7E-07	1.87
GD370414		Unknown	PCGI.052909	24	5.55	20.19	2.8E-10	1.86
TC297442		Unknown	GMGI.052909	21	0.99	3.58	9.1E-03	1.85
TC20944		Unknown	PCGI.052909	26	0.79	2.81	2.3E-02	1.83
TC125502	A7QKH7	Chromosome chr2 scaffold_112	allTIGR_Plant_2009	25	0.79	2.81	2.3E-02	1.83
TC13907	A7R5Y8	Chromosome undetermined scaffold_1099	PHVGI.052909	26	14.26	50.09	1.7E-22	1.81
TC321351	O80813	Ycf20-like protein	GMGI.052909	21	1.19	4.09	6.5E-03	1.78
TC15751	Q0PN09	Lateral organ boundaries domain protein	PHVGI.052909	26	2.97	10.22	1.4E-05	1.78
TC17710	Q2QWU3	Expressed protein	PCGI.052909	26	1.78	6.13	8.1E-04	1.78
TC280338	A9P7W1	Putative uncharacterized protein	GMGI.052909	26	12.28	41.40	4.4E-18	1.75
TC2391	A7NZN7	Chromosome chr6 scaffold_3	PCGI.052909	26	41.01	136.21	7.2E-55	1.73
GD387699	Q94A36	At1g50630/F17J6_15	PCGI.052909	26	1.39	4.60	4.6E-03	1.73
GD383583		Unknown	PCGI.052909	23	1.78	5.88	1.4E-03	1.72
BP077475	A2Q3K8	Remorin, C-terminal region	LJGI.052909	21	1.78	5.88	1.4E-03	1.72
TC18404	Q2HUZ5	Putative uncharacterized protein	PHVGI.052909	26	19.81	64.14	5.8E-26	1.69
TC12992	Q8VZE7	At2g31890/F20M17.7	PHVGI.052909	26	1.19	3.83	1.1E-02	1.69
TA35949_3635		P0413G02.3	allTIGR_Plant_2007	21	1.19	3.83	1.1E-02	1.69
TC18095	A7PA90	Chromosome chr14 scaffold_9	PHVGI.052909	22	0.79	2.56	4.0E-02	1.69

GD555233		Unknown	PCGI.052909	22	0.79	2.56	4.0E-02	1.69
TC291659	Q9FG54	Root cap protein 2-like protein	GMGI.052909	21	0.79	2.56	4.0E-02	1.69
NP9532897		Hypothetical protein	allTIGR_Plant_2009	21	0.79	2.56	4.0E-02	1.69
GD567642		Unknown	PCGI.052909	26	20.41	65.68	2.3E-26	1.69
FD787957		Unknown	PHVGI.052909	23	41.41	132.38	4.9E-51	1.68
TC21127	A9P9H0	Putative uncharacterized protein	PCGI.052909	26	2.58	8.18	2.2E-04	1.67
GD410621			PCGI.052909	22	4.36	13.80	1.5E-06	1.66
TC19688	Q2QKB5	U2AF small subunit	PHVGI.052909	26	3.37	10.48	3.5E-05	1.64
FE710186		Unknown	PHVGI.052909	21	0.99	3.07	2.7E-02	1.63
GD605786		Unknown	PCGI.052909	22	1.98	6.13	1.7E-03	1.63
TC325418	Q9SLM4	Putative uncharacterized protein At2g40980	GMGI.052909	25	0.99	3.07	2.7E-02	1.63
TC301786	Q8S8F5	Expressed protein	GMGI.052909	22	6.54	20.19	1.0E-08	1.63
TC10946	Q8L708	Putative uncharacterized protein At5g08200	PHVGI.052909	26	6.74	20.70	7.4E-09	1.62
TC9655	Q949N7	Putative uncharacterized protein At3g26890	PHVGI.052909	26	7.92	24.28	4.1E-10	1.62
TC311443	A7PCW1	Chromosome chr17 scaffold_12	GMGI.052909	26	1.59	4.86	5.6E-03	1.62
TC4118		Unknown	PCGI.052909	21	49.93	152.56	2.3E-55	1.61
GD506319		Unknown	PCGI.052909	22	16.64	49.58	1.6E-18	1.57
TC13251	A7NTV4	Chromosome chr18 scaffold_1	PHVGI.052909	26	1.39	4.09	1.3E-02	1.56
GD570201		Unknown	PCGI.052909	26	6.54	19.17	7.0E-08	1.55
TC19938		Unknown	PCGI.052909	26	12.48	36.54	9.6E-14	1.55
TC17749		Unknown	PHVGI.052909	26	2.97	8.69	3.0E-04	1.55
TC3922		Unknown	PCGI.052909	22	2.38	6.90	1.4E-03	1.54
TC14626	Q9T096	Protein yippee-like At4g27745	PHVGI.052909	26	1.78	5.11	6.5E-03	1.52
TC15330	A2Q1H0	Transferase putative	PHVGI.052909	26	11.89	33.99	1.6E-12	1.52
TC302751	Q0WWY1	Regulator of chromosome condensation-like protein	GMGI.052909	26	0.99	2.81	4.6E-02	1.50
EB698708		Unknown	allTIGR_Plant_2007	21	0.99	2.81	4.6E-02	1.50
GD429221		Unknown	PCGI.052909	26	29.52	82.80	1.4E-27	1.49
TC17131 or TC9644	Q8LKG1	Drm3	PHVGI.052909	26	44.38	124.20	2.2E-40	1.48
TC19672		Unknown	PHVGI.052909	26	1.19	3.32	3.2E-02	1.48
TC19610		Unknown	PCGI.052909	22	1.19	3.32	3.2E-02	1.48
TC2141		Unknown	PCGI.052909	22	2.38	6.64	2.3E-03	1.48
TC19953	A5BFM6	Putative uncharacterized protein	PHVGI.052909	26	2.58	7.16	1.6E-03	1.47
TC49245	Q2HSF1	WD40-like	LJGI.052909	22	2.97	8.18	7.9E-04	1.46
EG594350		Unknown	PHVGI.052909	26	1.59	4.34	1.5E-02	1.45
TC9661		Unknown	PCGI.052909	22	2.18	5.88	5.2E-03	1.43
GD619015		Unknown	PCGI.052909	26	2.18	5.88	5.2E-03	1.43
TC18441	Q8RXW8	Putative uncharacterized protein At5g6520	PHVGI.052909	26	21.20	56.99	2.3E-18	1.43
TC9619	A4GGF4	Putative uncharacterized protein ycf1	PHVGI.052909		195.35	519.28	5.3E-151	1.41

TC484		Unknown		PCGI.052909	22	3.37	8.94	6.3E-04	1.41
TC13162	A9PEK0	Putative uncharacterized protein		PHVGI.052909	26	64.59	170.96	1.2E-50	1.40
TC191781				allTIGR_Plant_2009	21	4.75	12.52	5.8E-05	1.40
GD441863	A7QHW9	Chromosome undetermined scaffold_100		PCGI.052909	26	3.96	10.22	3.5E-04	1.37
TC9626		Unknown		PHVGI.052909	26	2.18	5.62	8.3E-03	1.37
GD622234		Unknown		PCGI.052909	22	2.18	5.62	8.3E-03	1.37
TC10104	Q680K8	Putative uncharacterized protein At1g55760		PHVGI.052909	26	3.57	9.20	7.1E-04	1.37
TC15912	UPI000034F4BB	WD-40 repeat family protein / beige-related		PHVGI.052909	26	2.38	6.13	5.8E-03	1.37
TC6212		Unknown		PCGI.052909	26	1.59	4.09	2.5E-02	1.37
TC10023	A5BAT1	Putative uncharacterized protein		PHVGI.052909	26	1.39	3.58	3.6E-02	1.37
TC15497		Unknown		PHVGI.052909	26	1.39	3.58	3.6E-02	1.37
GD455759		Unknown		PCGI.052909	26	1.39	3.58	3.6E-02	1.37
TC4262		Unknown		PCGI.052909	23	18.62	47.79	1.2E-14	1.36
GD421377		Unknown		PCGI.052909	23	8.12	20.70	4.6E-07	1.35
GD434225		Unknown		PCGI.052909	26	6.14	15.59	1.3E-05	1.34
GD588250		Unknown		PCGI.052909	23	7.73	19.42	1.4E-06	1.33
TC8515	Q9SSR5	F6D8.15 protein		PHVGI.052909	26	14.26	35.78	5.9E-11	1.33
TC8834	Q9ZSJ7	Putative type 1 membrane protein		PHVGI.052909	26	38.44	96.09	9.7E-27	1.32
CA899860				PCGI.052909	26	2.97	7.41	3.1E-03	1.32
TC18800	Q9LK01	Hydrolase-like protein		PHVGI.052909	26	2.58	6.39	6.4E-03	1.31
TC16779 TC507	Q9FUP6	Suspensor-specific protein		PCGI.052909	26	7.73	19.17	2.1E-06	1.31
FG228855	A2Y700	Putative uncharacterized protein		PHVGI.052909	26	6.54	16.10	1.6E-05	1.30
GD541168		Unknown		PCGI.052909	21	8.72	21.47	6.1E-07	1.30
GD472424		Unknown		PCGI.052909	26	2.18	5.37	1.3E-02	1.30
TC11562	Q0JDG7	Os04g0404900 protein		PHVGI.052909	26	10.70	26.32	3.4E-08	1.30
TC310162		Unknown		GMGI.052909	23	4.16	10.22	6.1E-04	1.30
GD614632		Unknown		PCGI.052909	26	6.14	15.08	3.1E-05	1.30
TC11023	Q9LLM3	MTD1		PHVGI.052909	26	1.98	4.86	1.9E-02	1.29
FG232916		Unknown		PHVGI.052909	26	45.37	111.17	1.1E-29	1.29
TC1194	A7Q9H1	Chromosome chr19 scaffold_66		PCGI.052909	26	11.69	28.62	9.8E-09	1.29
TC12486	O23607	Putative uncharacterized protein dl4870c		PHVGI.052909	26	14.86	36.29	1.2E-10	1.29
TC10429	Q93VT6	Putative uncharacterized protein At5g08540		PHVGI.052909	26	5.55	13.54	8.5E-05	1.29
CA915903		Unknown		allTIGR_Plant_2007	26	23.77	58.01	3.9E-16	1.29
FG231283		Unknown		PHVGI.052909	26	3.57	8.69	1.7E-03	1.28
GE120834		Unknown		GMGI.052909	22	1.78	4.34	2.7E-02	1.28
TC13314	O49529	Predicted protein		PHVGI.052909	26	3.37	8.18	2.4E-03	1.28
TC282924	Q940R2	At1g04130/F20D22_10		GMGI.052909	25	11.29	27.34	2.9E-08	1.28
TC13355		Unknown		PCGI.052909	26	7.92	19.17	3.5E-06	1.27

GD488946		Unknown	PCGI.052909	26	4.56	10.99	4.7E-04	1.27
TC16867	A7Q9R4	Chromosome chr5 scaffold_67	PCGI.052909	26	4.36	10.48	6.6E-04	1.27
TC13508	A5B4Y5	Putative uncharacterized protein	PHVGI.052909	26	2.77	6.64	6.9E-03	1.26
TC17459	A5AZC8	Putative uncharacterized protein	PHVGI.052909	26	9.71	23.26	4.0E-07	1.26
BP533923		Unknown	allTIGR_Plant_2009	22	6.14	14.57	7.2E-05	1.25
FG231276		Unknown	PHVGI.052909	26	76.87	182.21	6.2E-45	1.25
TC190297	A7Q1C9	Chromosome chr10 scaffold_43	allTIGR_Plant_2009	23	9.51	22.49	8.5E-07	1.24
TC19013		Unknown	PHVGI.052909	22	3.37	7.92	3.7E-03	1.23
GD565457		Unknown	PCGI.052909	26	21.60	50.60	2.3E-13	1.23
TC12588	A9NXI7	Putative uncharacterized protein	PHVGI.052909	26	14.07	32.71	4.9E-09	1.22
GD586595		Unknown	PCGI.052909	25	3.96	9.20	2.0E-03	1.22
TC15721		Unknown	PCGI.052909	23	1.98	4.60	2.9E-02	1.22
TC18128	Q940R4	AT4g16560/dl4305c	PHVGI.052909	26	22.59	52.39	1.5E-13	1.21
TC12188	Q8LA64	Putative uncharacterized protein	PHVGI.052909	26	2.77	6.39	1.1E-02	1.20
TC11723		Unknown	PCGI.052909	26	3.57	8.18	4.0E-03	1.20
CB540180		Unknown	PHVGI.052909	26	1.78	4.09	4.2E-02	1.20
TC19171		Unknown	PHVGI.052909	26	6.14	14.06	1.6E-04	1.19
FD735381		Unknown	allTIGR_Plant_2009	21	2.58	5.88	1.5E-02	1.19
GD544036		Unknown	PCGI.052909	26	55.47	126.50	1.4E-29	1.19
TC20126		Unknown	PCGI.052909	22	19.22	43.70	3.6E-11	1.19
TC70630		Unknown	allTIGR_Plant_2009	21	5.75	13.03	3.2E-04	1.18
TC10636	A4Q3S1	Putative uncharacterized protein	PHVGI.052909	26	30.31	68.74	1.2E-16	1.18
TC9073	Q0E276	Os02g0265100 protein	PHVGI.052909	26	2.38	5.37	2.2E-02	1.17
GD315629	A7QNS9	Chromosome undetermined scaffold_134	PCGI.052909	26	4.75	10.73	1.2E-03	1.17
CA913426		Unknown	PCGI.052909	25	9.51	21.47	4.2E-06	1.17
CV540033	Q9SZ56	Putative uncharacterized protein AT4g31890	PHVGI.052909	26	13.67	30.41	6.6E-08	1.15
TC16637	A9PHQ9	Putative uncharacterized protein	PHVGI.052909	26	3.57	7.92	6.0E-03	1.15
EY726914		Unknown	allTIGR_Plant_2009	21	2.77	6.13	1.6E-02	1.14
TC19060	A7PG34	Chromosome chr6 scaffold_15	PHVGI.052909	25	13.87	30.67	7.0E-08	1.14
TC12475	Q8GSI6	Putative uncharacterized protein	PHVGI.052909	26	21.40	47.28	2.2E-11	1.14
CV543497		Unknown	PHVGI.052909	26	22.98	50.60	5.3E-12	1.14
TC4490		Unknown	PCGI.052909	26	11.29	24.79	1.5E-06	1.13
CV540123		Unknown	PHVGI.052909	26	3.96	8.69	4.5E-03	1.13
TC295587	A7P6G5	Chromosome chr9 scaffold_7	GMGI.052909	22	1.98	4.34	4.5E-02	1.13
TC16175		Unknown	PCGI.052909	26	6.54	14.31	2.7E-04	1.13
TC14775	A5C109	Putative uncharacterized protein	PHVGI.052909	26	15.45	33.73	2.4E-08	1.13
BE210310	Q8L951	Putative uncharacterized protein	GMGI.052909	24	2.58	5.62	2.3E-02	1.13
TC10856	O22826	Putative splicing factor	PHVGI.052909	26	3.17	6.90	1.2E-02	1.12

GD637538		Unknown		PCGI.052909	22	3.17	6.90	1.2E-02	1.12
TC10501		Unknown		PCGI.052909	26	12.48	27.09	6.7E-07	1.12
TC323610	Q0J0K4	Os09g0506900 protein		GMGI.052909	21	2.38	5.11	3.3E-02	1.10
TA4054_3886		Unknown		allTIGR_Plant_2007	26	12.68	27.09	1.0E-06	1.10
GD423362		Unknown		PCGI.052909	26	5.15	10.99	1.9E-03	1.09
TC9955		Unknown		PCGI.052909	22	8.32	17.63	9.3E-05	1.08
GD627044		Unknown		PCGI.052909	26	5.55	11.76	1.4E-03	1.08
GD606169		Unknown		PCGI.052909	26	2.77	5.88	2.4E-02	1.08
TC15278	A5AP27	Putative uncharacterized protein		PHVGI.052909	26	4.95	10.48	2.7E-03	1.08
TC301927	A9PG39	Putative uncharacterized protein		GMGI.052909	23	4.36	9.20	5.0E-03	1.08
TC15587	O64866	Expressed protein		PHVGI.052909	26	8.12	17.12	1.3E-04	1.08
TC21139		Unknown		PCGI.052909	26	21.40	44.98	6.1E-10	1.07
BP526808		Unknown		allTIGR_Plant_2009	21	6.93	14.57	4.4E-04	1.07
TC16452	A5C8Z8	Putative uncharacterized protein		PHVGI.052909	26	8.52	17.89	9.8E-05	1.07
TC18196	A9PJK5	Putative uncharacterized protein		PHVGI.052909	26	4.75	9.97	3.7E-03	1.07
FE705281	A9PGD0	Putative uncharacterized protein		PHVGI.052909	26	3.57	7.41	1.3E-02	1.06
TC11256	Q501H5	At1g55690		PHVGI.052909	26	9.11	18.91	7.7E-05	1.05
TC8962		Unknown		PHVGI.052909	26	4.56	9.46	5.2E-03	1.05
GD645178		Unknown		PCGI.052909	26	9.11	18.91	7.7E-05	1.05
TC19058	Q9LS71	Emb|CAB72194.1		PHVGI.052909	26	7.53	15.59	3.4E-04	1.05
GD536713		Unknown		PCGI.052909	26	6.93	14.31	6.3E-04	1.05
TC16398	Q9FPW6	POZ/BTB containing-protein AtPOB1		PHVGI.052909	26	47.95	98.39	5.1E-19	1.04
CB540889		Unkown		PHVGI.052909	22	8.72	17.89	1.5E-04	1.04
GD494929		Unkown		PCGI.052909	22	2.38	4.86	5.0E-02	1.03
GD395994		Unkown		PCGI.052909	21	8.52	17.38	2.0E-04	1.03
TC9138	A5BZB0	Putative uncharacterized protein		PHVGI.052909	26	3.76	7.67	1.4E-02	1.03
		Unkown		plantRNAtotal_april09	22	16.25	32.97	3.6E-07	1.02
TC12136		Unkown		PCGI.052909	22	3.17	6.39	2.7E-02	1.01
TC8854	A5AQ16	Putative uncharacterized protein		PHVGI.052909	26	4.95	9.97	5.6E-03	1.01
TC16310		Unkown		PHVGI.052909	26	3.57	7.16	1.9E-02	1.00

Down-regulated transcripts

Transcription regulation

GD519958	A8MS41	Carbon catabolite repressor protein 4 homolog 4		PCGI.052909	22	1.39	0.00	2.0E-02	-4.79
TC11635	Q38832	Auxin-responsive protein IAA14		PHVGI.052909	26	1.39	0.00	2.0E-02	-4.79
TC10315	Q5YLQ7	Ethylene-responsive element binding factor		PHVGI.052909	26	2.97	0.26	1.6E-03	-3.54
TC1944	O65597	Putative uncharacterized protein M3E9.200		PCGI.052909	25	2.18	0.26	1.3E-02	-3.09
GD532891	Q5EEQ0	Zinc finger protein		PCGI.052909	26	2.97	0.51	7.0E-03	-2.54

TC17800	Q8GZ43	RanBP2-type zinc finger protein At1g67325	PHVGI.052909	23	4.36	0.77	9.4E-04	-2.51
CB542396	Q06A73	PHD1	PHVGI.052909	26	4.16	1.02	4.5E-03	-2.03
TC16895	Q4PRK5	Pseudo response regulator 3	PHVGI.052909	26	4.16	1.02	4.5E-03	-2.02
TC15593	A5AWW8	Putative uncharacterized protein	PHVGI.052909	26	5.15	1.28	1.5E-03	-2.01
TC15547	Q0PJI3	MYB transcription factor MYB139	PHVGI.052909	26	3.96	1.02	6.9E-03	-1.95
TC7573	Q8L8V0	Transcription co-activator-like protein	PCGI.052909	26	17.24	4.60	1.0E-08	-1.91
TC15823	Q7Y0Z9	Bell-like homeodomain protein 3	PHVGI.052909	26	5.55	1.53	1.8E-03	-1.86
EX304406	Q0HA68	DELLA protein	PHVGI.052909	26	3.57	1.02	1.6E-02	-1.80
CV538288	Q7XTV6	OSJNBa0010D21.10 protein	PHVGI.052909	26	2.58	0.77	4.8E-02	-1.75
TC9336	Q45EZ4	RAV-like DNA-binding protein	PHVGI.052909	26	19.61	5.88	8.9E-09	-1.74
TC10858	Q0WNR6	Putative DNA-binding protein	PHVGI.052909	26	8.92	2.81	2.0E-04	-1.67
TC314353	Q9C9H1	Putative zinc finger protein	GMGI.052909	26	5.55	1.79	4.2E-03	-1.63
TC308879	A4ZGR0	Transcription factor bZIP34	GMGI.052909	25	3.76	1.28	2.4E-02	-1.56
TC11353	Q0GPH5	BZIP transcription factor bZIP62	PHVGI.052909	26	7.33	2.56	1.6E-03	-1.52
FD786790	Q2PJS4	WRKY6	PHVGI.052909	26	12.28	4.34	4.6E-05	-1.50
FE689535	Q6ER77	Metallo-beta-lactamase protein-like	PHVGI.052909	26	12.09	4.34	6.5E-05	-1.48
TC9553	Q0PJJ8	MYB transcription factor MYB93	PHVGI.052909	26	4.95	1.79	1.2E-02	-1.47
TC8622	Q2VWB7	Prf interactor 30137	PHVGI.052909	26	9.11	3.32	6.3E-04	-1.46
NP7260353		Disease resistance protein; Zinc finger, C2H2-type	MTGI.071708	25	5.94	2.30	9.0E-03	-1.37
TC18859	Q2LMF3	MYB2	PHVGI.052909	26	17.43	6.90	7.6E-06	-1.34
CV533766	A2Q5Q2	Zinc finger, GATA-type	PHVGI.052909	26	10.90	4.34	4.7E-04	-1.33
TC16274	Q10LG3	Zinc finger C3HC4 type family protein expressed	PHVGI.052909	26	8.52	3.58	3.2E-03	-1.25
TC14700	Q00423	HMG-Y-related protein A	PHVGI.052909	26	37.64	15.84	3.6E-10	-1.25
TC16399	Q2HS28	Transcription factor IIA helical	PHVGI.052909	26	12.48	5.37	4.5E-04	-1.22
TC343409	Q9SV30	GATA transcription factor 10	GMGI.052909	21	26.15	11.50	5.5E-07	-1.19
TC8347	A4ZVU9	CCAAT-binding transcription factor	PHVGI.052909	26	25.16	11.24	1.3E-06	-1.16
TC20433	Q0GPG4	BZIP transcription factor bZIP109	PCGI.052909	23	20.01	9.20	2.9E-05	-1.12
TC11220	A7LHF7	WRKY8	PHVGI.052909	26	14.26	6.64	5.2E-04	-1.10
TC8673	A5A8C1	C2-H2 zinc finger protein	PHVGI.052909	26	21.20	10.22	4.3E-05	-1.05
TC18603	A1ECK5	Putative multiple stress-responsive zinc-finger protein	PHVGI.052909	26	96.09	46.51	2.6E-18	-1.05
TC9222	Q9ZRB9	Homeobox 1 protein	PHVGI.052909	26	18.23	8.94	2.0E-04	-1.03
FE700223	Q9SYH4	Nuclear transcription factor Y subunit A-5	PHVGI.052909	26	8.32	4.09	1.3E-02	-1.03
TC17929	O82116	Zinc finger protein	PHVGI.052909	26	6.14	3.07	3.8E-02	-1.00
Signal transduction								
TC12632	O80920	Abscisic acid receptor PYL4	PHVGI.052909	26	5.75	0.00	6.7E-08	-6.84
TC279226	P62163	Calmodulin-2	GMGI.052909	26	2.58	0.00	6.5E-04	-5.69
TC8988	Q9LX66	Probable receptor-like protein kinase At3g46290 precursor	PHVGI.052909	26	2.58	0.00	6.5E-04	-5.69
TC37902	Q5QQ33	ADP-ribosylation factor 1	allTIGR_Plant_2009	22	1.59	0.00	1.1E-02	-4.99

CB541284	Q96477	LRR protein	PHVGI.052909	22	1.59	0.00	1.1E-02	-4.99
EV281217	Q9LR15	ER lumen protein retaining receptor	GMGI.052909	26	1.19	0.00	3.6E-02	-4.57
TC13200	Q9MB06	Serine/threonine protein phosphatase	PHVGI.052909	26	2.38	0.26	7.7E-03	-3.22
TC13128	O80920	Abscisic acid receptor PYL4	PHVGI.052909	26	2.97	0.51	7.0E-03	-2.54
FE897685	A6YAQ1	Ethylene receptor	PHVGI.052909	26	20.41	5.88	2.0E-09	-1.80
TC291387	Q1RUA5	Annexin, type V	GMGI.052909	26	2.58	0.77	4.8E-02	-1.75
TC12776	Q9ZR53	Annexin-like protein	PHVGI.052909	26	22.59	7.67	1.1E-08	-1.56
FK554351	O82062	39 kDa EF-Hand containing protein	GMGI.052909	26	2.97	1.02	5.0E-02	-1.54
TC18087	A5C962	Putative uncharacterized protein	PHVGI.052909	26	118.87	44.21	3.8E-35	-1.43
TC9174	Q9SCA1	Calcium-binding protein	PHVGI.052909	26	8.12	3.07	1.7E-03	-1.41
TC11596	A9PIP7	Putative uncharacterized protein	PHVGI.052909	26	86.18	34.24	1.7E-23	-1.33
CV529064	O80575	6 7-dimethyl-8-ribityllumazine synthase chloroplast precursor	PHVGI.052909	25	4.36	1.79	3.5E-02	-1.28
FE693449	Q94F62	BRASSINOSTEROID INSENSITIVE 1-associated receptor kinase 1 precursor	PHVGI.052909	26	4.36	1.79	3.5E-02	-1.28
TC10438	O80920	Abscisic acid receptor PYL4	PHVGI.052909	26	25.16	10.99	7.7E-07	-1.20
TC314254	Q946Y7	Syntaxin-61	GMGI.052909	24	22.19	9.71	3.7E-06	-1.19
TC14232	Q9SV55	AFP homolog 2	PHVGI.052909	26	9.11	4.09	4.2E-03	-1.16
TC14342	O65732	Annexin	PHVGI.052909	26	33.28	15.59	1.1E-07	-1.09
TC19495	Q9XED8	Auxin response factor 9	PHVGI.052909	26	18.03	8.94	2.6E-04	-1.01
Transport								
TC286776	Q8VYR7	Boron transporter 1	GMGI.052909	26	2.38	0.00	1.1E-03	-5.57
TC15430	A4ZVI6	Phosphate transporter	PHVGI.052909	26	1.78	0.00	6.4E-03	-5.16
TC315977	A5ASS0	Putative uncharacterized protein	GMGI.052909	26	1.78	0.00	6.4E-03	-5.16
TC19979	Q6S9Z3	Allantoin permease	PHVGI.052909	26	1.59	0.00	1.1E-02	-4.99
TC333004	Q94FN3	Phosphatidylinositol transfer-like protein II	GMGI.052909	22	7.33	0.26	1.2E-08	-4.84
TC21330	Q5DVT5	Plasma membrane intrinsic protein 2;5	PHVGI.052909	24	1.39	0.00	2.0E-02	-4.79
TC21465	Q41709	Ferritin-2, chloroplast precursor	PHVGI.052909	24	1.39	0.00	2.0E-02	-4.79
TC31929	Q6S9Z3	Allantoin permease	PHVGI.052909	26	1.19	0.00	3.6E-02	-4.57
BU547481	UPI000034EE33	Transporter-related	GMGI.052909	26	1.19	0.00	3.6E-02	-4.57
TC342320	Q4PKP6	Mitochrondrial voltage-dependent anion-selective channel	GMGI.052909	26	1.19	0.00	3.6E-02	-4.57
TC343750	Q9ZUT3	ABC transporter I family member 16	GMGI.052909	21	5.55	0.26	1.6E-06	-4.44
TC15969	Q0WP36	Sulfate transporter like protein	PHVGI.052909	26	4.56	0.26	2.4E-05	-4.16
TC11041	Q3ECP7	General substrate transporter	PHVGI.052909	26	4.95	0.51	5.2E-05	-3.28
TC26430	O49377	Vesicle-associated membrane protein 711	PHVGI.052909	23	2.38	0.26	7.7E-03	-3.22
TC295541	Q9LHN7	Similarity to amino acid transporter	GMGI.052909	21	4.36	0.51	2.4E-04	-3.09
TC16994	Q9LNH6	Novel plant SNARE 12	PHVGI.052909	24	2.18	0.26	1.3E-02	-3.09
TA4384_3988		RNA-binding region RNP-1 (RNA recognition motif); Calcium-binding EF- hand	allTIGR_Plant_2007	21	2.18	0.26	1.3E-02	-3.09
TC11657	Q8LAI4	Putative amino acid transport protein	PHVGI.052909	26	1.78	0.26	3.5E-02	-2.80
TC9383	Q8LE45	Nodulin-like protein	PHVGI.052909	26	6.14	1.02	5.3E-05	-2.59

TC14349	Q949G4	N3 like protein	PHVGI.052909	26	5.75	1.02	1.3E-04	-2.49
TC14343	Q9SA38	F3O9.19 protein	PHVGI.052909	26	60.63	12.01	9.2E-35	-2.34
TC12460	Q9FH68	Genomic DNA, chromosome 5, TAC clone:K16E1	PHVGI.052909	26	6.14	1.28	1.8E-04	-2.26
TC9999	Q8LDF6	Putative mitochondrial dicarboxylate carrier protein	PHVGI.052909	26	56.07	12.27	5.2E-30	-2.19
TC30771	O22124	Proton pyrophosphatase	PHVGI.052909	26	19.22	4.60	1.8E-10	-2.06
TC326494	A7NWQ9	Non-specific lipid-transfer protein	GMGI.052909	22	10.90	2.81	4.1E-06	-1.95
TC15925	Q94KJ7	Vacuolar protein sorting-associated protein 33 homolog	PCGI.052909	26	23.58	6.13	1.0E-11	-1.94
TC10406	A5AUB0	Putative uncharacterized protein	PHVGI.052909	26	6.74	1.79	4.1E-04	-1.91
FE692883	Q9S9N8	Metal transporter Nramp6	PHVGI.052909	26	3.76	1.02	1.0E-02	-1.88
FD786515	Q9SJI6	Putative uncharacterized protein At2g42700	PHVGI.052909	26	3.76	1.02	1.0E-02	-1.88
TC343392	Q5W273	PDR-like ABC transporter	GMGI.052909	26	3.57	1.02	1.6E-02	-1.80
TC14385	Q9C521	Putative uncharacterized protein At1g77610	PHVGI.052909	22	6.74	2.04	9.9E-04	-1.72
FE708024	Q7Y1Q0	Sucrose transporter-like protein	PHVGI.052909	26	11.49	3.58	1.9E-05	-1.68
TC12270	A5C1M4	Putative uncharacterized protein	PHVGI.052909	26	10.50	3.58	1.1E-04	-1.55
TC18384	Q0WP01	Similar to peptide transporter	PHVGI.052909	26	68.15	24.53	9.3E-22	-1.47
TC23286	A5C2M2	Putative uncharacterized protein	PHVGI.052909	24	3.96	1.53	3.5E-02	-1.37
TC302204	A3A494	Putative uncharacterized protein	GMGI.052909	26	8.32	3.32	2.4E-03	-1.32
TC13372	Q2HUJ7	V-ATPase subunit C	PHVGI.052909	26	5.75	2.30	1.3E-02	-1.32
TC5542	Q2HSW3	Sec61beta	PCGI.052909	26	16.44	6.64	2.0E-05	-1.31
TC304699	A7NUZ2	Putative monosaccharide-H+ symporter	GMGI.052909	21	13.27	5.37	1.3E-04	-1.31
TC19189	A2Q3R8	Vesicle transport v-SNARE; t-snare	PHVGI.052909	26	47.35	19.17	3.3E-13	-1.30
DB988154	O82485	Oligopeptide transporter 7	GMGI.052909	26	6.93	2.81	6.4E-03	-1.30
TC13277	Q9C5H4	VHS domain-containing protein At3g16270	PHVGI.052909	26	33.28	13.54	1.3E-09	-1.30
TC11034	A2Q1V6	Cysteine protease ATG4	PHVGI.052909	25	3.76	1.53	5.0E-02	-1.30
TC14563	Q84WV4	Putative uncharacterized protein At4g01810	PHVGI.052909	24	7.53	3.07	4.6E-03	-1.30
TC10913	Q107W9	Small basic intrinsic protein 1	PHVGI.052909	26	104.01	44.98	2.1E-24	-1.21
TC15784	A3DSX4	Sucrose transport protein SUF1	PHVGI.052909	26	18.43	8.18	3.3E-05	-1.17
TC14698	Q00M90	Membrane protein-like protein	PHVGI.052909	26	11.89	5.37	1.1E-03	-1.15
TC8923	Q94G17	TatC	PHVGI.052909	26	12.28	5.62	1.1E-03	-1.13
TC19270	Q2PEZ3	Putative importin alpha	PHVGI.052909	26	22.78	10.48	8.0E-06	-1.12
TC16855	Q59IV5	Plastidic phosphate translocator-like protein2	PHVGI.052909	26	22.19	10.22	1.1E-05	-1.12
TC12323	Q9ARM2	Putative component of high affinity nitrate transporter	PHVGI.052909	26	20.21	9.46	3.7E-05	-1.10
TC15883	Q7XJI9	Katanin	PHVGI.052909	26	51.71	24.53	6.3E-11	-1.08
TC9987	Q9SFU0	Protein transport protein Sec24-like At3g07100	PHVGI.052909	26	7.53	3.58	1.5E-02	-1.07
TC9855	Q8LPK1	Putative chloroplast outer membrane protein	PHVGI.052909	26	40.22	19.42	1.6E-08	-1.05
TC10954	Q9M8K5	F28L1.7 protein	PCGI.052909	22	15.65	7.67	5.7E-04	-1.03
TC9997	Q59I53	Mitochondrial F1-ATPase gamma subunit	PHVGI.052909	26	313.43	155.12	1.9E-53	-1.01
TC10369	Q69X19	Putative small calcium-binding mitochondrial carrier 2	PHVGI.052909	26	8.72	4.34	1.2E-02	-1.00

Stress/defense

TC29471	A2Q191	Short-chain dehydrogenase/reductase SDR	PHVGI.052909	25	82.02	0.00	7.2E-104	-10.68
TC12631	Q9C9V6	Putative uncharacterized protein T23K23.25	PHVGI.052909	26	4.16	0.00	6.6E-06	-6.38
EX304605	Q4TZI9	GIR1	PHVGI.052909	26	2.38	0.00	1.1E-03	-5.57
TC294705	Q39807	Protease inhibitor	GMGI.052909	24	1.98	0.00	3.6E-03	-5.31
TC19583	Q9FLI9	RAR1	PCGI.052909	26	1.19	0.00	3.6E-02	-4.57
TC19365	A2Q3R6	Poly(ADP-ribose) polymerase catalytic region	PHVGI.052909	25	1.19	0.00	3.6E-02	-4.57
TC302215	Q8GUW3	1-aminocyclopropane-1-carboxylic acid oxidase	GMGI.052909	25	1.19	0.00	3.6E-02	-4.57
TC11224	P24102	Peroxidase 22 precursor	PHVGI.052909	26	43.19	3.83	3.8E-37	-3.49
TC15192	Q9T0K6	Putative uncharacterized protein At4g13350	PHVGI.052909	26	2.18	0.26	1.3E-02	-3.09
BE821454		ATP-dependent DNA ligase; Metal-dependent phosphohydrolase, HD region; TGS; DNA polymerase III clamp loader subunit, C-terminal	allTIGR_Plant_2007	22	2.18	0.26	1.3E-02	-3.09
TC11803	A2Q4E5	Disease resistance protein	PHVGI.052909	22	18.43	2.30	1.2E-14	-3.00
TC10874	Q8GZ10	Putative uncharacterized protein	PHVGI.052909	26	3.96	0.51	6.3E-04	-2.95
TC16224	Q8GZF0	Resistance protein KR4	PHVGI.052909	21	1.98	0.26	2.1E-02	-2.95
NP7938883		low molecular weight heat shock protein PvHSP17-19;The partial cds predicted product is similar to the carboxy-half of plant-low molecular weight heat shock proteins; cytoplasmic class I lmw-HSP	PHVGI.052909	26	1.78	0.26	3.5E-02	-2.80
FK017125	Q84JS4	Putative uncharacterized protein At5g47740	GMGI.052909	26	1.78	0.26	3.5E-02	-2.80
TC16365	Q93VZ6	2-oxoglutarate-dependent dioxygenase	PHVGI.052909	22	3.17	0.51	4.4E-03	-2.63
TC2981	Q9ZUZ3	Putative auxin-regulated protein	PCGI.052909	22	3.17	0.51	4.4E-03	-2.63
TC346376	Q9SUC0	Probable 3-hydroxyisobutyrate dehydrogenase mitochondrial precursor	GMGI.052909	22	2.97	0.51	7.0E-03	-2.54
TC279546	A5BZY3	Glutamyl-tRNA reductase	GMGI.052909	22	4.36	0.77	9.4E-04	-2.51
TC13684	Q4LAW5	Putative ethylene response protein	PHVGI.052909	26	3.96	0.77	2.4E-03	-2.37
TC44083	Q9MF85	Orf155b protein	LJGI.052909	26	2.38	0.51	2.8E-02	-2.22
CV542275	Q6YIA0	Disease resistance protein-like protein MsR1	PHVGI.052909	26	3.37	0.77	8.9E-03	-2.14
TC9474	Q9XFL5	Peroxidase 4	PHVGI.052909	26	8.52	2.04	2.8E-05	-2.06
TC21187	Q2HUD2	Heat shock protein Hsp70	PCGI.052909	22	3.96	1.02	6.9E-03	-1.95
TC17196	Q7XIG4	Putative uncharacterized protein OJ1339_F05.122	PHVGI.052909	26	4.95	1.28	2.3E-03	-1.95
TC13759	Q9C588	Putative uncharacterized protein At5g21990	PHVGI.052909	26	6.74	1.79	4.1E-04	-1.91
TC16553	Q40374	Pathogenesis-related protein PR-1 precursor	PHVGI.052909	26	88.36	23.51	3.5E-39	-1.91
TC14728	Q8LJ85	Putative calreticulin	PHVGI.052909	26	22.78	6.39	1.2E-10	-1.83
TC16074	Q2HT58	Putative lectin-related	PHVGI.052909	26	4.56	1.28	5.2E-03	-1.83
FE683413	O22987	T19F6.16 protein	PHVGI.052909	26	6.14	1.79	1.3E-03	-1.78
TC13919	UPI000034F043	ATPP2-A13	PHVGI.052909	26	3.37	1.02	2.3E-02	-1.72
TC22064	Q6RYA0	Salicylic acid-binding protein 2	PHVGI.052909	22	3.17	1.02	3.4E-02	-1.63
TC290953	Q8LCK4	Growth-on protein GRO10	GMGI.052909	22	5.55	1.79	4.2E-03	-1.63
TC14171	Q9AVG9	S-adenosyl-L-methionine:salicylic acid carboxyl methyltransferase	PHVGI.052909	26	12.48	4.09	1.5E-05	-1.61
CB541638	A2Q365	BTB/POZ; Superoxide dismutase, copper/zinc binding; NPH3	PHVGI.052909	26	13.08	4.34	1.1E-05	-1.59

TC10353	Q9C8L4	Putative hydroxyacylglutathione hydrolase 3 mitochondrial precursor	PHVGI.052909	26	5.35	1.79	6.0E-03	-1.58
TC332012	A7TUG5	AT-hook DNA-binding protein	GMGI.052909	22	4.56	1.53	1.2E-02	-1.57
TC11141	Q9FH12	Axi 1 (Auxin-independent growth promoter)-like protein	PHVGI.052909	26	7.53	2.56	1.1E-03	-1.56
TC288269	A5BZK7	Putative uncharacterized protein	GMGI.052909	26	3.76	1.28	2.4E-02	-1.56
TC11217	Q5QIA9	Peroxisomal ascorbate peroxidase	PHVGI.052909	26	2.97	1.02	5.0E-02	-1.54
TC122315	Q8S529	Cytosolic aldehyde dehydrogenase RF2D	MTGI.071708	23	21.40	7.67	8.3E-08	-1.48
TC14498	Q94AY3	E3 ubiquitin protein ligase DRIP2	PHVGI.052909	26	15.45	5.62	7.1E-06	-1.46
FD787258	A5BHU7	Putative uncharacterized protein	PHVGI.052909	26	9.51	3.58	6.4E-04	-1.41
TC8424	O65158	1-aminocyclopropane-1-carboxylate oxidase	PHVGI.052909	26	31.90	12.01	2.6E-10	-1.41
TC8310	Q9FQF9	Lipoxygenase	PHVGI.052909	26	141.66	53.67	1.8E-40	-1.40
TC18289	O04076	ACC-oxidase	PHVGI.052909	26	10.10	3.83	4.7E-04	-1.40
GO025552	Q9SYU1	Pathogenesis-related protein	LJGI.052909	24	5.35	2.04	1.3E-02	-1.39
TC16767	A9PG97	Putative uncharacterized protein	PHVGI.052909	26	13.27	5.11	6.9E-05	-1.38
CV533361	Q6T2Z6	Cyclin d3	PHVGI.052909	26	15.26	5.88	1.9E-05	-1.38
CV538151	Q6TAF8	Blight resistance protein SH20	PHVGI.052909	26	3.96	1.53	3.5E-02	-1.37
TC37655	Q9LJU1	Similarity to nodulin	LJGI.052909	22	17.63	6.90	5.6E-06	-1.35
TC8324	O49385	Putative uncharacterized protein F10N7.120	PHVGI.052909	26	4.56	1.79	2.5E-02	-1.35
CA653043	Q67WR2	Probable GDP-L-fucose synthase 1	allTIGR_Plant_2009	21	9.71	3.83	9.0E-04	-1.34
TC11087	Q9M1T6	Serine/proline-rich	PHVGI.052909	25	5.15	2.04	1.8E-02	-1.33
TC9928	A5C9U1	Putative uncharacterized protein	PHVGI.052909	26	8.32	3.32	2.4E-03	-1.32
TC14053	Q9LYR4	Transaldolase-like protein	PHVGI.052909	26	216.75	88.68	4.9E-54	-1.29
TC15955	Q940E6	Putative defense associated acid phosphatase	PHVGI.052909	26	4.36	1.79	3.5E-02	-1.28
TC281580	Q6T2Z7	Cyclin d2	GMGI.052909	26	4.36	1.79	3.5E-02	-1.28
TC17645	A2Q440	Harpin-induced 1	PHVGI.052909	26	200.10	82.29	1.4E-49	-1.28
TC17290	Q9ZR17	Putative alcohol dehydrogenase	PHVGI.052909	26	15.45	6.39	5.0E-05	-1.27
TC8780	Q43680	Mung bean seed albumin	PHVGI.052909	26	780.01	324.30	1.7E-184	-1.27
GD411322	Q2HU33	Kinesin motor region	PCGI.052909	26	6.14	2.56	1.2E-02	-1.27
BI969381	A5BUB4	Putative uncharacterized protein	GMGI.052909	25	6.74	2.81	8.8E-03	-1.26
TC322953	A5ASZ0	Putative uncharacterized protein	GMGI.052909	22	9.71	4.09	1.7E-03	-1.25
TC9526	A6XER5	ERAD RING E3	PHVGI.052909	26	17.43	7.41	2.6E-05	-1.23
TC10368	Q9LXC9	Soluble inorganic pyrophosphatase 1 chloroplast precursor	PHVGI.052909	26	63.60	27.09	6.8E-16	-1.23
TC15478	Q705X3	Rho GDP dissociation inhibitor 2	PHVGI.052909	26	5.94	2.56	1.7E-02	-1.22
TC19758	Q6W5F3	Microtubule-associated protein 1 light chain 3	PHVGI.052909	26	4.16	1.79	4.8E-02	-1.22
TC15317	Q39807	Protease inhibitor	PHVGI.052909	26	411.90	180.68	2.6E-89	-1.19
TC14724	Q45EZ4	RAV-like DNA-binding protein	PHVGI.052909	26	185.64	82.03	1.2E-40	-1.18
TC11602	Q9ZWN0	GPI-anchored protein	PHVGI.052909	26	6.93	3.07	1.2E-02	-1.18
TC11733	A7Q2Q0	Thioredoxin domain 2; Thioredoxin fold	PHVGI.052909	26	32.89	14.57	2.4E-08	-1.17
TC15099	Q3IA99	Disease resistance protein	PHVGI.052909	26	4.56	2.04	4.7E-02	-1.16

TC9649	Q40367	Peroxidase precursor	PHVGI.052909	26	87.77	39.87	4.5E-19	-1.14
TC11030	Q9ZS51	Peroxisomal membrane protein PMP22	PHVGI.052909	26	12.88	5.88	7.7E-04	-1.13
TC16721	A8IXV1	Universal stress protein family protein	PHVGI.052909	26	6.14	2.81	2.2E-02	-1.13
TC12210	A5AUY6	Putative uncharacterized protein	PHVGI.052909	22	14.46	6.64	3.9E-04	-1.12
TC11911	A2Q503	Heat shock protein DnaJ	PHVGI.052909	26	10.50	4.86	2.8E-03	-1.11
TC18706	Q0GXX6	Auxin conjugate hydrolase	PHVGI.052909	23	4.95	2.30	4.5E-02	-1.11
TC14703	Q7X9S5	Fiber protein Fb15	PHVGI.052909	26	23.58	10.99	7.4E-06	-1.10
TC15140	Q52UN1	Cyclin-related protein 1	PHVGI.052909	24	95.10	44.47	1.9E-19	-1.10
EG594345	Q9LFF9	Inorganic pyrophosphatase-like protein	PHVGI.052909	25	118.87	55.97	1.4E-23	-1.09
CV543400	Q9SJA7	Probable sarcosine oxidase	PHVGI.052909	26	25.16	12.01	6.4E-06	-1.07
TC16783	Q2LD62	Putative copper ion-binding laccase	PHVGI.052909	26	50.12	24.02	2.0E-10	-1.06
CB540029	Q9FSZ6	Putative mitochondrial glyoxalase II	PHVGI.052909	26	8.52	4.09	9.9E-03	-1.06
TC19695	Q2PER1	Putative uncharacterized protein	PHVGI.052909	22	30.31	14.57	8.5E-07	-1.06
TC20143	Q9ZNZ6	Peroxidase precursor	PHVGI.052909	26	9.31	4.60	9.0E-03	-1.02
Carbonhydrate metabolism								
TC9251	Q94FP3	Succinate dehydrogenase subunit 3	PHVGI.052909	26	2.77	0.51	1.1E-02	-2.44
TC293059	O64897	Trehalose-6-phosphate phosphatase	GMGI.052909	22	8.72	2.56	1.2E-04	-1.77
TC9013	A8C8H3	Glutamate decarboxylase	PHVGI.052909	26	3.17	1.02	3.4E-02	-1.63
TC11712	Q5NE21	Carbonic anhydrase	PHVGI.052909	26	8.72	2.81	2.8E-04	-1.63
FD787806	O23503	Glucosyltransferase like protein	PHVGI.052909	26	3.76	1.28	2.4E-02	-1.56
FE692167	P54242	Glucose-6-phosphate isomerase, cytosolic 2	PHVGI.052909	22	18.82	7.41	3.0E-06	-1.34
FD787253	Q38IX1	Glyceraldehyde-3-phosphate dehydrogenase A subunit	PHVGI.052909	26	5.75	2.30	1.3E-02	-1.32
TC10657	Q9ZNX1	NAD-dependent isocitrate dehydrogenase precursor	PHVGI.052909	26	8.92	3.83	3.2E-03	-1.22
TC10870	A7NYM8	Enolase	PCGI.052909	26	9.11	4.09	4.2E-03	-1.16
Energy metabolism								
TA56_74648		Ribulose bisphosphate carboxylase small chains, chloroplast precursor	allTIGR_Plant_2007	22	1.59	0.00	1.1E-02	-4.99
TC287515	Q7Y0D4	Putative thioredoxin	GMGI.052909	22	1.59	0.00	1.1E-02	-4.99
TC282091	Q2MJ17	Cytochrome P450 monooxygenase CYP72A65	GMGI.052909	22	1.19	0.00	3.6E-02	-4.57
TC11165	Q2LAL2	Cytochrome P450 monooxygenase CYP76O2	PHVGI.052909	26	2.38	0.26	7.7E-03	-3.22
CV543462	Q6WNQ8	CYP81E8	PHVGI.052909	26	1.78	0.26	3.5E-02	-2.80
TC207787	Q96035	Cytochrome oxidase subunit 3	allTIGR_Plant_2009	23	56.86	8.69	2.3E-38	-2.71
TC14609	A0MAV5	Allene oxide synthase	PHVGI.052909	26	5.94	1.02	8.4E-05	-2.54
CV532273	Q9ZRV5	Basic blue copper protein	PHVGI.052909	26	2.58	0.51	1.8E-02	-2.33
TC8882	Q5PYQ	Chloroplast oxygen-evolving enhancer protein	PHVGI.052909	26	2.38	0.51	2.8E-02	-2.22
TC17696	P14226	Oxygen-evolving enhancer protein 1, chloroplast precursor	PHVGI.052909	26	3.37	0.77	8.9E-03	-2.14
TC40879	Q6YSJ7	NADH dehydrogenase subunit 7	LJGI.052909	26	4.56	1.28	5.2E-03	-1.83
TC18728	Q2LAK0	Cytochrome P450 monooxygenase CYP701A16	PHVGI.052909	26	130.36	41.40	3.5E-47	-1.65
FG230417	O81971	Cytochrome P450 71D9	PHVGI.052909	26	7.73	2.81	1.7E-03	-1.46

FE898928	P42027	NADH-ubiquinone oxidoreductase 20 kDa subunit, mitochondrial precursor	PHVGI.052909	26	4.75	1.79	1.8E-02	-1.41
TC18940	Q9SWS4	Ripening related protein	PHVGI.052909	22	27.14	10.73	2.1E-08	-1.34
TC11202	Q41001	Blue copper protein precursor	PHVGI.052909	26	64.98	27.09	8.6E-17	-1.26
TC23125	Q8S4C0	Isoflavone synthase	PHVGI.052909	26	956.53	421.41	3.6E-203	-1.18
TC14299	Q2MJ18	Cytochrome P450 monooxygenase CYP72A59	PHVGI.052909	26	11.29	5.11	1.5E-03	-1.14
TC12823	Q69WE3	NADH-ubiquinone oxidoreductase-related-like protein	PHVGI.052909	26	210.80	96.60	7.4E-43	-1.13
TC17597	O65576	ABC1 protein	PHVGI.052909	26	5.55	2.56	3.1E-02	-1.12
CB541671	O49394	Cytochrome P450-like protein	PHVGI.052909	26	7.53	3.58	1.5E-02	-1.07
TC9515	Q7XZW1	Putative NADH dehydrogenase	PHVGI.052909	26	171.18	83.05	2.9E-31	-1.04
FG232344	Q9ZRV5	Basic blue copper protein	PHVGI.052909	26	8.32	4.09	1.3E-02	-1.03
Amino acid metabolism								
BQ856324	A1YYP7	Glutamine synthetase	allTIGR_Plant_2009	21	1.39	0.00	2.0E-02	-4.79
FE680918	Q9LJQ4	Muconate cycloisomerase-like protein	PHVGI.052909	26	1.19	0.00	3.6E-02	-4.57
TC11839	O49543	Cysteine desulfurase 1 mitochondrial precursor	PHVGI.052909	26	2.77	0.51	1.1E-02	-2.44
TC10435	Q5F2M9	Glutamate dehydrogenase 1	PHVGI.052909	26	17.43	4.86	1.7E-08	-1.84
TC17707	P19143	Phenylalanine ammonia-lyase class 3	PHVGI.052909	26	7.33	2.30	7.4E-04	-1.67
TC11346	Q6JJ29	Prephenate dehydratase	PHVGI.052909	26	15.65	5.37	2.4E-06	-1.54
TC9914	Q6ULR9	SAT5	PHVGI.052909	26	32.69	11.50	1.7E-11	-1.51
TC17998	Q9FLY0	Similarity to ornithine cyclodeaminase	PHVGI.052909	26	11.49	4.34	1.8E-04	-1.40
TC16047	Q9LIR4	Dihydroxy-acid dehydratase	PHVGI.052909	22	18.03	6.90	2.9E-06	-1.39
TC8559	Q9FFW8	Tryptophan synthase beta chain	PHVGI.052909	22	9.51	3.83	1.2E-03	-1.31
TC13526	Q5QLG0	Membrane protein-like	PHVGI.052909	26	4.16	1.79	4.8E-02	-1.22
CB539420	A5YT88	Cysteine synthase	PHVGI.052909	26	14.66	6.39	1.7E-04	-1.20
TC10982	A4PU48	S-adenosyl-L-methionine synthetase	PHVGI.052909	26	335.62	162.53	6.5E-60	-1.05
TC16647	Q05758	Ketol-acid reductoisomerase, chloroplast precursor	PHVGI.052909	26	7.33	3.58	1.9E-02	-1.03
Lipid metabolism								
TC14544	Q84V30	Phosphatidylserine decarboxylase	PHVGI.052909	26	1.19	0.00	3.6E-02	-4.57
GD452583	Q0WWR0	Very-long-chain fatty acid condensing enzyme CUT1 like protein	PCGI.052909	26	6.93	0.77	1.8E-06	-3.18
TC19714	Q49IM2	Lipase 1	PHVGI.052909	26	1.98	0.26	2.1E-02	-2.95
TC18367	A2Q1D5	Esterase/lipase/thioesterase	PHVGI.052909	26	1.98	0.26	2.1E-02	-2.95
TC36057	Q43804	Oleosin 1	allTIGR_Plant_2009	21	1.98	0.26	2.1E-02	-2.95
FD796484	Q7XEM4	Fatty acid elongase putative expressed	PHVGI.052909	26	2.38	0.51	2.8E-02	-2.22
FE899153	UPI000034F5BC	phospholipase C	PHVGI.052909	26	2.18	0.51	4.3E-02	-2.09
TC11439	Q9M7D7	Non-specific lipid-transfer protein	PHVGI.052909	21	2.18	0.51	4.3E-02	-2.09
TC18234	Q41244	Lipoxygenase	PHVGI.052909	26	16.64	4.60	3.2E-08	-1.86
TC8686	Q8LBT8	Putative phosphatidylglycerotransferase	PHVGI.052909	26	2.77	0.77	3.2E-02	-1.86
TC14436	A2WVB6	Putative uncharacterized protein	PHVGI.052909	26	9.91	2.81	2.9E-05	-1.82
TC9699	A2Y6K4	Putative uncharacterized protein	PHVGI.052909	22	5.35	1.53	2.6E-03	-1.80

TC307431	O04946	Enoyl-ACP reductase precursor	GMGI.052909	26	4.36	1.53	1.7E-02	-1.51
TC278147	Q8L3X9	3-oxoacyl-[acyl-carrier-protein] synthase mitochondrial precursor	GMGI.052909	21	7.13	2.56	2.3E-03	-1.48
TC12878	Q2HUX9	Esterase/lipase/thioesterase	PHVGI.052909	26	5.94	2.30	9.0E-03	-1.37
TC15306	A5C9Q5	Putative uncharacterized protein	PHVGI.052909	26	11.09	4.34	3.4E-04	-1.35
TC10580	A4Q7K6	Plant lipid transfer/seed storage/trypsin-alpha amylase inhibitor	PHVGI.052909	26	234.77	100.94	1.4E-53	-1.22
TC13495	A1L4Y2	Alcohol dehydrogenase-like 3	PHVGI.052909	26	5.55	2.56	3.1E-02	-1.12
Secondary metabolism								
TC331881	P19142	Phenylalanine ammonia-lyase class 2	GMGI.052909	21	1.19	0.00	3.6E-02	-4.57
TC8948	A9PJ96	Putative uncharacterized protein	PHVGI.052909	26	7.53	1.02	1.9E-06	-2.88
TC10052	P49440	Chalcone synthase 17	PHVGI.052909	26	185.24	61.59	1.1E-62	-1.59
TC9356	P31687	4-coumarate--CoA ligase 2	PHVGI.052909	26	13.08	5.11	9.5E-05	-1.36
TC1678	A2Q2G0	Strictosidine synthase	PCGI.052909	26	14.46	5.88	6.9E-05	-1.30
TC12466	O22810	Putative cinnamoyl-CoA reductase	PHVGI.052909	26	3.76	1.53	5.0E-02	-1.30
CB540276	Q944G3	Acetyl Co-A acetyltransferase	PHVGI.052909	26	3.76	1.53	5.0E-02	-1.30
TC15519	Q3HRZ0	Putative cinnamoyl-CoA reductase-like protein	PHVGI.052909	26	102.03	42.93	4.1E-25	-1.25
TC302697	Q5MK23	ARV1	GMGI.052909	21	7.13	3.32	1.5E-02	-1.10
Other metabolisms								
TC344920	Q2QU89	Pentatricopeptide putative expressed	GMGI.052909	21	1.59	0.00	1.1E-02	-4.99
CV540513	Q8W2E3	3-hydroxy-3-methylglutaryl coenzyme A	PHVGI.052909	26	2.77	0.26	2.8E-03	-3.44
TC14454	Q6KAW1	Putative esterase	PHVGI.052909	26	13.08	1.53	5.3E-11	-3.09
TC11311	Q682L2	Monooxygenase putatve	PHVGI.052909	26	8.72	3.32	1.2E-03	-1.39
TC10033	Q6E593	Benzoyl coenzyme A: benzyl alcohol benzoyl transferase	PHVGI.052909	26	17.63	7.92	6.0E-05	-1.15
TC10717	Q6KAW1	Putative esterase	PHVGI.052909	26	21.00	9.46	1.2E-05	-1.15
TC17573	Q9FGI4	Genomic DNA chromosome 5 P1 clone:MPA22	PHVGI.052909	26	581.89	262.71	1.3E-118	-1.15
TC18184	Q5DQ95	4-amino-4-deoxychorismate lyase	PHVGI.052909	26	18.23	8.69	1.2E-04	-1.07
FG230474	A2Q3Y3	NAD-dependent epimerase/dehydratase	PHVGI.052909	26	13.08	6.39	1.6E-03	-1.03
Cell wall synthesis, organization								
TC286839	Q9FF77	Pectinesterase	GMGI.052909	24	4.16	0.00	6.6E-06	-6.38
CV531082	Q9M9Y5	Probable galacturonosyltransferase 6	PHVGI.052909	26	2.97	0.00	2.1E-04	-5.89
FG230794	Q8GTJ0	Xyloglucan endotransglycosylase	PHVGI.052909	26	27.74	0.77	6.0E-31	-5.18
TC193775	A7BJ77	Xylanase inhibitor	allTIGR_Plant_2009	26	1.59	0.00	1.1E-02	-4.99
TC287478	A4ZYQ7	Secondary wall-associated glycosyltransferase family 8D	GMGI.052909	26	1.59	0.00	1.1E-02	-4.99
TC338675	Q6XP47	Cellulose synthase	GMGI.052909	26	1.39	0.00	2.0E-02	-4.79
TC341207	Q10B12	Glycoside hydrolase family 28 protein putative expressed	GMGI.052909	22	1.19	0.00	3.6E-02	-4.57
TC12228	Q9LKY8	Proline-rich protein	PHVGI.052909	26	26.55	1.53	3.2E-26	-4.11
TC323585	Q940Q8	AT5g61840/mac9_140	GMGI.052909	23	3.17	0.26	9.8E-04	-3.63
TC11172	Q03773	Glucan endo-1,3-beta-glucosidase precursor ((1->3)-beta- glucan endohydrolase) ((1->3)-beta-glucanase)	PHVGI.052909	26	122.64	10.22	5.6E-105	-3.58
AM797506	Q8LF99	Probable xyloglucan endotransglucosylase/hydrolase protein 6 precursor	allTIGR_Plant_2009	23	7.92	0.77	1.5E-07	-3.37

195

TC330165	Q9FVQ2	Endo-beta-1 4-glucanase putative	GMGI.052909	22	2.38	0.26	7.7E-03	-3.22
TC331628	A2SY66	Vicianin hydrolase	GMGI.052909	21	2.58	0.51	1.8E-02	-2.33
TC333567	Q9M0F7	Extensin-like protein	GMGI.052909	22	7.53	1.53	2.6E-05	-2.30
TC10943	Q43070	UDP-glucose 4-epimerase	PHVGI.052909	26	2.38	0.51	2.8E-02	-2.22
TC16298	Q9LUI1	Extensin protein-like	PHVGI.052909	26	3.37	0.77	8.9E-03	-2.14
TC280687	A0ZNK1	Pectin methylesterase 3	GMGI.052909	25	34.08	8.18	1.7E-17	-2.06
TC13942	Q9AR81	Germin-like protein precursor	PHVGI.052909	26	5.15	1.53	3.9E-03	-1.75
TC284857	Q9FF78	Pectinesterase	GMGI.052909	26	5.75	1.79	2.9E-03	-1.68
CV538457	Q9ZT82	Putative glucan synthase component	PHVGI.052909	25	4.75	1.53	8.3E-03	-1.63
TC306127	Q8LK71	Extensin-like protein	GMGI.052909	21	148.00	51.62	2.1E-47	-1.52
TC15321	Q5TIN3	Alpha-1 6-xylosyltransferase	PHVGI.052909	26	54.88	19.42	3.3E-18	-1.50
FE677604	Q8GUZ9	Cellulose synthase-like protein D4	PHVGI.052909	26	6.34	2.30	4.5E-03	-1.46
TC14646	Q6EPQ1	dTDP-D-glucose 4 6-dehydratase-like	PHVGI.052909	22	333.64	124.71	7.5E-95	-1.42
FE697591	Q09WE7	UDP-sugar pyrophosphorylase 1	PHVGI.052909	26	12.48	5.11	2.5E-04	-1.29
TC8333	Q5ZQK6	Fructan 1-exohydrolase	PHVGI.052909	26	18.23	7.67	1.4E-05	-1.25
TC193875	Q5NE19	1,4-alpha-glucan-maltohydrolase	allTIGR_Plant_2009	21	115.90	48.81	2.9E-28	-1.25
TC12227	A1YZ21	Xyloglucan endotransglycosylase precursor	PCGI.052909	25	121.65	51.37	1.8E-29	-1.24
TC19294	A5C6V7	Galactose-1-phosphate uridylyltransferase	PHVGI.052909	26	28.93	12.27	5.0E-08	-1.24
TC18794	Q9SCP2	Probable pectate lyase 12 precursor	PHVGI.052909	26	5.94	2.56	1.7E-02	-1.22
TC16408	Q0GA85	Glycoside hydrolase family 1 protein	PHVGI.052909	26	4.16	1.79	4.8E-02	-1.22
TC22207	O50044	2-dehydro-3-deoxyphosphooctonate aldolase	PHVGI.052909	24	4.16	1.79	4.8E-02	-1.22
TC17835	Q8S9A5	Glucosyltransferase like protein	PHVGI.052909	26	6.93	3.07	1.2E-02	-1.18
TC17044	Q9FSZ9	Putative extracellular dermal glycoprotein	PHVGI.052909	26	82.22	36.80	1.9E-18	-1.16
TC15956	Q9LYF6	Arabinogalactan peptide 15 precursor	PHVGI.052909	26	2186.08	991.80	0.0E+00	-1.14
TC8422	Q7XAS3	Beta-D-glucosidase	PHVGI.052909	26	82.62	38.59	4.0E-17	-1.10
TC15078	Q9ARU3	Putative xylosyltransferase I	PHVGI.052909	26	42.00	19.68	2.4E-09	-1.09
TC12406	Q41120	Hydroxyproline-rich glycoprotein	PHVGI.052909	26	275.39	129.56	1.4E-52	-1.09
TC18996	A2TEJ5	Xyloglucan endotransglycosylase/hydrolase XTH-21	PHVGI.052909	26	198.72	94.81	2.5E-37	-1.07
CV542742	Q5MB21	Xyloglucan endotransglucosylase/hydrolase	PHVGI.052909	22	23.58	4.86	5.3E-14	-2.28
TC14600	Q09083	Hydroxyproline-rich glycoprotein precursor	PHVGI.052909	26	1591.12	785.57	3.9E-265	-1.02
TC17940	Q9FNT1	Alpha-expansin	PHVGI.052909	26	58.45	28.88	3.1E-11	-1.02

Replication and Repair

TC292156	Q9LTW3	DNA-3-methyladenine glycosidase I-like protein	GMGI.052909	24	99.85	40.12	1.6E-26	-1.32
TC19575	Q9FK21	Similarity to WD-containing protein	PHVGI.052909	26	33.28	13.80	2.4E-09	-1.27

Cytoskeleton

CX548387	Q9M7M9	Profilin-4	GMGI.052909	26	3.96	0.00	1.2E-05	-6.31
TC10981	Q6F4H4	Actin	PHVGI.052909	26	19.81	8.43	7.3E-06	-1.23
TC19436	Q5VKJ6	Actin	PHVGI.052909	25	17.43	7.92	7.9E-05	-1.14

Protein translation, processing and degradation

TC14499	A5CBL0	Putative uncharacterized protein	PHVGI.052909	25	10.50	0.00	6.9E-14	-7.71
TC21212	P25698	Elongation factor 1-alpha	PHVGI.052909	24	3.37	0.00	6.5E-05	-6.07
TC308772	Q06H23	Ubiquitin carrier protein	GMGI.052909	26	2.18	0.00	2.0E-03	-5.45
TC24604	Q9AV87	60S ribosomal protein L21	PHVGI.052909	24	1.98	0.00	3.6E-03	-5.31
EG562984	Q2PYP4	RING-box protein	PHVGI.052909	24	1.78	0.00	6.4E-03	-5.16
BE037973	A1YMY0	Ribosomal protein S27	allTIGR_Plant_2009	21	1.59	0.00	1.1E-02	-4.99
CA912233	Q8RWZ2	U-box domain-containing protein 39	PCGI.052909	26	1.39	0.00	2.0E-02	-4.79
TC337490	Q2HVS3	Ribosomal protein L34e	GMGI.052909	25	1.39	0.00	2.0E-02	-4.79
TC25027	Q7X9K1	Ribosomal Pr 117	PHVGI.052909	24	1.39	0.00	2.0E-02	-4.79
CV539942	Q6Z2M5	Putative small nuclear ribonucleoprotein polypeptide E	PHVGI.052909	26	1.19	0.00	3.6E-02	-4.57
TC117538	Q0DBP0	Ribosomal protein L1	allTIGR_Plant_2009	21	1.19	0.00	3.6E-02	-4.57
TC23167	O23714	Proteasome subunit beta type-2-A	PHVGI.052909	24	2.58	0.26	4.6E-03	-3.33
FD794444	Q8GWV5	U-box domain-containing protein 3	PHVGI.052909	26	1.78	0.26	3.5E-02	-2.80
TC291152	Q5XF85	RING-H2 finger protein ATL4J precursor	GMGI.052909	24	1.78	0.26	3.5E-02	-2.80
TC16624	P29344	30S ribosomal protein S1 chloroplast precursor	PHVGI.052909	26	3.17	0.51	4.4E-03	-2.63
TC9894	UPI000016329 1	S1 RNA-binding domain-containing protein	PHVGI.052909	26	2.77	0.51	1.1E-02	-2.44
TC16868	Q9LJL8	Emb|CAB43653.1	PHVGI.052909	26	2.58	0.51	1.8E-02	-2.33
TC18164	A5BMQ9	Putative uncharacterized protein	PHVGI.052909	26	3.37	0.77	8.9E-03	-2.14
TC19842	UPI0000196D 09	ubiquitin family protein	PHVGI.052909	26	2.18	0.51	4.3E-02	-2.09
TC9060	Q9LN71	E3 ubiquitin-protein ligase At1g12760	PHVGI.052909	26	11.49	2.81	1.2E-06	-2.03
FD788585	Q9FPS4	Ubiquitin carboxyl-terminal hydrolase 23	PHVGI.052909	26	3.96	1.02	6.9E-03	-1.95
TC309913	A5BJG3	Putative uncharacterized protein	GMGI.052909	22	63.20	18.40	4.8E-26	-1.78
TC284112		18S ribosomal RNA gene	GMGI.052909	26	9.71	3.07	1.0E-04	-1.66
TC20536	A0EVX1	EBP1	PHVGI.052909	24	3.17	1.02	3.4E-02	-1.63
TC341074	Q93Y09	Serine carboxypeptidase-like 45 precursor	GMGI.052909	22	4.75	1.53	8.3E-03	-1.63
TC16753	Q9LZ26	Aspartyl aminopeptidase-like protein	PHVGI.052909	26	3.96	1.28	1.7E-02	-1.63
TC17117	Q6YS30	DEAD-box ATP-dependent RNA helicase 5	PHVGI.052909	26	5.55	1.79	4.2E-03	-1.63
TC15199	P25698	Elongation factor 1-alpha	PHVGI.052909	24	3.96	1.28	1.7E-02	-1.63
TC8681	A5C114	Putative uncharacterized protein	PHVGI.052909	26	8.52	2.81	4.1E-04	-1.60
TC18451	Q4U4M3	Subtilisin-like protease	PHVGI.052909	26	19.22	6.64	2.0E-07	-1.53
TC11765	A9P931	Putative uncharacterized protein	PHVGI.052909	26	178.71	71.30	1.0E-46	-1.33
TC9895	A4Q7L2	ANTH	PHVGI.052909	26	29.32	12.01	1.5E-08	-1.29
TC12933	O64982	26S protease regulatory subunit 7	PHVGI.052909	26	25.56	10.48	1.3E-07	-1.29
TC23006	Q2XTB8	Putative translation initiation factor eIF-1A-like	PHVGI.052909	24	4.95	2.04	2.5E-02	-1.28
TC11736	O48844	26S proteasome regulatory subunit (RPN2) putative	PHVGI.052909	26	101.64	42.93	7.4E-25	-1.24
TC17712	Q67Y83	Serine carboxypeptidase-like 51 precursor	PHVGI.052909	24	54.29	23.00	6.7E-14	-1.24

TC8674	A5BSZ9	Putative uncharacterized protein	PHVGI.052909	26	4.16	1.79	4.8E-02	-1.22
TC12872	O49607	Subtilisin proteinase-like	PHVGI.052909	25	12.88	5.88	7.7E-04	-1.13
TC17844	Q8LBL5	E3 ubiquitin-protein ligase PRT1	PHVGI.052909	26	43.98	20.96	2.0E-09	-1.07
FG230469	Q677B0	Ribosomal protein L18A	PHVGI.052909	26	9.11	4.34	7.2E-03	-1.07
TC10973	Q6RJY1	60S ribosomal protein L12	PHVGI.052909	26	864.80	413.74	1.5E-155	-1.06
TC15721	A2XAA7	Putative uncharacterized protein	PHVGI.052909	26	194.56	94.04	1.4E-35	-1.05
TC10535	Q8LJR8	RING-H2 finger protein	PHVGI.052909	26	18.23	8.94	2.0E-04	-1.03
TC17712	A8MR86	Uncharacterized protein At2g27920.2	PHVGI.052909	26	65.18	32.46	3.5E-12	-1.01
TC282796	Q84LM4	Acylamino acid-releasing enzyme	GMGI.052909	22	6.14	3.07	3.8E-02	-1.00

Nucleotide Metabolism

TC12836	P51820	Bifunctional dihydrofolate reductase-thymidylate synthase (DHFR-TS) [Includes: Dihydrofolate reductase ; Thymidylate synthase]	PHVGI.052909	26	6.14	2.30	6.4E-03	-1.42
CV536867	Q9SMC1	Quinolinate phosphoribosyltransferase	PHVGI.052909	26	8.32	3.32	2.4E-03	-1.32
TC11440	Q8VZX0	Adenylosuccinate-AMP lyase	PHVGI.052909	26	25.36	11.76	2.9E-06	-1.11
CX129670	Q52K88	Nudix hydrolase 13 mitochondrial precursor	PHVGI.052909	26	6.34	3.07	2.9E-02	-1.05

Protein posttranslational modification

TC17219	Q9LW62	Casein kinase	PHVGI.052909	26	2.77	0.00	3.6E-04	-5.79
TC17517	Q0WL08	Putative serine/threonine protein kinase	PHVGI.052909	26	2.18	0.00	2.0E-03	-5.45
TC9223	Q8GYA4	Cysteine-rich receptor-like protein kinase 10 precursor	PHVGI.052909	26	1.39	0.00	2.0E-02	-4.79
TC8754	A5B005	Putative uncharacterized protein	PHVGI.052909	26	3.37	0.51	2.7E-03	-2.72
TC135907	Q9LDC1	CRK1 protein	MTGI.071708	23	8.12	1.28	1.9E-06	-2.67
FG230882	Q9SUI2	Phosphatidylinositol-4-phosphate 5-kinase 7	PHVGI.052909	26	3.96	0.77	2.4E-03	-2.37
TC12812	Q4VYF4	SNF1-related protein kinase regulatory beta subunit 1	PHVGI.052909	26	4.95	1.02	8.0E-04	-2.28
TC18854	Q5YD56	Calcium/calmodulin-regulated receptor-like kinase	PHVGI.052909	26	2.38	0.51	2.8E-02	-2.22
TC17809	Q7G6W1	Putative receptor-like protein kinase	PHVGI.052909	26	12.28	3.32	1.7E-06	-1.89
FE691898	Q1W203	NAK-type protein kinase	PHVGI.052909	26	3.76	1.02	1.0E-02	-1.88
TC11144	A5C729	Putative uncharacterized protein	PHVGI.052909	26	8.12	2.30	1.6E-04	-1.82
TC294508	Q1EPA3	Protein kinase family protein	GMGI.052909	21	3.37	1.02	2.3E-02	-1.72
TC16264	Q6UY57	Lectin-like receptor kinase 1;1	PHVGI.052909	26	20.21	6.13	6.8E-09	-1.72
TC318430	Q9LY50	Receptor kinase-like protein	GMGI.052909	24	9.91	3.07	7.0E-05	-1.69
TC14363	A5C4Y3	Putative uncharacterized protein	PHVGI.052909	26	27.74	8.69	2.4E-11	-1.67
TC11066	O82469	Protein phosphatase-2C	PHVGI.052909	26	3.17	1.02	3.4E-02	-1.63
CV543376	UPI0000197 0FF	Leucine-rich repeat transmembrane protein kinase putative	PHVGI.052909	26	6.34	2.04	2.1E-03	-1.63
TC15262	Q9LY50	Receptor kinase-like protein	PHVGI.052909	26	8.52	3.07	8.6E-04	-1.47
TC330616	Q9LVM0	Receptor-like protein kinase	GMGI.052909	26	4.16	1.53	2.5E-02	-1.44
FE708647	Q5JK52	Probable NAD kinase 1	PHVGI.052909	26	6.93	2.56	3.3E-03	-1.44
CV541472	O49449	Protein phosphatase 2C-like protein	PHVGI.052909	26	6.74	2.56	4.6E-03	-1.40
TC13115	Q9LKY3	Pti1 kinase-like protein	PHVGI.052909	26	135.52	52.13	6.7E-38	-1.38

NP7938857	Q9XED4	Receptor-like protein kinase homolog RK20-1	PHVGI.052909	26	66.57	26.07	6.6E-19	-1.35
TC12882	A5B9X1	Putative uncharacterized protein	PHVGI.052909	26	70.73	28.37	2.8E-19	-1.32
TC8807	Q8SA64	NIMA-related protein kinase	PHVGI.052909	26	6.93	2.81	6.4E-03	-1.30
TC14015	A2Q2Z4	Protein kinase	PHVGI.052909	26	24.37	9.97	2.5E-07	-1.29
TC312564	Q6RC06	Serine/threonine protein kinase	GMGI.052909	22	4.36	1.79	3.5E-02	-1.28
TC8488	Q2QLI7	Protein kinase domain containing protein expressed	PHVGI.052909	26	23.38	9.97	1.1E-06	-1.23
TC8736	Q6H6V1	Putative receptor protein kinase PERK	PHVGI.052909	26	26.75	11.50	2.3E-07	-1.22
TC317438	Q9ZU46	Putative receptor-like protein kinase	GMGI.052909	21	4.16	1.79	4.8E-02	-1.22
TC28410	Q0WPA7	Receptor-like protein kinase	PHVGI.052909	24	12.68	5.88	1.0E-03	-1.11
TC16580	Q5DUG7	Protein kinase-like protein	PHVGI.052909	26	173.36	81.01	3.4E-34	-1.10
FD789495	Q9LKZ6	Receptor-like protein kinase 1	PHVGI.052909	26	5.35	2.56	4.2E-02	-1.07
TC285184	Q0WR59	Receptor protein kinase-like	GMGI.052909	24	18.43	8.94	1.6E-04	-1.04
TC13879	O65846	Serine/threonine protein phosphatase	PHVGI.052909	26	7.33	3.58	1.9E-02	-1.03
TC18559	Q6QA01	CDPK-related protein kinase	PHVGI.052909	26	21.20	10.48	6.9E-05	-1.02
FE683462	Q1X8N2	Protein phosphatase 2C-related	PHVGI.052909	26	20.01	9.97	1.3E-04	-1.01
RNA processing and modification								
CV533429	UPI00001633 B7	RNA-binding protein putative	PHVGI.052909	26	2.97	1.02	5.0E-02	-1.54
TC333869	Q8H0U8	DEAD-box ATP-dependent RNA helicase 42	GMGI.052909	26	14.86	5.88	3.7E-05	-1.34
TC8503	Q2HRG6	RNA-binding region RNP-1	PHVGI.052909	22	7.92	3.58	8.1E-03	-1.15
Unknown/unclassfied								
EY729086		Unknown	allTIGR_Plant_2009	21	5.94	0.00	3.7E-08	-6.89
TC47075	A7QUR8	Chromosome chr1 scaffold_180	allTIGR_Plant_2009	22	4.16	0.00	6.6E-06	-6.38
GD375422		Unknown	PCGI.052909	23	2.97	0.00	2.1E-04	-5.89
TC14144		Chromosome chr16 scaffold_86	PHVGI.052909	26	2.58	0.00	6.5E-04	-5.69
TC38099	A7QFK2	Chromosome chr8 scaffold_88	allTIGR_Plant_2009	22	2.18	0.00	2.0E-03	-5.45
TC11837		Unknown	PCGI.052909	25	1.59	0.00	1.1E-02	-4.99
GD552168		Unknown	PCGI.052909	21	1.59	0.00	1.1E-02	-4.99
CK753482		Unknown	allTIGR_Plant_2007	21	1.59	0.00	1.1E-02	-4.99
TC159120	A7Q1N2	Chromosome chr7 scaffold_44	allTIGR_Plant_2009	22	1.59	0.00	1.1E-02	-4.99
CD396102		Hypothetical protein At5g19330	allTIGR_Plant_2007	21	1.59	0.00	1.1E-02	-4.99
CV536149	A7QR15	Chromosome undetermined scaffold_147	PHVGI.052909	26	1.39	0.00	2.0E-02	-4.79
TC16332	Q7X9C0	NIN-like protein 2	PHVGI.052909	26	1.39	0.00	2.0E-02	-4.79
TC345200	A5BAS1	Putative uncharacterized protein	GMGI.052909	25	1.39	0.00	2.0E-02	-4.79
TC288753		Unknown	GMGI.052909	22	1.39	0.00	2.0E-02	-4.79
CX708370		Unknown	GMGI.052909	24	1.39	0.00	2.0E-02	-4.79
CV521730		Unknown	allTIGR_Plant_2007	22	1.39	0.00	2.0E-02	-4.79
BP614541		Unknown	allTIGR_Plant_2009	21	1.39	0.00	2.0E-02	-4.79
DY619532	A7Q9M6	Chromosome chr5 scaffold_67	allTIGR_Plant_2009	22	1.39	0.00	2.0E-02	-4.79

TC8781	A2WQB8	Putative uncharacterized protein	PHVGI.052909	26	1.19	0.00	3.6E-02	-4.57
TC10348	O04133	SRC2	PHVGI.052909	26	1.19	0.00	3.6E-02	-4.57
CV543253	A5BPM3	Putative uncharacterized protein	PHVGI.052909	22	1.19	0.00	3.6E-02	-4.57
TC12180	A0EPI4	ERD15	PHVGI.052909	26	1.19	0.00	3.6E-02	-4.57
FE711194	A2Y909	Putative uncharacterized protein	PHVGI.052909	24	1.19	0.00	3.6E-02	-4.57
CB539173	Q9M3Z3	Putative PTS protein	PHVGI.052909	26	1.19	0.00	3.6E-02	-4.57
TC15735	A7PMF3	Chromosome chr14 scaffold_21	PHVGI.052909	25	1.19	0.00	3.6E-02	-4.57
GD294489		Unknown	PCGI.052909	26	1.19	0.00	3.6E-02	-4.57
GD635081		Unknown	PCGI.052909	26	1.19	0.00	3.6E-02	-4.57
TC345202	Q0WNN6	Putative uncharacterized protein At3g53010	GMGI.052909	22	1.19	0.00	3.6E-02	-4.57
TC326690		Unknown	GMGI.052909	21	1.19	0.00	3.6E-02	-4.57
TC338955	Q9XEX8	Remorin 1	GMGI.052909	26	1.19	0.00	3.6E-02	-4.57
TC322165	A7PY71	Chromosome chr15 scaffold_37	GMGI.052909	26	1.19	0.00	3.6E-02	-4.57
CV241221		Hypothetical protein At1g15200	allTIGR_Plant_2007	21	1.19	0.00	3.6E-02	-4.57
NP7273300			allTIGR_Plant_2009	22	1.19	0.00	3.6E-02	-4.57
TC46454	A7R1J7	Chromosome undetermined scaffold_359	allTIGR_Plant_2009	21	1.19	0.00	3.6E-02	-4.57
TC320212		Unknown	allTIGR_Plant_2009	23	1.19	0.00	3.6E-02	-4.57
TC16896		Unknown	allTIGR_Plant_2009	21	1.19	0.00	3.6E-02	-4.57
CV543094		Unknown	PHVGI.052909	26	4.56	0.26	2.4E-05	-4.16
GD649405		Unknown	PCGI.052909	22	4.16	0.26	7.0E-05	-4.02
GD311359		Unknown	PCGI.052909	25	8.12	0.77	8.8E-08	-3.41
FE710851		Unknown	PHVGI.052909	26	2.58	0.26	4.6E-03	-3.33
TC296093	A5BYD2	Putative uncharacterized protein	GMGI.052909	21	2.58	0.26	4.6E-03	-3.33
TA73258_3847		Unknown	allTIGR_Plant_2007	22	2.38	0.26	7.7E-03	-3.22
TC10257	A0T2G1	NPR-1	PHVGI.052909	26	2.18	0.26	1.3E-02	-3.09
CB542725	Q2PF01	Putative cytosolic factor	PHVGI.052909	26	2.18	0.26	1.3E-02	-3.09
EG948471	A9PBL2	Putative uncharacterized protein	PHVGI.052909	26	2.18	0.26	1.3E-02	-3.09
TA2828_3886		Hypothetical protein	allTIGR_Plant_2007	26	2.18	0.26	1.3E-02	-3.09
TC129949	A7QKC7	Chromosome chr2 scaffold_112	allTIGR_Plant_2009	26	2.18	0.26	1.3E-02	-3.09
TC18298		Unknown	PHVGI.052909	26	3.96	0.51	6.3E-04	-2.95
TC10706	Q0JFK8	Os01g0974600 protein	PHVGI.052909	26	3.96	0.51	6.3E-04	-2.95
TC8654	A5C6X9	Putative uncharacterized protein	PHVGI.052909	26	1.98	0.26	2.1E-02	-2.95
FD788432	A5C2P6	Putative uncharacterized protein	PHVGI.052909	26	1.98	0.26	2.1E-02	-2.95
TC18464		Unknown	PCGI.052909	26	1.98	0.26	2.1E-02	-2.95
CV541653	Q9FKM0	Genomic DNA chromosome 5 P1 clone:MUA2	PHVGI.052909	26	11.69	1.53	1.6E-09	-2.93
DV565253		Unknown	PHVGI.052909	26	3.57	0.51	1.7E-03	-2.80
CV536411	Q0E4A5	Os02g0128300 protein	PHVGI.052909	22	1.78	0.26	3.5E-02	-2.80
TC9897	Q3EA05	Uncharacterized protein At4g16695.2	PCGI.052909	26	1.78	0.26	3.5E-02	-2.80

AM782203	Q9FIL2	Gb|AAD32776.1	allTIGR_Plant_2009	22	1.78	0.26	3.5E-02	-2.80
TC318399		Unknown	GMGI.052909	26	3.37	0.51	2.7E-03	-2.72
TC14780		Unknown	PHVGI.052909	26	3.17	0.51	4.4E-03	-2.63
GD294386		Unknown	PCGI.052909	26	6.34	1.02	3.3E-05	-2.63
TC23612	A5BY91	Putative uncharacterized protein	PHVGI.052909	24	4.56	0.77	5.9E-04	-2.57
CV537247	A9PBT4	Putative uncharacterized protein	PHVGI.052909	26	2.97	0.51	7.0E-03	-2.54
TC300846	Q2HUM6	Putative uncharacterized protein	GMGI.052909	25	2.97	0.51	7.0E-03	-2.54
CV542024	A7PEK8	Chromosome chr11 scaffold_13	PHVGI.052909	26	33.68	6.13	4.5E-21	-2.46
TC7355		Unknown	PCGI.052909	26	2.77	0.51	1.1E-02	-2.44
GD474982		Unknown	PCGI.052909	26	4.16	0.77	1.5E-03	-2.44
FD795641	A9P9J5	Putative uncharacterized protein	PHVGI.052909	26	25.95	4.86	2.8E-16	-2.42
TC21034		Unknown	PCGI.052909	22	12.09	2.30	3.7E-08	-2.39
TC13891		Unknown	PCGI.052909	26	3.96	0.77	2.4E-03	-2.37
TC9689	A5BK56	Putative uncharacterized protein	PHVGI.052909	26	6.54	1.28	7.4E-05	-2.36
TC10739	A2Q1H6	EXS, C-terminal	PHVGI.052909	26	9.11	1.79	2.5E-06	-2.35
FG230624	Q7XIZ2	Putative uncharacterized protein OJ1048_C10.1	PHVGI.052909	26	2.58	0.51	1.8E-02	-2.33
TC9068	Q01I40	OSIGBa0092M08.12 protein	PHVGI.052909	26	2.58	0.51	1.8E-02	-2.33
GD535902		Unknown	PCGI.052909	26	2.58	0.51	1.8E-02	-2.33
TC14935	Q9FMI8	Arabidopsis thaliana genomic DNA chromosome 5 P1 clone:MHJ24	PHVGI.052909	26	2.38	0.51	2.8E-02	-2.22
TC323623	A7PL26	Chromosome chr7 scaffold_20	GMGI.052909	21	2.38	0.51	2.8E-02	-2.22
FG230670		Unknown	PHVGI.052909	26	8.12	1.79	2.2E-05	-2.18
FD795306	Q9XEF2	Putative uncharacterized protein T07M07.11	PHVGI.052909	26	4.56	1.02	1.9E-03	-2.16
AW734437	A7PUN8	Chromosome chr7 scaffold_31	GMGI.052909	23	3.37	0.77	8.9E-03	-2.14
TC4009	Q8LAN7	Acyltransferase-like protein	PCGI.052909	24	12.28	2.81	2.3E-07	-2.13
GD600695		Unknown	PCGI.052909	22	22.98	5.37	1.7E-12	-2.10
CV536776	A5AI06	Putative uncharacterized protein	PHVGI.052909	26	2.18	0.51	4.3E-02	-2.09
GD830341		Unknown	GMGI.052909	22	2.18	0.51	4.3E-02	-2.09
GD553110		Unknown	PCGI.052909	26	7.53	1.79	7.9E-05	-2.07
TC281642	A7PHH8	Unknown	GMGI.052909	22	23.58	5.62	1.4E-12	-2.07
CA916148		Unknown	PCGI.052909	26	21.40	5.11	1.6E-11	-2.07
CV533974		Unknown	PHVGI.052909	26	3.17	0.77	1.4E-02	-2.05
CB543596	Q6NQ19	At5g25170	PHVGI.052909	26	3.17	0.77	1.4E-02	-2.05
TC13551	Q9FE06	Putative phi-1 protein	PHVGI.052909	26	61.62	15.08	5.7E-30	-2.03
TC19346	Q84K42	Putative uncharacterized protein At1g68500	PHVGI.052909	26	7.13	1.79	1.8E-04	-2.00
CV543983	Q7XYV8	Seed specific protein Bn15D89A	PHVGI.052909	26	8.12	2.04	6.3E-05	-1.99
CV542770	A8C978	Forisome	PHVGI.052909	26	6.93	1.79	2.7E-04	-1.95
BW622006		Unknown	LJGI.052909	25	4.95	1.28	2.3E-03	-1.95
FE710515	Q9M840	T27C4.12 protein	PHVGI.052909	26	2.97	0.77	2.1E-02	-1.95

TC334890	A7QJ17	Chromosome chr2 scaffold_105	GMGI.052909	22	2.97	0.77	2.1E-02	-1.95
TC13726	Q0WP25	Putative uncharacterized protein At5g05310	PHVGI.052909	26	6.74	1.79	4.1E-04	-1.91
FD787048		Unknown	PHVGI.052909	26	9.51	2.56	2.6E-05	-1.90
TC329239		Unknown	GMGI.052909	25	3.76	1.02	1.0E-02	-1.88
CV542013	A5BKD7	Putative uncharacterized protein	PHVGI.052909	24	10.30	2.81	1.4E-05	-1.87
FE693125	Q1HIU5	Ankyrin repeat BTB/POZ domain-containing protein	PHVGI.052909	26	2.77	0.77	3.2E-02	-1.86
TC8455	A5B9U8	Putative uncharacterized protein	PHVGI.052909	26	2.77	0.77	3.2E-02	-1.86
FE706867	A7NUG8	Chromosome chr18 scaffold_1	PHVGI.052909	22	2.77	0.77	3.2E-02	-1.86
CV534710	Q0JNE6	Os01g0300600 protein	PHVGI.052909	26	4.56	1.28	5.2E-03	-1.83
GD506389		Unknown	PCGI.052909	26	6.34	1.79	9.0E-04	-1.83
TC139797	A5C2C7	Putative uncharacterized protein	MTGI.071708	24	6.34	1.79	9.0E-04	-1.83
GD532151		Unknown	PCGI.052909	26	14.46	4.09	3.7E-07	-1.82
TC15603	A2Q343	Putative uncharacterized protein	PHVGI.052909	26	8.12	2.30	1.6E-04	-1.82
GD578172		Unknown	PCGI.052909	21	11.69	3.32	5.5E-06	-1.81
CB541634		Unknown	PHVGI.052909	26	26.94	7.67	3.6E-12	-1.81
BI893491		Unknown	GMGI.052909	22	3.57	1.02	1.6E-02	-1.80
TC293878	A7PYC0	Chromosome chr15 scaffold_37	GMGI.052909	21	3.57	1.02	1.6E-02	-1.80
FE702397	A5BAS2	Putative uncharacterized protein	PHVGI.052909	26	11.49	3.32	8.0E-06	-1.79
TC1264	A9PCD8	Putative uncharacterized protein	PCGI.052909	26	6.14	1.79	1.3E-03	-1.78
GD581183		Unknown	PCGI.052909	26	4.36	1.28	7.7E-03	-1.77
TC344853	A7Q3P5	Chromosome chr13 scaffold_48	GMGI.052909	21	23.38	6.90	2.3E-10	-1.76
GD339172		unknown	PCGI.052909	26	5.15	1.53	3.9E-03	-1.75
CV544163		unknown	PHVGI.052909	26	2.58	0.77	4.8E-02	-1.75
CV535980	Q9FY58	Putative uncharacterized protein T5K6_60	PHVGI.052909	26	2.58	0.77	4.8E-02	-1.75
TC326297	A7PEE0	Chromosome chr11 scaffold_13	GMGI.052909	26	2.58	0.77	4.8E-02	-1.75
TC337324	A5BSI8	Putative uncharacterized protein	GMGI.052909	26	2.58	0.77	4.8E-02	-1.75
TC172830	A7P0J1	Chromosome chr19 scaffold_4	allTIGR_Plant_2009	21	2.58	0.77	4.8E-02	-1.75
TC331520	A5C958	Putative uncharacterized protein	GMGI.052909	26	5.94	1.79	2.0E-03	-1.73
TC17282	A7P6N1	Chromosome chr9 scaffold_7	allTIGR_Plant_2009	23	5.94	1.79	2.0E-03	-1.73
TC8964	Q8L7A5	Expressed protein	PHVGI.052909	26	3.37	1.02	2.3E-02	-1.72
TC12202	A9PAA8	Putative uncharacterized protein	PHVGI.052909	26	10.90	3.32	2.5E-05	-1.71
CV531451	A5AXC1	Putative uncharacterized protein	PHVGI.052909	26	4.16	1.28	1.1E-02	-1.70
GD626648		Unknown	PCGI.052909	25	4.95	1.53	5.7E-03	-1.69
TC9878		Unknown	PCGI.052909	26	4.95	1.53	5.7E-03	-1.69
FG230783		Unknown	PHVGI.052909	22	22.98	7.16	1.1E-09	-1.68
CB556091	A7P113	Chromosome chr19 scaffold_4	PHVGI.052909	26	6.54	2.04	1.5E-03	-1.68
TC307997	A7NVT9	Chromosome chr18 scaffold_1	GMGI.052909	22	6.54	2.04	1.5E-03	-1.68
GD428323		Unknown	PCGI.052909	25	7.33	2.30	7.4E-04	-1.67

FG229144		Unknown	PHVGI.052909	26	3.17	1.02	3.4E-02	-1.63
FD793371	A2XYC3	Putative uncharacterized protein	PHVGI.052909	26	4.75	1.53	8.3E-03	-1.63
TC19137		Unknown	PHVGI.052909	26	3.96	1.28	1.7E-02	-1.63
GD393345		Unknown	PCGI.052909	21	3.96	1.28	1.7E-02	-1.63
TC8495	Q6NLB1	F-box protein At2g26850	PHVGI.052909	26	14.66	4.86	3.1E-06	-1.59
TC11809	O82273	Putative uncharacterized protein At2g31110	PHVGI.052909	26	6.93	2.30	1.5E-03	-1.59
TC9823	A5BQI7	Putative uncharacterized protein	PHVGI.052909	26	12.28	4.09	2.2E-05	-1.59
TC15153		Unknown	PCGI.052909	26	27.54	9.20	1.7E-10	-1.58
TC15545	Q9LHJ3	Gb|AAD15386.1	PHVGI.052909	26	5.35	1.79	6.0E-03	-1.58
FE699996	A7PUA3	Chromosome chr7 scaffold_31	PHVGI.052909	26	4.56	1.53	1.2E-02	-1.57
TC12246	A2XKS0	Putative uncharacterized protein	PHVGI.052909	26	18.82	6.39	1.9E-07	-1.56
TC14444	A7PDY6	Chromosome chr11 scaffold_13	PHVGI.052909	26	3.76	1.28	2.4E-02	-1.56
TC10135	A5C224	Putative uncharacterized protein	PHVGI.052909	26	3.76	1.28	2.4E-02	-1.56
GD492429		Unknown	PCGI.052909	22	3.76	1.28	2.4E-02	-1.56
TC19349	Q94C55	Putative uncharacterized protein At3g27640	PHVGI.052909	26	5.94	2.04	4.4E-03	-1.54
TC15055	A9T531	Predicted protein	PHVGI.052909	26	8.92	3.07	4.3E-04	-1.54
TC24241	A7QHQ6	Chromosome chr8 scaffold_99	allTIGR_Plant_2009	24	2.97	1.02	5.0E-02	-1.54
TC3688	Q9MF99	Orf214 protein	PCGI.052909	26	8.12	2.81	8.3E-04	-1.53
TC15271	Q94F28	Putative uncharacterized protein	PHVGI.052909	26	23.58	8.18	8.4E-09	-1.53
GD521039		Unknown	PCGI.052909	26	14.66	5.11	6.6E-06	-1.52
TC13271	O22847	Expressed protein	PHVGI.052909	26	4.36	1.53	1.7E-02	-1.51
TC9346	Q9S7A6	T1B9.2 protein	PHVGI.052909	26	4.36	1.53	1.7E-02	-1.51
GD598671		Unknown	PCGI.052909	25	4.36	1.53	1.7E-02	-1.51
TC301653	A0MEI7	Putative uncharacterized protein	GMGI.052909	22	4.36	1.53	1.7E-02	-1.51
GD639749		Unknown	PCGI.052909	22	18.03	6.39	7.3E-07	-1.50
TC8661	A2Q5V9	Putative uncharacterized protein	PHVGI.052909	26	17.24	6.13	1.4E-06	-1.49
TC9725		Unknown	PCGI.052909	26	5.75	2.04	6.3E-03	-1.49
CV542587	A7QNP9	Chromosome undetermined scaffold_133	PHVGI.052909	26	16.44	5.88	2.6E-06	-1.48
TC15847	Q0IT26	Os11g0425600 protein	PHVGI.052909	22	3.57	1.28	3.5E-02	-1.48
TC5084		Unknown	PCGI.052909	22	3.57	1.28	3.5E-02	-1.48
TC16235	A7PDC5	Chromosome chr17 scaffold_12	PHVGI.052909	26	12.09	4.34	6.5E-05	-1.48
FE701261	Q8L9E9	Putative uncharacterized protein	PHVGI.052909	26	8.52	3.07	8.6E-04	-1.47
GD418477		Unknown	PCGI.052909	26	4.95	1.79	1.2E-02	-1.47
GD466470		Unknown	PCGI.052909	26	4.95	1.79	1.2E-02	-1.47
GD459897		Unknown	PCGI.052909	26	11.29	4.09	1.2E-04	-1.47
TC16888		Unknown	PHVGI.052909	26	7.73	2.81	1.7E-03	-1.46
FE695232	A5BCD4	Putative uncharacterized protein	PHVGI.052909	26	4.16	1.53	2.5E-02	-1.44
TC18711	Q9ZS47	Arbuscular mycorrhiza protein	PHVGI.052909	26	11.09	4.09	1.7E-04	-1.44

FE708168	Q8GTE4	Putative uncharacterized protein 274	PHVGI.052909	26	5.55	2.04	8.9E-03	-1.44
BU548137		Unknown	GMGI.052909	26	4.16	1.53	2.5E-02	-1.44
TC18621		Unknown	PHVGI.052909	26	71.72	26.58	6.2E-22	-1.43
CV541821		Unknown	PHVGI.052909	26	26.15	9.71	7.4E-09	-1.43
TC13895	A5C2H3	Putative uncharacterized protein	PHVGI.052909	26	8.92	3.32	8.8E-04	-1.42
TC6671		Unknown	PCGI.052909	26	13.67	5.11	3.6E-05	-1.42
TC8944	A5AXU6	Putative uncharacterized protein	PHVGI.052909	26	19.81	7.41	5.9E-07	-1.42
TC11828	A5BPK4	Putative uncharacterized protein	PHVGI.052909	26	76.28	28.62	8.0E-23	-1.41
GD464542		Unknown	PCGI.052909	22	4.75	1.79	1.8E-02	-1.41
CA916403		Unknown	PCGI.052909	26	6.74	2.56	4.6E-03	-1.40
TC11033	Q93W28	AT4g15540/dl3810w	PHVGI.052909	26	5.35	2.04	1.3E-02	-1.39
FE711393		Unknown	PHVGI.052909	22	7.33	2.81	3.3E-03	-1.38
TC12190	Q9FX61	T6J4.11 protein	PHVGI.052909	26	7.33	2.81	3.3E-03	-1.38
TC299534	Q9SMR9	Putative uncharacterized protein T5J17.10	GMGI.052909	22	17.83	6.90	4.0E-06	-1.37
TC8835	A7QWS6	Chromosome chr4 scaffold_208	PCGI.052909	26	37.64	14.57	1.7E-11	-1.37
FE897118		Unknown	PHVGI.052909	26	3.96	1.53	3.5E-02	-1.37
TC20043	O80543	Uncharacterized protein At1g22800	PHVGI.052909	26	3.96	1.53	3.5E-02	-1.37
BI315678		Unknown	GMGI.052909	22	3.96	1.53	3.5E-02	-1.37
TC323783	A9PBG4	Putative uncharacterized protein	GMGI.052909	22	5.94	2.30	9.0E-03	-1.37
BQ583196	A7PFF7	Chromosome chr11 scaffold_14	allTIGR_Plant_2009	21	41.41	16.10	2.0E-12	-1.36
FE711503	O82178	Pentatricopeptide repeat-containing protein At2g35130	PHVGI.052909	26	21.60	8.43	4.6E-07	-1.36
TC55943	A7QGT9	Chromosome chr16 scaffold_94	allTIGR_Plant_2009	21	15.65	6.13	2.0E-05	-1.35
DY475323		DENN (AEX-3) domain-containing protein-like	allTIGR_Plant_2007	21	12.28	4.86	1.8E-04	-1.34
CV533448		Unknown	PHVGI.052909	26	14.86	5.88	3.7E-05	-1.34
GD360834		Unknown	PCGI.052909	22	7.73	3.07	3.3E-03	-1.33
TC14272	A5AIS4	Putative uncharacterized protein	PHVGI.052909	26	20.60	8.18	1.2E-06	-1.33
TC15174		Unknown	PCGI.052909	26	12.88	5.11	1.3E-04	-1.33
CB541823	Q41041	Outer envelope membrane protein	PHVGI.052909	26	28.93	11.50	8.2E-09	-1.33
CB542699		Unknown	PHVGI.052909	26	8.32	3.32	2.4E-03	-1.32
TC6951		Unknown	PCGI.052909	26	12.09	4.86	2.5E-04	-1.32
GD660429	A7P5Q3	Chromosome chr4 scaffold_6	PCGI.052909	24	45.77	18.40	6.1E-13	-1.31
TC295864	A7Q9W0	Chromosome chr8 scaffold_68	GMGI.052909	24	15.85	6.39	2.7E-05	-1.31
TC12729	Q9LPR9	F11F12.20 protein	PHVGI.052909	26	19.02	7.67	4.1E-06	-1.31
TC18504	A5AL18	Putative uncharacterized protein	PHVGI.052909	26	6.93	2.81	6.4E-03	-1.30
GD388208	Q0DV44	Os03g0151000 protein	PCGI.052909	22	3.76	1.53	5.0E-02	-1.30
TC2570		Unknown	PCGI.052909	26	11.89	4.86	3.4E-04	-1.29
TC15005		Unknown	PCGI.052909	26	130.56	53.41	3.2E-33	-1.29
TC16305	A2X722	Putative uncharacterized protein	PHVGI.052909	26	20.60	8.43	2.2E-06	-1.29

TC11966	A5C0I5	Putative uncharacterized protein	PHVGI.052909	26	16.84	6.90	2.0E-05	-1.29
TC298242	A2Q3J4	Dilute	GMGI.052909	24	8.72	3.58	2.4E-03	-1.28
GD632745		Unknown	PCGI.052909	26	4.36	1.79	3.5E-02	-1.28
TC8943	A7PU84	Putative uncharacterized protein	PHVGI.052909	26	24.77	10.22	2.4E-07	-1.28
GD489242		Unknown	PCGI.052909	24	25.95	10.73	1.3E-07	-1.27
TC21399		Unknown	PCGI.052909	26	16.05	6.64	3.6E-05	-1.27
CV543519	A7QKT5	Chromosome undetermined scaffold_114	PHVGI.052909	26	5.55	2.30	1.7E-02	-1.27
GD432215		Unknown	PCGI.052909	24	5.55	2.30	1.7E-02	-1.27
TC13396	Q8VY14	Putative uncharacterized protein At4g02880	PHVGI.052909	26	27.54	11.50	7.0E-08	-1.26
TC10631	Q9LMJ7	F10K1.25 protein	PHVGI.052909	22	62.41	26.07	3.9E-16	-1.26
TC17252		Unknown	PHVGI.052909	26	23.18	9.71	8.4E-07	-1.26
GD294100	Q9FGZ0	Genomic DNA chromosome 5 TAC clone: K6M13	PCGI.052909	26	17.04	7.16	2.6E-05	-1.25
TC10444	A2Q1V5	Smr protein/MutS2 C-terminal	PHVGI.052909	26	18.62	7.92	1.4E-05	-1.23
TC18868	A9P948	Putative uncharacterized protein	PHVGI.052909	26	28.13	12.01	9.2E-08	-1.23
GD560283		Unknown	PCGI.052909	26	32.29	13.80	1.0E-08	-1.23
GD409398		Unknown	PCGI.052909	26	7.13	3.07	8.6E-03	-1.22
FD787051		Unknown	PHVGI.052909	26	19.61	8.43	9.9E-06	-1.22
TC18673		Unknown	PHVGI.052909	24	4.75	2.04	3.4E-02	-1.22
TC16326	Q75HW3	Putative uncharacterized protein OSJNBb0092G21.2	PHVGI.052909	26	27.34	11.76	1.7E-07	-1.22
TC20114	Q94A46	At2g44500/F4I1.31	PHVGI.052909	26	33.88	14.57	5.6E-09	-1.22
TC16712	A5B2I4	Putative uncharacterized protein	PHVGI.052909	26	5.35	2.30	2.4E-02	-1.22
TC324335	A7PDY5		GMGI.052909	23	5.35	2.30	2.4E-02	-1.22
TC19441	A5AT40	Putative uncharacterized protein	PHVGI.052909	26	6.54	2.81	1.2E-02	-1.22
CB543281	A3BRY9	Putative uncharacterized protein	PHVGI.052909	26	43.19	18.66	5.3E-11	-1.21
TC333526		Unknown	GMGI.052909	26	86.58	37.57	1.9E-20	-1.20
TC9176	O04342	Expressed protein	PHVGI.052909	26	22.19	9.71	3.7E-06	-1.19
DT661629		Unknown	PHVGI.052909	26	58.84	25.81	4.2E-14	-1.19
GD621965		Unknown	PCGI.052909	26	24.37	10.73	1.4E-06	-1.18
TC16389	A9PJY7	Putative uncharacterized protein	PHVGI.052909	26	8.12	3.58	6.0E-03	-1.18
TC19740		Unknown	PHVGI.052909	22	20.21	8.94	1.3E-05	-1.18
EC749366		Unknown	allTIGR_Plant_2007	21	6.34	2.81	1.6E-02	-1.17
GD570987		Unknown	PCGI.052909	22	58.64	26.07	9.6E-14	-1.17
CB556122	A8C977	Forisome	PHVGI.052909	26	11.49	5.11	1.1E-03	-1.17
CA913335		Unknown	PCGI.052909	26	17.63	7.92	6.0E-05	-1.15
TC9058	Q8GYW1	Putative uncharacterized protein At5g40450/MPO12_160	PHVGI.052909	26	28.93	13.03	2.7E-07	-1.15
CB539266	A9PGP2	Putative uncharacterized protein	PHVGI.052909	26	16.44	7.41	1.1E-04	-1.15
CV542039		Unknown	PHVGI.052909	26	7.92	3.58	8.1E-03	-1.15
TC16500	Q9FPI4	AT5g16110	PHVGI.052909	26	7.92	3.58	8.1E-03	-1.15

GD313065		Unknown	PCGI.052909	21	7.92	3.58	8.1E-03	-1.15
CV543952	A5C8N1	Putative uncharacterized protein	PHVGI.052909	26	15.26	6.90	2.1E-04	-1.14
TC18946		Unknown	PHVGI.052909	26	22.59	10.22	6.2E-06	-1.14
TC15785	Q5HZ39	At4g27460	PHVGI.052909	26	29.32	13.29	2.6E-07	-1.14
GD376922		Unknown	PCGI.052909	26	7.33	3.32	1.1E-02	-1.14
FG229590	A5BA49	Putative uncharacterized protein	PHVGI.052909	26	25.36	11.50	1.7E-06	-1.14
GD374309		Unknown	PCGI.052909	26	6.74	3.07	1.6E-02	-1.14
GD497933		Unknown	PCGI.052909	22	33.68	15.33	3.8E-08	-1.14
TC8410	A3BFW3	Putative uncharacterized protein	PHVGI.052909	26	23.58	10.73	4.4E-06	-1.14
TC20016	Q94BP7	Putative uncharacterized protein At5g40740	PHVGI.052909	26	22.39	10.22	8.2E-06	-1.13
TC10626	Q9ASQ1	At1g04290/F19P19_27	PHVGI.052909	26	15.65	7.16	2.1E-04	-1.13
TC20147	A2WXH1	Putative uncharacterized protein	PHVGI.052909	26	8.92	4.09	5.6E-03	-1.12
GD463445		Unknown	PCGI.052909	24	17.83	8.18	7.7E-05	-1.12
GD328316		Unknown	PCGI.052909	26	5.55	2.56	3.1E-02	-1.12
TC21184		Unknown	PCGI.052909	26	11.09	5.11	2.0E-03	-1.12
CV541981		Unknown	PHVGI.052909	26	8.32	3.83	7.8E-03	-1.12
FE683916		Unknown	PHVGI.052909	22	16.05	7.41	2.0E-04	-1.11
TC11102	A5BV51	Putative uncharacterized protein	PHVGI.052909	26	87.37	40.38	2.2E-18	-1.11
TC15242	Q9LQ84	T1N6.13 protein	PHVGI.052909	26	32.49	15.08	1.2E-07	-1.11
TC13777	Q8LKV1	GAGA-binding protein	PHVGI.052909	26	14.26	6.64	5.2E-04	-1.10
TC292378	A2Q3A0	Putative uncharacterized protein	GMGI.052909	26	11.49	5.37	1.9E-03	-1.10
TC19102	Q84WK2	At1g44770	PHVGI.052909	26	25.16	11.76	3.8E-06	-1.10
BQ481798		Unknown	PHVGI.052909	26	8.72	4.09	7.5E-03	-1.09
TC11777		Unknown	PCGI.052909	23	39.62	18.66	8.2E-09	-1.09
GD489688		Unknown	PCGI.052909	24	5.94	2.81	3.0E-02	-1.08
TC51597	A7Q3V8	Chromosome chr13 scaffold_48	allTIGR_Plant_2009	26	38.83	18.40	1.5E-08	-1.08
EX532874		Unknown	MTGI.071708	21	30.71	14.57	5.0E-07	-1.08
TC17587	Q3E7L8	Uncharacterized protein At5g19400.1	PHVGI.052909	26	17.24	8.18	1.8E-04	-1.08
GE039563		Unknown	GMGI.052909	22	21.00	9.97	3.4E-05	-1.08
FE708941		Unknown	PHVGI.052909	26	7.53	3.58	1.5E-02	-1.07
CV530660	O23119	Putative uncharacterized protein F19G10.1	PHVGI.052909	26	7.53	3.58	1.5E-02	-1.07
TC15979		Unknown	PHVGI.052909	26	15.06	7.16	4.8E-04	-1.07
GD618460		Unknown	PCGI.052909	26	9.11	4.34	7.2E-03	-1.07
GD600637		Unknown	PCGI.052909	26	9.11	4.34	7.2E-03	-1.07
CV530959	Q8S9L9	At2g42180/T24P15.9	PHVGI.052909	26	17.63	8.43	1.7E-04	-1.06
GD615612		Unknown	PCGI.052909	26	15.45	7.41	4.6E-04	-1.06
TC15296	O23120	Putative uncharacterized protein F10G19.2	PHVGI.052909	26	20.21	9.71	6.1E-05	-1.06
TC2023		Unknown	PCGI.052909	26	11.69	5.62	2.5E-03	-1.06

GD327096		Unknown		PCGI.052909	21	49.93	24.02	2.5E-10	-1.06
FD791492		Unknown		PHVGI.052909	26	61.02	29.39	2.8E-12	-1.05
GD534609		Unknown		PCGI.052909	26	19.61	9.46	8.3E-05	-1.05
GD432150		Unknown		PCGI.052909	26	40.22	19.42	1.6E-08	-1.05
GD424676		Unknown		PCGI.052909	25	6.34	3.07	2.9E-02	-1.05
TC15686	Q0WSC	Putative uncharacterized protein At1g53380		PHVGI.052909	26	7.92	3.83	1.4E-02	-1.05
TC317318	Q9FSF7	O-linked GlcNAc transferase like		GMGI.052909	21	137.10	66.70	3.3E-25	-1.04
TC17149	O48796	F24O1.5		PHVGI.052909	26	7.33	3.58	1.9E-02	-1.03
CV529898		Unknown		PHVGI.052909	26	5.75	2.81	4.0E-02	-1.03
TC11145	Q9ZVZ7	T25N20.6		PHVGI.052909	26	5.75	2.81	4.0E-02	-1.03
TC13542	Q94BN5	Putative uncharacterized protein At5g50900		PHVGI.052909	26	5.75	2.81	4.0E-02	-1.03
TC17366	Q8GVB8	Fw2.2		PHVGI.052909	26	33.88	16.61	3.5E-07	-1.03
TC16282		Unknown		PCGI.052909	26	248.64	122.15	1.9E-43	-1.03
TC9934		Unknown		PCGI.052909	25	8.32	4.09	1.3E-02	-1.03
TC15963		Unknown		PHVGI.052909	26	12.48	6.13	2.2E-03	-1.03
GD320371		Unknown		PCGI.052909	26	10.90	5.37	4.5E-03	-1.02
TC15318	A7PCQ7	Chromosome chr17 scaffold_12		PHVGI.052909	26	9.31	4.60	9.0E-03	-1.02
FG640364	Q9LIM3	Arabidopsis thaliana genomic DNA chromosome 3 BAC clone:F4B12		allTIGR_Plant_2009	22	33.09	16.36	6.2E-07	-1.02
GD384383		Unknown		PCGI.052909	22	14.46	7.16	1.1E-03	-1.02
GD448732		Unknown		PCGI.052909	26	7.73	3.83	1.8E-02	-1.01
TC289363	A7PYS2	Chromosome chr12 scaffold_38		GMGI.052909	26	6.14	3.07	3.8E-02	-1.00
TC11257	O80914	Putative uncharacterized protein At2g38370		PHVGI.052909	26	6.14	3.07	3.8E-02	-1.00

SUPPLEMENTAL DATA FOR CHAPTER 3

Proteomic analysis of polyethylene glycol-induced osmotic stress in root tips of common bean (*Phaseolus vulgaris* **L.**)

Zhong-Bao Yang[1], Dejene Eticha[1], Hendrik Führs[1], Sébastien Gallien[2], Dimitri Heintz[3], Alain Van Dorsselaer[2], Idupulapati Madhusudana Rao[4], Walter Johannes Horst[1]

[1] Institute of Plant Nutrition, Leibniz Universität Hannover, Herrenhaeuser Str. 2, D-30419 Hannover, Germany

[2] Laboratoire de Spectrométrie de Masse Bio-organique, IPHC-DSA, Université de Strasbourg, CNRS, UMR7178, 25 rue Becquerel, 67087 Strasbourg, France

[3] Institut de Biologie Mooléculaire des Plantes (IBMP), 28 rue Goethe, CNRS-UPR2357, Université de Strasbourg, 67083 Strasbourg, France

[4] International Center for Tropical Agriculture (CIAT), AA 6713, Cali, Colombia

(To be submitted)

Supplementary Figure S1 Close-ups of the decreased (A) and increased (B) apoplastic proteins in response to PEG in the root tips of common bean genotype VAX 1. The intact Coomassie-stained 2D IEF/SDS–PAGE gels of the apoplastic proteins were shown in Fig. 5.
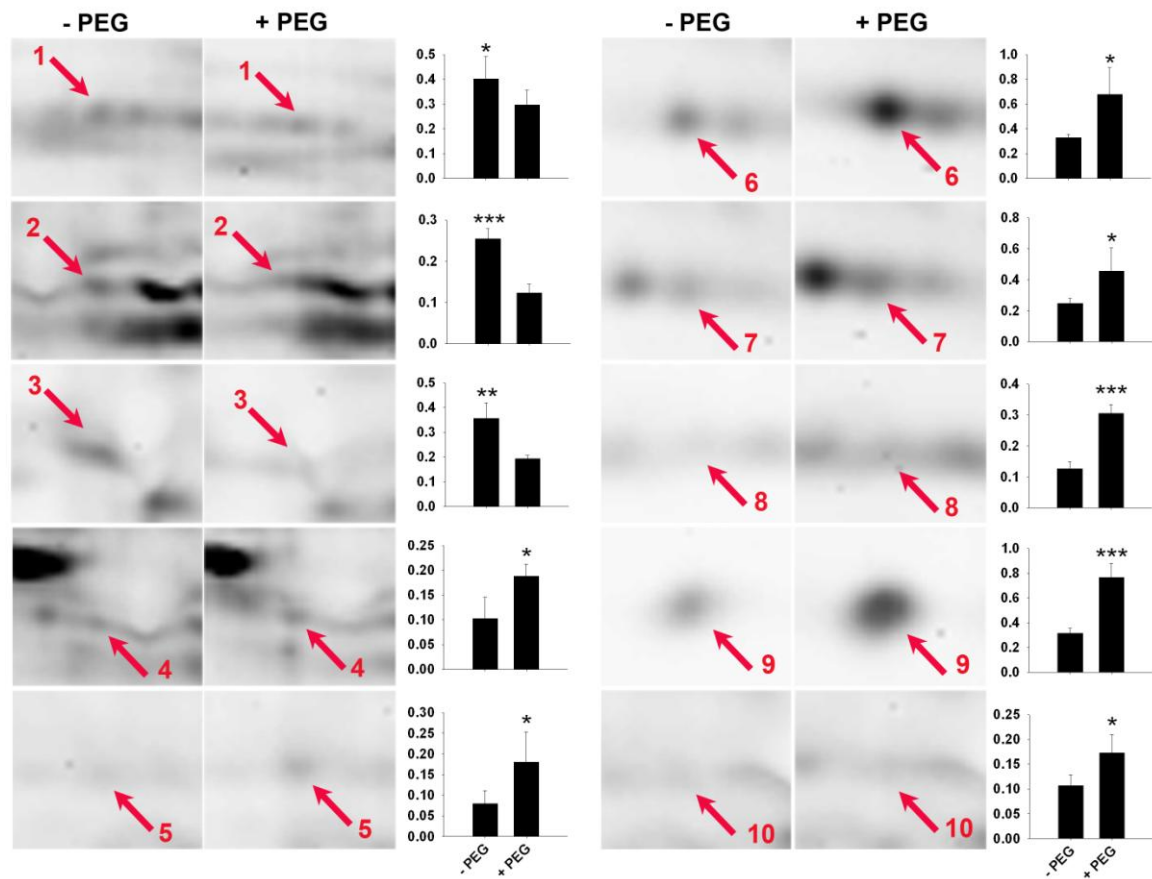
Supplementary Figure S2 Close-ups of the decreased and increased phosphoproteins in response to PEG in the root tips of common bean genotype VAX 1, and the corresponding changes of relative volume in these ten phosphoproteins were presented. The intact Pro-Q DPS-stained 2D IEF/SDS–PAGE gels of the total phophoproteins were shown in Fig. 6A. The symbol *, ** and *** denote significant differences at $P < 0.05$, 0.01 and 0.001, respectively.

SUPPLEMENTAL DATA FOR CHAPTER 4

Physiological and molecular analysis of the interaction between aluminum toxicity and drought stress in common bean (*Phaseolus vulgaris* L.)

Zhong-Bao Yang[1], Dejene Eticha[1], Alfonso Albacete[2], Idupulapati Madhusudana Rao[3], Thomas Roitsch[2], Walter Johannes Horst[1]

[1] Institute of Plant Nutrition, Leibniz Universität Hannover, Herrenhaeuser Str. 2, D-30419 Hannover, Germany

[2] Institute of Plant Science, Universität Graz, Schubertstrasse 51, A-8010 Graz, Austria

[3] International Center for Tropical Agriculture (CIAT), AA 6713, Cali, Colombia

(To be submitted)
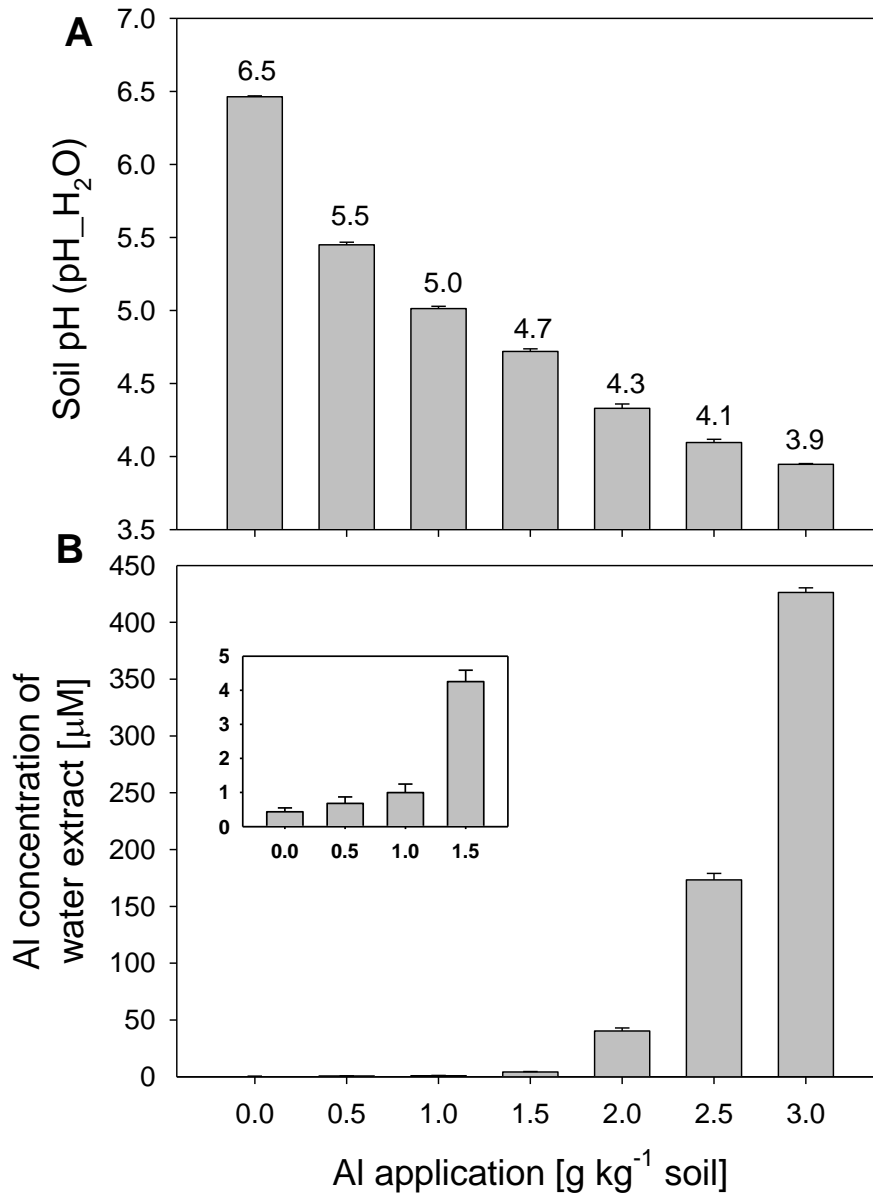
Supplemental Figure S1 Soil pH (pH_H_2O) (A) and the corresponding Al concentrations in the water extracts (B) at different levels of Al application (0 to 3.0 g kg^{-1} soil). 10 mg air dried soil was incubated in 20 ml distilled water (pH_H_2O), and shaken for 1 h, then the soil pH and Al concentrations were determined. In B, the inserted graph shows the downscaled data for the Al supplies from 0 to 1.5 g kg^{-1} soil.
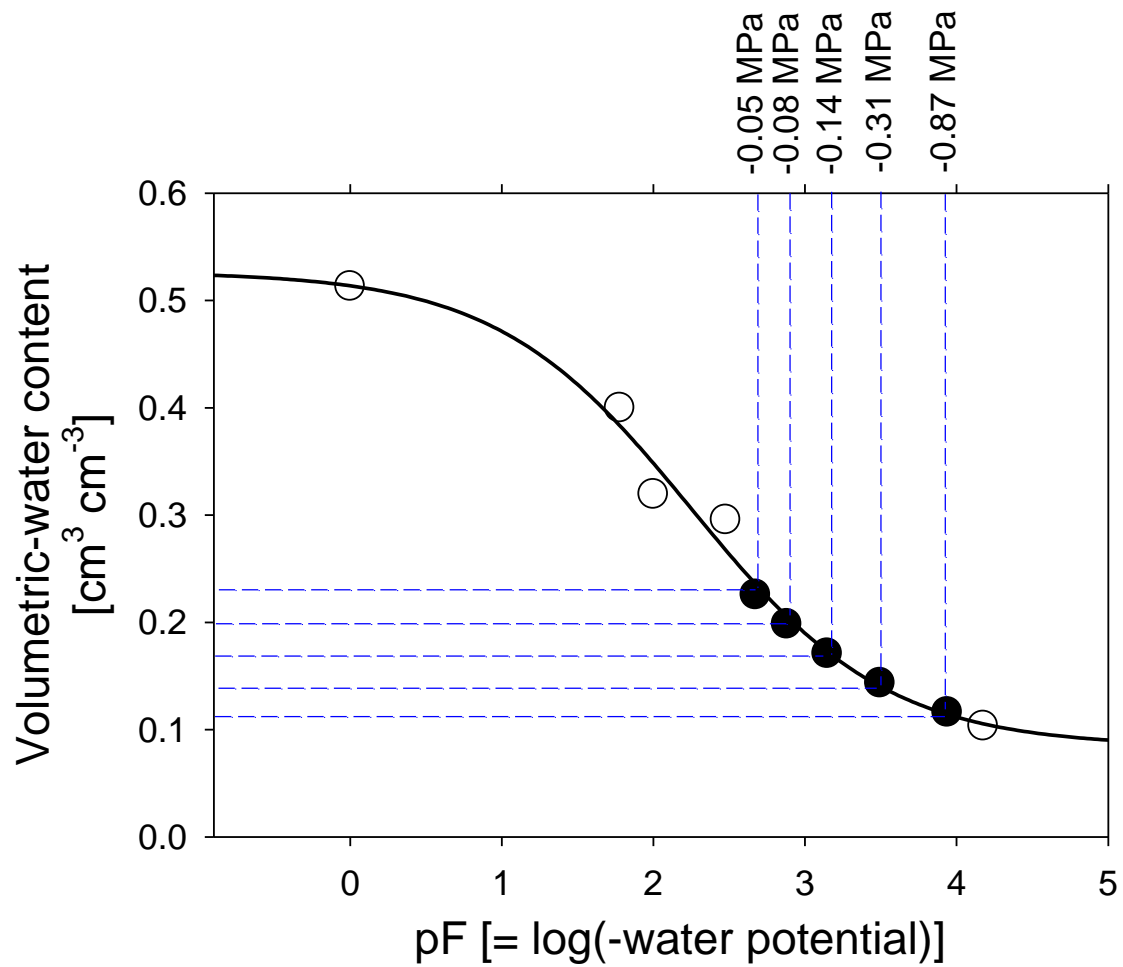
Supplemental Figure S2 The soil water retention curve of an Oxisol from the Llanos region of Colombia. The filled dots indicate the soil-moisture treatments used in the present study; the corresponding soil-water potentials in MPa are presented on the top of the graph.
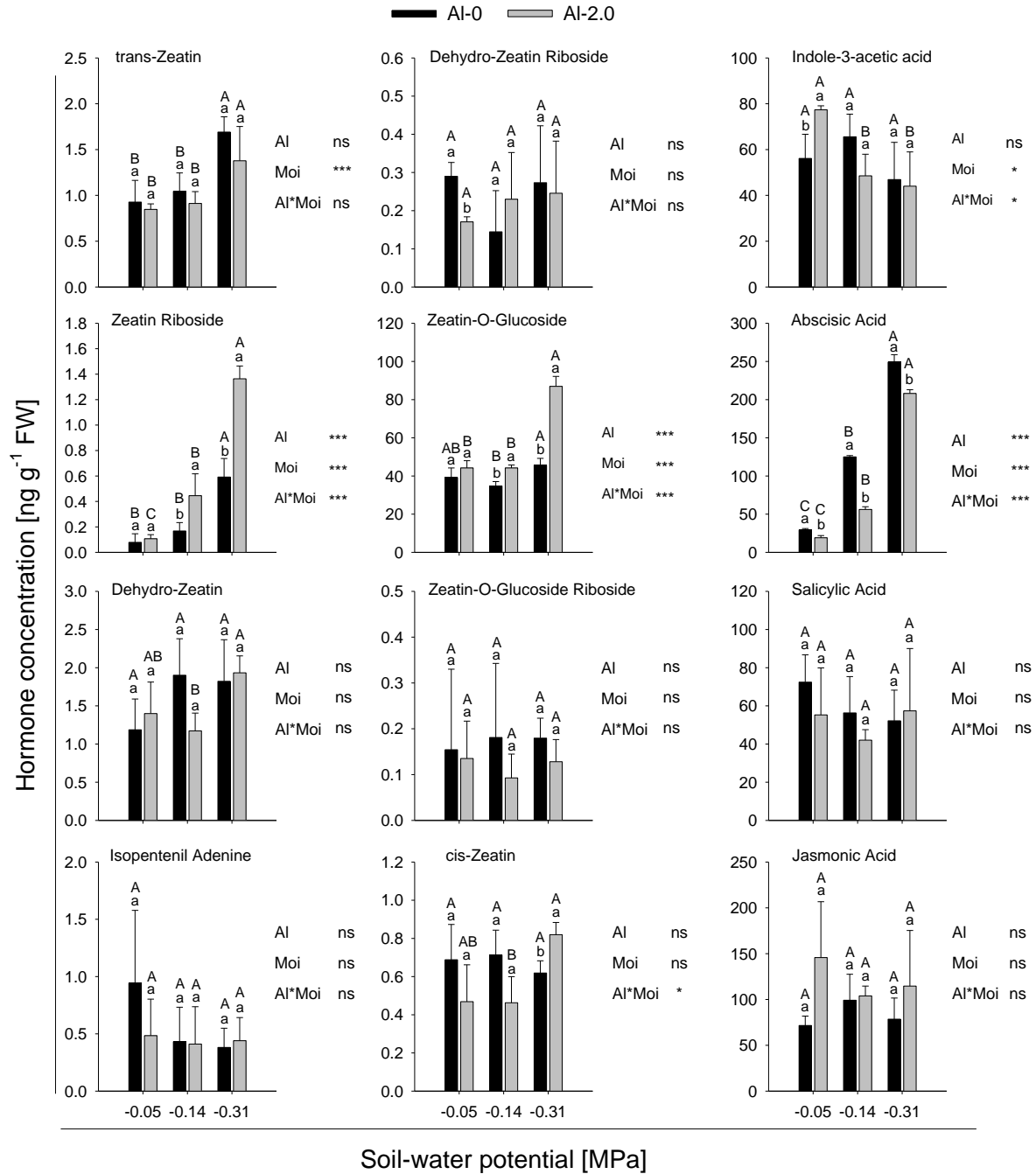
Supplemental Figure S3 Phytohormone concentrations in the 1-cm root tips of the common bean genotype VAX 1 as affected by soil moisture and Al supply (g kg^{-1} soil). Two-day-old seedlings were grown in soil for 24 h. Bars represent means $\pm$ SD, n = 3. Means with different small and capital letters are significantly different at $P < 0.05$ (Tukey test) for the comparison of Al treatments within soil moisture and comparison of soil-moisture treatments within Al treatments, respectively. For the ANOVA, *, *** denote significant differences at $P < 0.05$, $P < 0.001$, respectively. ns = not significant.

Supplemental Table S1 List of genes and specific primer pairs used for quantitative gene expression analysis.

Candidate genes	Primer pairs (5'→3')*		Amplicon size (bp)	TC/GB Acc. No.
P5CS (VuP5CS protein)	(+) GACAGTGCTGCTGTTTTCCA	(-) AAACCCTCTACTCCCACAGGA	128	TC14708
SUS (Sucrose synthase 2)	(+) GCATGGCCTCATGAAAGAGT	(-) GAAAGCAGGCTGAACGAAAG	133	TC11609
AQP (Aquaporin)	(+) CCACATCACCATCCTCACTG	(-) ATTGCCAAACCTCCTGTGAC	102	TC14630
KS-DHN (KS-type dehydrin SLTI629)	(+) CATAGCAGTGAGGGCTGTGA	(-) CAAAGCAGTGGGGTTACACA	157	TC23304
CYP701A (Cytochrome P450 monooxygenase CYP701A16)	(+) GGATGCAACATGGACAAGAA	(-) AACCTGCACACACCCTCTTC	136	TC18728
PvLEA18 (PvLEA-18)	(+) ACCAAAGACTGGTCGAGGTG	(-) GGCAGTGTAGGAGGTGGTGT	141	TC17584
BEG (Glucan endo-1, 3-beta-glucosidase precursor)	(+) ATGGAAGACTTGGCAACGAC	(-) GCCTCTCAAAGCTCCAAGAA	122	TC11172
HRGP (Hydroxyproline-rich glycoprotein)	(+) CCTGTCTTGATGGTGAAGCA	(-) TTCATTTGTTGCAGGCTGAC	114	CV543261
PRP (Proline-rich protein)	(+) GCAAGTGTTGTGCATTGCTT	(-) TGGAAGCCAGAAGGAACTGT	160	TC12228
LTP (Protease inhibitor/seed storage/lipid transfer protein family protein)	(+) CCTCAGCAGCACAAGATGAG	(-) TGACAGCAATCTGAGGGTTG	147	CV542382
XTHa (Xyloglucan endotransglycosylase precursor)	(+) ATATGTCATCGGAGGGTCCA	(-) TTGGTAGGGTCGAACCAAAG	151	TC12227
XTHb (Xyloglucan endotransglucosylase/hydrolase)	(+) TTTGACCAACCCATGAAGGT	(-) GCATTCACTGAGGCTTCACA	153	CV542742
bZIP (bZip transcription factor)	(+) AAACTGCCACTTCCCTCCTT	(-) TCTCCTGTGCTTCCTTTCGT	127	TC17978
MYB (MYB transcription factor MYB134)	(+) CCGATTCCGACAAAATGAAC	(-) GCATCAGGTGTGTTCAGCTC	136	TC13287
NCED (9-cis-epoxycarotenoid dioxygenase)	(+) GCTCGAAGCTTCCATCAAAC	(-) ATCTGCAAGCATCCCTCAGT	143	AF190462
ZEP (Zeaxanthin epoxidase)	(+) CCTCATCACAAGGTGGGAGT	(-) CCTTTCTCTTTGCAGCCAAC	108	TC20513
AAO1 (Abscisic aldehyde oxidase 1)	(+) TGCAACATCTTGGTCGAGAG	(-) AAGTTCACAGCTCGCAGGTT	113	TC30901
AAO2 (Abscisic aldehyde oxidase 2)	(+) TGCTGGGAGCACTACATCAG	(-) TTGACAGAGCCCATTTCCTC	117	TC25061
IPT1 (Isopentenyltransferase 1)	(+) AAGGACAAGGTGGTGGTGAT	(-) TTGCATTTTGTCGGAGTTGA	114	BW662125
IPT2 (Isopentenyltransferase 2)	(+) TGCCAGGATCAAGATCAACA	(-) GCTCTTAGCGAGAACGTGGT	160	CV543443
IPT3 (Isopentenyltransferase 3)	(+) GTCAACTCAGACAAAATGCAA	(-) ACAGTGCCAAGCAGATGATG	104	CA784528
CYP735A (cytochrome P450 monooxygenase 735A)	(+) TCGTTGTGCTCAAGCAAGTC	(-) GCAGAGTCTCCACCTCCATC	107	CV535867
ZOGT (Zeatin O-glucosyltransferase)	(+) GTTTCTCCTCCTCCCAATCC	(-) GCCATGAGGGAGTCATTGAT	155	AF116858
βGlc (β-glucosidase)	(+) GGAGGTGTGAACAAGGAAGG	(-) CTTGAGGAAGGTCCCAATGA	109	TC27431
CKX1 (Cytokinin oxidase/dehydrogenase 1)	(+) GGAAGAAACCCTTGTGGTGA	(-) ACAAGCCTTTTGAACGCAAC	152	FE674332
CKX2 (Cytokinin oxidase/dehydrogenase 2)	(+) CCAATGGTCCTGATGGACTT	(-) GCACTCTCCATGCTTCCTCT	129	FE709123
MATE (Citrate transporter family) (Eticha et al., 2010)	(+) CTGGATGCAGTTTCAAGAGAG	(-) ACTCCAGCAGCTGCAAGTTC	138	CV535133
ACCO (ACC-oxidase) (Eticha et al., 2010)	(+) GAAGATGGCGCAAGAAGAAG	(-) TGGAGCAAAGGTTCAAGGAG	105	AB002667
β-Tubulin (Eticha et al., 2010)	(+) CCGTTGTGGAGCCTTACAAT	(-) GCTTGAGGGTCCTGAAACAA	117	CV530631

* (+) and (-) indicate forward and reverse primers, respectively.

CURRICULUM VITAE

Personal Data

Name: Zhongbao Yang

Date of Birth: November 28, 1979

Place of birth: Tancheng, Shandong province, PR China

Sex / Marital Status: Male / Married

Nationality: PR China

E-mail: zhongbao@pflern.uni-hannover.de

Education

2007 - 2011   PhD. Gottfried Wilhelm Lebniz University of Hannover, Faculty of Natural Science, Institute of Plant Nutrition, Hannover, Germany.

2004 - 2007   Master of Agriculture, Jilin University, College of Plant Science, Changchun, PR China.

2000 - 2004   Bachelor of Agriculture, Laiyang Agricultural College, Department of Horticulture, Laiyang, PR China

Main Research

- Adaptation of plants to adverse soil conditions (aluminum toxicity, drought stress, manganese toxicity).

Awards

- Scholarship award from China Scholarship Council (CSC)

- Poster awards (2nd)

   Yang ZB, Eticha D, Rao IM, Horst WJ (2008) The interaction between aluminium toxicity and drought stress in common bean (*Phaseolus vulgaris* L.). Abstract and Poster in Annual Conference of the German Society of Plant Nutrition. pp 39.

Scientific Publications

A. *Peer-reviewed Journal articles*

1. **Yang ZB**, Eticha D, Rao IM, Roitsch T, Horst WJ. Physiological and molecular analysis of the interaction between aluminum toxicity and drought stress in common bean (*Phaseolus vulgaris* L.). (To be submitted)

2. **Yang ZB**, Eticha D, Führs H, Gallien S, Heintz D, Dorsselaer AV, Rao IM, Roitsch T, Horst WJ. Proteomic analysis of polyethylene glycol-induced osmotic stress in root tips of common bean (*Phaseolus vulgaris* L.). (To be submitted)

3. **Yang ZB**, Eticha D, Rotter B, Rao IM, Horst WJ (2011) Physiological and molecular analysis of polyethylene glycol-induced reduction of aluminium accumulation in the root tips of common bean (*Phaseolus vulgaris*). *New Phytologist* (in press)

4. **Yang ZB**, Eticha D, Rao IM, Horst WJ (2010) Alteration of cell-wall porosity is involved in osmotic stress-induced enhancement of aluminium resistance in *Phaseolus vulgaris* L. *Journal of Experimental Botany*. 61: 3245-3258.

5. Eticha D, Zahn M, Bremer M, **Yang Z**, Rangel AF, Rao IM, Horst WJ (2010) Transcriptomic analysis reveals differential gene expression in response to aluminium in common bean (*Phaseolus vulgaris*) genotypes. *Annals of Botany*. 105: 1119-1128.

6. Shi ZY, Wang FY, Zhang C, **Yang ZB** (2011) Exploitation of phosphorus patches with different phosphorus enrichment by three arbuscular mycorrhizal fungi. *Journal of Plant Nutrition* (In press)

7. **Yang ZB**, You JF, Xu MY, Yang ZM (2009). Interaction between aluminum toxicity and manganese toxicity in soybean (*Glycine max*). *Plant and Soil*. 319：277-289.

8. **Yang ZB**, You JF, Yang ZM (2007). Aluminum lightens the adverse effects of excessive Mn on growth of soybean (*Glycine max*). *Journal of Plant Physiology and Molecular Biology* 33: 574-580 (In Chinese)

9. **Yang ZB**, You JF, Yang ZM (2007). Manganese uptake and transportation as well as antioxidant response to excess manganese in plants. *Journal of Plant Physiology and Molecular Biology* 33: 480-488 (In Chinese)

10. **Yang ZB**, Wang MY, Liu RJ (2005). Effects of exogenous nutrients and hormones on colonization and sporulation of AM fungi. *Mycosystema* 24: 277-282 (in Chinese)

B. *Papers published in conference proceedings*

11. **Yang ZB**, Eticha D, Rao IM, Horst WJ (2010) Transcriptional characterization of polyethylene glycol-induced reduction in aluminium binding of bean (*P. vulgaris* L.) root tips. Abstract and Poster in Annual Conference of the German Society of Plant Nutrition. pp48

12. **Yang ZB**, Eticha D, Rao IM, Horst WJ (2009) Osmotic stress improves aluminium-resistance in *Phaseolus Vulgaris* L. by changing cell wall porosity. Abstract and Poster in Annual Conference of the German Society of Plant Nutrition. pp71

13. Yang ZM, **Yang ZB**, You JF. (2009). Interaction between aluminum toxicity and manganese toxicity in soybean. IN: Hong Liao et al edited, Plant-Soil interactions at low pH: a nutritiomic approach-Proceedings of the 7th International Symposium on Plant-Soil Interactions at low pH. ISBN 978-7-5623-3309-7. pp 200-201

14. **Yang ZB**, Eticha D, Rao IM, Horst WJ (2008) The interaction between aluminium toxicity and drought stress in common bean (*Phaseolus vulgaris* L.). Abstract and Poster in Annual Conference of the German Society of Plant Nutrition. 23-24 September 2008, Page 39

15. **Yang ZB**, Yang ZM (2006). The interactions between Al and Mn at low pH in soybean (*Glycine max*. L). Symposium of plant stress physiology ecology and molecular biology. Xinjiang, China, Pp76. Academic published in Chinese

Erklärung zur Dissertation

gemäß §6(1) der Promotionsordnung der Naturwissenschaftlichen Fakultät der Gottfried Wilhelm Leibniz Universität Hannover

für die Promotion zum Dr. rer. nat.

Hierdurch erkläre ich, dass ich meine Dissertation mit dem Titel

The Interaction between Aluminium Toxicity and Drought Stress in Common Bean (*Phaseolus vulgaris* L.). Physiological and Molecular Aspects

selbständig verfasst und die benutzten Hilfsmittel und Quellen sowie gegebenenfalls die zu Hilfeleistungen herangezogenen Institutionen vollständig angegeben habe.

Die Dissertation wurde nicht schon als Masterarbeit, Diplomarbeit oder andere Prüfungsarbeit verwendet.

ACKNOWLEDGEMENTS